

RAYLEIGH WAVE SCATTERING  
ACROSS STEP DISCONTINUITIES

by

DOUGLAS ROBERT NATHMAN  
S.B., Massachusetts Institute  
of Technology  
(1979)

SUBMITTED IN PARTIAL FULFILLMENT  
OF THE REQUIREMENTS FOR THE  
DEGREE OF

MASTER OF SCIENCE

at the

MASSACHUSETTS INSTITUTE OF TECHNOLOGY

September 1980

© Massachusetts Institute of Technology 1980

Signature of Author.....  
Department of Earth & Planetary Sciences  
August 25, 1980

Approved by.....  
Jacques Chamuel  
Draper Laboratory Supervisor

Certified by.....  
Nafi Toksöz  
Thesis Supervisor

Accepted by.....  
Chairman, Departmental Graduate Committee

**WITHDRAWN**  
MASSACHUSETTS INSTITUTE  
OF TECHNOLOGY  
**FROM**  
APR 2 1981  
**MIT LIBRARIES**  
LIBRARIES

# RAYLEIGH WAVE SCATTERING ACROSS STEP DISCONTINUITIES

by

DOUGLAS ROBERT NATHMAN

Submitted to the Department of Earth and Planetary  
Sciences on August 25, 1980 in partial  
fulfillment of the requirements for the  
Degree of Master of Science in  
Earth and Planetary Sciences

## ABSTRACT

Propagation of Rayleigh waves across discontinuities comparable to wavelength was investigated using two-dimensional ultrasonic models. Specially designed transducers sensitive to Rayleigh waves were used to generate and detect ultrasonic waves in nickel sheets through magnetostrictive transduction. Different discontinuities (steps and mountain-like features) were cut along the edge of the nickel sheets. Reflection and transmission coefficients were determined for each discontinuity. Computer plots showing amplitude and phase spectra are also presented. Wave velocities in the nickel sheets are 2.776 km/sec for the Rayleigh waves and 5.082 km/sec for the longitudinal body waves.

For the step discontinuities a difference exists between the scattering of waves incident on an upstep and those incident on a downstep. A significant amount of energy is scattered as body waves in both cases, but is more severe for the upsteps. The reflection and transmission coefficients are dependent on frequency. Reflected waves from the upsteps show phase shifts which are fairly constant. The downstep phase shifts change significantly with frequency. The reflected signals from the steps were found to be composed of two components: one from the base of the step and one from the top of the step. The transmitted wave contains both direct surface waves and scattered body waves which are converted back into surface waves. Due to scattering and interference from the different components the amplitude spectra are often irregular shapes. The empirical relationship  $h = \lambda/8 + (\lambda/2)n$  ( $n=0,1,2,\dots$ ) in conjunction with the equation  $c = f\lambda$  was found to correspond to frequency dips in the amplitude spectra of the reflected waves, in some cases.

The mountain-like shapes studied included ramps, pyramids, and rectangular 'mountains'.

The reflected and transmitted waves from the ramp were found to be small. The base of the ramp causes large amounts of conversions from Rayleigh waves to body waves. The ramp's transmitted wave is also composed of a surface wave component and a converted body wave component. Reflection from a pyramid decreases as the pyramid's height is decreased. The transmitted wave is made up of a body wave component which travels through the base of the pyramid, and a surface wave component which travels along the perimeter of the shape. The converted component is larger than the surface one. Similar results were found for the rectangular mountains.

Diffacted body waves from a corner are larger in certain directions; i.e.  $+30^\circ$  of the line traveled by the Rayleigh waves before hitting the corner. These diffracted waves must be taken into account when studying surface wave propagation.

Thesis Supervisor: M. Nafi Toksöz

Title: Professor of Geophysics

## ACKNOWLEDGEMENTS

The author expresses his sincere thanks to all who helped make this thesis possible: my thesis advisor, Prof. Nafi Toksöz, for his many hours of help, understanding, and patience--from the Mojave Desert to the Green Building; my supervisor at Draper Lab, Jacques Chamuel, for uncountable hours of guidance and insight; Terry S. Neiman, of M.I.T., for constantly prodding me onward; Elvis Costello and Joe Strummer for inspiration while writing many rough drafts; to my good friends Matt Dolan, Glen Gawarkiewicz, Dave Gould, and Theodore A. Peck III for their valiant work on the figures; to Ken Tubman for help with the computer work; to Joseph W. Chapman for yet another greatly appreciated late night typing job; and to everyone who wished me luck along the way. A special thanks goes out to Andy Walton for putting up with everything.

This research was conducted partly at the C. S. Draper Laboratory, Inc., and partly at M.I.T. in a cooperative effort. At C. S. Draper the work was supported under contract F-04704-78-C-0002 with the Ballistic Missile Office of the U.S. Air Force and CSDL Independent Research and Development project no. 18325. At M.I.T. the research effort was supported by the Advanced Research Projects Agency, monitored by the Air Force Office of Scientific Research, under contract F-44620-75-C-0064.

## TABLE OF CONTENTS

	<u>Page</u>
Abstract	2
Acknowledgements	4
Table of Contents	5
List of Figures	6
I. INTRODUCTION	9
II. ULTRASONIC MODELING APPROACH	13
III. RESULTS	16
3.1 Steps	
3.2 Mountain-Like Features	
IV. SUMMARY AND CONCLUSION	23
Figures	27
List of Symbols and Abbreviations	65
APPENDIX A. Amplitude and phase spectra plots shown with reflection and transmission coefficients for the steps	66
APPENDIX B. Amplitude and phase spectra plots shown with reflection and transmission coefficients for the mountain-like features	111
REFERENCES	142

## LIST OF FIGURES

	<u>Page</u>
Figure 1. Experimental Set-Up	27
Figure 2. Picture of a Typical Seismogram	28
Figure 3. Placement of Transducers for Reflection from a Step	29
Figure 4. Placement of Transducers for Transmission Through a Step	30
Figure 5. Comparison of Infinite Upstep and Infinite Downstep Reflections	31
Figure 6. Comparison of Infinite Upstep and Infinite Downstep Transmitted Waves (scale changed from previous figure)	32
Figure 7. Amplitude and Phase Spectra for the Infinite Upstep Model	33
Figure 8. Reflection and Transmission Coefficients for the Infinite Upstep Model (Reflection coefficient= reflected signal/incident signal; Transmission coefficient=transmitted signal/incident signal.)	34
Figure 9. Amplitude and Phase Spectra for the Infinite Downstep Model	35
Figure 10. Reflection and Transmission Coefficients for the Infinite Downstep Model	36
Figure 11. Phase Shift Plots of Reflections from Infinite Step Model	37
Figure 12. 6 mm Step Seismograms	38

Figure 13.	
6 mm Upstep Amplitude and Phase Spectra. (The amplitude scale is in arbitrary units. The relative amplitude for the direct, reflected, and transmitted spectra represent the correct values. Phase spectra are shown in fractions of a cycle. Frequency is in MHz.)	39
Figure 14.	
6 mm Upstep Reflection and Transmission Coefficients	40
Figure 15.	
6 mm Downstep Amplitude and Phase Spectra	41
Figure 16.	
6 mm Downstep Reflection and Transmission Coefficients	42
Figure 17.	
Phase Shift Plots of 6 mm Step Reflections	43
Figure 18.	
2 mm Step Seismograms	44
Figure 19.	
2 mm Upstep Amplitude and Phase Spectra	45
Figure 20.	
2 mm Upstep Reflection and Transmission Coefficients	46
Figure 21.	
2 mm Downstep Amplitude and Phase Spectra	47
Figure 22.	
2 mm Downstep Reflection and Transmission Coefficients	48
Figure 23.	
Phase Shift Plots of 2 mm Step Reflections	49
Figure 24.	
Seismograms for the Complete Upstep Case (Step heights are rounded to the nearest millimeter.)	50
Figure 25.	
Seismograms for the Complete Downstep Case	53
Figure 26.	
The Two Components of the Reflected Rayleigh Wave	56

Figure 27.		
Seismograms of Ramps and Trapezoidal Models		57
Figure 28.		
Seismograms of Pyramids		58
Figure 29.		
Seismograms of Rectangular Mountains		59
Figure 30.		
Paths of the Transmitted Wave Components for the Ramps		61
Figure 31.		
Components of Transmitted Wave Through Pyramids.		
(The left column shows the complete transmitted signal. The right column shows the effect of damping the top of the pyramid thereby allowing only the converted component of the transmitted wave to pass through.)		62
Figure 32.		
Diffracted Body Waves		63
Figure 33.		
Summary of Model Shapes and Signal Waveshapes		65



## CHAPTER I

### INTRODUCTION

The earth is often modeled as a laterally homogeneous medium comprised of many parallel layers. In this simplified view, changes in densities and velocities are functions only of depth or radius. While this approximation makes many theoretical formulations possible, the earth is in actuality laterally heterogeneous. Surface topographical features as well as geologic structure vary laterally.

Surface wave propagation across lateral heterogeneities is a complex phenomenon. The aim of this thesis was to study this problem using two-dimensional scaled ultrasonic models. The modeling technique is described in detail in the next section.

Numerous efforts have been made to study surface waves in the past. Theoretical, experimental, and in situ methods have been employed.

Using analytical methods Hudson and Knopoff (1964) used a Green's function to compute reflection and transmission coefficients of surface Rayleigh waves incident normal to the corner of a homogeneous elastic wedge. Mal and Knopoff (1965) used a similar method to find coefficients for Rayleigh waves incident on a step change in elevation. McGarr and Alsop

(1967) employed an approximate variational method to study Rayleigh waves normally incident on vertical discontinuities in plane layered structures. One weak point of this method is that it accounts for only the Rayleigh waves generated at the boundary. Lapwood (1961) used operational methods to analytically attack the problem of a Rayleigh pulse impinging onto a corner and found that the transmitted wave was of a different shape than the incident one. These results agree qualitatively with de Bremaecker's (1958) experimental results. More recently, finite element and finite difference methods (Munasinghe and Farnell, 1973) have also been used.

Other theoretical studies have examined reflection and transmission from different shaped boundaries, such as steps and grooves (Li, 1972; Tuan and Li, 1974; Curtis and Redwood, 1975; Otto, 1977; Parekh and Tuan, 1977), as well as the general problem of topographic irregularities (Gilbert and Knopoff, 1960; Hudson and Knopoff, 1967; Thapar, 1970; Bouchon, 1973; Farshad and Ahmadi, 1974; Deresiewicz, 1974; Sills, 1978.)

Because of the complexities imposed by a heterogeneous media, all of the theoretical analyses involve some form of approximation or a numerical method. How accurate these approximations are and how well the numerical methods converge is not well known at this time.

Experimental modeling work has been carried out by Oliver et al. (1954); Knopoff and Gangi (1960), who looked at wedges;

Toksöz and Anderson (1963), who used piezoelectric transducers on brass sheets; and Pilant et al. (1964) who observed the behavior of waves incident upon a corner as a function of angle. Dally and Lewis (1968) show that reflection and transmission coefficients depend heavily on the angle of the wedge being observed. Here and in a later paper (Lewis and Dally, 1970) they used a photoelastic approach to view the waves, yet it is not easy to separate unwanted wave types and interfering modes using this method. Martel et al. (1977) compared reflection and transmission coefficients and their relation to step height. As the coefficients were, for the most part, fairly small a significant amount of the incident energy is obviously being scattered into body waves.

All these studies point out the fact that the Rayleigh waves are quite sensitive to small changes in the shape of the discontinuity. Modeling can provide a relatively fast and easy way of analyzing this phenomenon. Two-dimensional modeling is a very useful tool in understanding complicated aspects of wave propagation and will eventually lead to effective three-dimensional models.

The scope of this thesis was to determine the effect of different topographical shapes on Rayleigh waves, using the magnetostrictive seismic ultrasonic modeling approach introduced by Chamuel (1979). Scattering across two-dimensional steps was studied and reflection and transmission coef-

ficients were obtained to determine the effect of step height. Then, the experiments were extended to several 'mountain-like' shapes and, once again, scattering across these topographical features was analyzed.

## CHAPTER II

### ULTRASONIC MODELING APPROACH

Two-dimensional models are a useful way to investigate Rayleigh wave scattering across surface irregularities and changes in topography. A thin plate is used to model the earth and the topographical features being examined are cut along the edge of the plate.

Elastic waves were generated and detected in a magnetostrictive material (the thin plate) through contactless magnetostrictive transduction. Specially designed transducers (Chamuel, 1977) consisting of electromagnetic coils were utilized in the experiments. Reflection, transmission, and scattering across discontinuities were studied by placing the source and receiver transducers in different positions. A 0.02 inch thick sheet of Nickel 200 was chosen as a magnetostrictive material. The received signal was displayed on an oscilloscope, where it was photographed and recorded.

When a current is applied to the source transducer a local stress is produced in the nickel sheet. This results in a deformation which travels away from the source. Magnetostriction is the change in a body's dimensions due to magnetization. This change in size is associated with domain orientation. In

a ferromagnetic material the magnetization in one small region, or domain, may be oriented in a different direction from that of another domain. In an unmagnetized material the individual domains, within which the magnetic dipole moments are aligned, are oriented at random. As the material is magnetized, by being placed in an external magnetic field, two things happen. First, the domains which are favorably oriented with respect to the field increase in size while the others decrease in size. Then, the direction of magnetization within each domain rotates toward the applied field. Therefore, the section of the nickel sheet adjacent to the source undergoes a change in dimensions and the outgoing wave arrives at the receiver at time  $t=x/c$ ; where  $x$  is the distance between the transducers and  $c$  is the velocity of the wave in the nickel sheet.

As we were concerned with investigating Rayleigh wave behavior, measurements were made along the edge of the nickel sheets where the surface waves travel (see Figure 1). Magnetostrictive transducers which fit around the edge of the nickel sheets were used. These transducers generally have a broader frequency response than piezoelectric transducers. The system response extended over the range 50-400 kHz.

A typical picture of the direct and reflected Rayleigh waves is shown in Figure 2. In this figure [1] represents the longitudinal body waves; [2] represents the direct Rayleigh wave traveling from the source to the receiver; [3] represents the

Rayleigh wave reflected back from the discontinuity. [4] represents the reflection from the far edge of the sheet.

In this study when investigating scattering across various sizes of steps, waves incident on upsteps as well as waves incident on downsteps have been studied. Figure 3 shows the placement of the transducers to observe the direct wave and the wave reflected from an upstep (top figure) and the direct wave and the wave reflected from a downstep (lower figure). Figure 4 shows the transducer arrangement for transmission through a step.

The goal was to observe the effect of step height on the reflection and transmission coefficients and to see the differences between the upstep and the downstep cases. Also the scattering across several 'mountain-like' shapes was studied.

## CHAPTER III

## RESULTS

The experimental results are presented in two sections. The reflection and transmission coefficients for different step-like shapes are discussed first, followed by a second section discussing the effects of mountain-like topographical features.

### 3.1 Steps

We found the Rayleigh wave velocity in the nickel sheets used to be  $c=2.776$  mm/ $\mu$ sec and the longitudinal wave velocity to be  $c_p=5.082$  mm/ $\mu$ sec. (These units scale one-to-one to km/sec.)

A large cut was made in a nickel sheet approximating an 'infinite' step (many wavelengths long). The same sheet was used to study the effects of an infinite upstep and an infinite downstep on Rayleigh wave propagation.

Figure 5 shows the reflections for both the upstep and downstep cases. The upstep reflection is much smaller than the reflection from the downstep. The transmitted waves for both cases are shown in Figure 6. Once again we see that the amplitude is slightly greater in the downstep case. As both reflection and transmission are smaller for an upstep, more



energy is scattered into body waves in the upstep case. Figures 7 - 10 show amplitude and phase spectra and reflection and transmission coefficients for the Infinite Step. In Figure 11 plots of the phase shift for the reflected waves are presented. While the phase of the upstep reflection is fairly constant, the downstep reflection varies greatly with frequency.

Examining the 6 mm step we see similar results. Both the reflected and transmitted waves are larger for the downstep case. We again see phase reversal for the reflected wave. The 2 mm step, the smallest one studied, shows high amounts of transmitted energy, as is expected. (Figures 12 - 17 show the data for the 6 mm step and Figures 18 - 23 show the data for the 2 mm step.)

We now turn to the case of the steps in general. The direct, reflected and transmitted wave shapes are shown in Figures 24 and 25 for upsteps and downsteps, respectively. (Plots of amplitude and phase spectra, as well as reflection and transmission coefficients are displayed in Appendix A.)

Looking at the complete picture of wave scattering across steps we make several observations. The reflected signal is consistently larger from a downstep than from an upstep of the same height. The transmitted wave, in general, is also larger in the downstep case. This confirms our earlier observation that an upstep causes more scattering of energy than does a downstep.

Examining the two sets individually, we find that the reflected upstep signal appears to 'spread out' as the step height ( $h$ ) becomes larger. As the duration of the reflected signal increases its average amplitude decreases. The downstep reflection experiences a similar phenomenon, but, in this case, when the signal 'spreads out' the first of the two apparent components stays at approximately the same amplitude even as  $h$  is increased--very unlike the upstep case. In both upstep and downstep cases the transmitted signal duration increases.

When the incident wave 'hits' the base of the step, a portion of the wave is reflected, another part is converted into body waves, and a third part is transmitted. The transmitted wave continues traveling up the side of the step. At the top of the step, another boundary is reached causing new reflections. Once again, some of the energy continues onward as the transmitted wave, but some of the energy is reflected back down the step. This signal, together with the first reflection from the base of the step, make up the complete reflected wave (see Figure 26). (This holds for upstep and downstep reflections.)

Therefore, when the incident wave is in the form of a single pulse, the reflected wave will be composed of two pulses. The two reflected wave components can have different amplitudes and frequency contents. The time delay of the two

signals is contributing to the interference of the reflected waves.

As the points of reflection for the two pulses are separated by the distance  $h$  (the step height), the reflected component from the top will arrive at the receiver at time  $2h/c$  after the reflection from the base arrives. When  $h$  is not very large, the two pulses arrive close together in time and combine to form one pulse. As the size of the step is increased the reflection from the top becomes more delayed and the two pulses start to destructively interfere with one another. If the step height is made large enough, they will be discerned as individual pulses.

The reflected and transmitted signals are made up of several components causing the spectra of the reflection and transmission coefficients to be irregular and complex. The amplitude spectra, especially for the upstep case, show 'lips' due to the interference at certain frequencies. It was observed that the interfering frequencies of the reflected signals follow the equation  $h = \lambda/8 + (\lambda/2)n$  ( $n=0,1,2,3.$ ), where  $\lambda$  denotes the wavelength. Additional studies are needed to verify this empirical relation.

### 3.2 Mountain-Like Features

We next looked at scattering across several mountain-like shapes. Again, these shapes were cut along the edge of nickel

sheets. The wave shapes and the dimensions of the mountain features are shown in Figures 27 - 29. (Amplitude and phase spectra as well as reflection and transmission coefficients are displayed in Appendix B.)

Reflection and transmission from these mountain-like features show many interesting characteristics. In the case of the ramp, the reflected signal is small as is expected. Yet, the transmitted signal is small, also. Instead of the Rayleigh wave being easily transmitted up the ramp, it is converted into body waves at the base of the ramp.

Comparing the two ramps, we see that for the lower ramp the transmitted wave (both up and down the slope) appears to be a clean pulse. The higher ramp shows us that the transmitted wave is actually comprised of two parts. The first portion has traveled through the interior of the sheet as a converted body wave, while the later arriving portion of the transmitted signal is the surface component which follows the outline of the ramp along the edge of the sheet. Figure 30 shows the different paths traveled by the two components of the ramp's transmitted wave.

Perhaps the most intriguing event occurs in the pyramid case. The reflected wave decreases slightly as the height of the pyramid is decreased. The transmitted wave clearly shows that it is composed of two distinct components. By damping the top of the pyramid to attenuate the waves traveling along

this path, we see that the purely surface component forms the second part of the transmitted wave. The leading portion of the transmitted wave has traveled through the base of the pyramid as a converted body wave. Emerging from the base it becomes converted back into a Rayleigh wave. This converted pulse is also larger than the pure surface wave component traveling along the perimeter of the pyramid.

Figure 31 shows the complete transmitted wave for the pyramid and then shows the same wave with the top of the pyramid--and the wave traveling over the top of the pyramid--damped to reveal only the converted transmitted component. This clearly shows the two distinct components of the transmitted wave. (Calculation of travel times confirms this, also.)

The reflection and transmission from the rectangular mountain shapes are not very sensitive to changes in the height or width of the mountain. A reflection from a wider mountain shows ringing from multiple internal reflections.

Comparing the mountains with pyramids of equal height we unexpectedly (from intuition) find the reflection to be larger from the pyramid. Again, the sharp corner at the mountain base--similar to that in the upstep case--creates a large amount of scattering into body waves.

Comparing the trapezoid (a shape half way between the pyramids and the rectangular mountains) to Pyramid #3 (both the same height) we find the pyramid's reflection to be larger.

The transmitted waves for the two shapes look very different from one another.

To get an idea of the direction of diffraction of Rayleigh waves from a corner we placed transducers as shown in Figure 32a. We found the diffracted body waves are larger in some directions than in others (Figure 32b).

## CHAPTER IV

### SUMMARY AND CONCLUSION

Ultrasonic modeling is a useful and practical way of studying surface wave propagation across various shaped discontinuities. Rayleigh wave scattering from topographical features is quickly displayed by the modeling technique and the results often defy intuition (see Figure 33). In this study the Rayleigh waves were generated and detected using contactless magnetostrictive transduction in a nickel sheet.

Two main types of features were studied: steps and mountains. Reflection and transmission coefficients and amplitude and phase spectra were calculated for all cases. Wave velocities were found to be 2.776 km/sec for the Rayleigh waves and 5.082 km/sec for the longitudinal body waves.

For the steps, it was found that a significant difference exists between scattering from an upstep and a downstep. The upstep reflection is significantly smaller than the downstep, as illustrated with the Infinite Step. The upstep's transmitted wave is also smaller implying that more energy is converted into body waves in the upstep case.

Reflected waves from the steps show phase shifts as is expected, but the upstep shows a phase shift which is fairly constant while the downstep phase shift changes significantly

with frequency.

The surface waves impinging on the steps are subject to tremendous amounts of scatter and conversions into body waves. The reflected signal increases in duration with step height. This occurs because the reflected signal is composed of two components: a reflection from the base of the step and a reflection from the wave which continues up the step and is then reflected back by the top of the step. These two components constructively interfere when the step height is small and may not be detected. The transmitted wave, also, is made up of two main components. One is the surface component traveling along the edge of the step, and the other is a diffracted component which is converted to a body wave at the base of the step. The body wave travels through the interior of the nickel sheet and is converted back to a Rayleigh wave as it emerges onto the edge of the sheet. This diffracted component travels at body wave velocities inside the sheet. Since it also travels a shorter distance than the surface component, it will arrive first, followed by the surface component.

Due to the large amounts of scattering and interference between the different components, the amplitude spectra are often irregular shapes. Looking at the reflected amplitude spectra many dips in amplitude are observed. The empirical



relation  $h = \lambda/8 + (\lambda/2)n$  ( $n=0,1,2,3\dots$ ) in conjunction with the equation  $c=f\lambda$  was found to correspond to the frequency dips in the amplitude spectra, in some cases.

The mountain-like shapes studied included ramps, pyramids, and rectangular mountains. Like the steps these were cut along the edge of the nickel sheets.

The wave reflected from the ramp was small in amplitude. The transmitted wave was small too, however. Instead of the Rayleigh waves easily traveling up the ramp they are largely converted into body waves at the base of the ramp.

Similar to the steps, the ramp's transmitted wave is also made up of two components. The diffracted portion and the surface portion may not be discernable for small ramps. As the two path lengths diverge the two components have a larger delay and are easier to detect. The reflected wave from the ramp is smaller than that from a step of the same height.

Reflection from a pyramid decreases as the pyramid's height is decreased. The transmitted wave for the pyramid shows many interesting phenomena. The transmitted wave contains two distinct signals: a converted portion which travels through the base of the pyramid; and the surface component which travels along the perimeter of the shape. The converted pulse (Rayleigh wave to body wave and then back to Rayleigh wave) arrives first and is larger than the surface component. The difference in the path lengths traveled and the difference

in velocities determine the separation in time of the two pulses.

Small changes in the height and width of the rectangular mountains do not considerably change the reflected and transmitted waves. Comparing these mountains to pyramids of the same height we find the pyramid reflection to be larger. This means that--as in the upstep case--the corner of the mountain is causing heavy conversion of surface waves into body waves.

We also found that the diffracted body waves from a corner are larger in an area  $\pm 30^\circ$  of the line traveled by the Rayleigh waves before hitting the corner.

From these experiments it is clear that Rayleigh wave propagation across topographical features contains many interesting facets. Future studies can shed more light on some questions raised here.

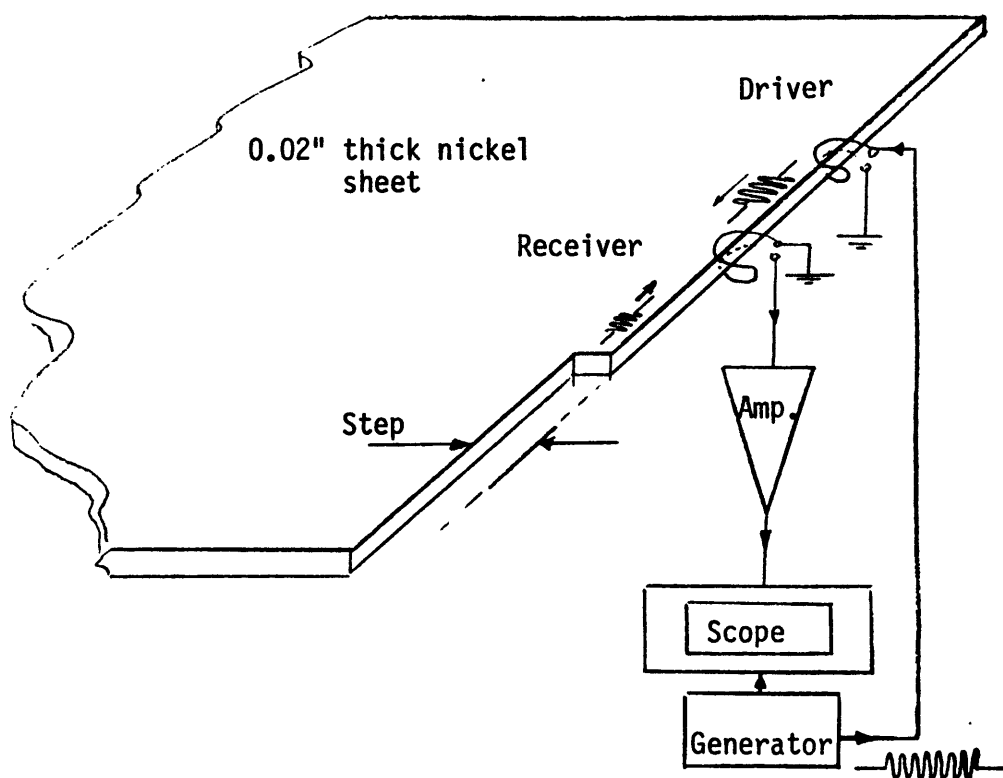
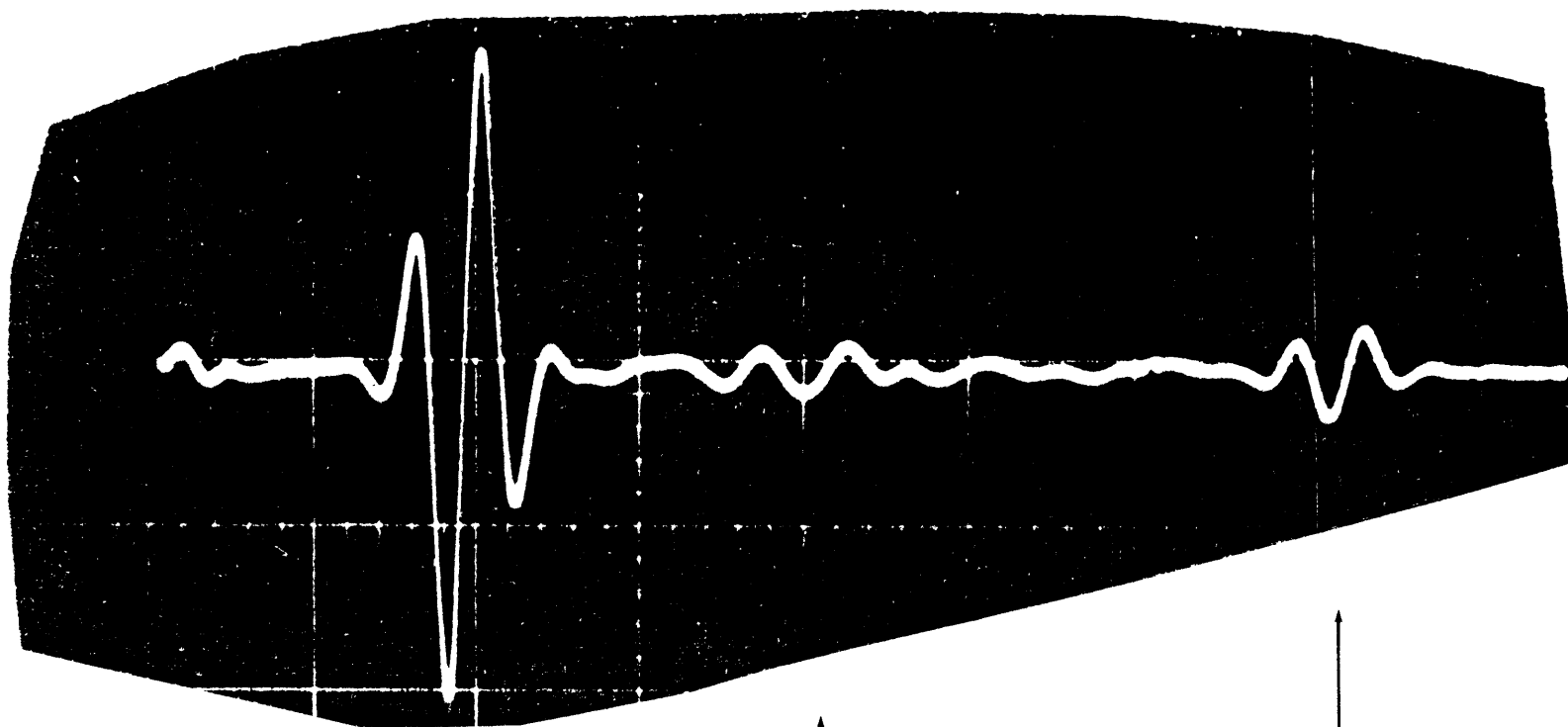


Figure 1.



[1]

[2]

[4]

Figure 2.

[3]

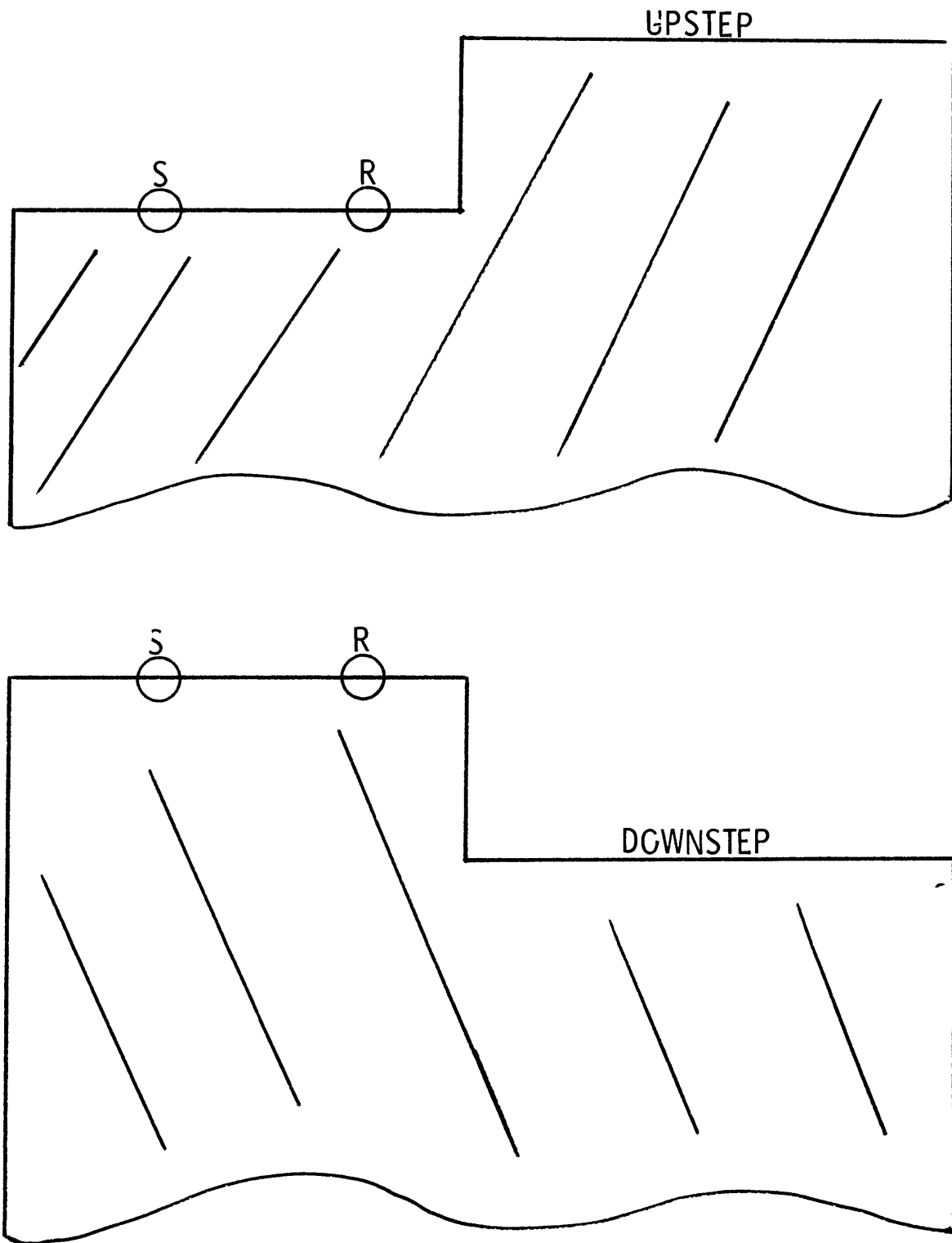


Figure 3.

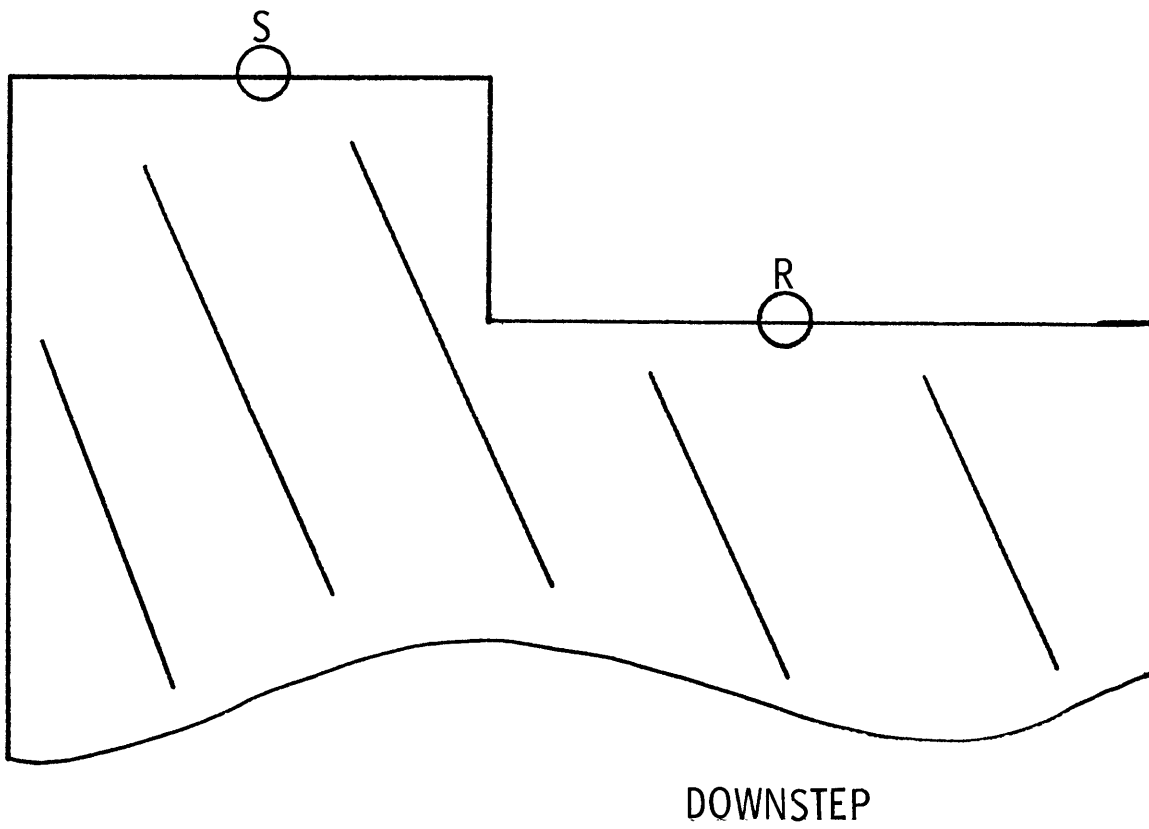
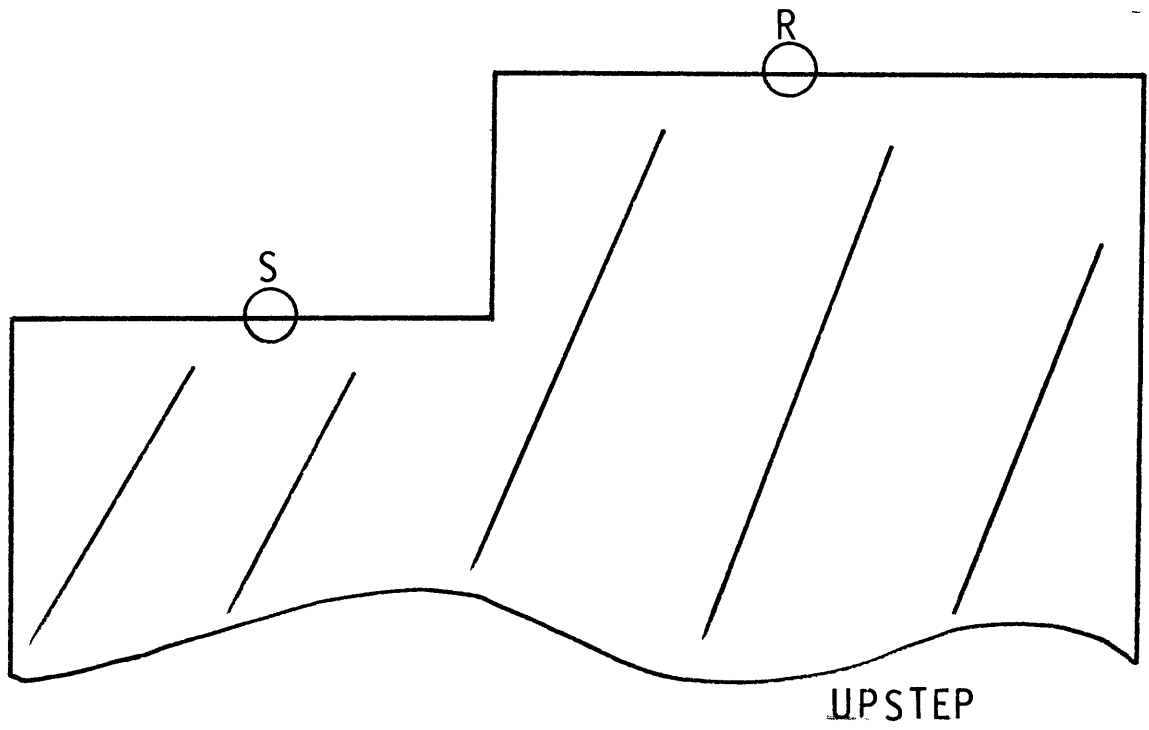


Figure 4.

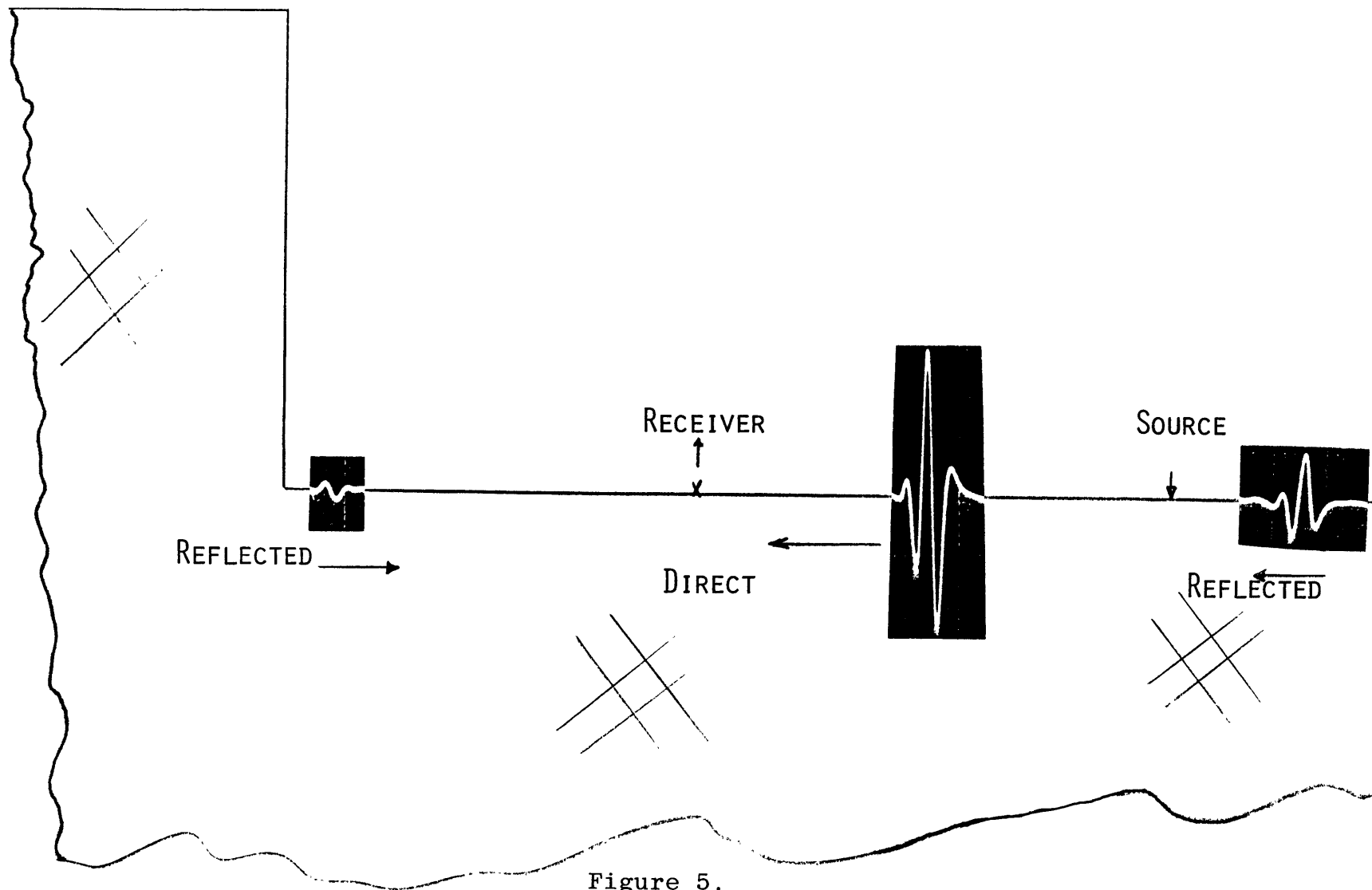
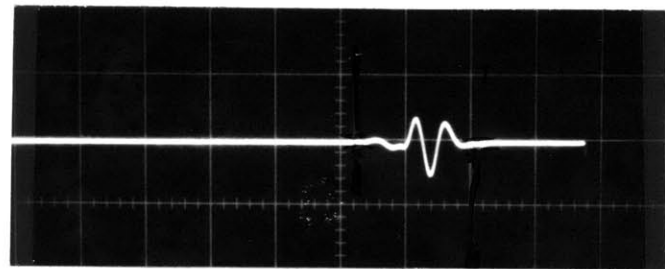
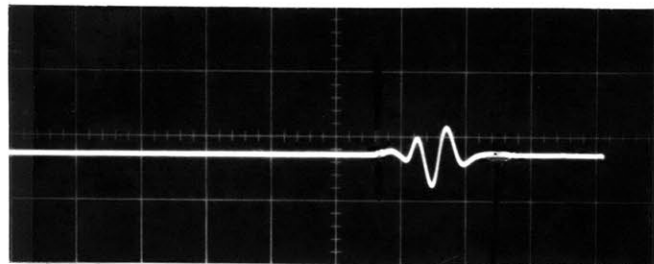


Figure 5.



UPSTEP



DOWNSTEP

Figure 6.



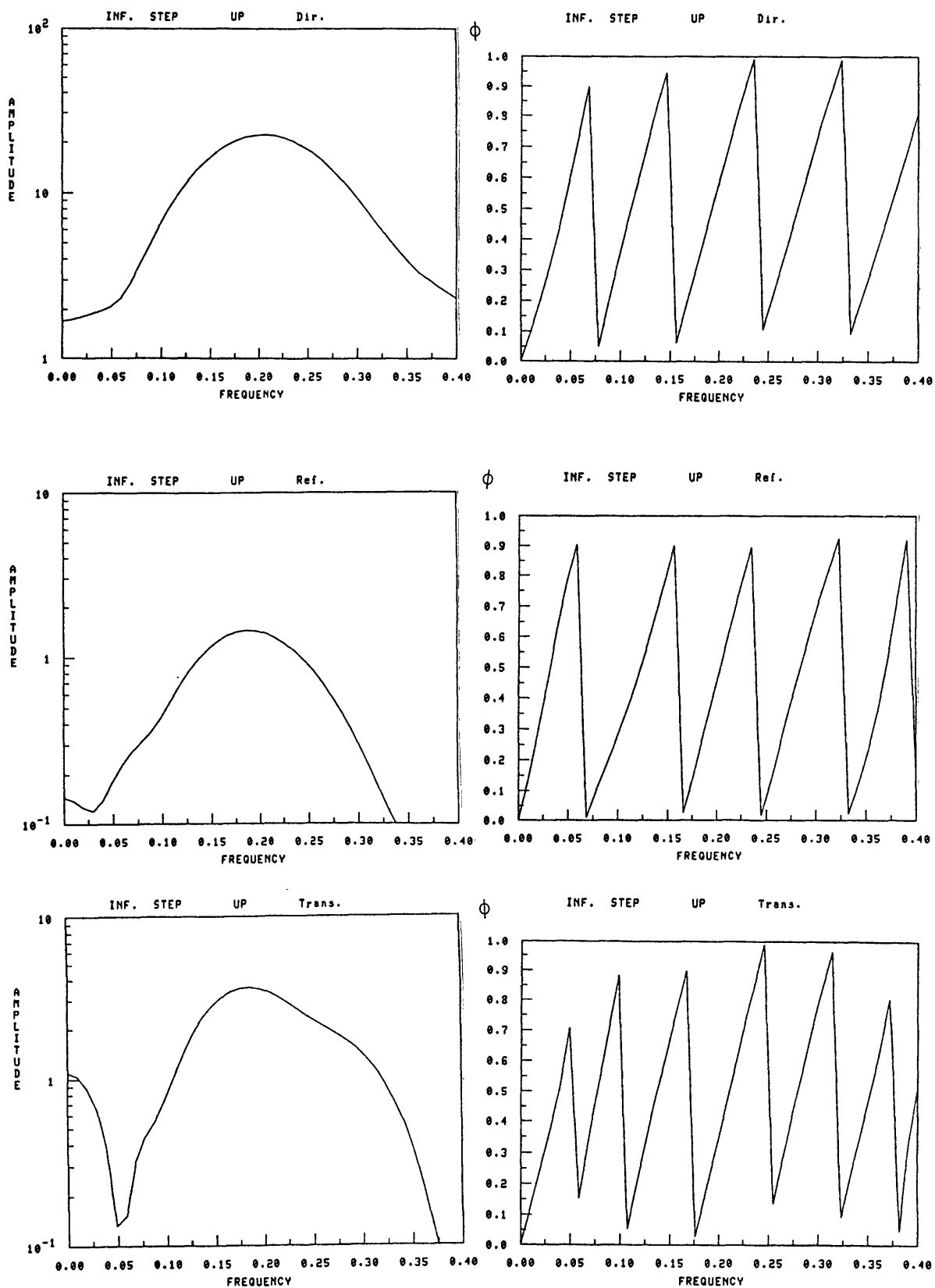
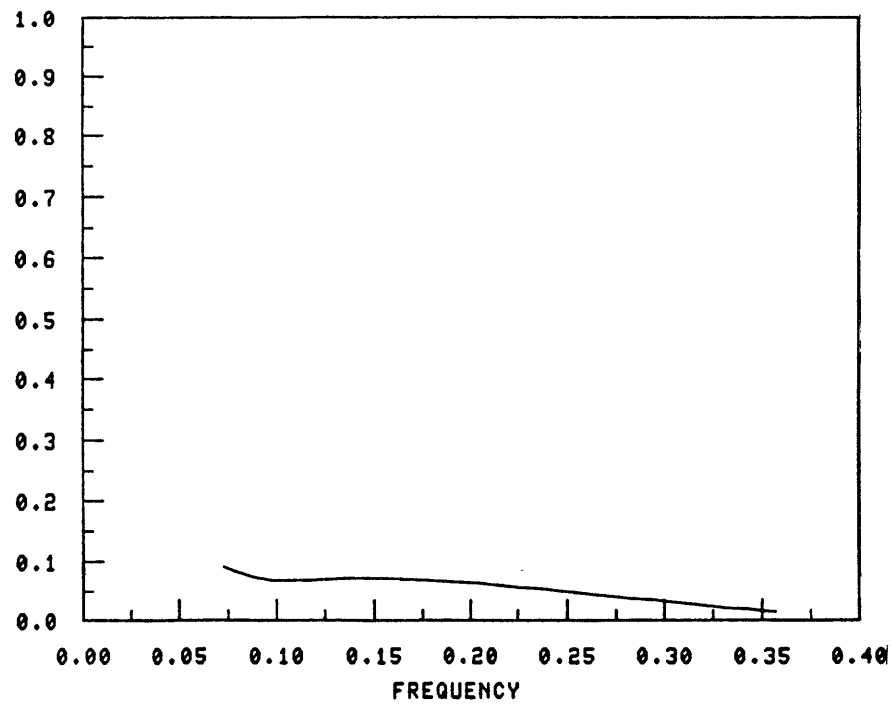


Figure 7.

REF. COEFF. (Inf. Step UP)



TRANS. COEFF. (Inf. Step UP)

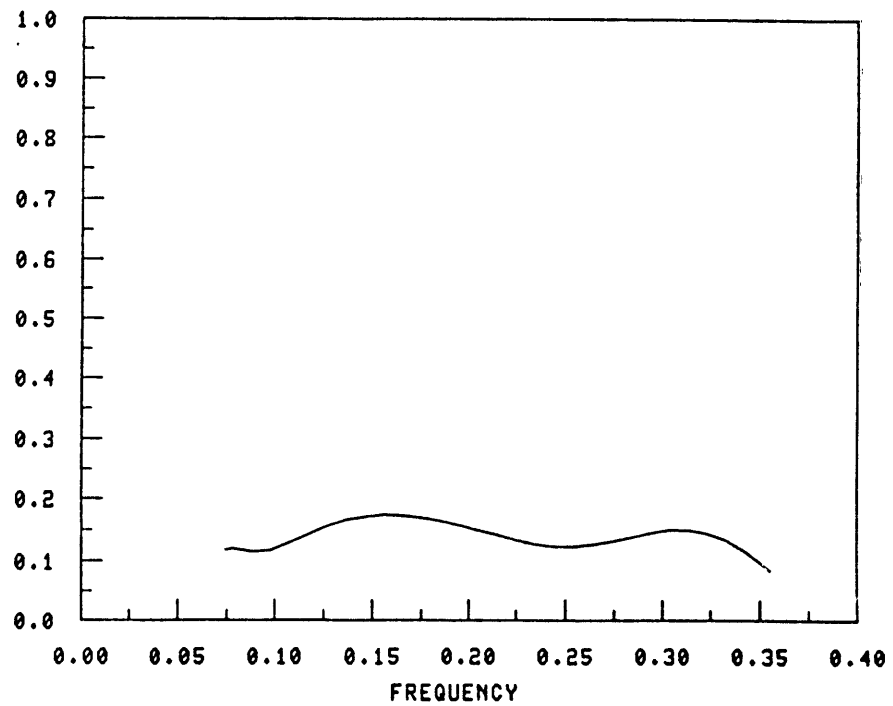


Figure 8.

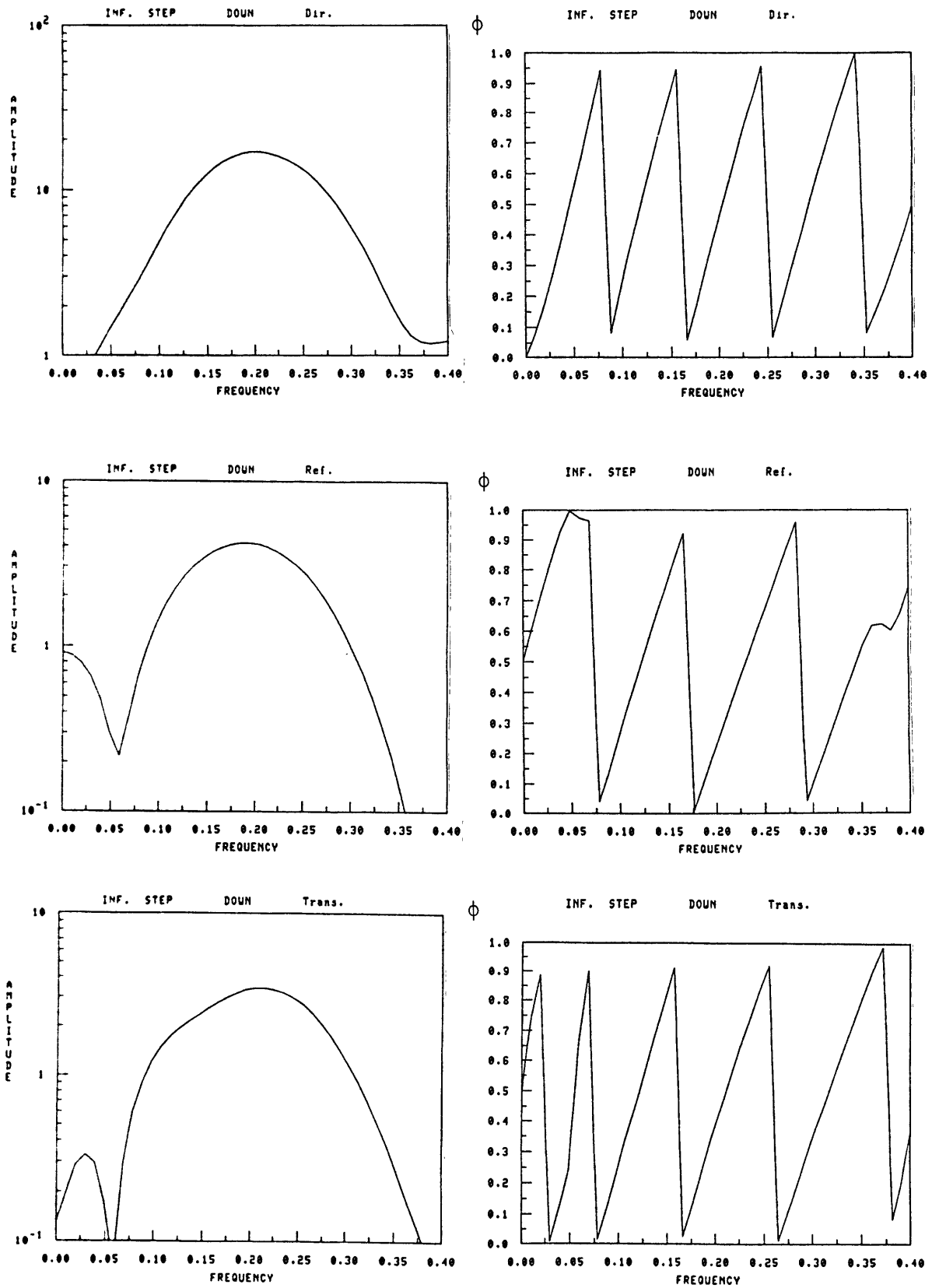
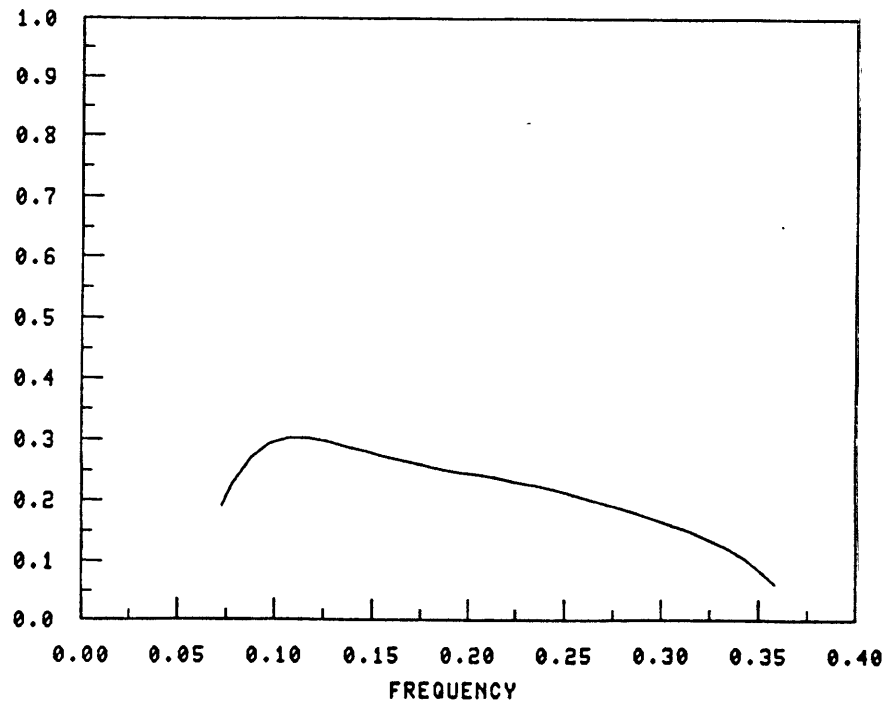


Figure 9.

REF. COEFF. (Inf Step DOWN)



TRANS. COEFF. (Inf. Step DOWN)

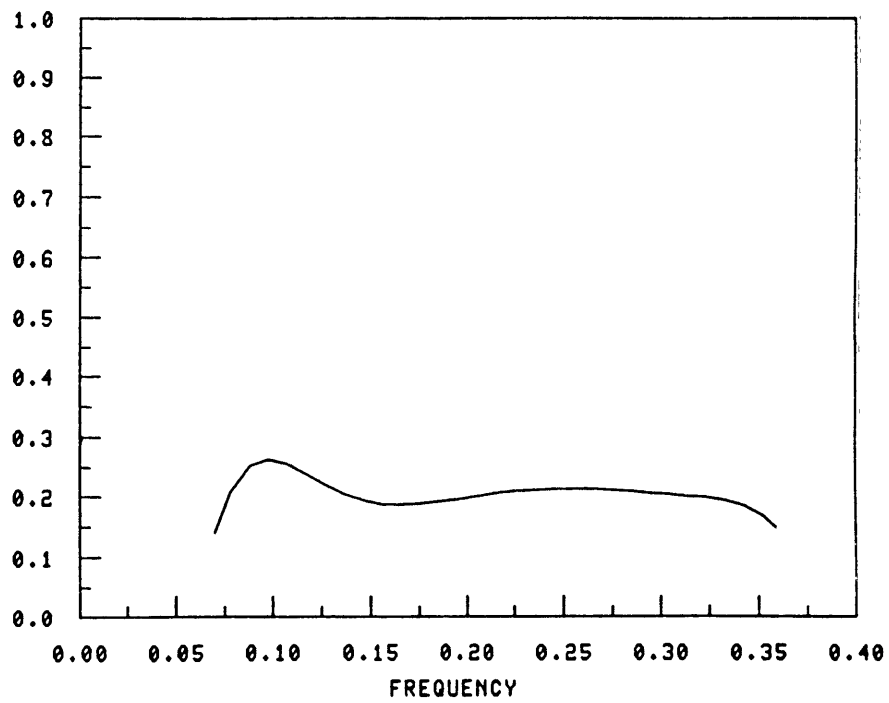


Figure 10.

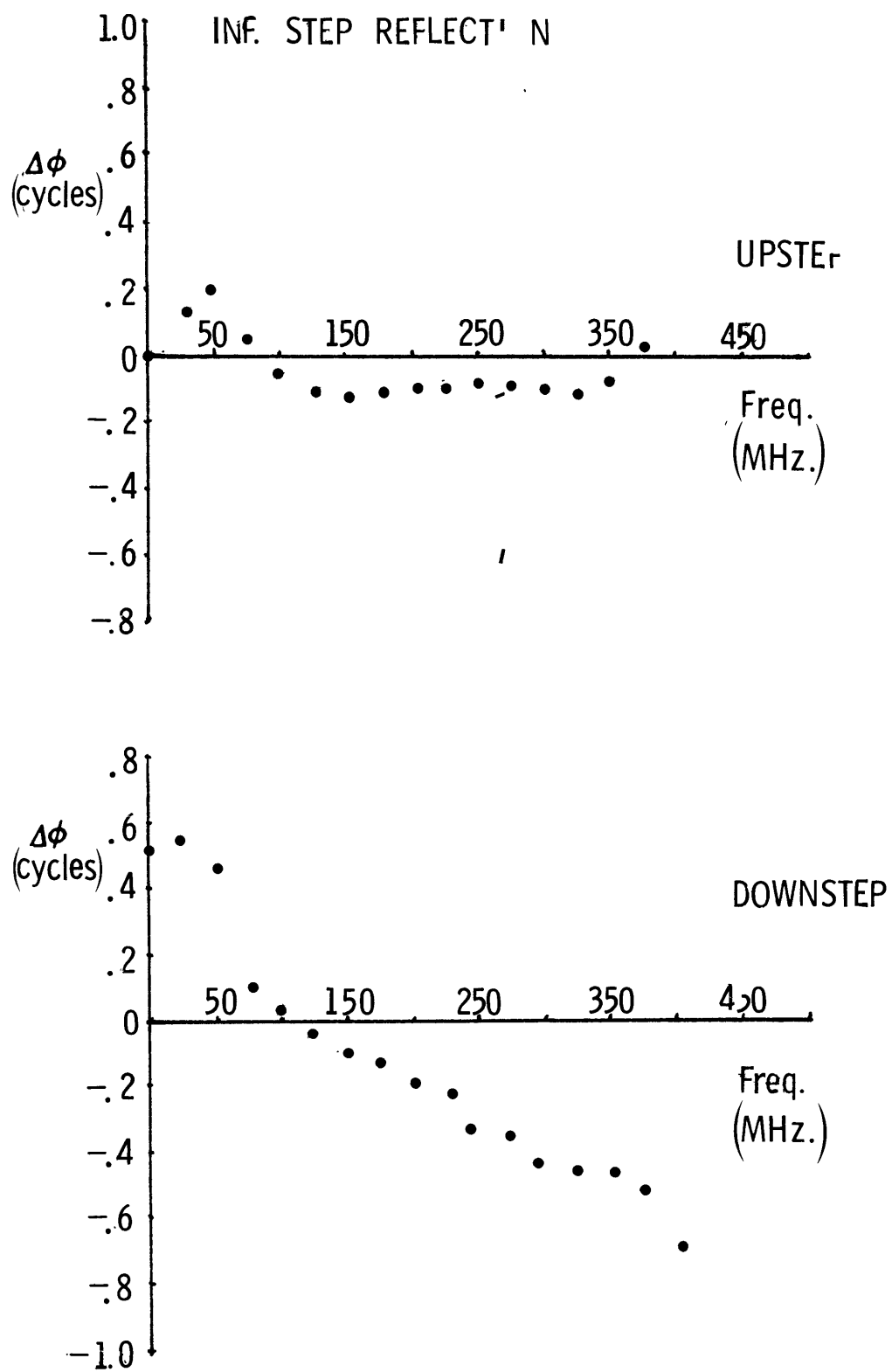


Figure 11.

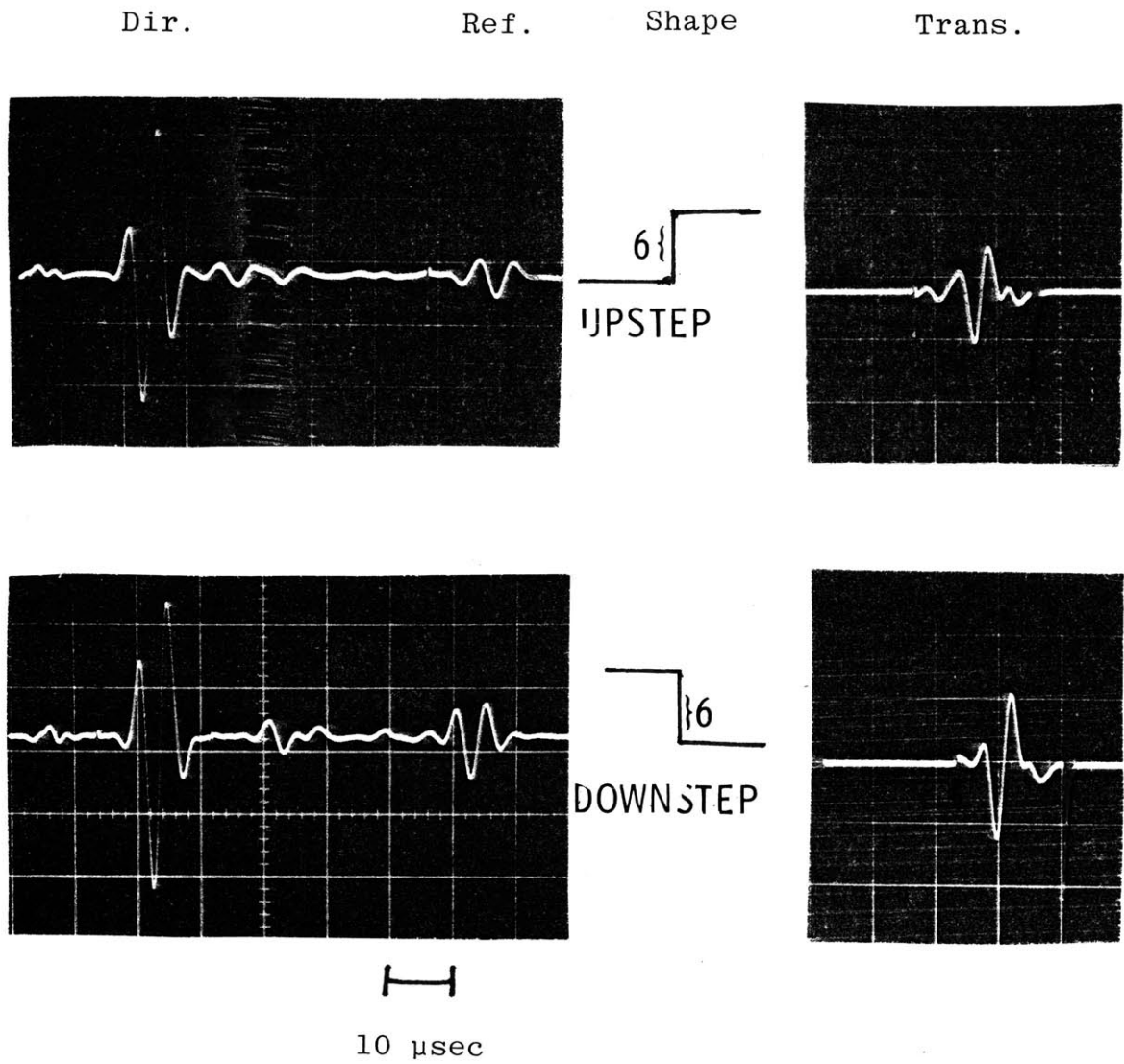


Figure 12.

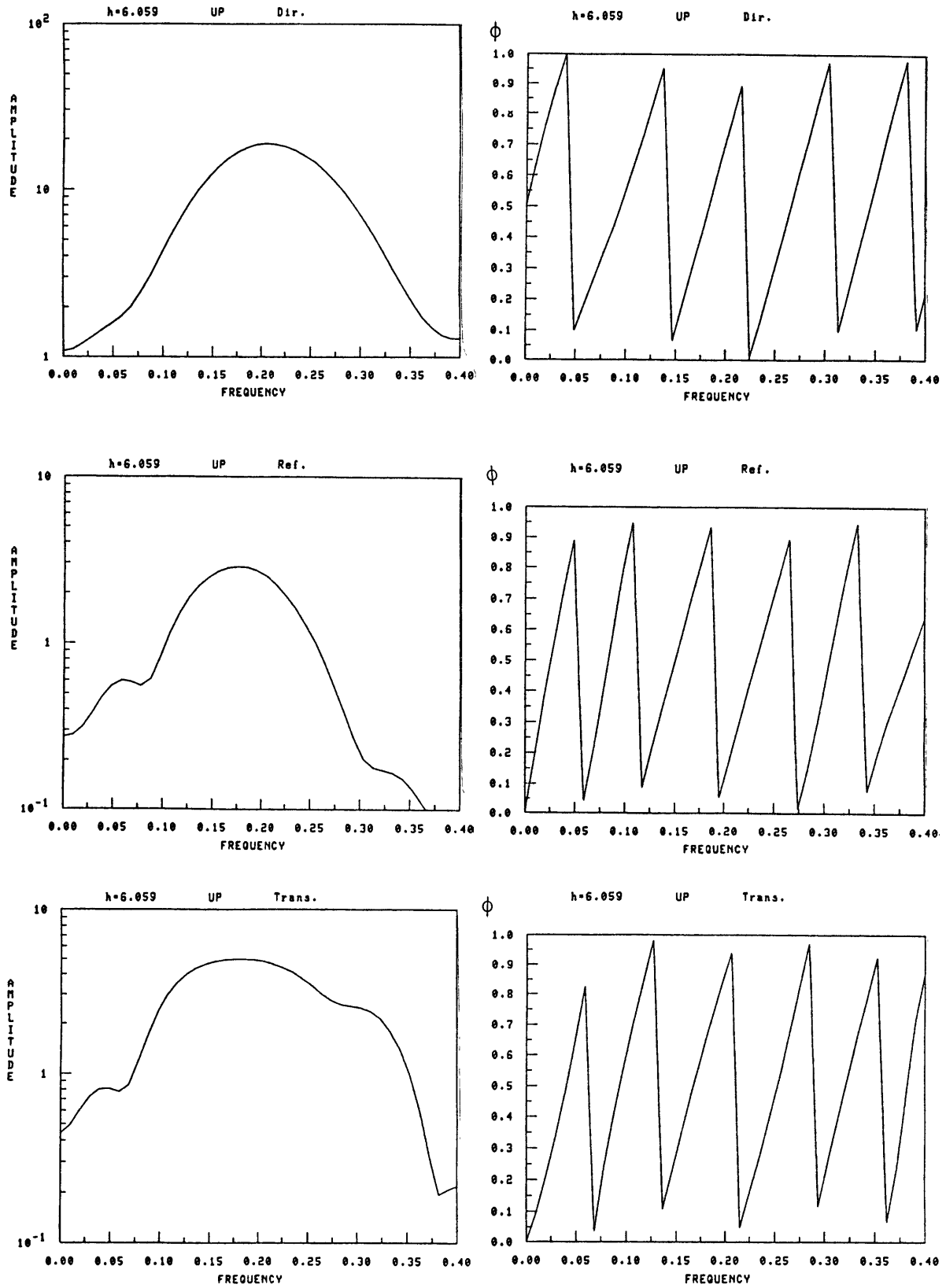
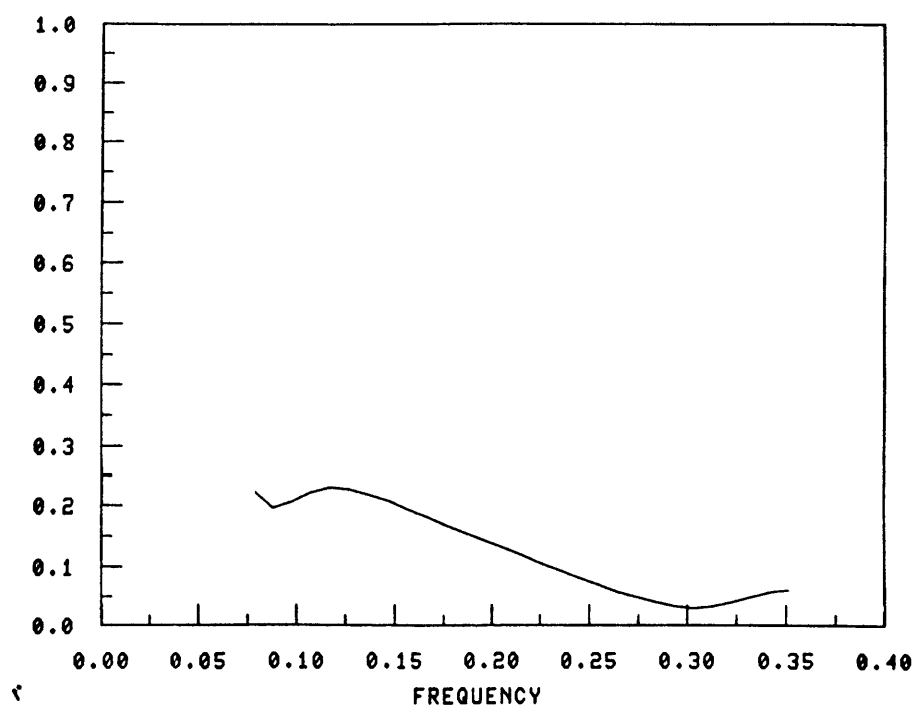


Figure 13.

REF. COEFF. (h=6.059 UP)



TRANS. COEFF. (h=6.059 UP)

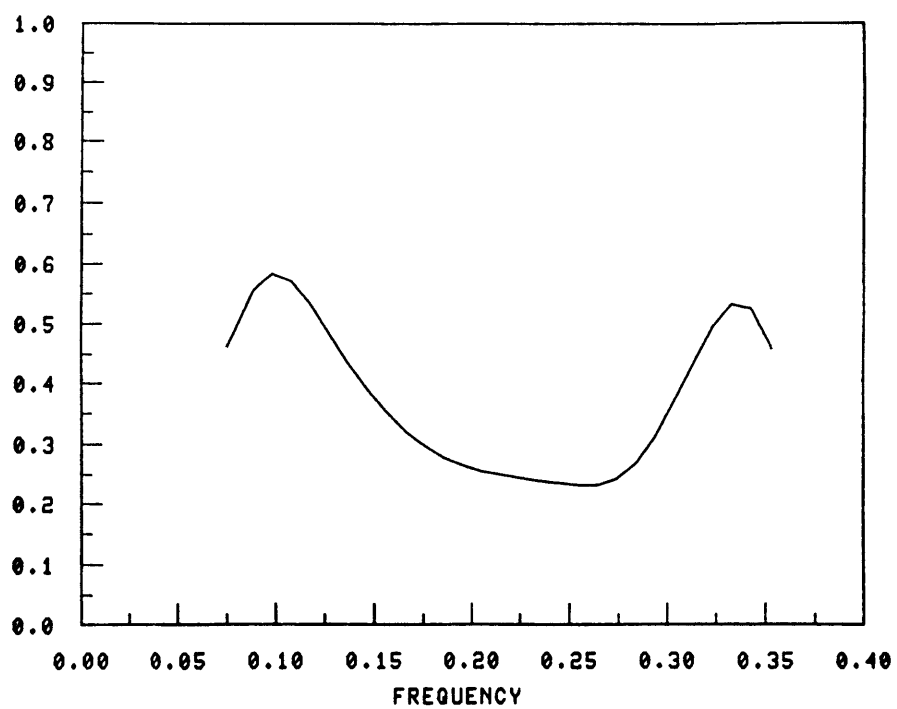


Figure 14.



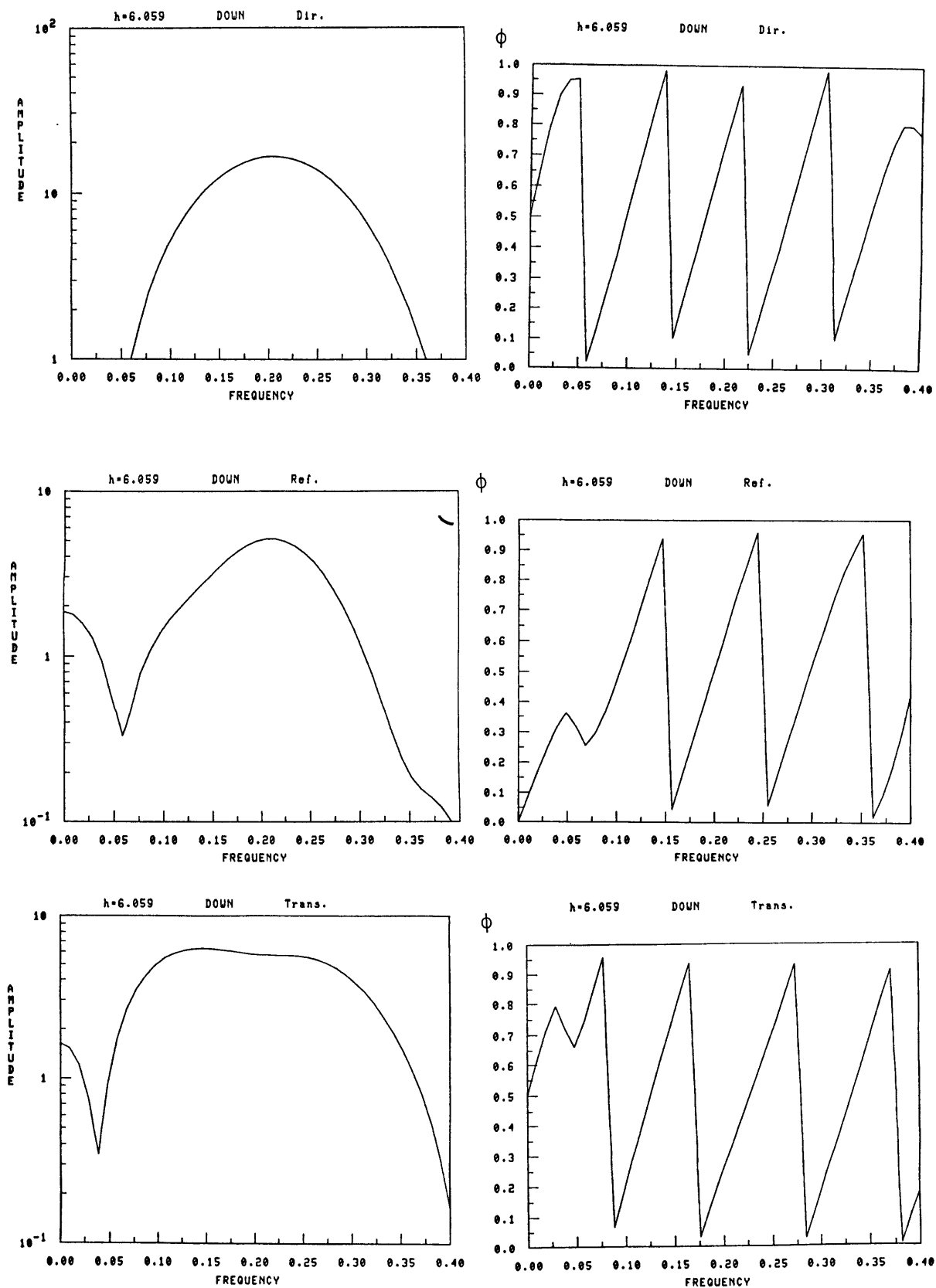
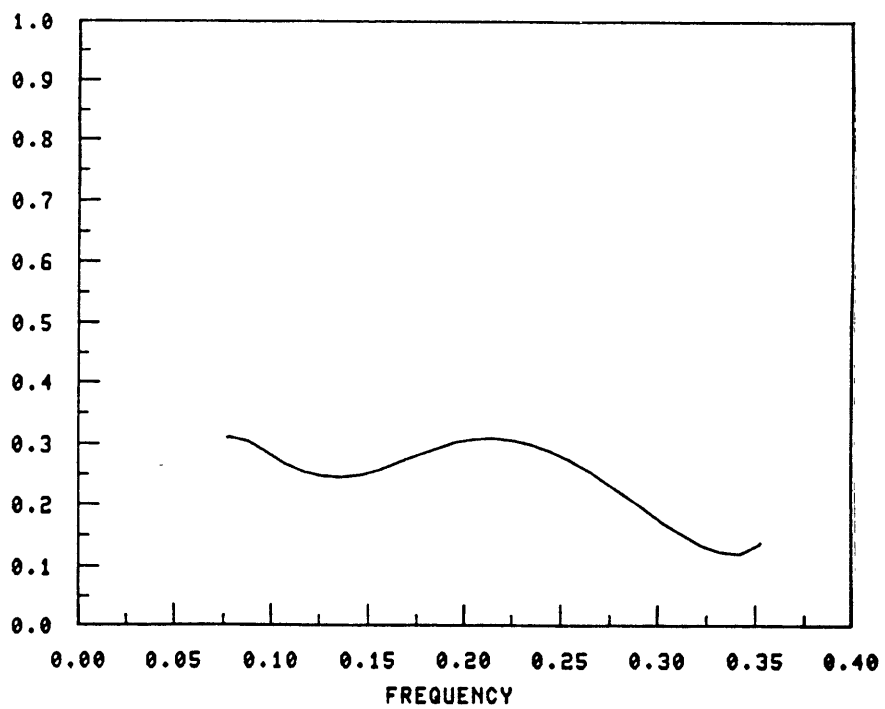


Figure 15.

REF. COEFF. (h=6.059 DOWN)



TRANS. COEFF. (h=6.059 DOWN)

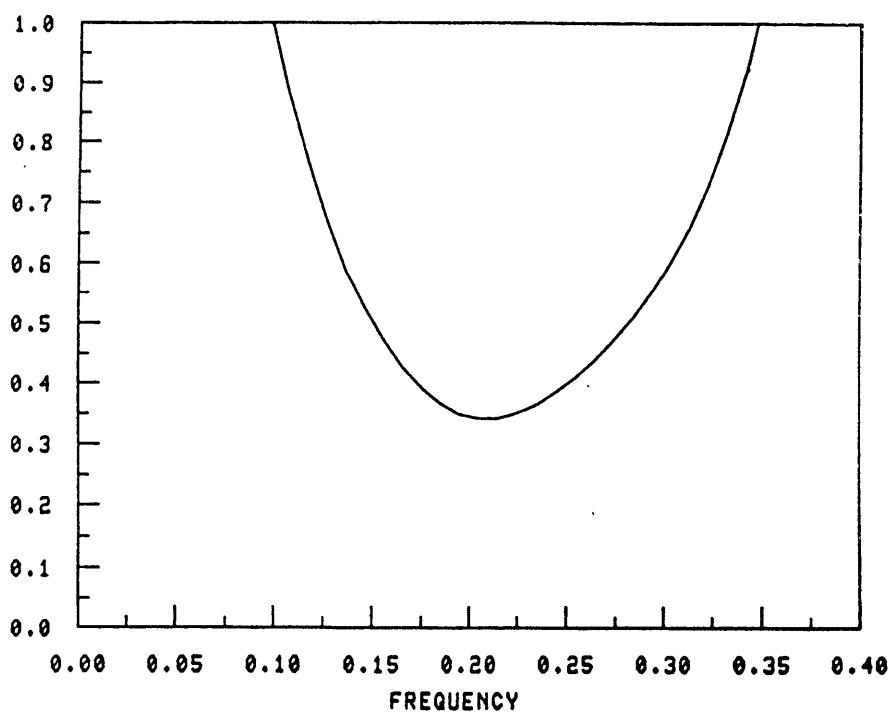


Figure 16.

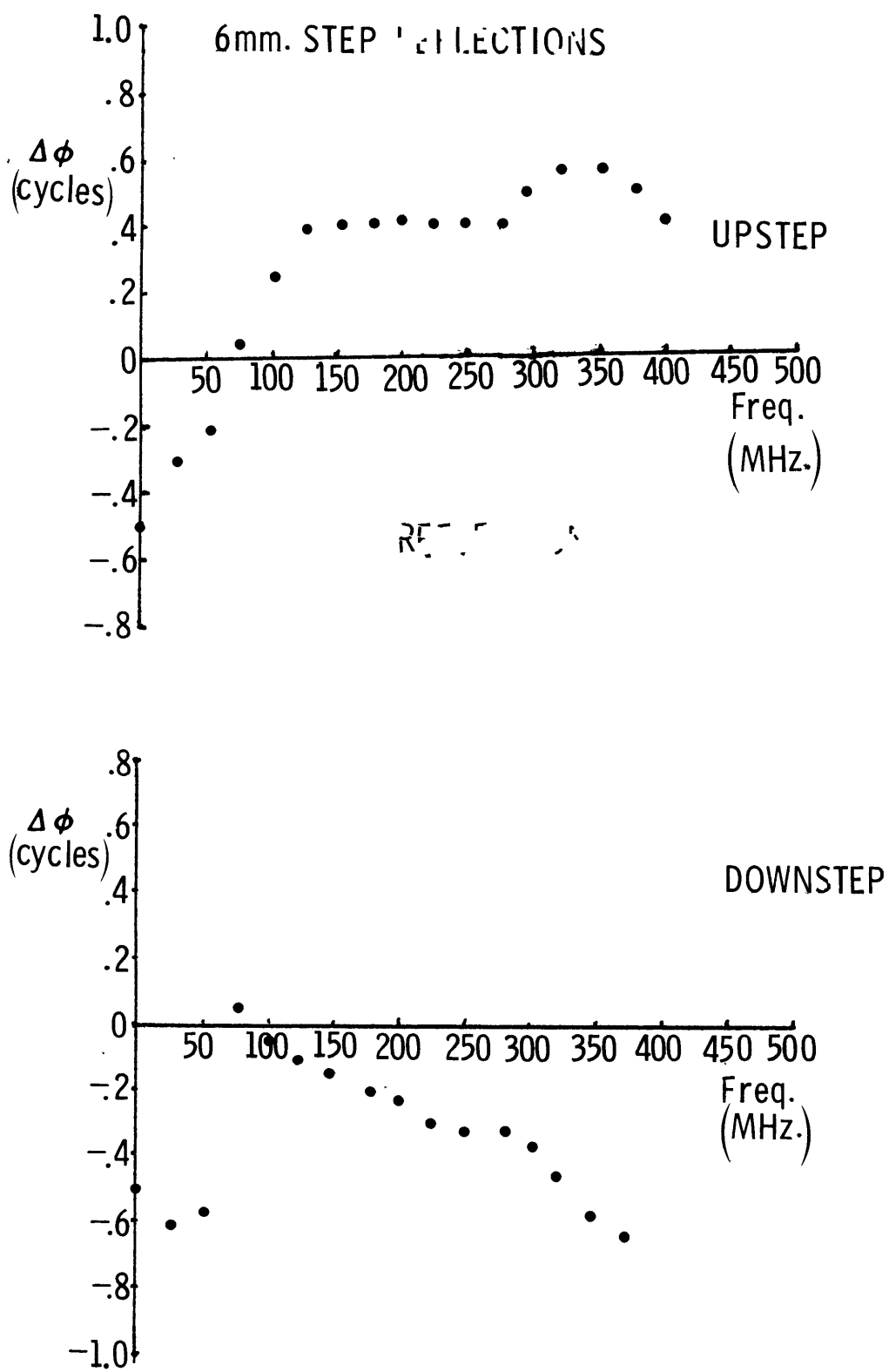


Figure 17.

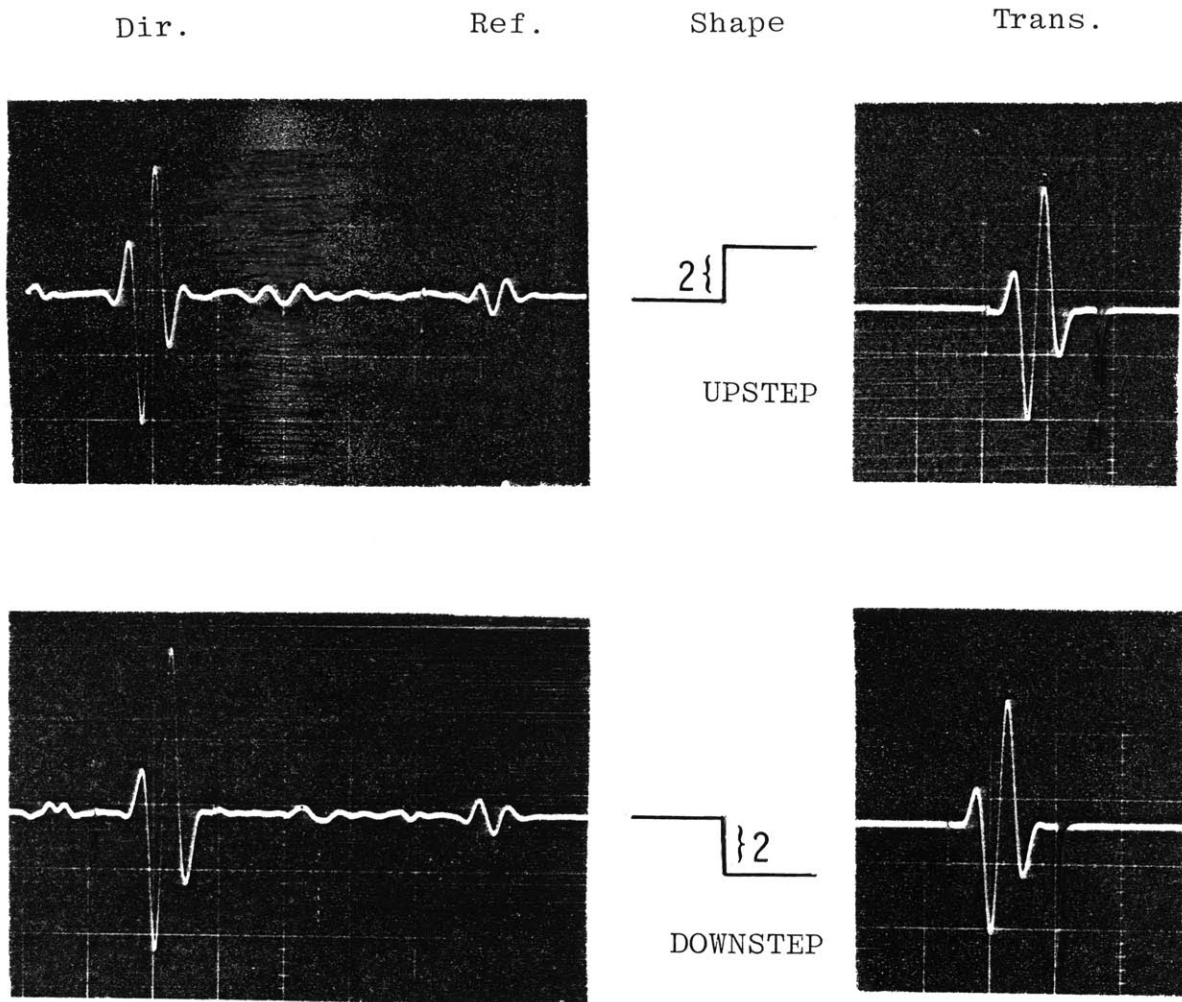


Figure 18.

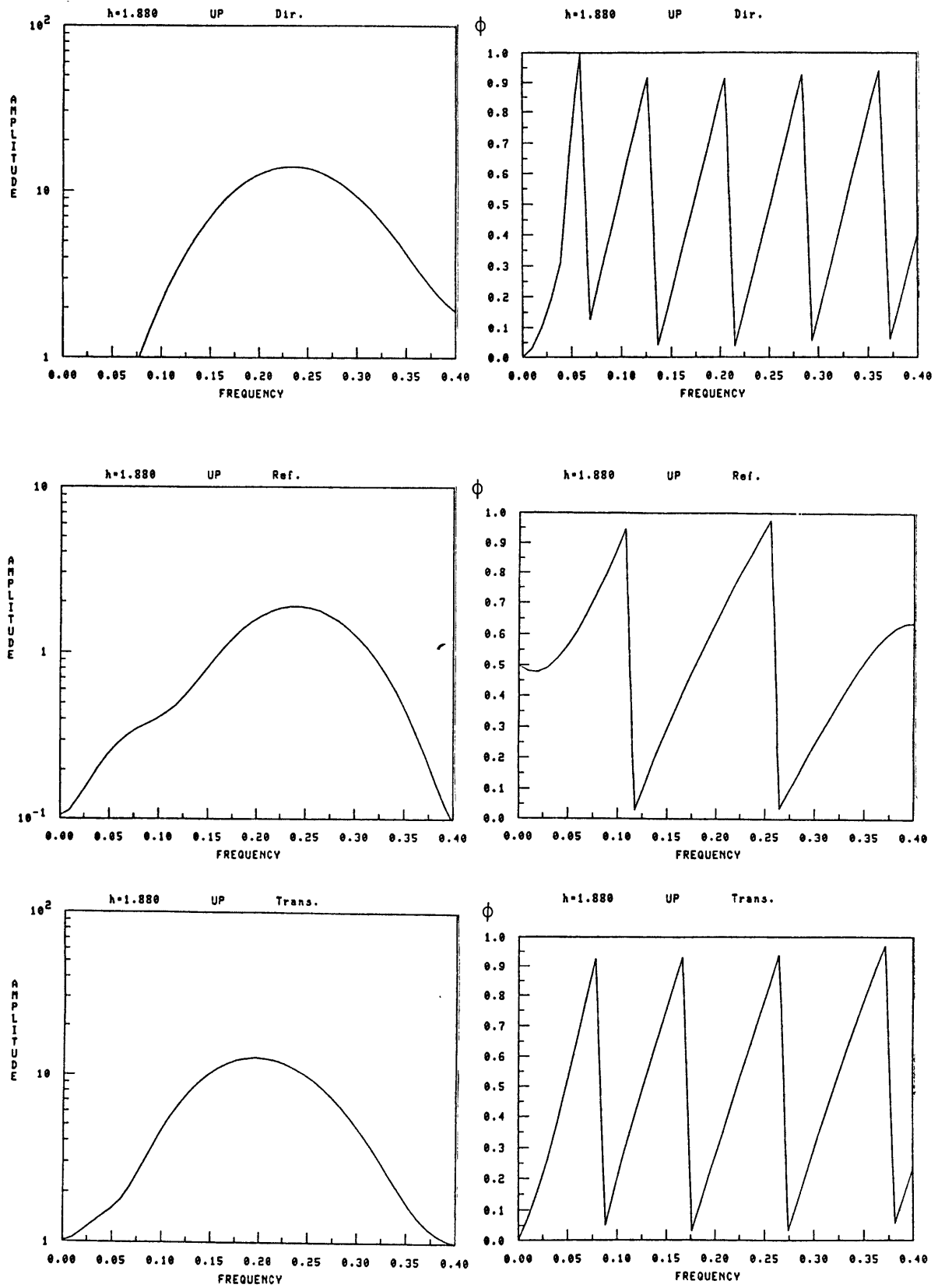
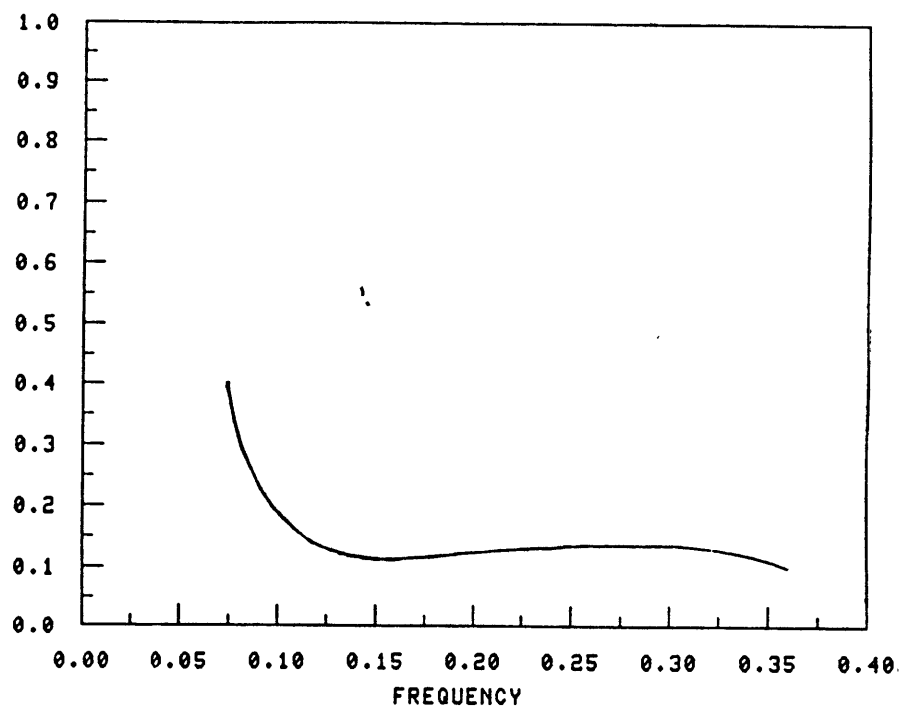


Figure 19.

REF. COEFF. (h=1.880 UP)



TRANS. COEFF. (h=1.880 UP)

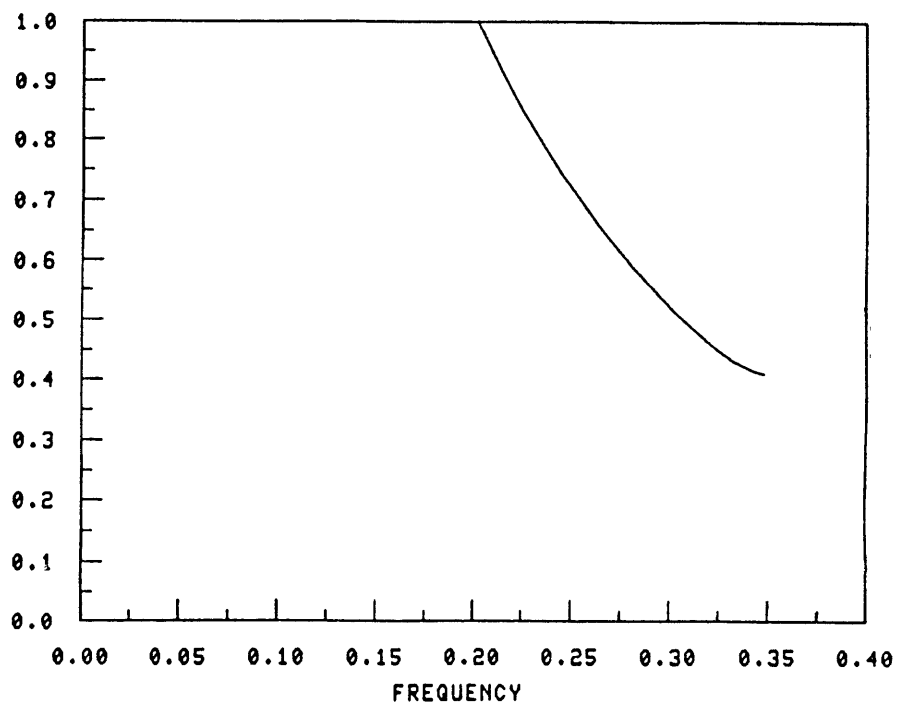


Figure 20.

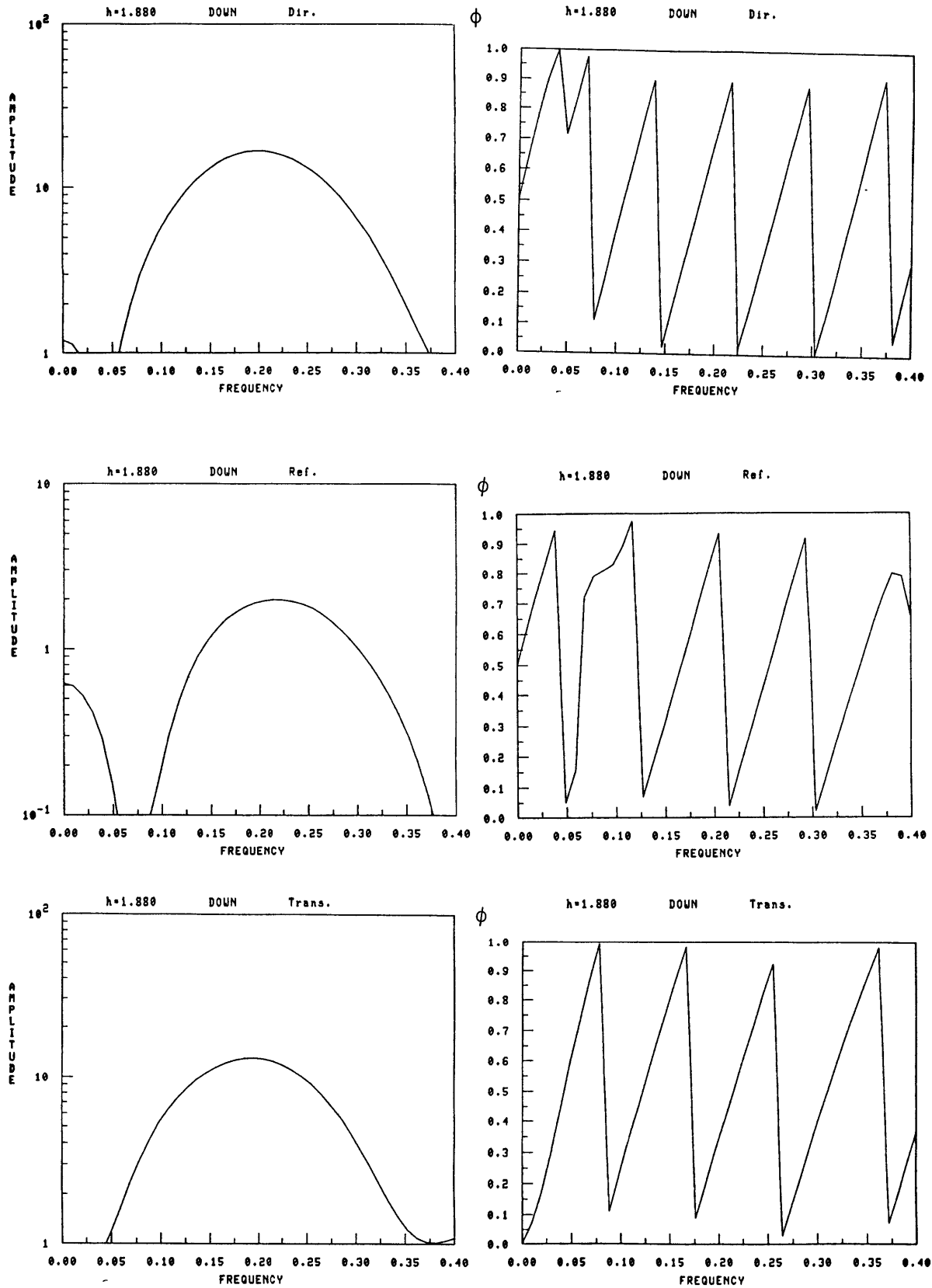
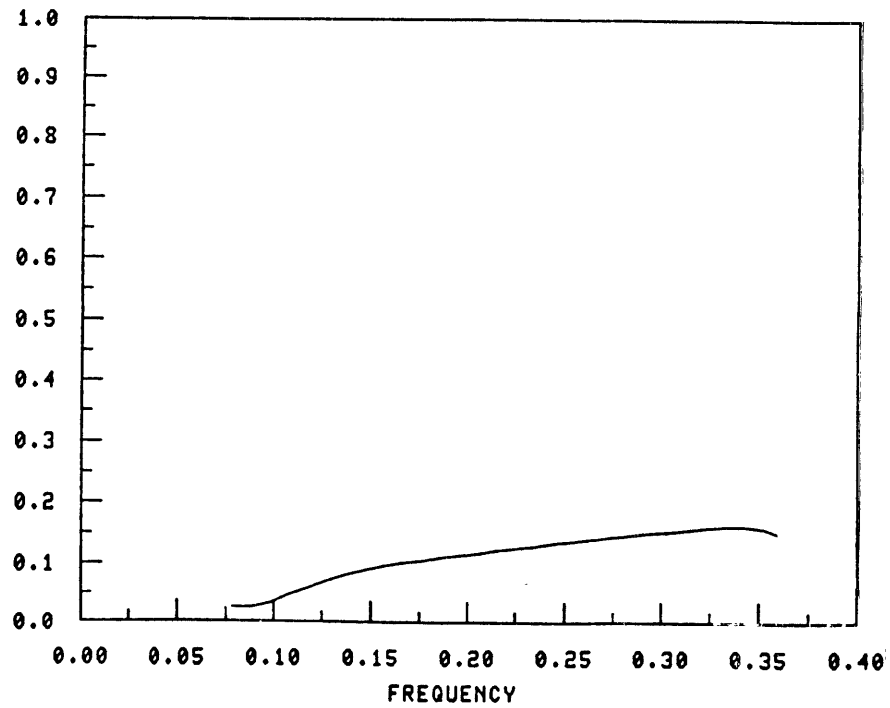


Figure 21.

REF. COEFF. (h=1.880 DOWN)



TRANS. COEFF. (h=1.880 DOWN)

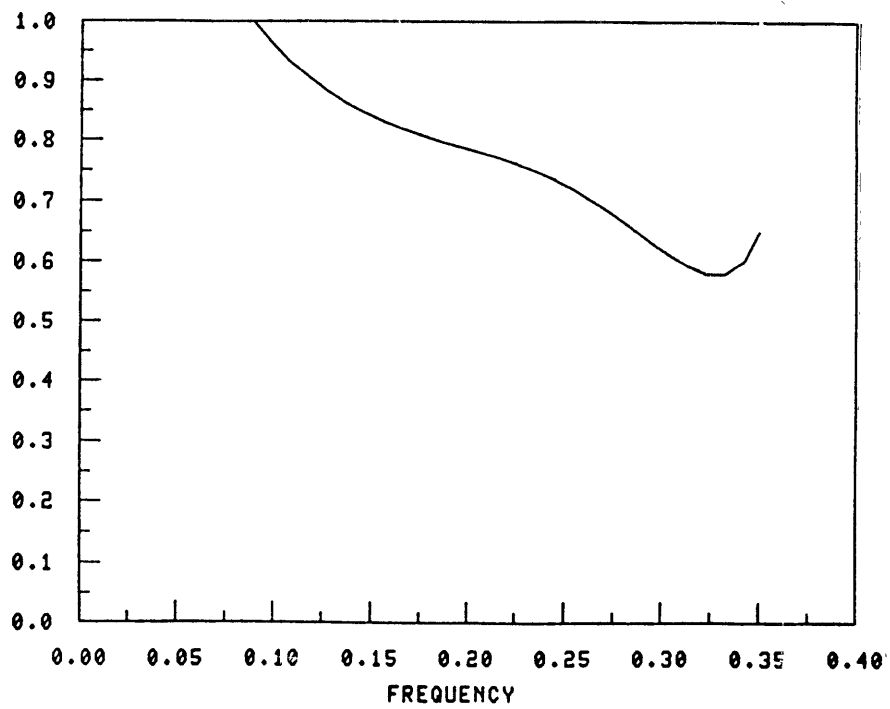


Figure 22.



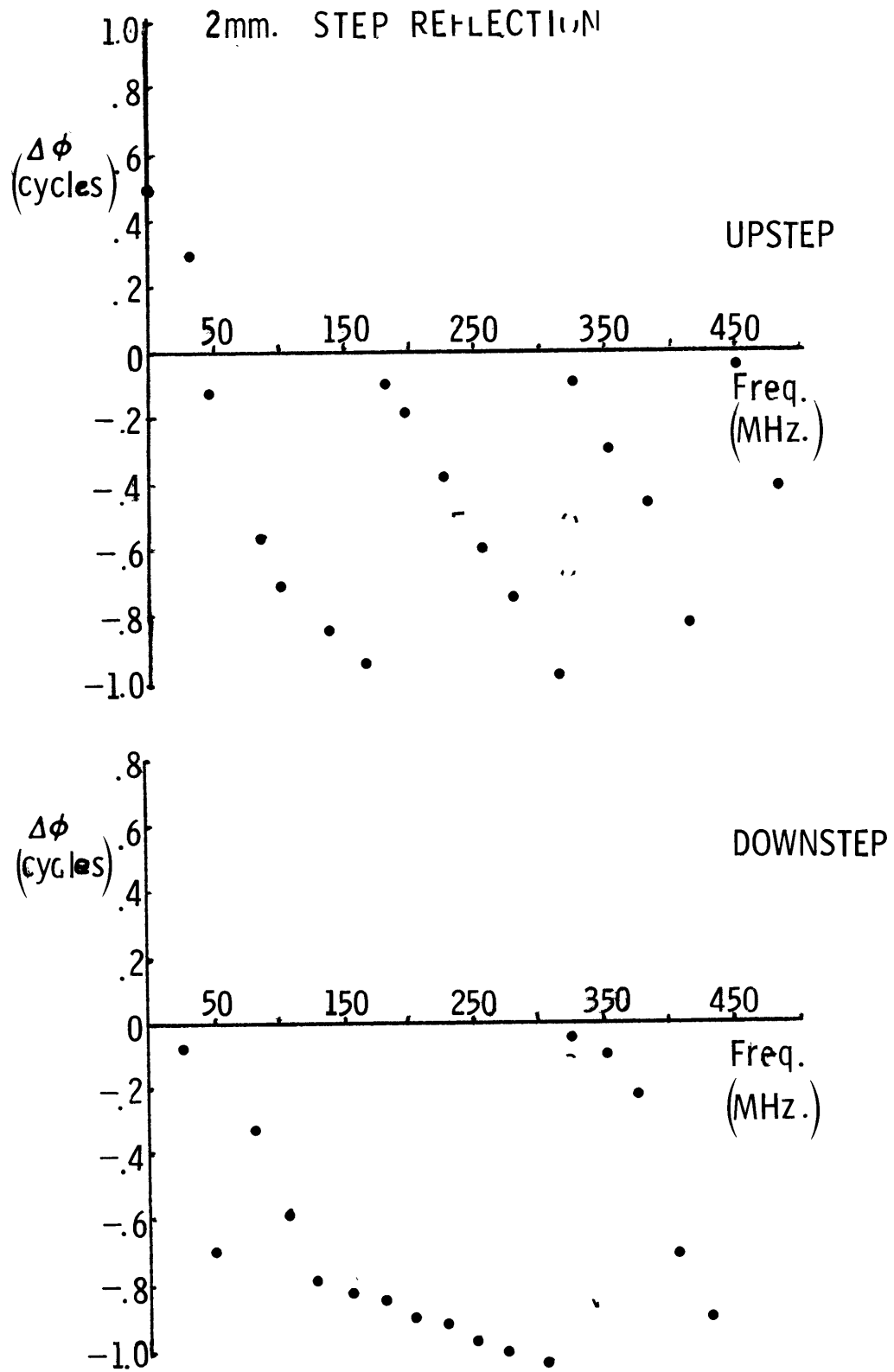


Figure 23.

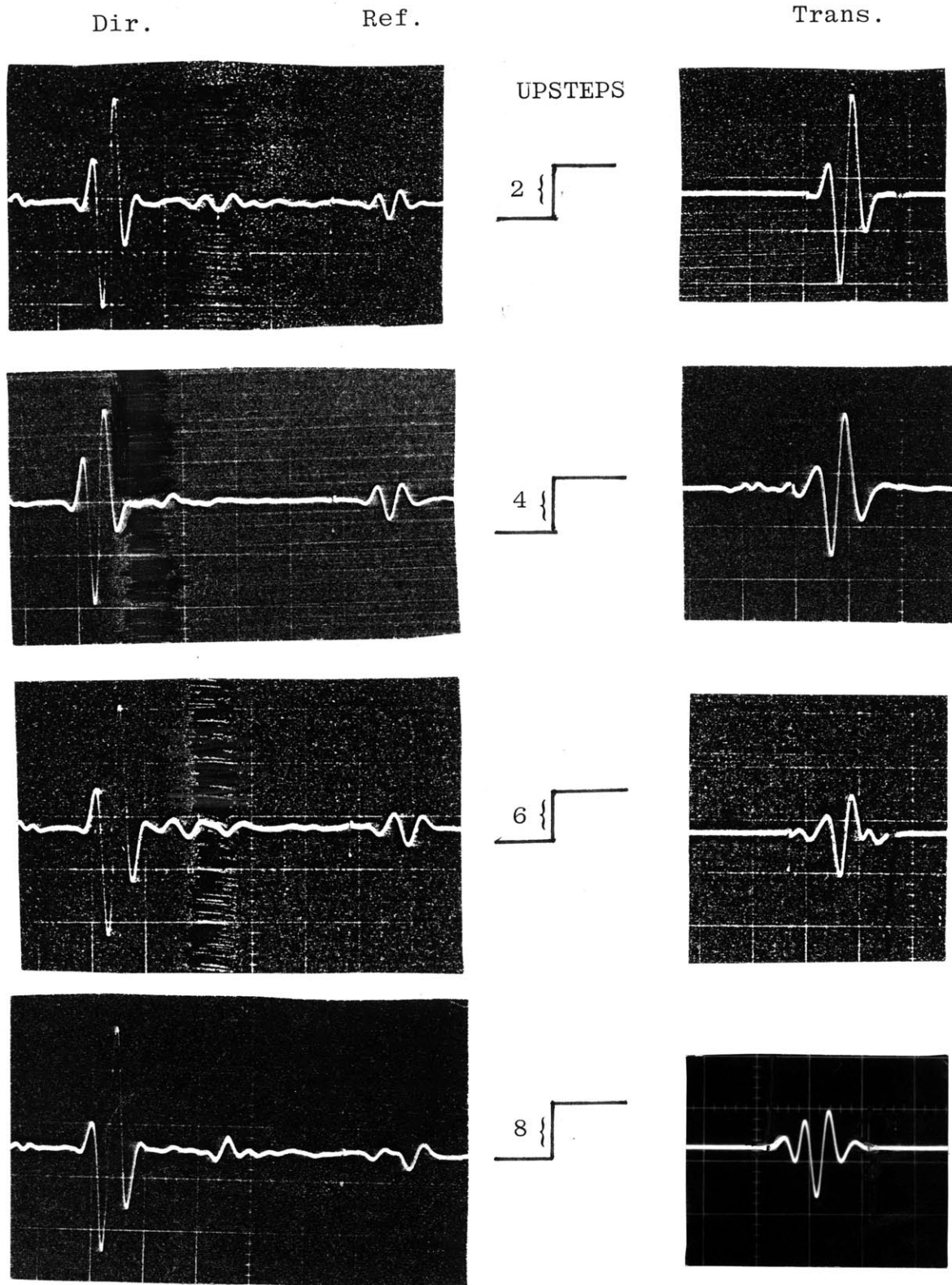


Figure 24a.

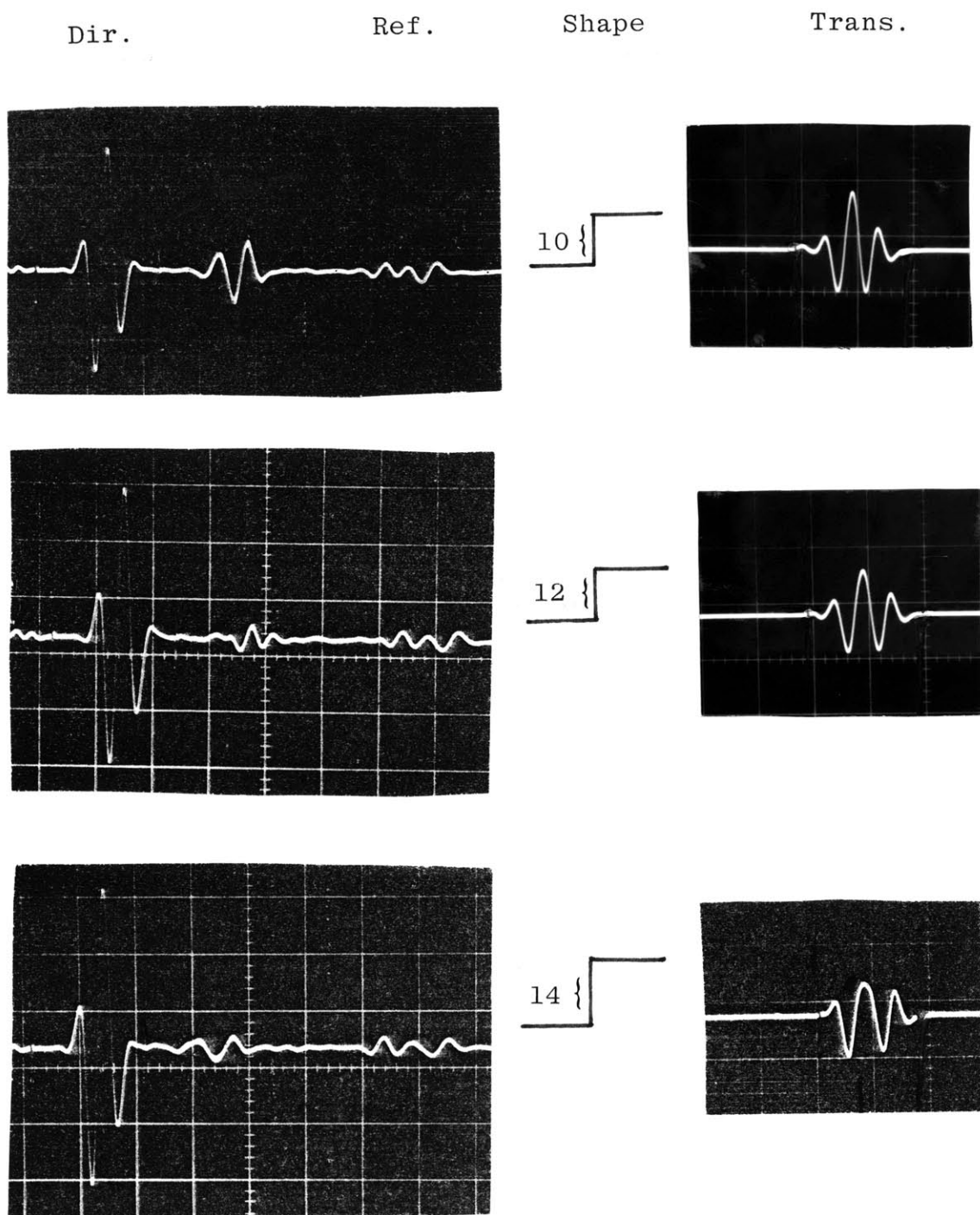


Figure 24b.

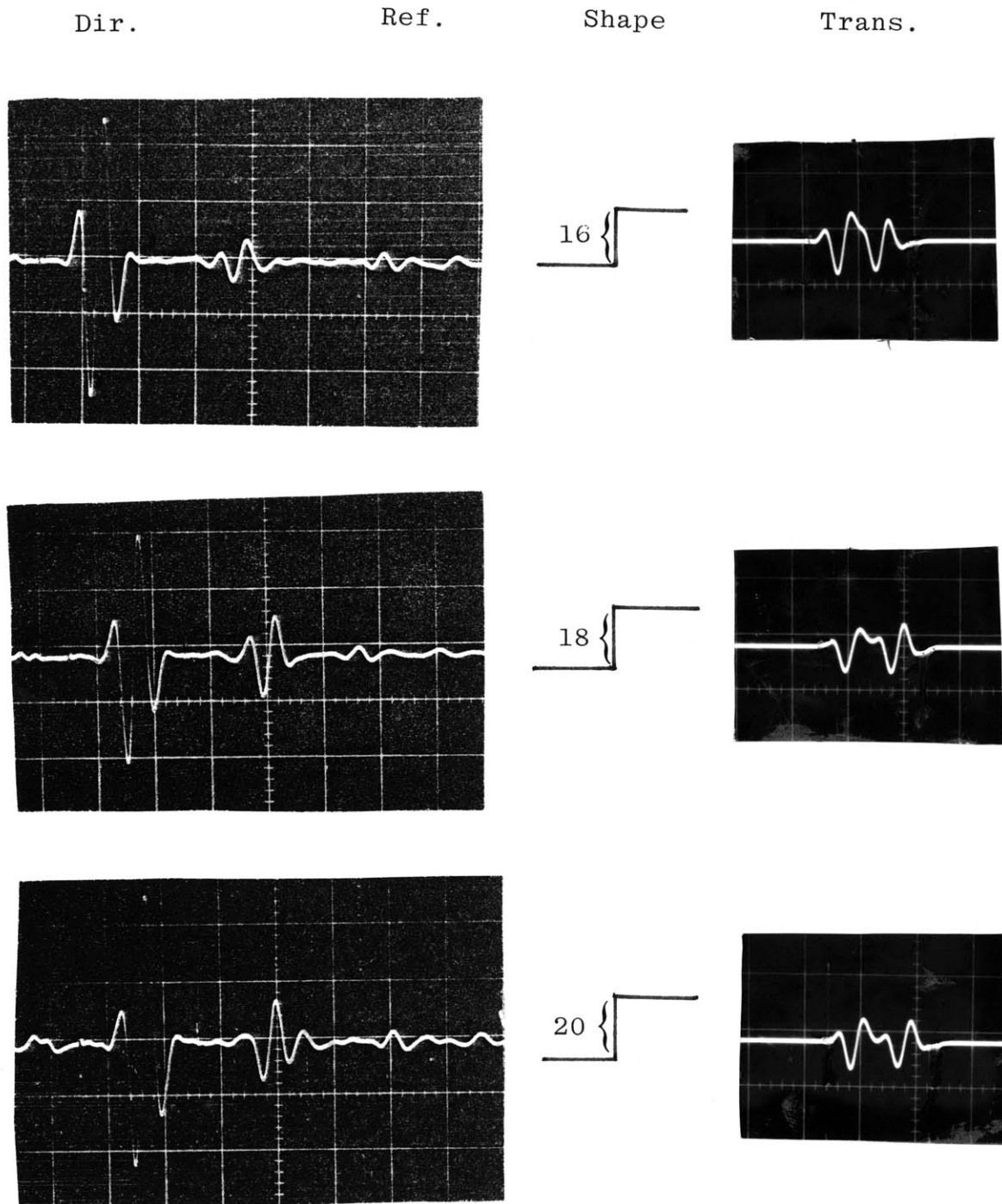


Figure 24c.

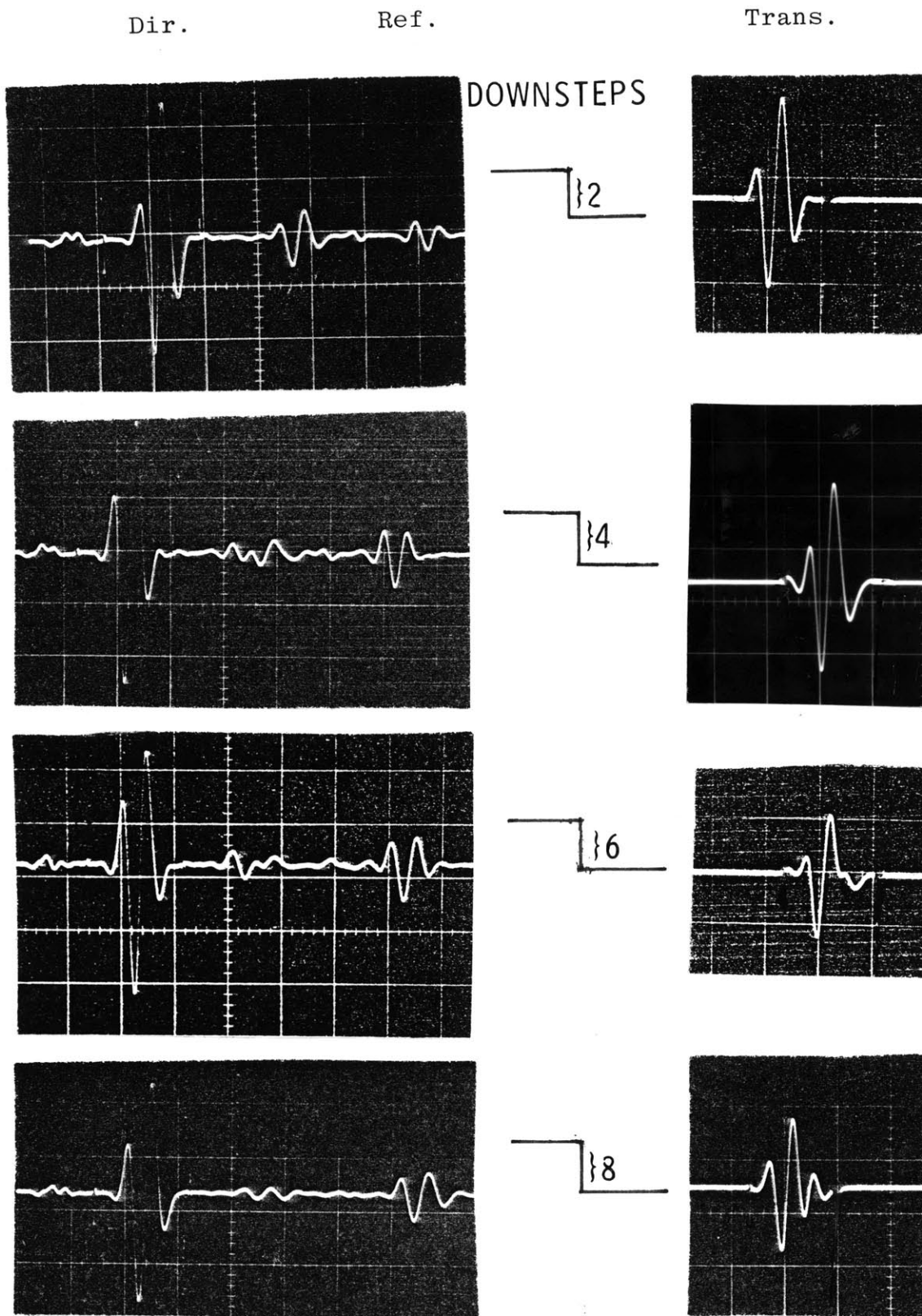


Figure 25a.

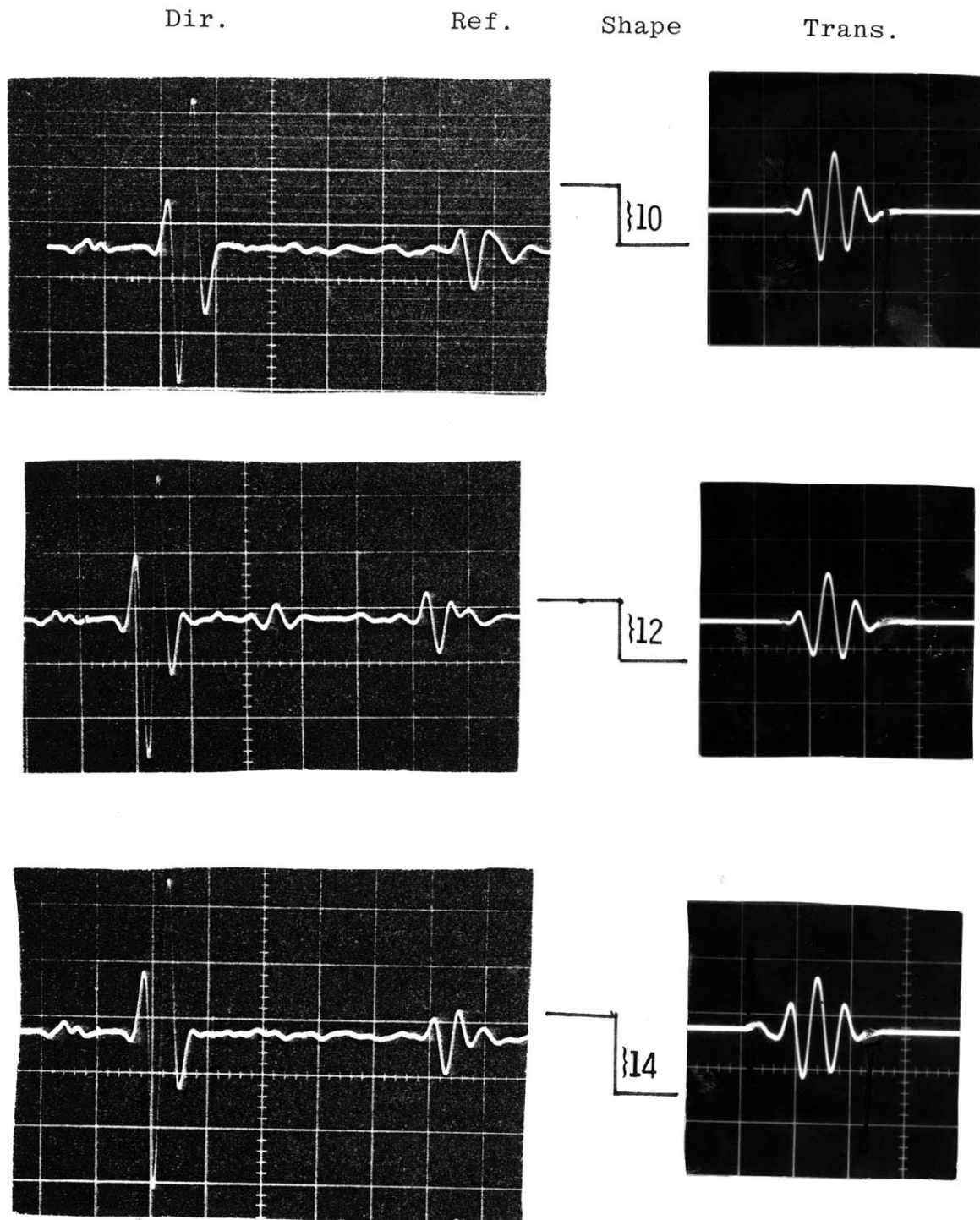


Figure 25b.

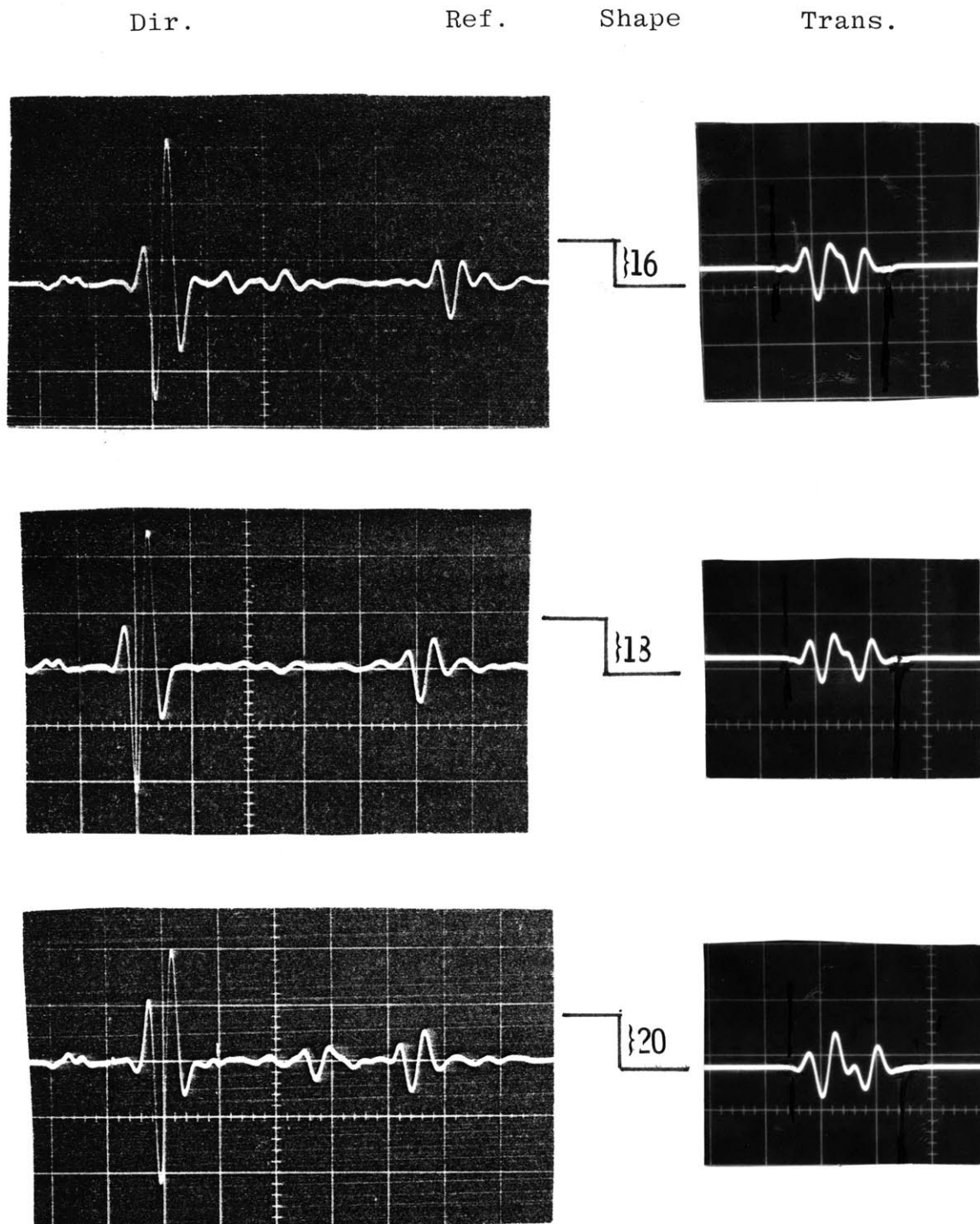


Figure 25c.

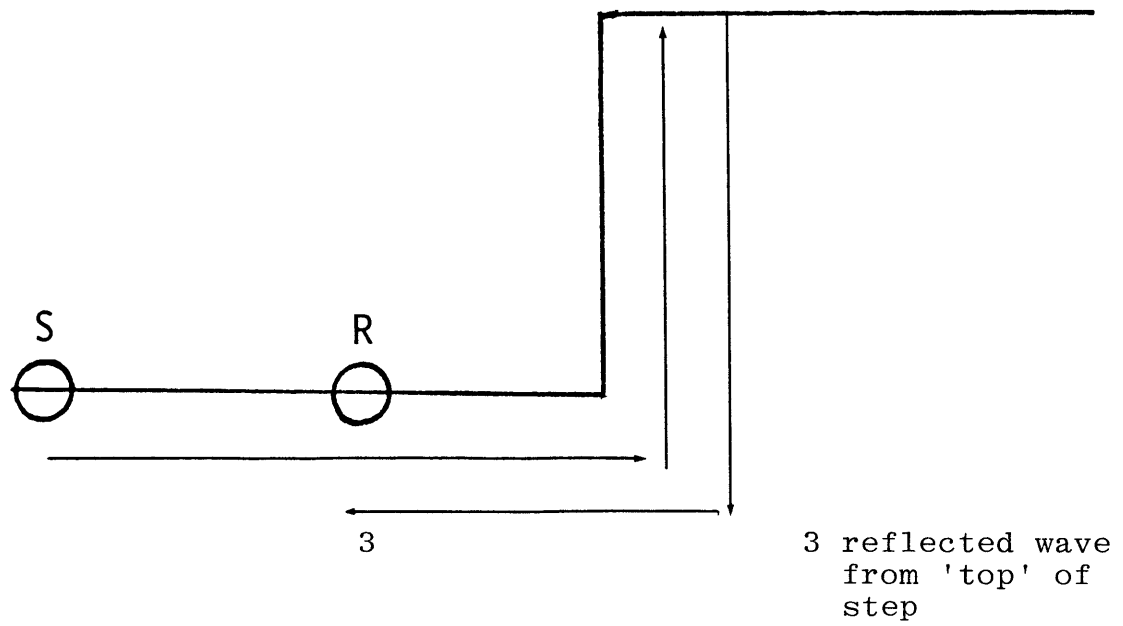
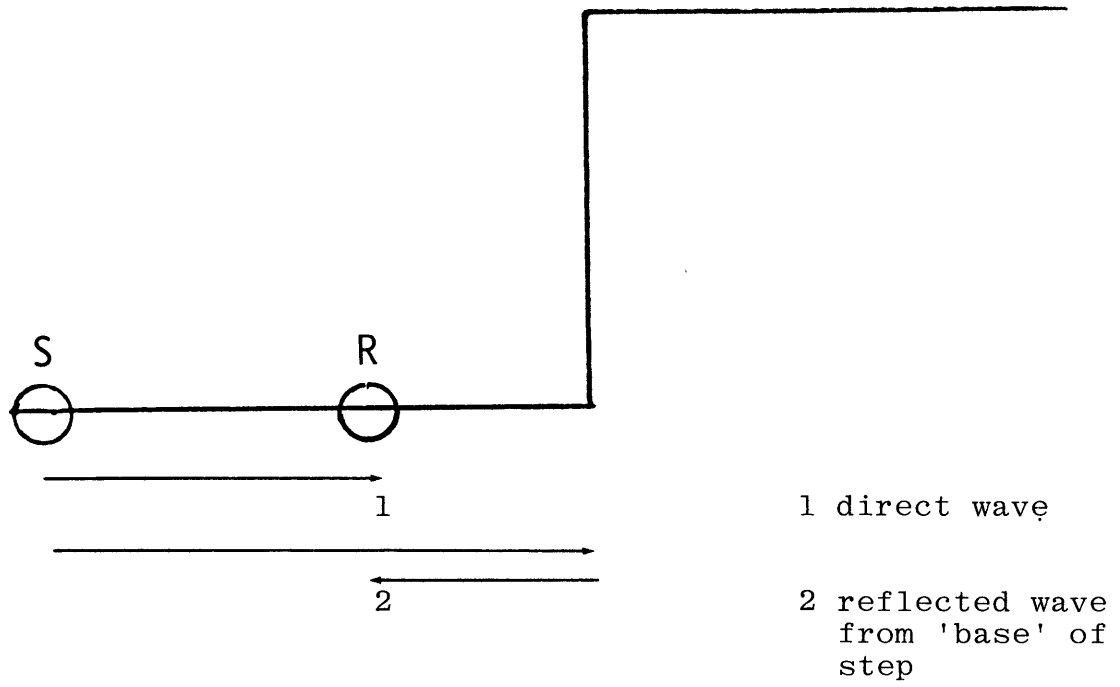


Figure 26



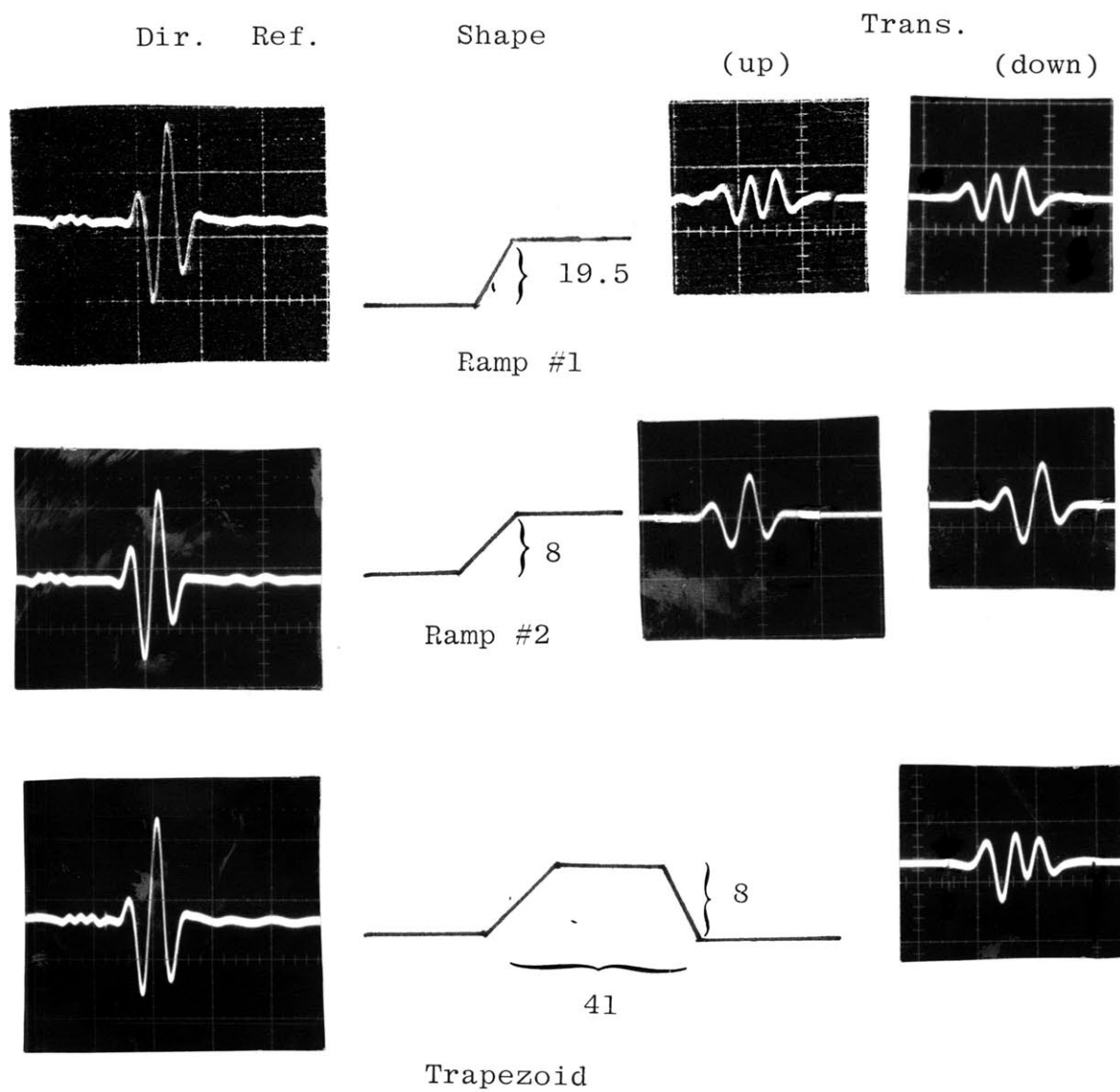


Figure 27.

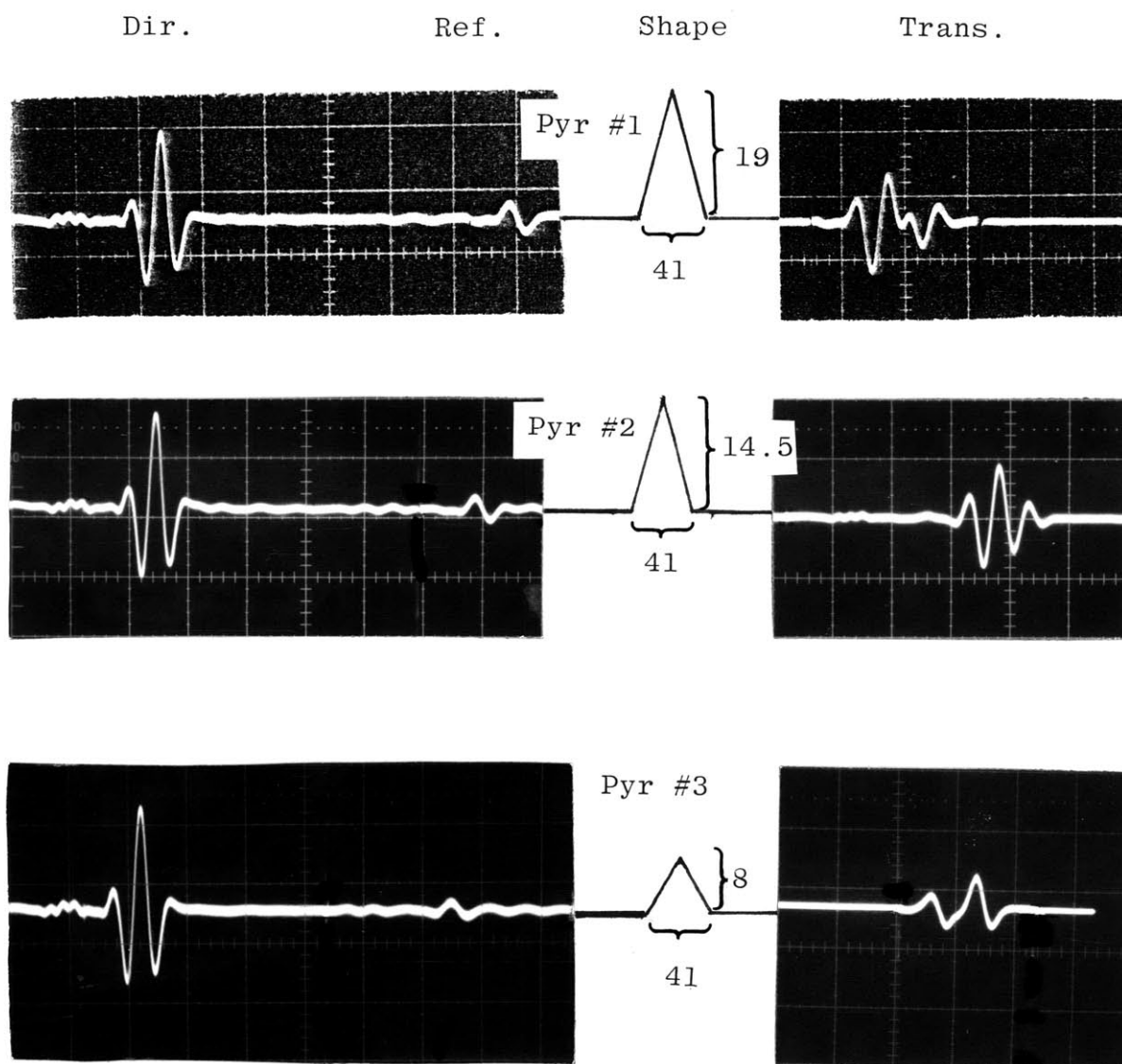


Figure 28.

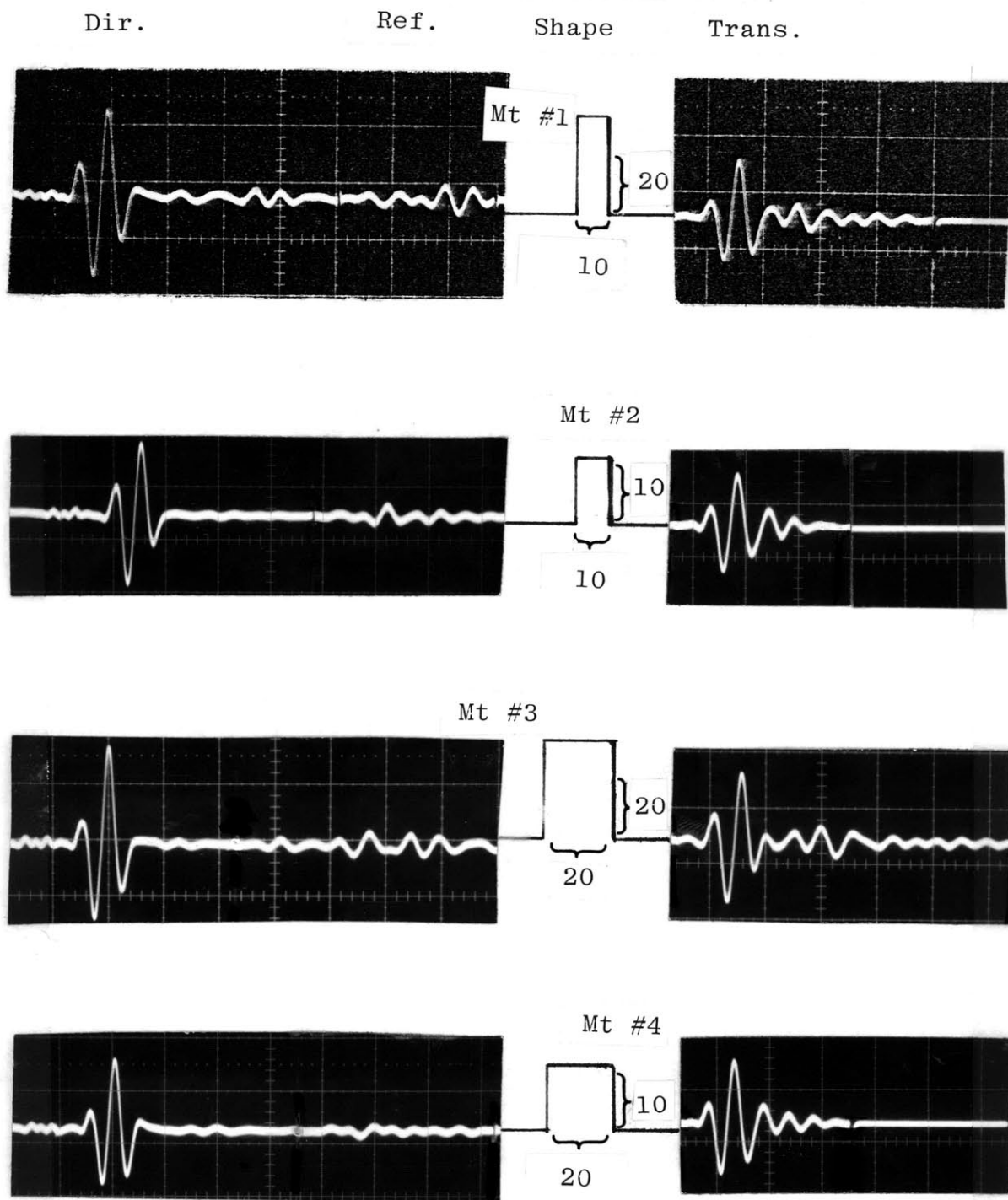


Fig. 29a

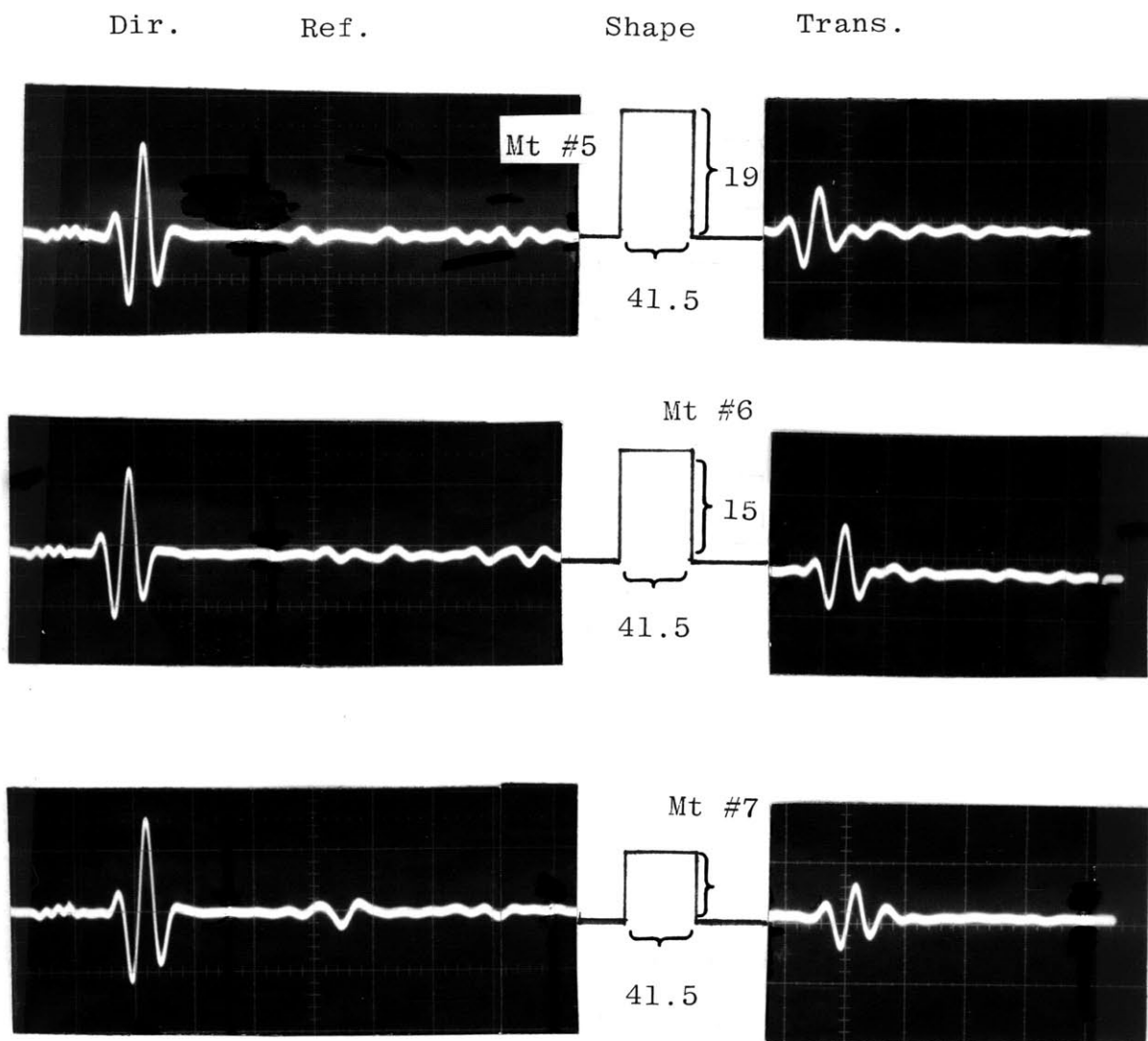


Fig. 29b

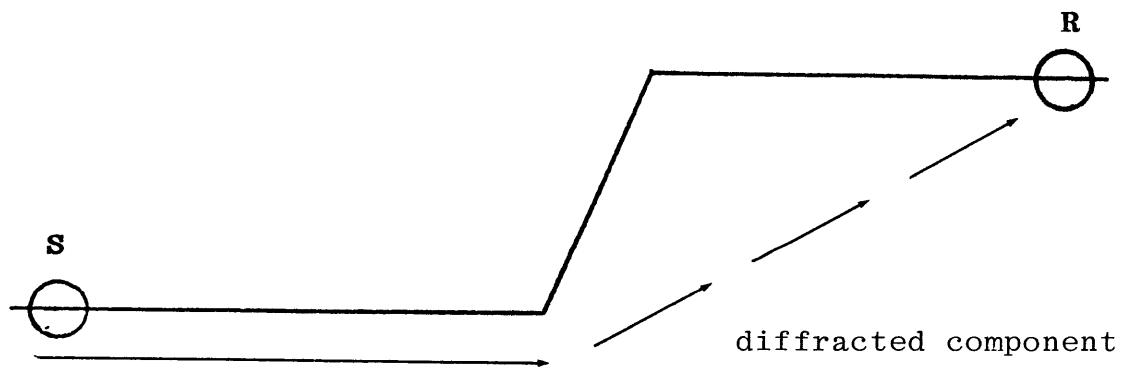
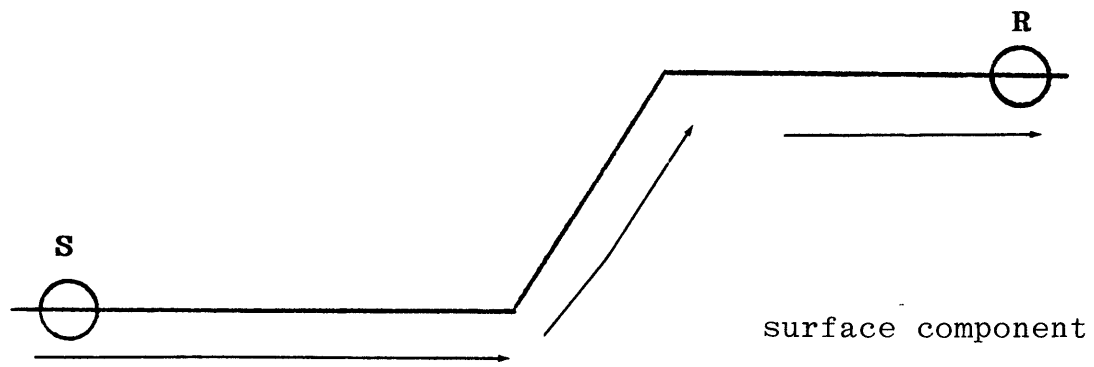
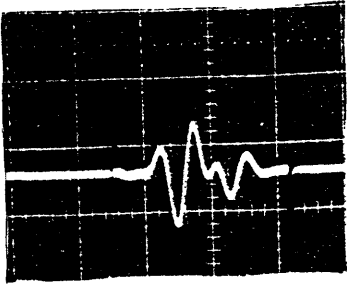
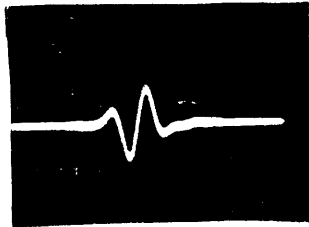
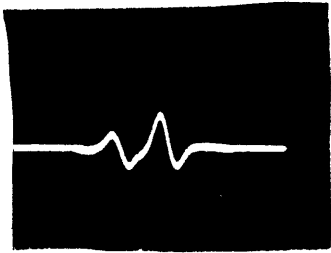
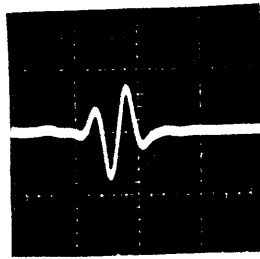
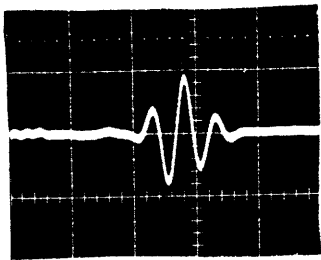
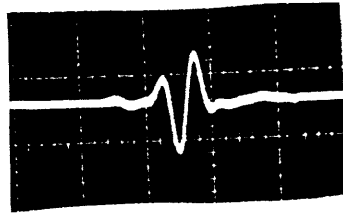


Figure 30

complete trans-  
mitted wave



converted component

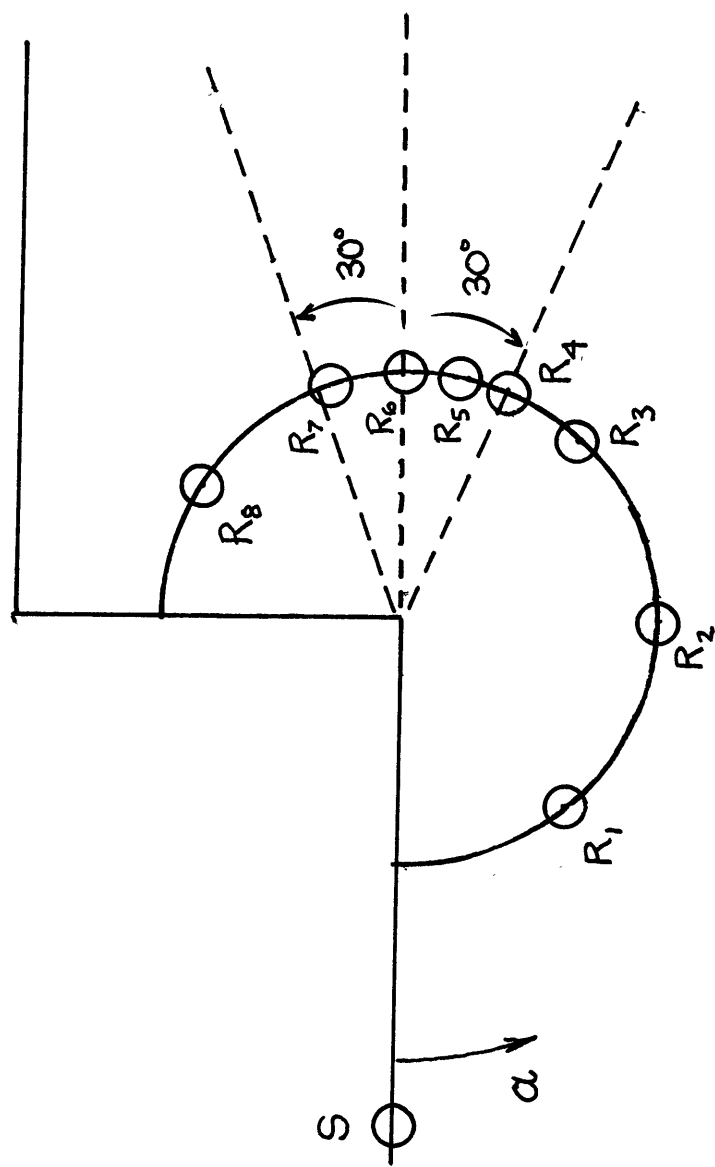


path of  
converted  
component



path of  
surface  
component

Figure 31.



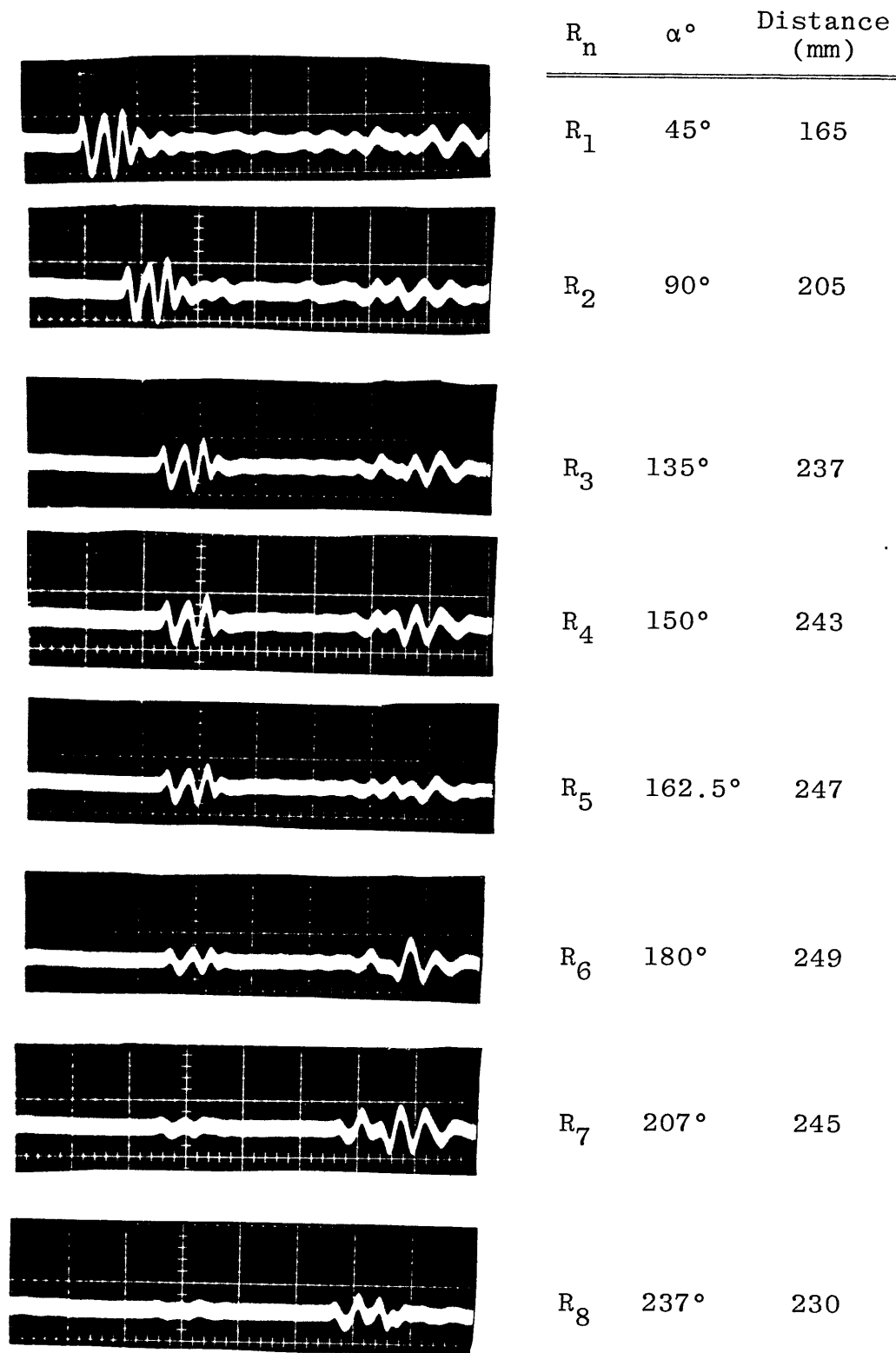


Figure 32b.



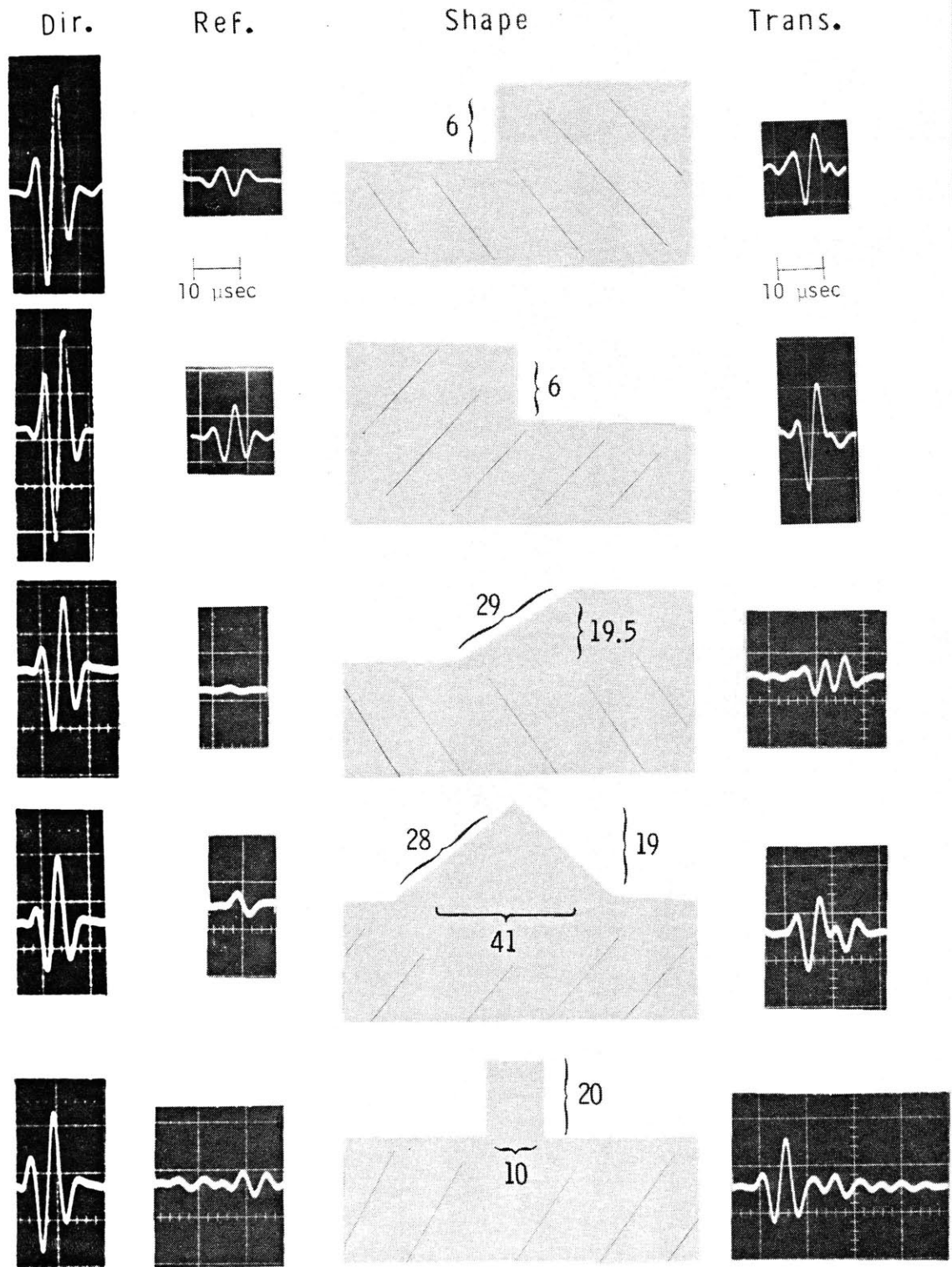


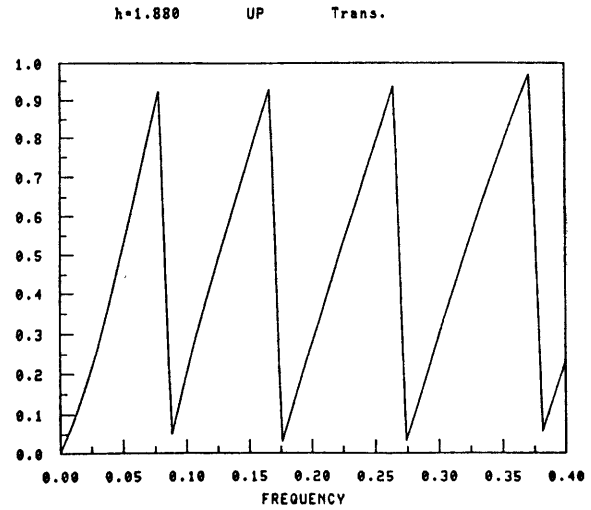
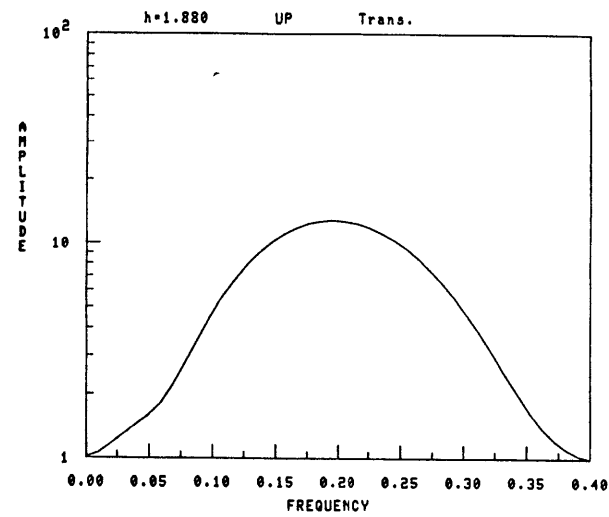
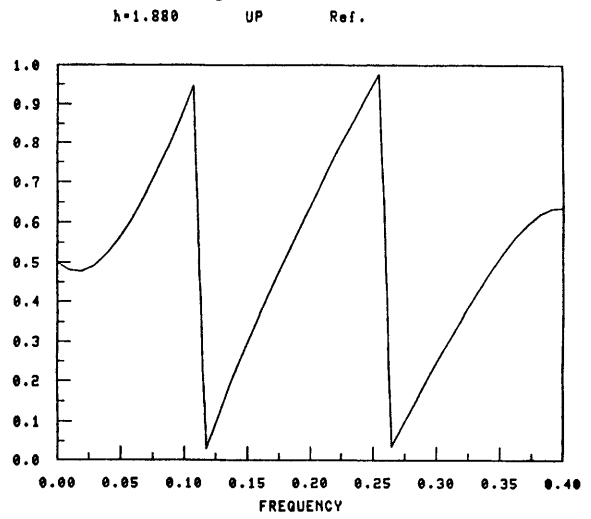
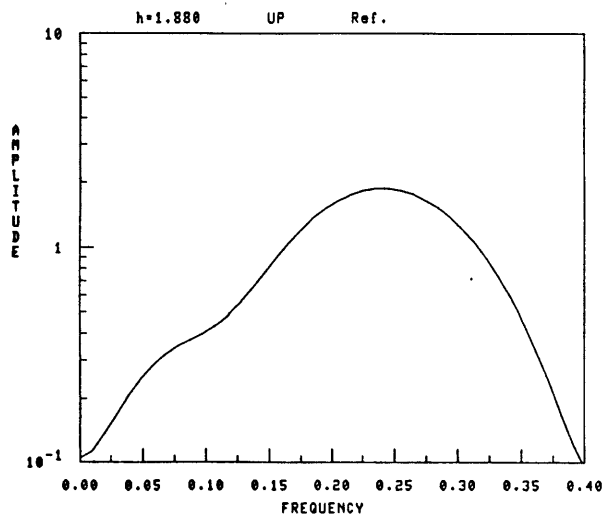
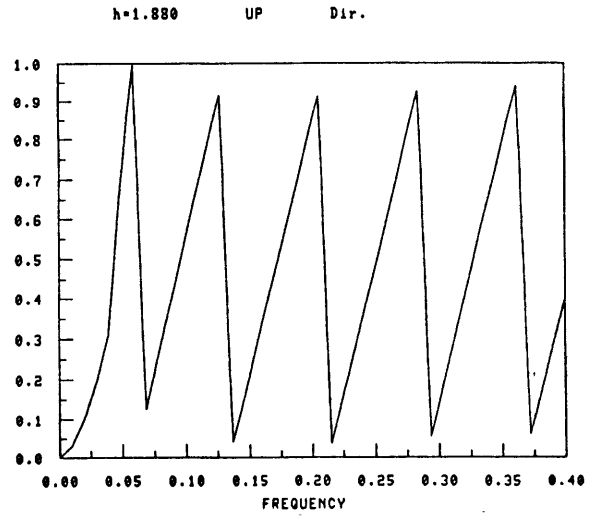
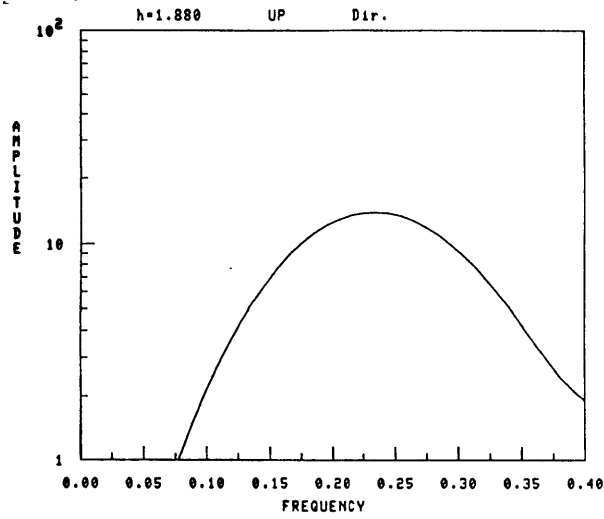
Figure 33.

## LIST OF SYMBOLS AND ABBREVIATIONS

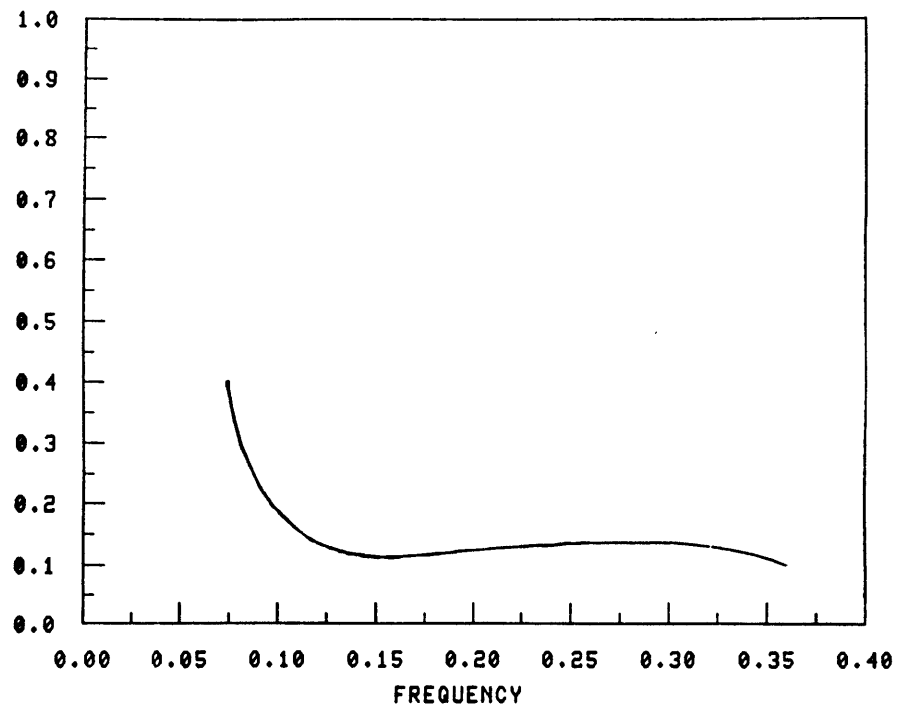
c	Rayleigh wave velocity
$c_p$	longitudinal body wave velocity
h	step height
f	frequency
$\lambda$	wavelength
R	reflection coefficient
T	transmission coefficient
Dir.	direct (incident wave)
Ref.	reflected wave
Trans.	transmitted wave
Pyr	pyramid feature
Mt	rectangular mountain feature
Trap.	trapezoid feature

## APPENDIX A

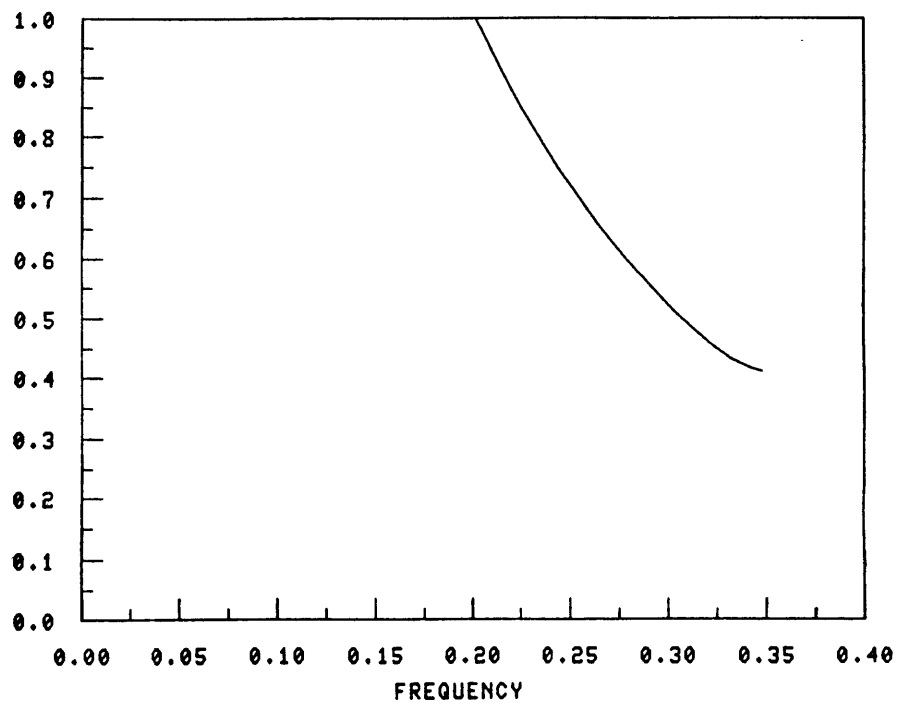
This appendix contains the amplitude and phase spectra plots as well as the reflection and transmission coefficient curves for all of the step discontinuities. (The amplitude spectra are displayed in the left column and the phase spectra are in the right column.) The seismograms were digitized and then the plots were generated by computer. The Amplitude scale is in arbitrary units. The relative amplitude for each set (direct, reflected, and transmitted) represents the correct values. The phase spectra are shown in fractions of a cycle. The units on the frequency axis are MHz.

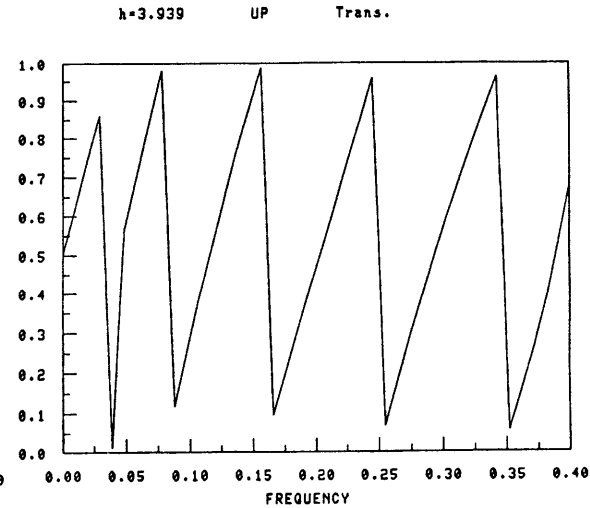
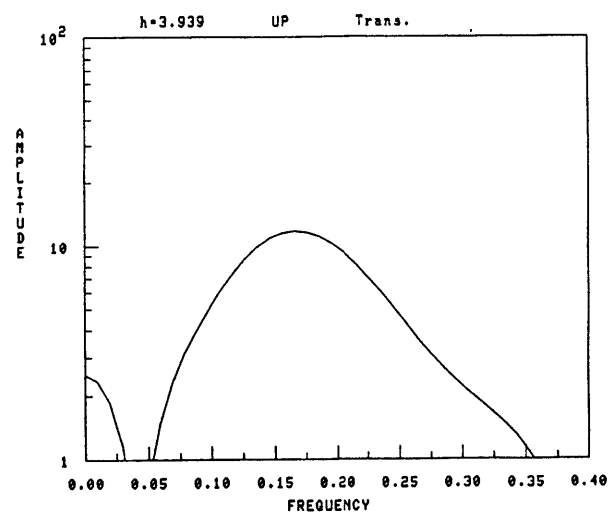
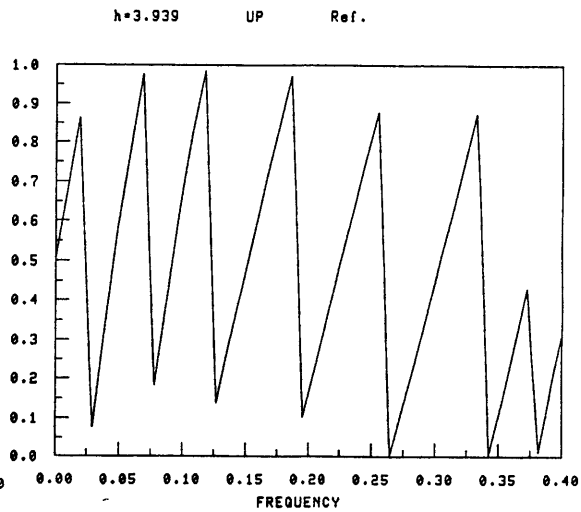
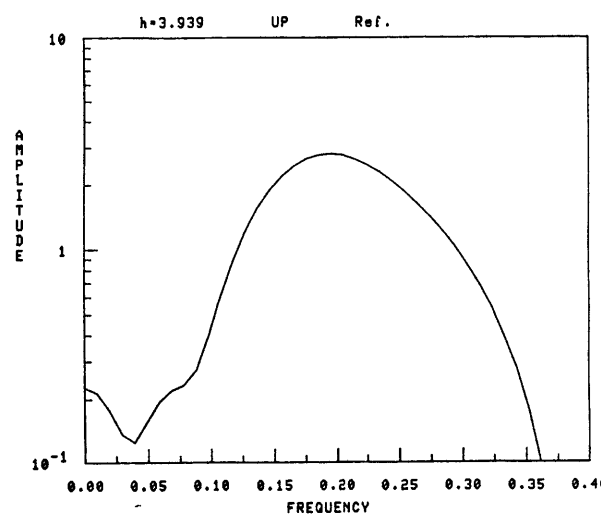
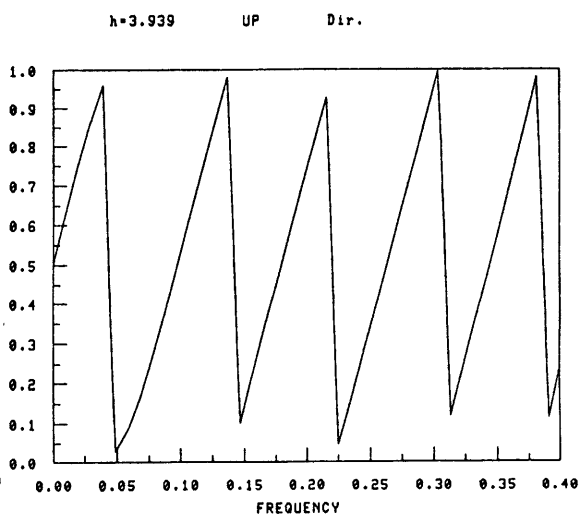
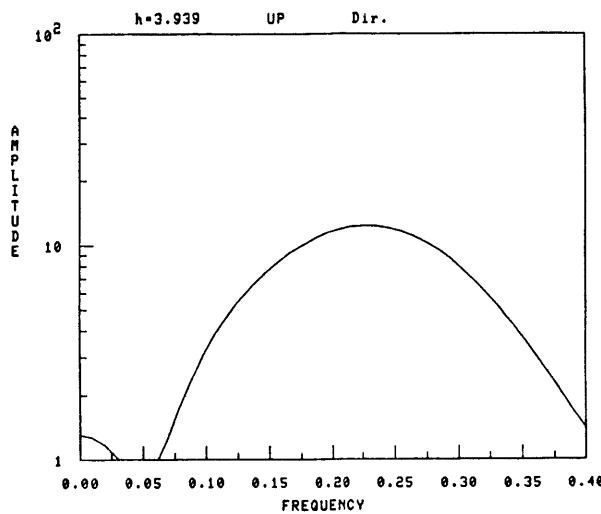


REF. COEFF. (h=1.880 UP)

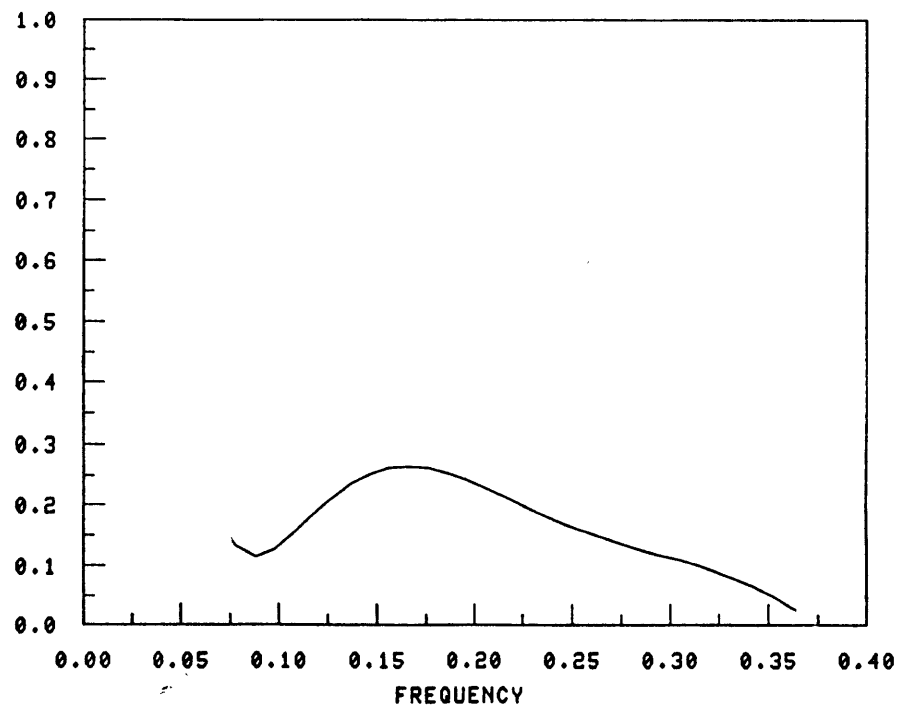


TRANS. COEFF. (h=1.880 UP)

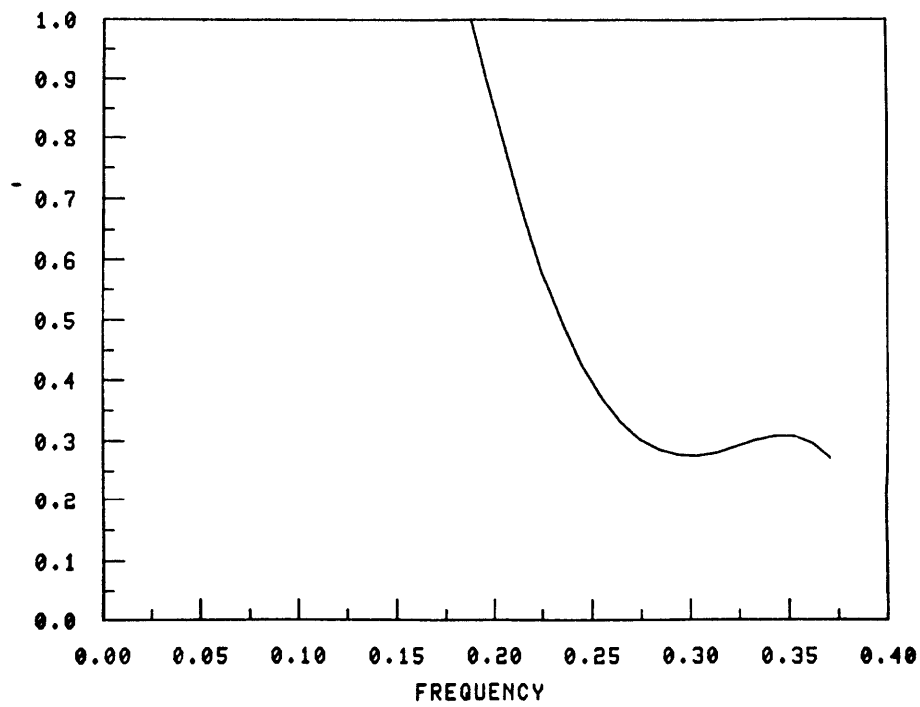


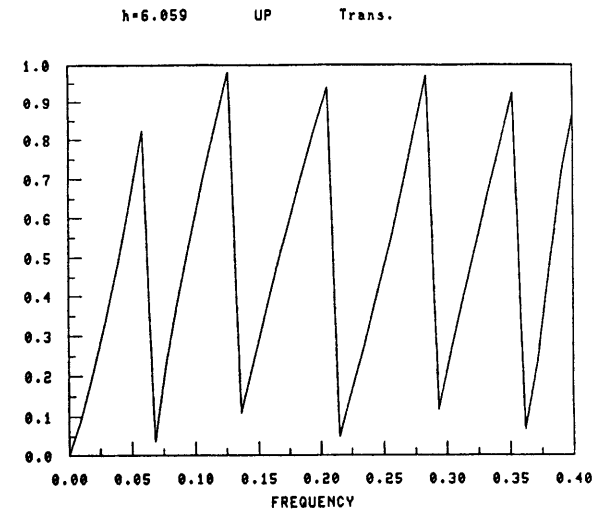
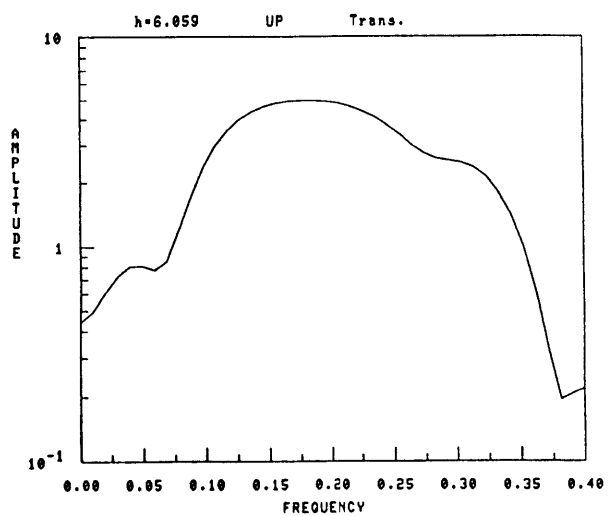
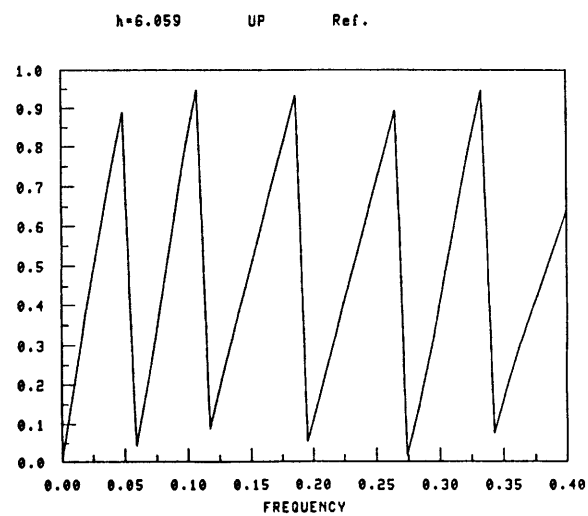
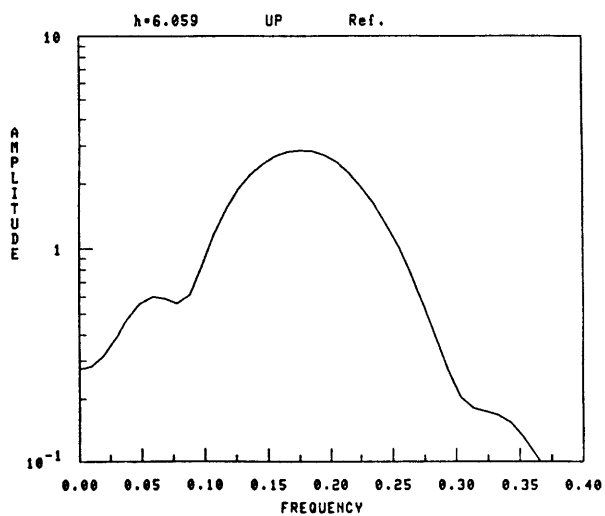
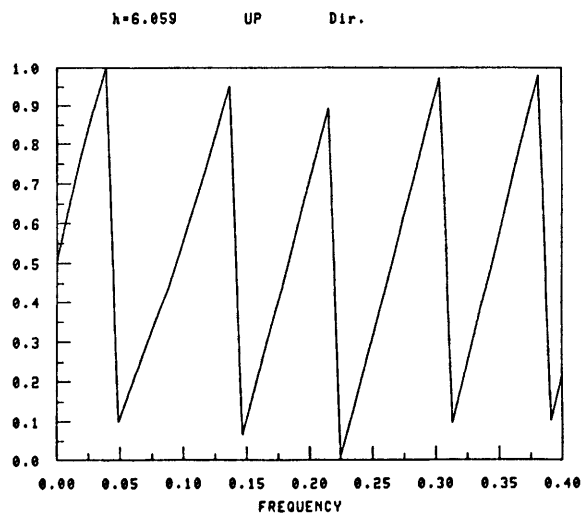
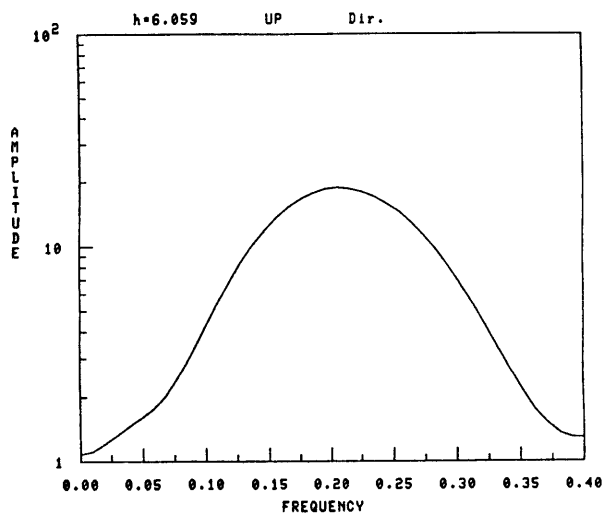


REF. COEFF. (h=3.939 UP)



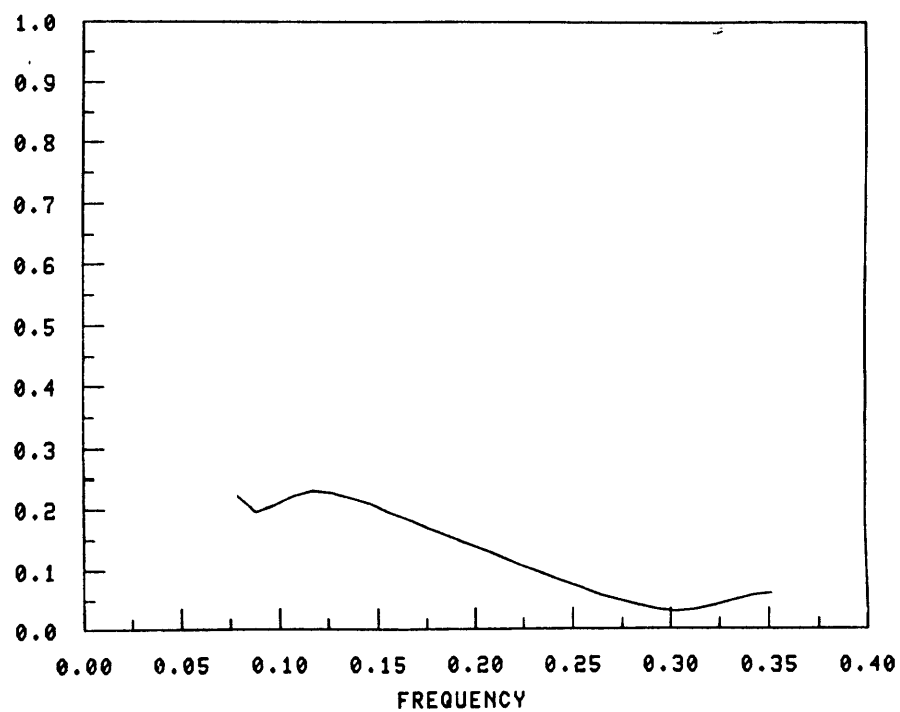
TRANS. COEFF. (h=3.939 UP)



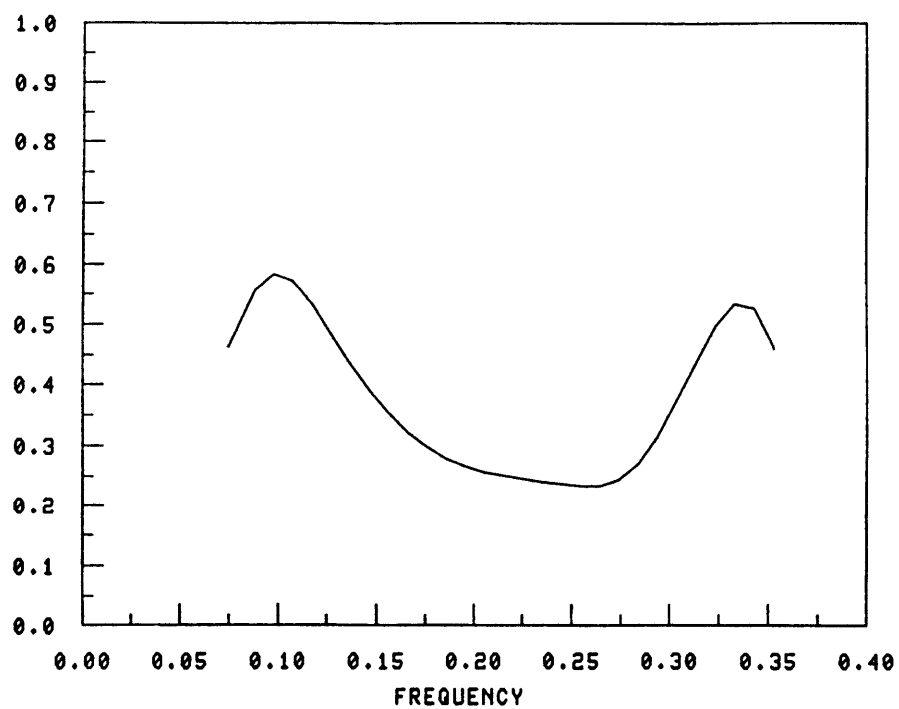


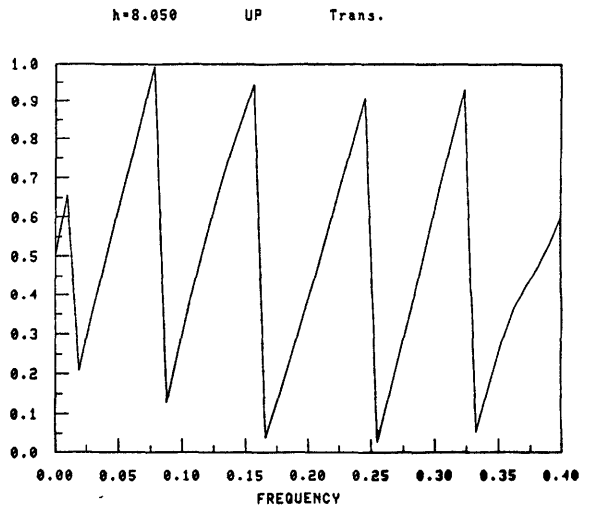
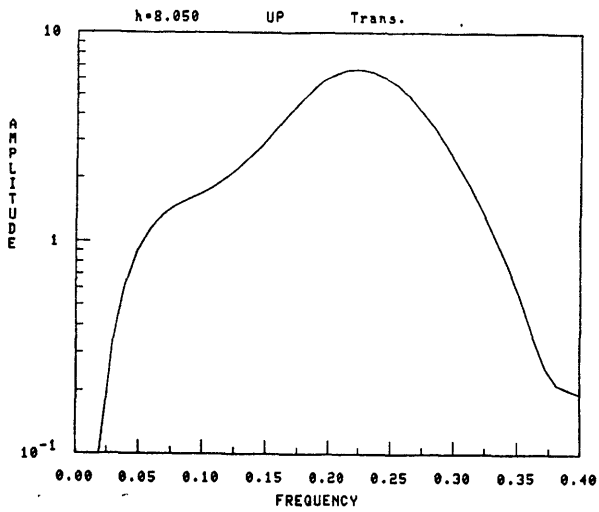
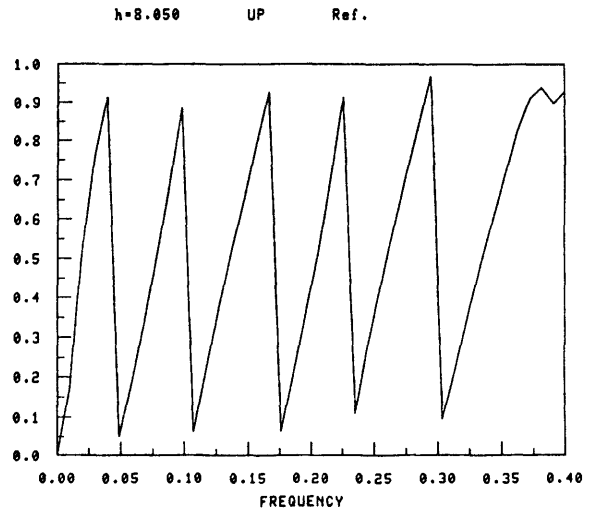
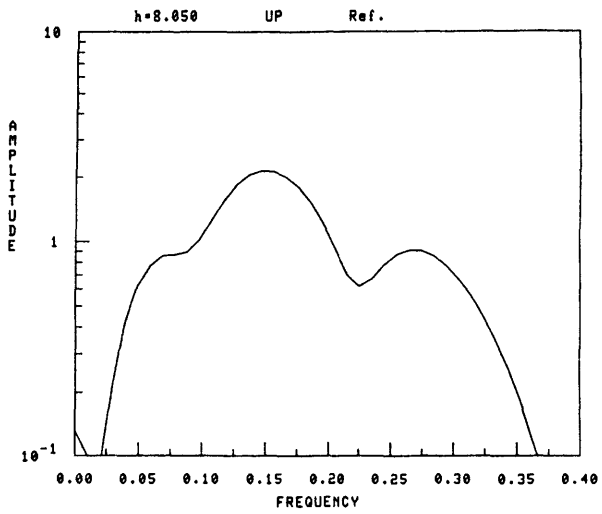
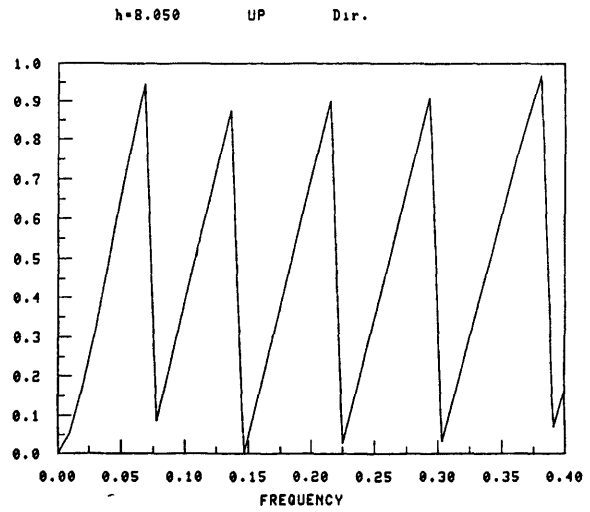
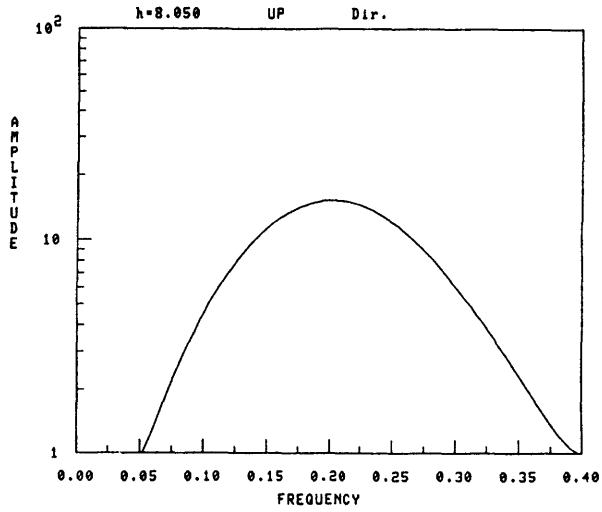


REF. COEFF. (h=6.059 UP)

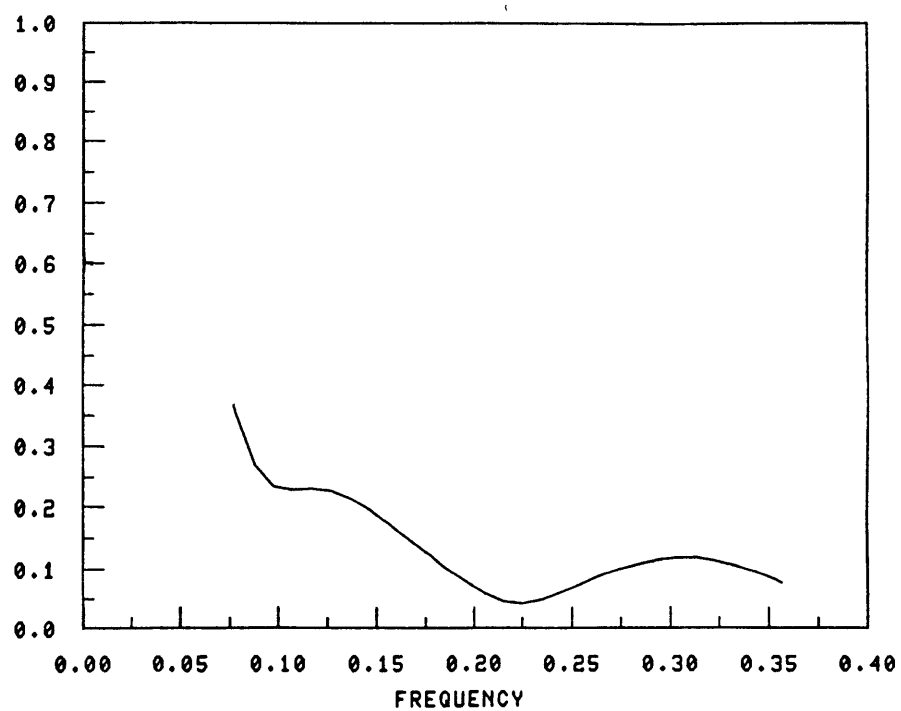


TRANS. COEFF. (h=6.059 UP)

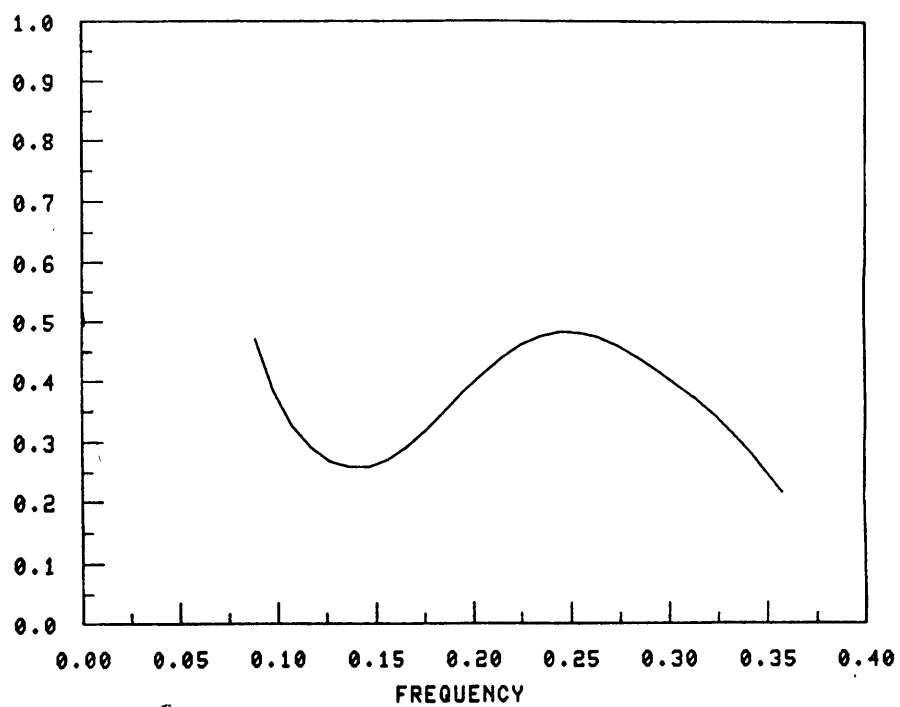


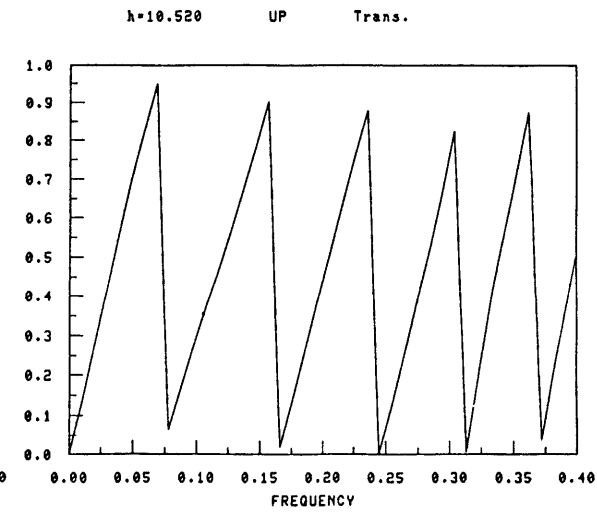
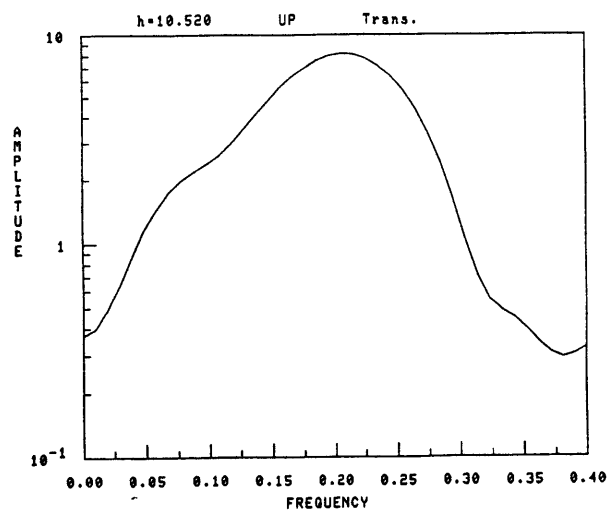
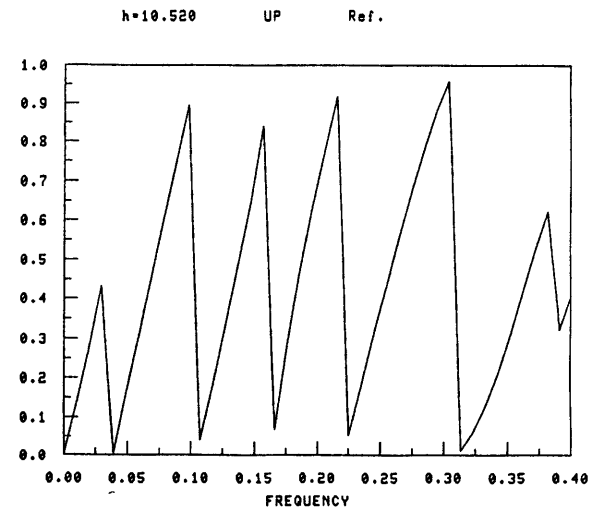
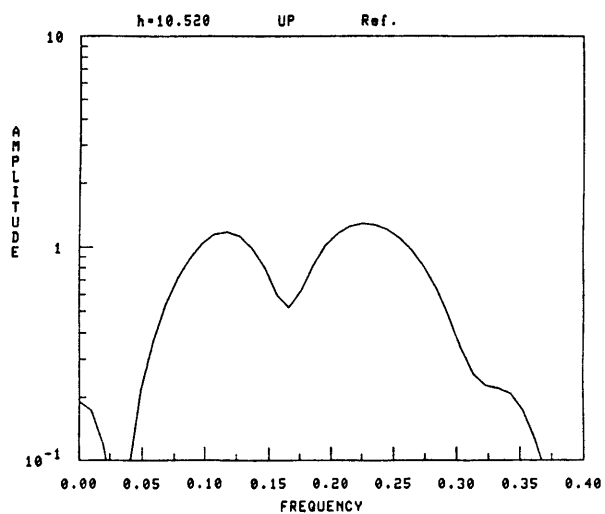
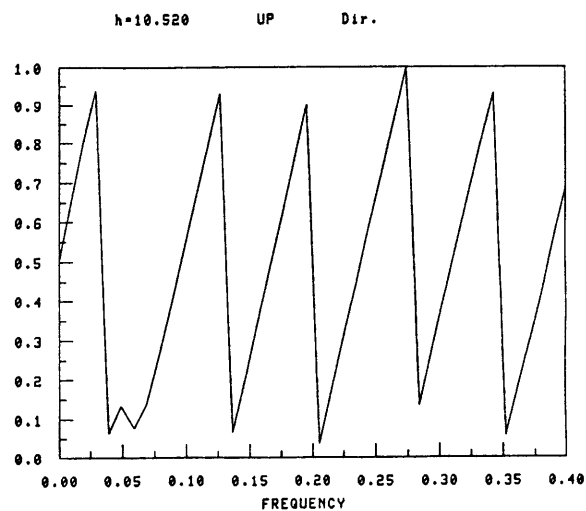
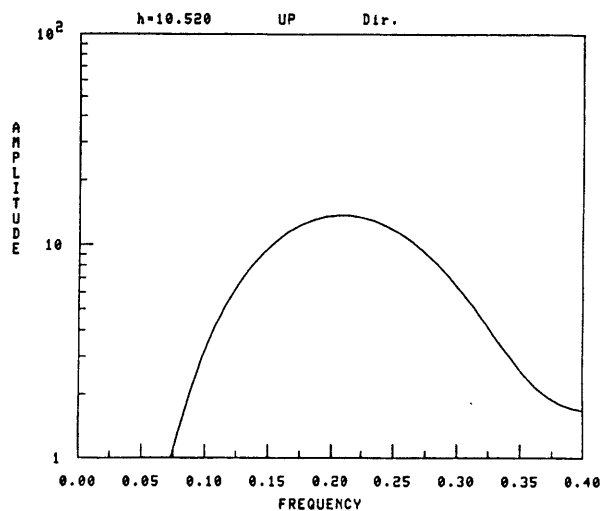


REF. COEFF. (h=8.050 UP)

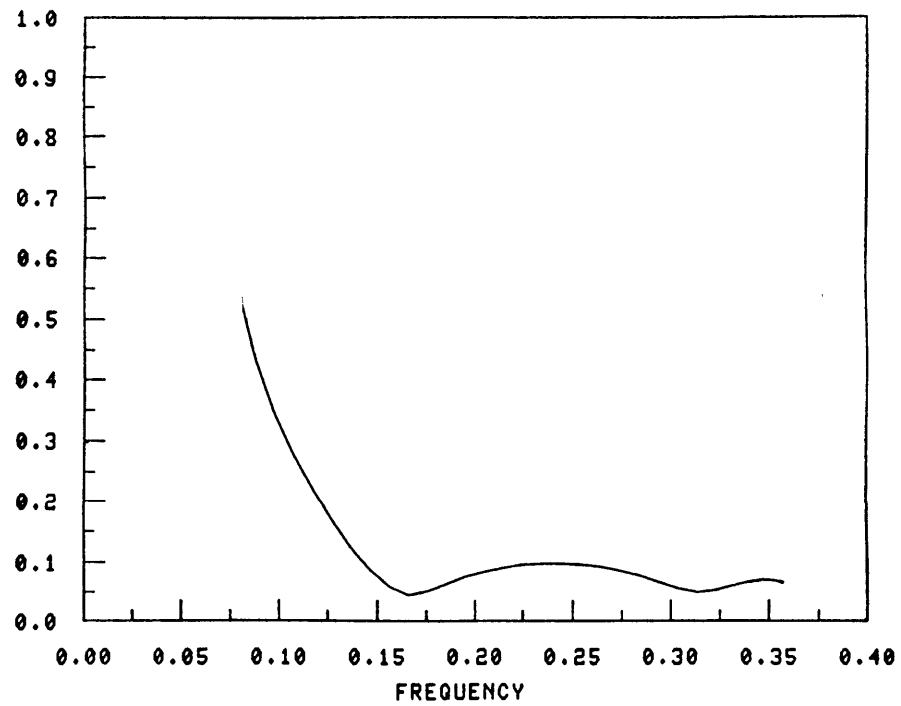


TRANS. COEFF. (h=8.050 UP)

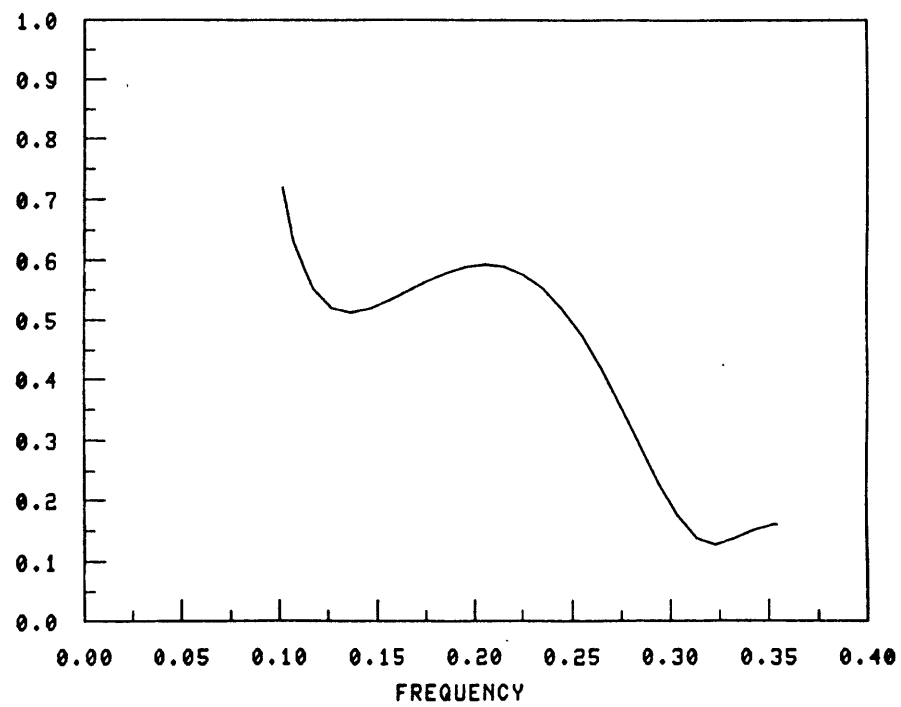


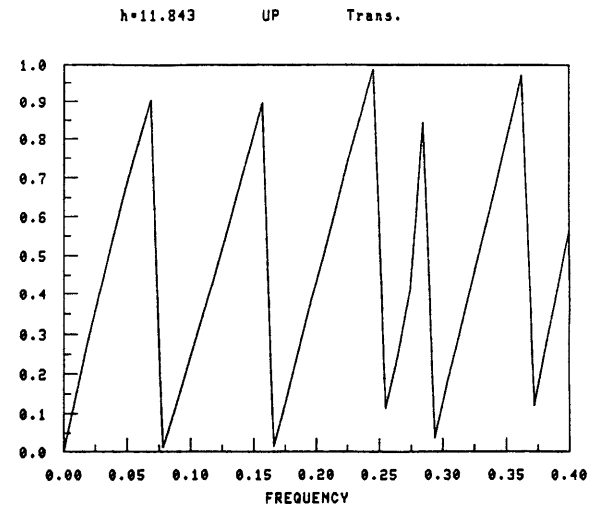
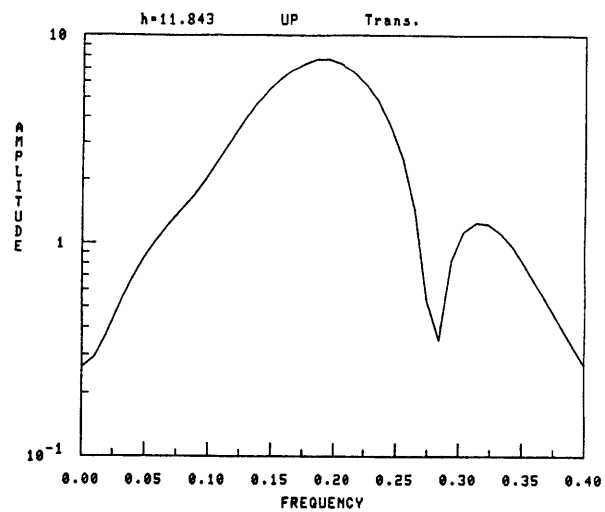
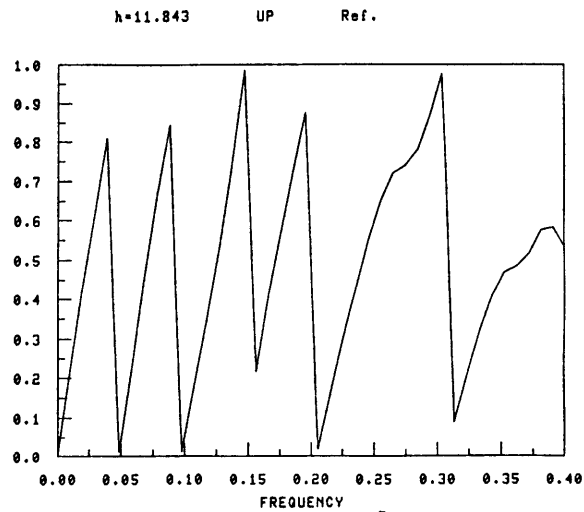
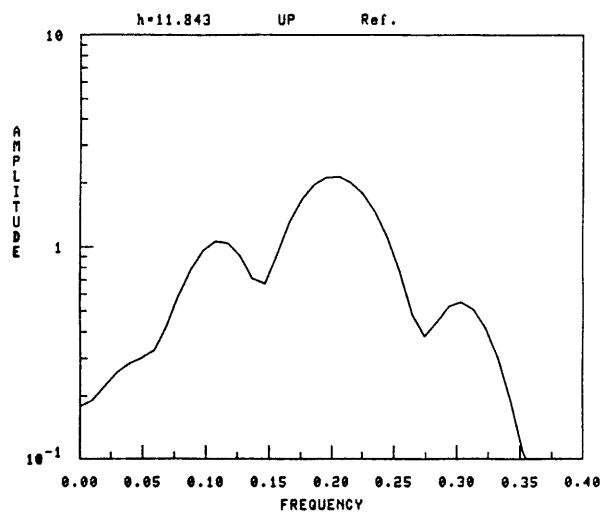
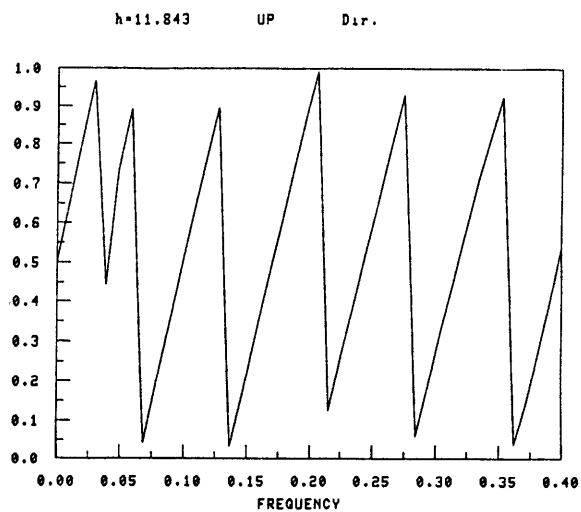
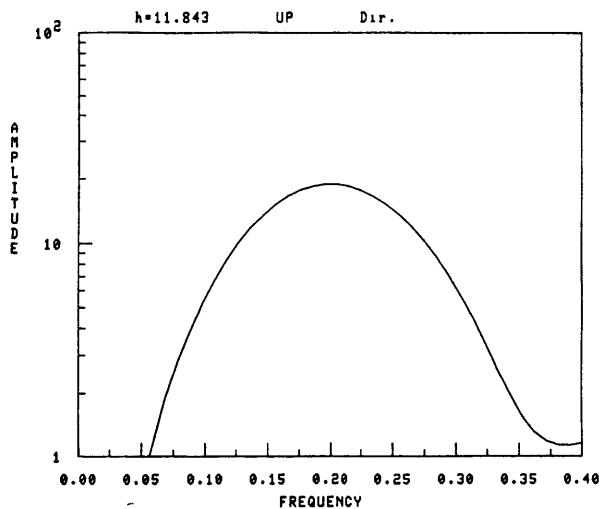


REF. COEFF. (h=10.520 UP)

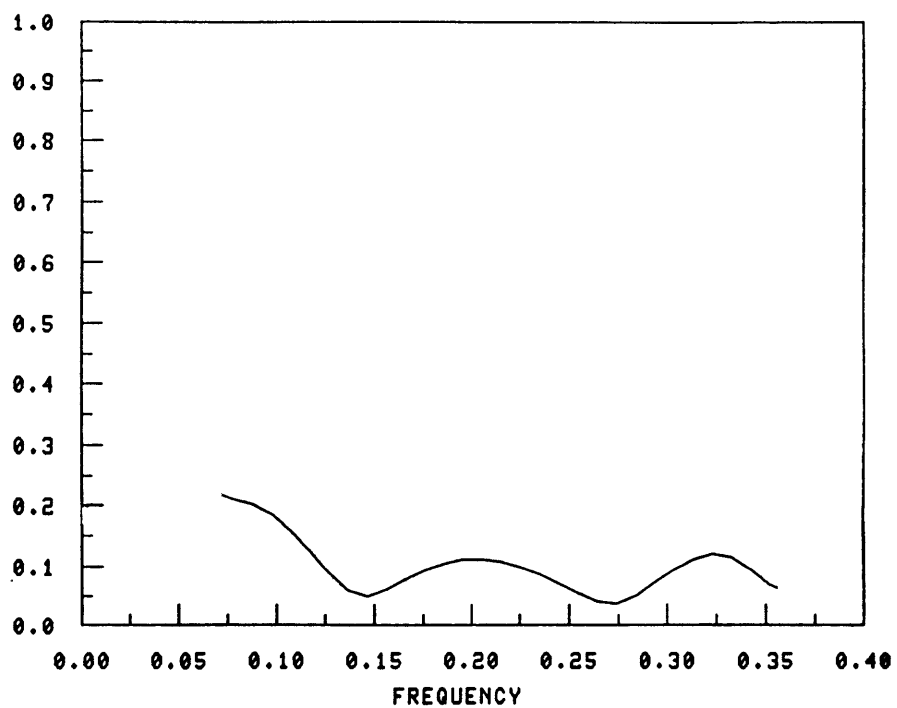


TRANS. COEFF. (h=10.520 UP)

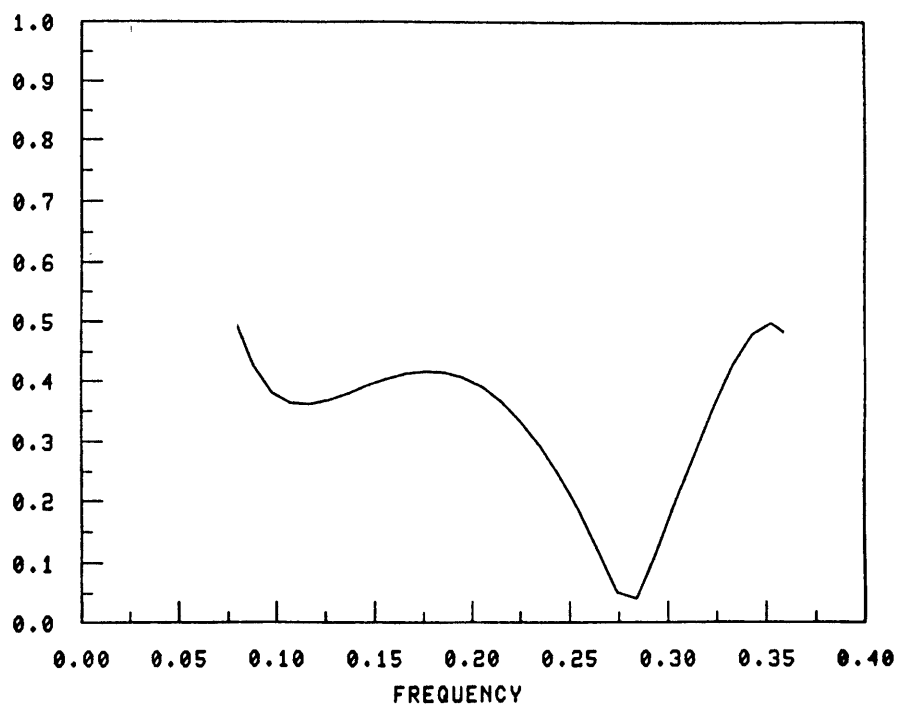


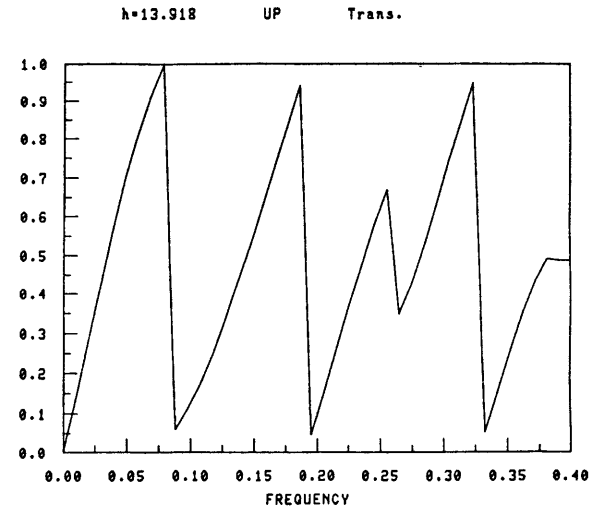
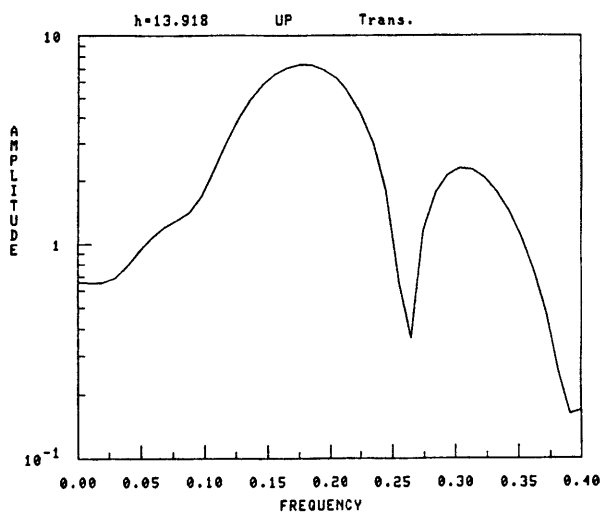
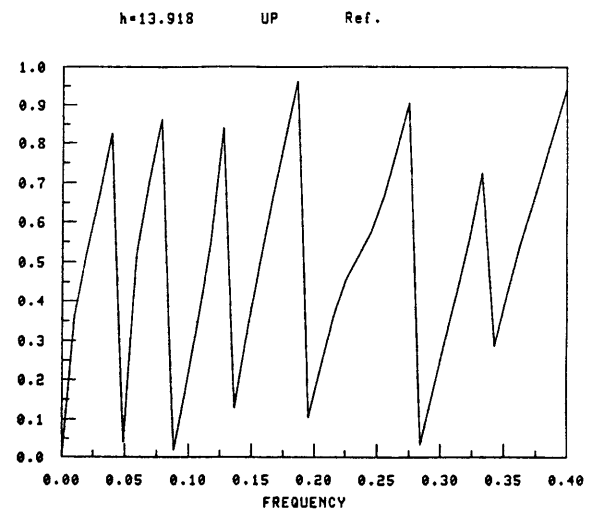
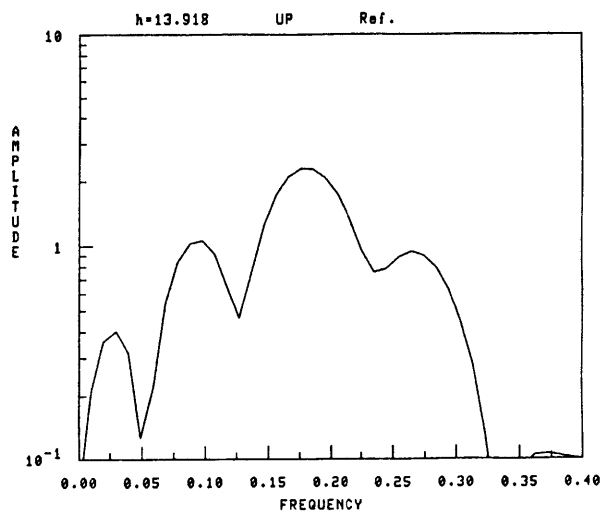
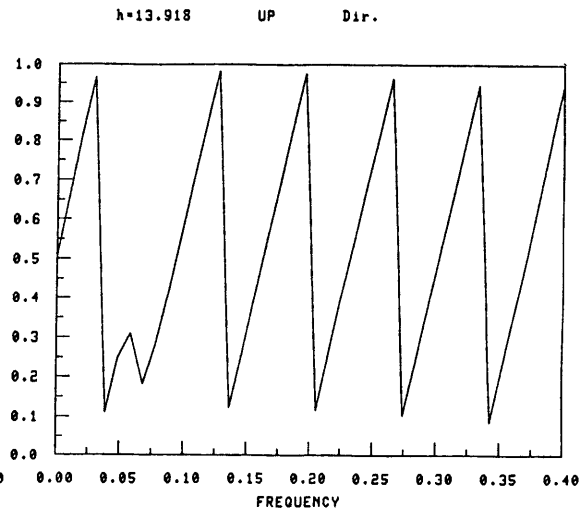
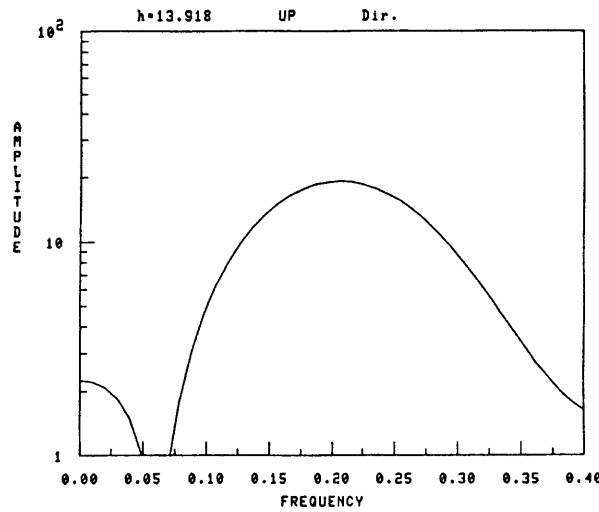


REF. COEFF. (h=11.843 UP)



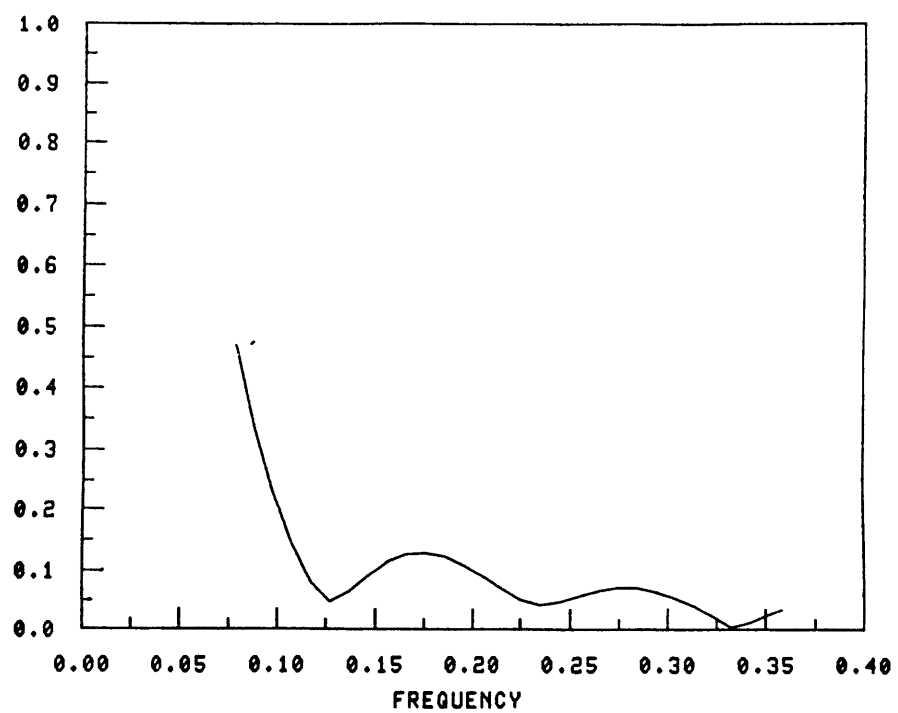
TRANS. COEFF. (h=11.843 UP)



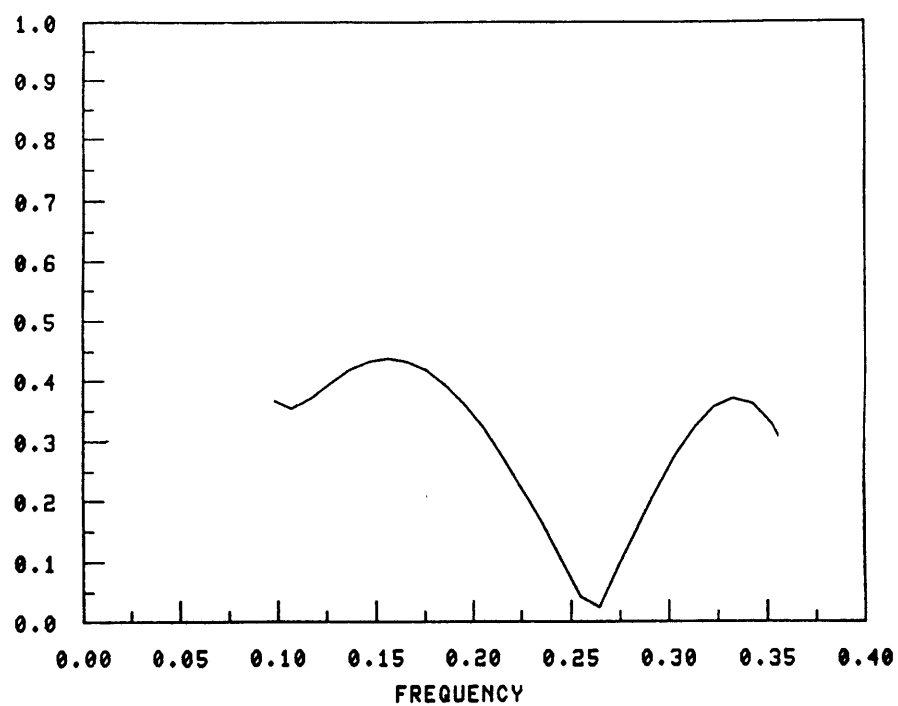


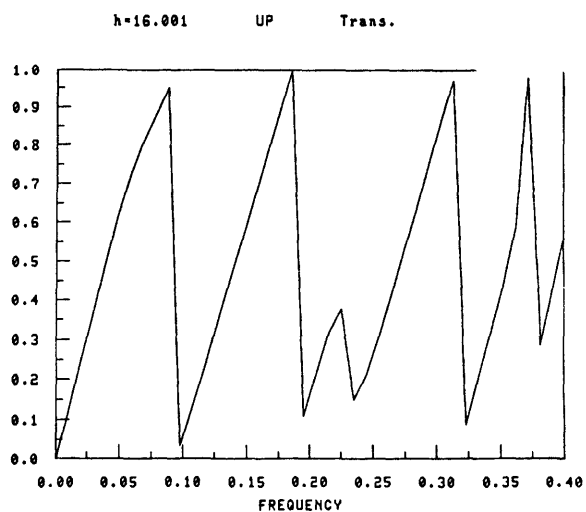
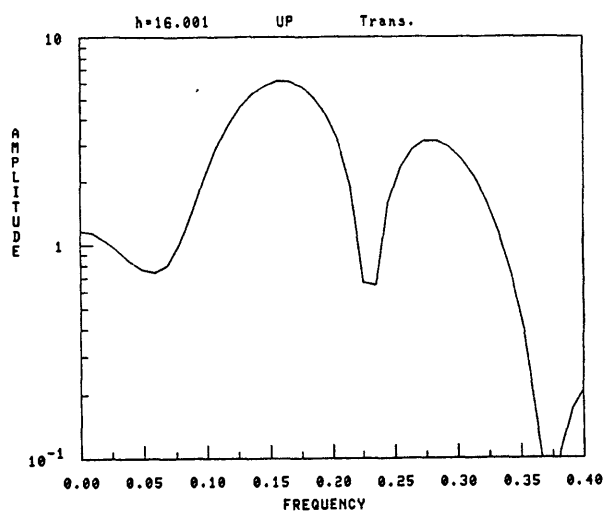
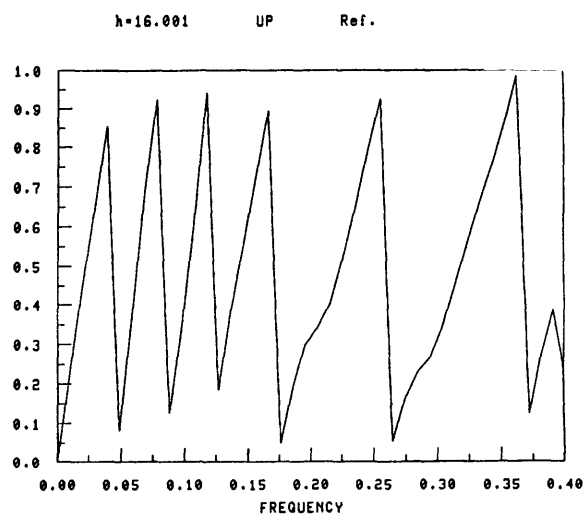
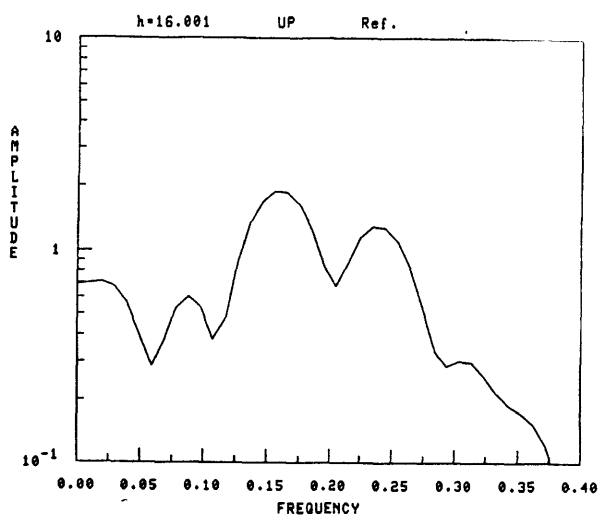
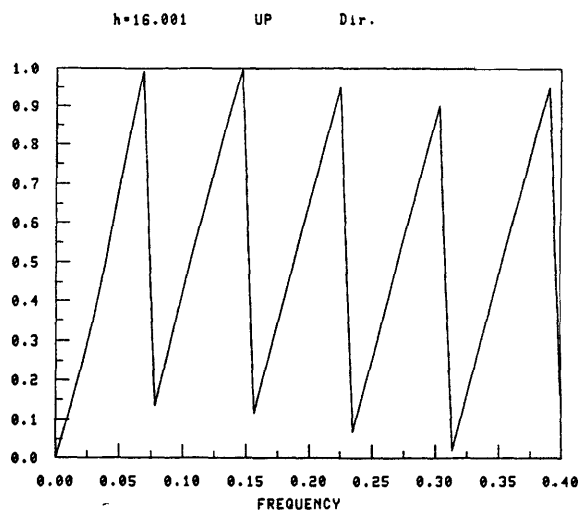
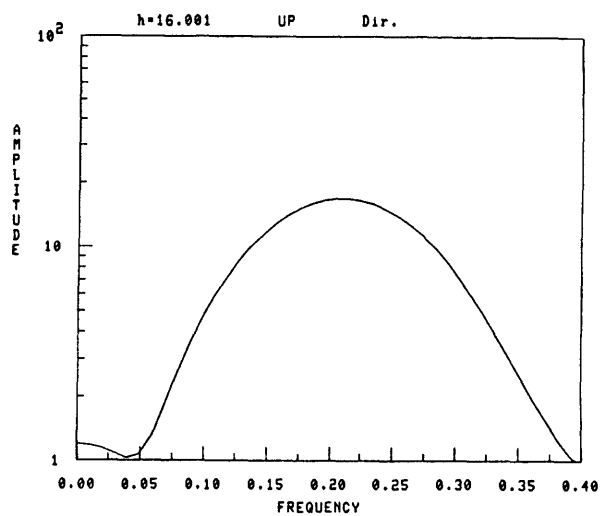


REF. COEFF. (h=13.918 UP)

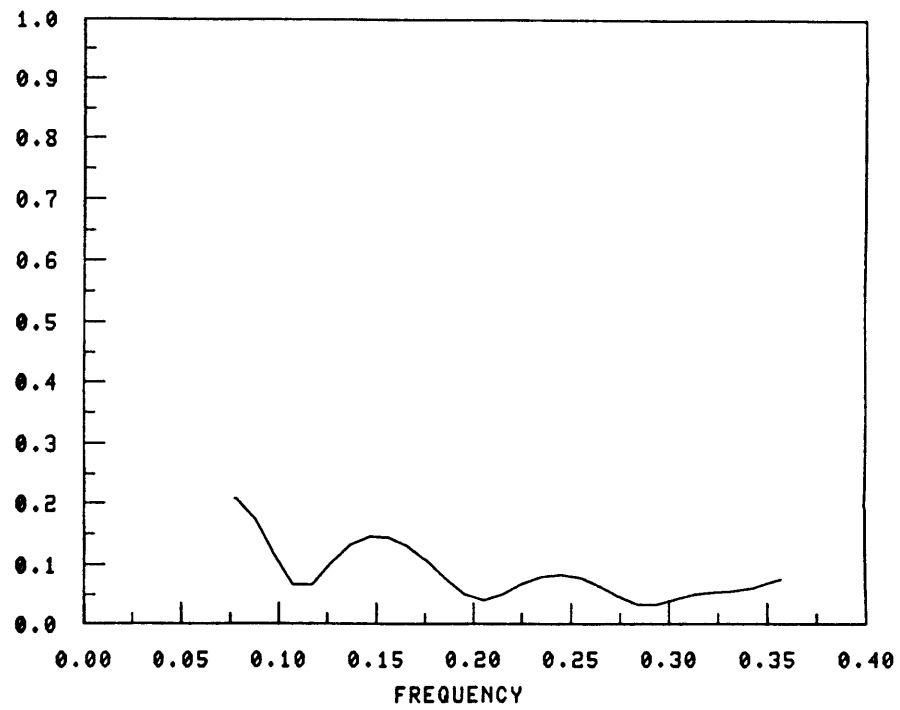


TRANS. COEFF. (h=13.918 UP)

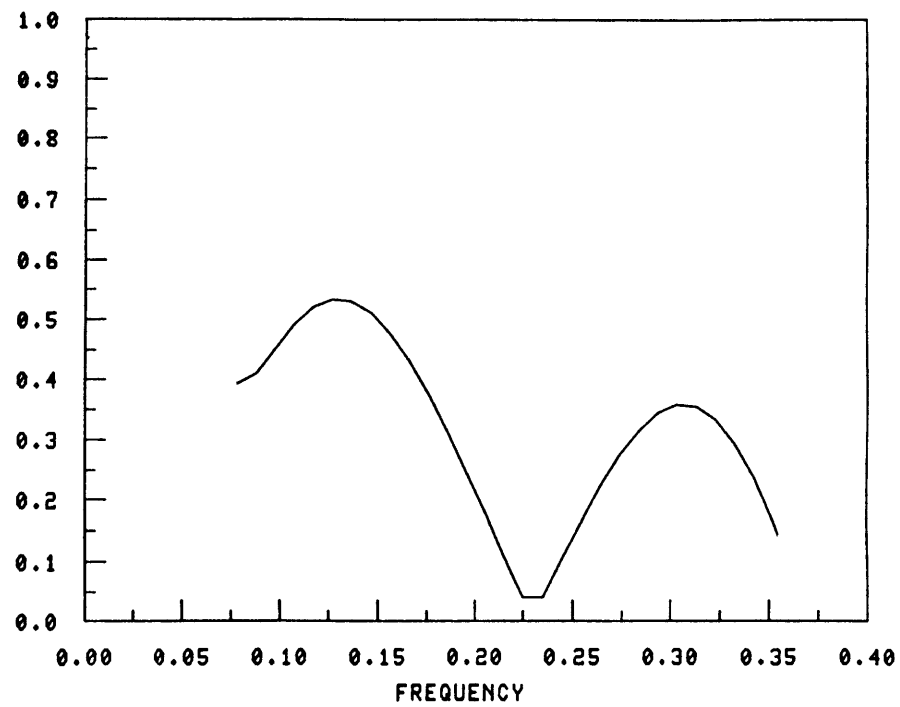


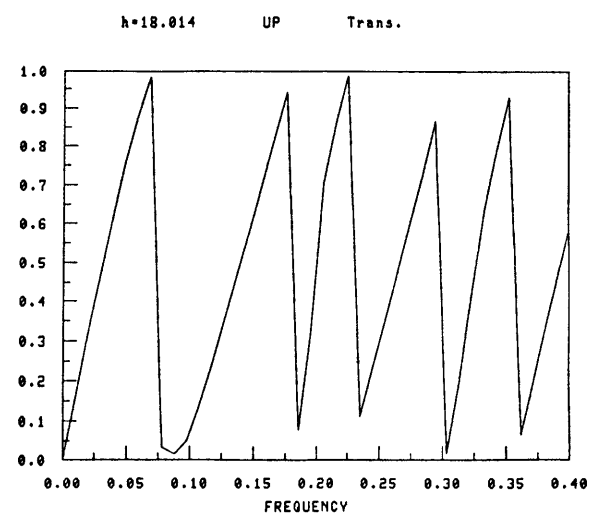
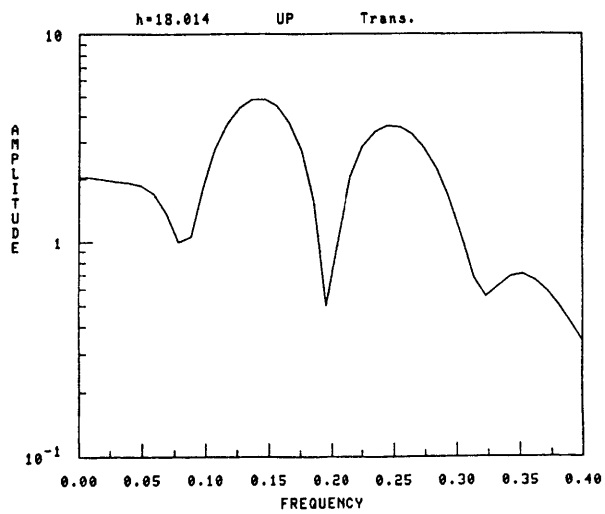
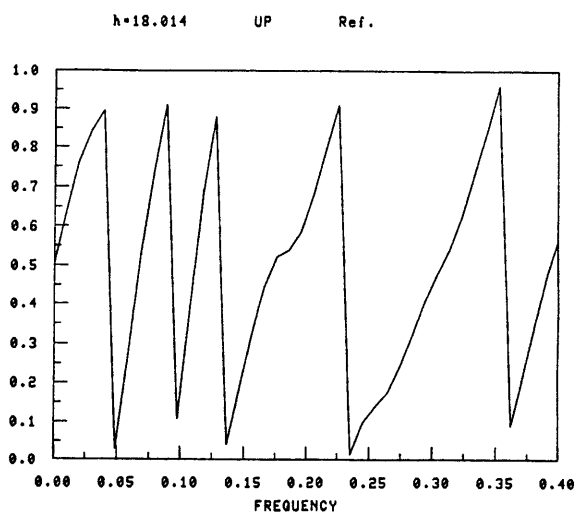
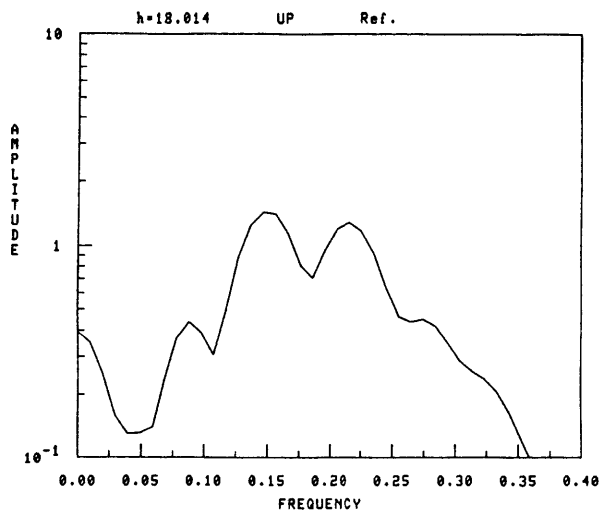
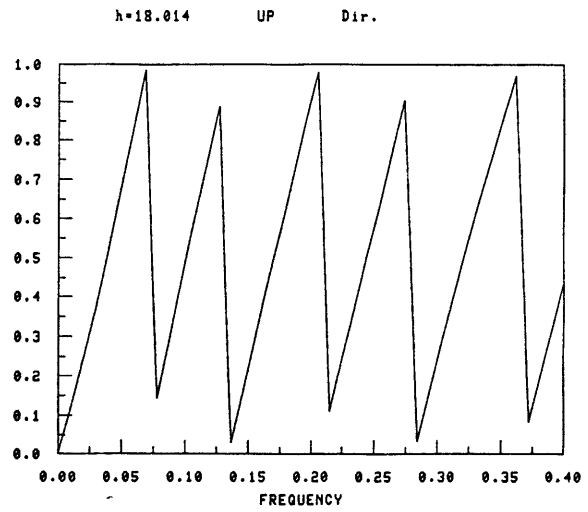
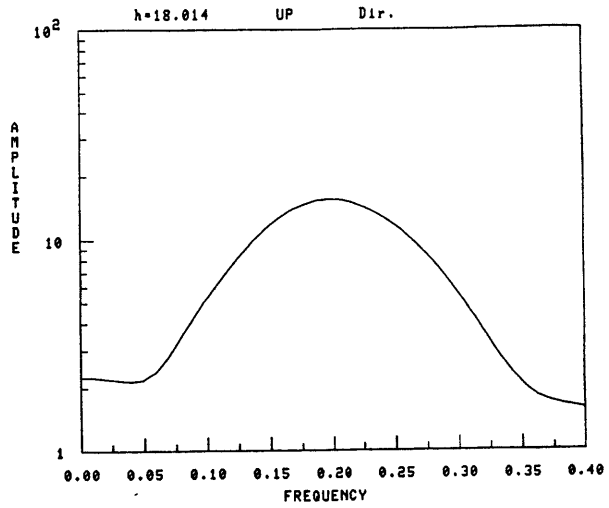


REF. COEFF. (h=16.001 UP)

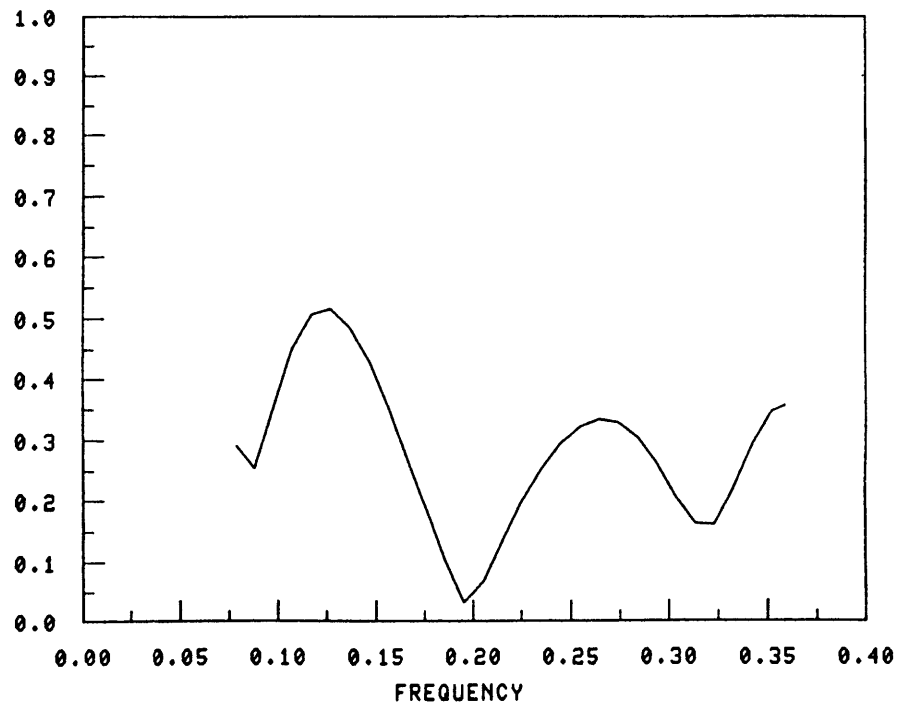


TRANS. COEFF. (h=16.001 UP)

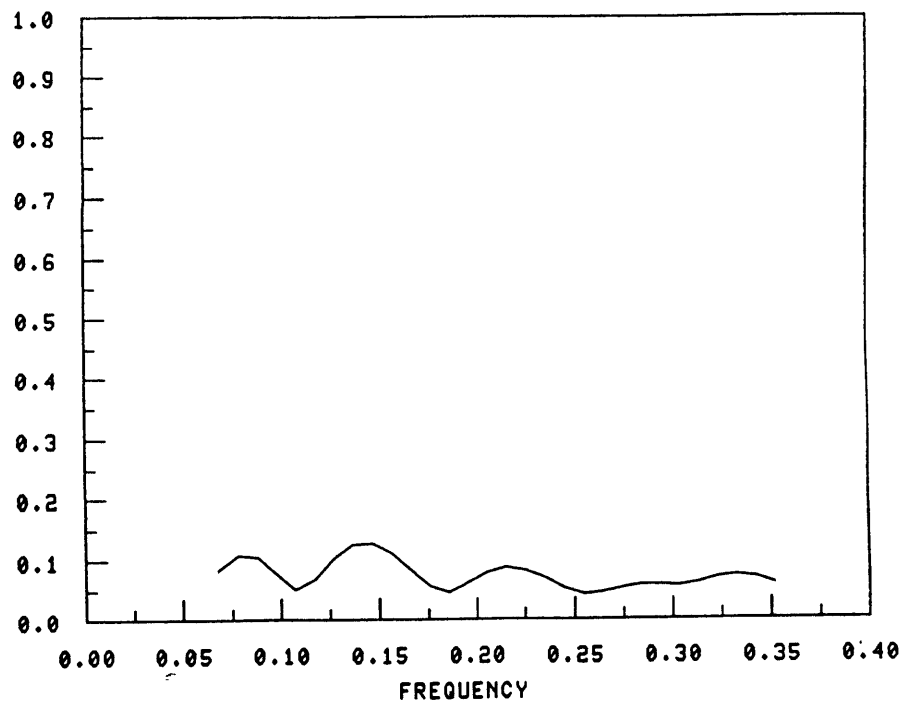


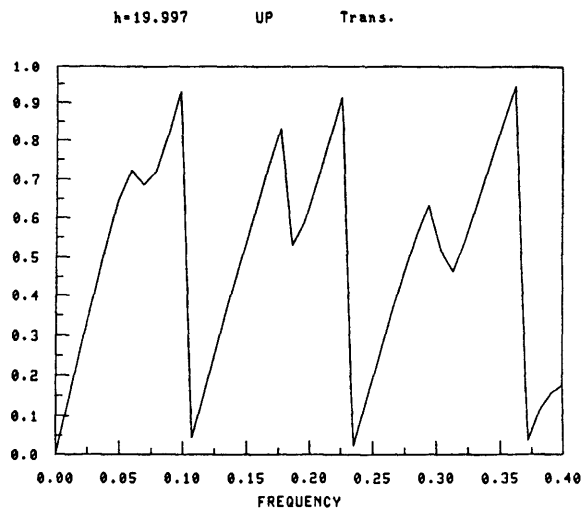
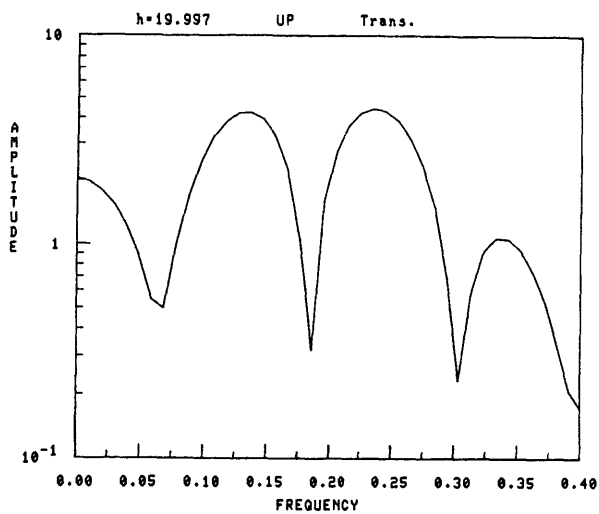
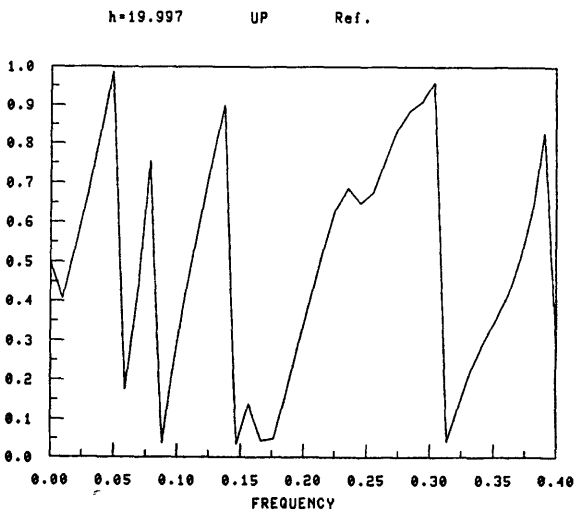
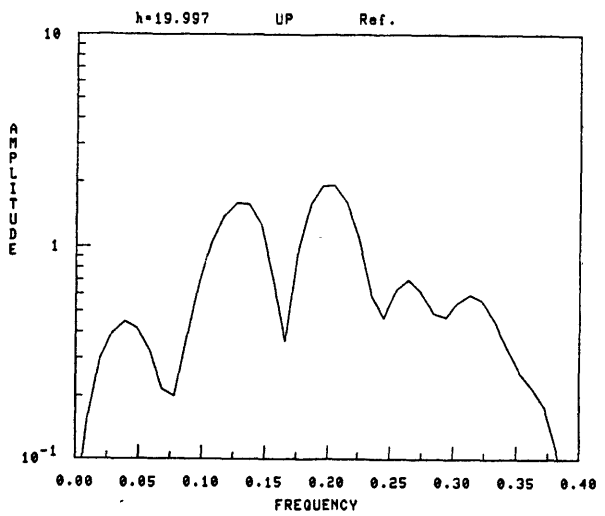
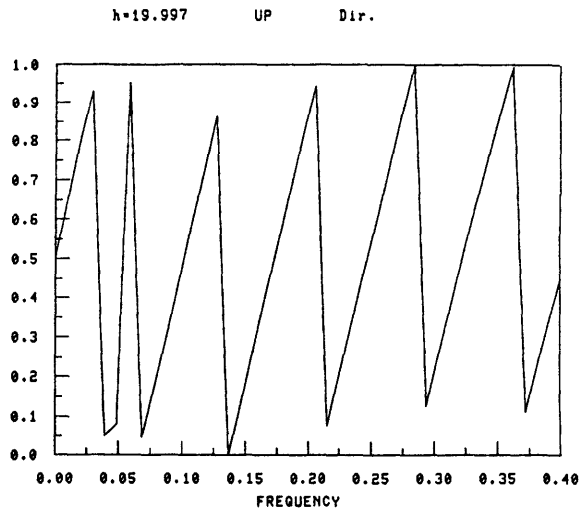
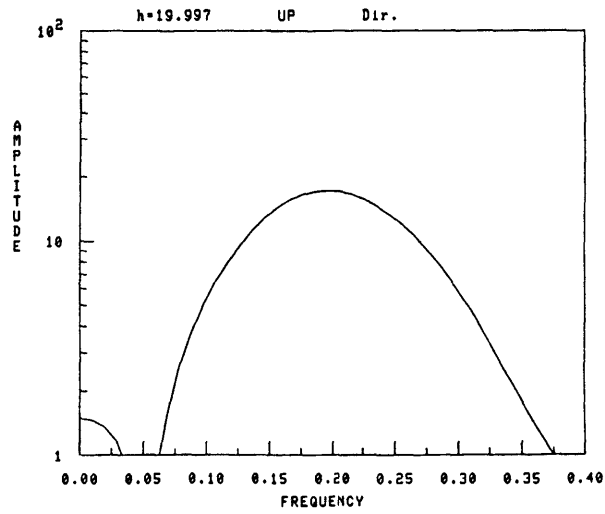


TRANS. COEFF. (h=18.014 UP)

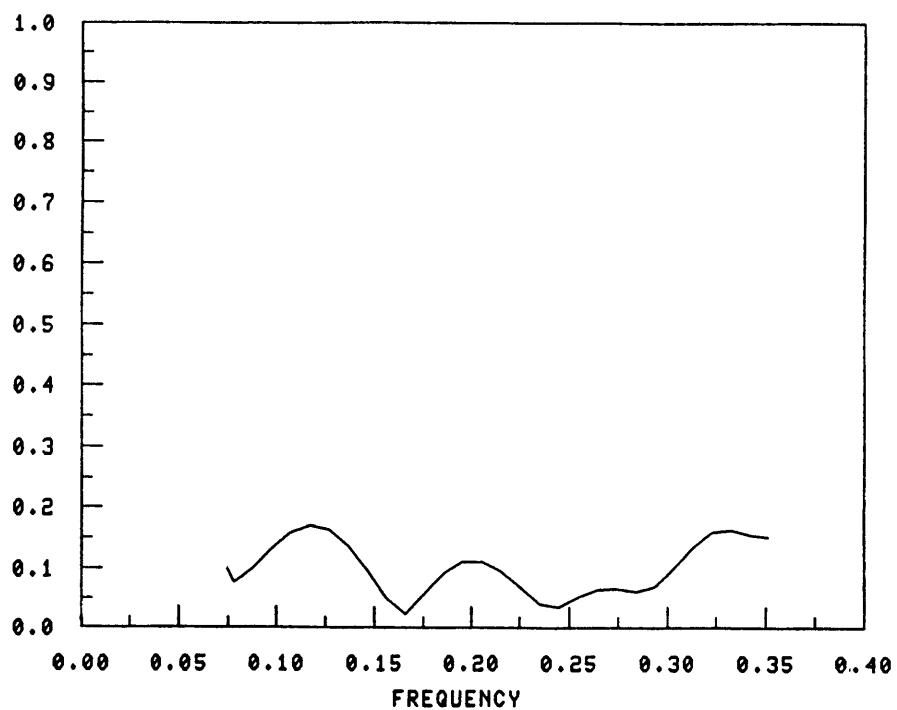


REF. COEFF. (h=18.014 UP)

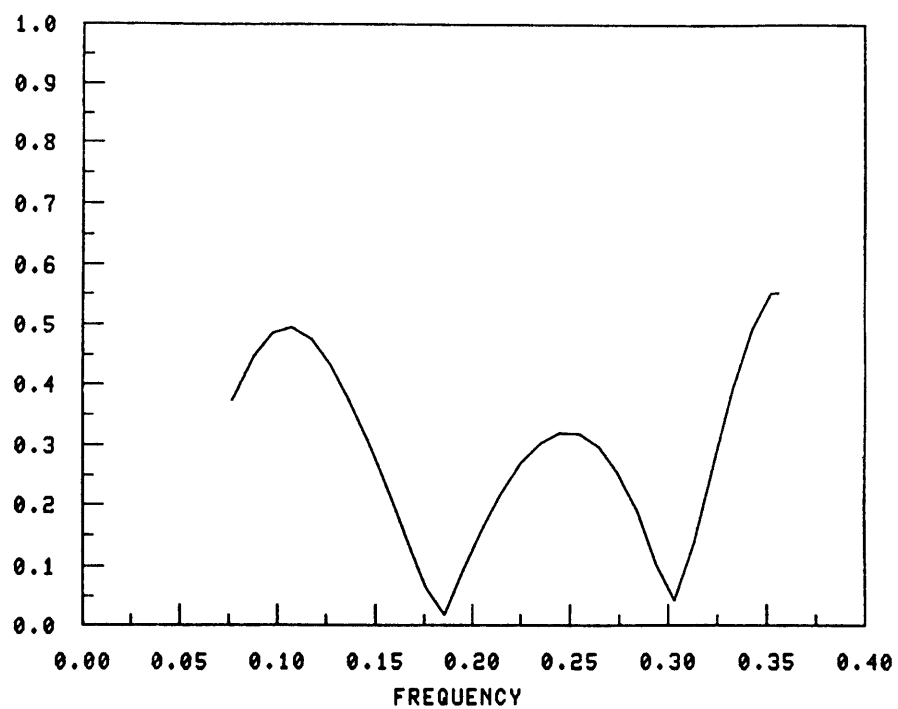


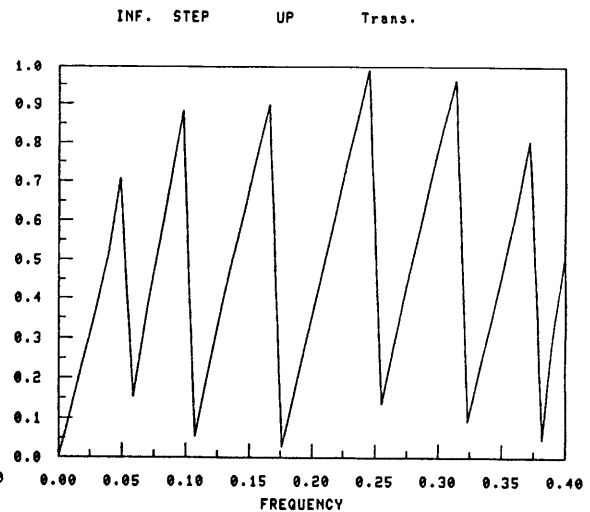
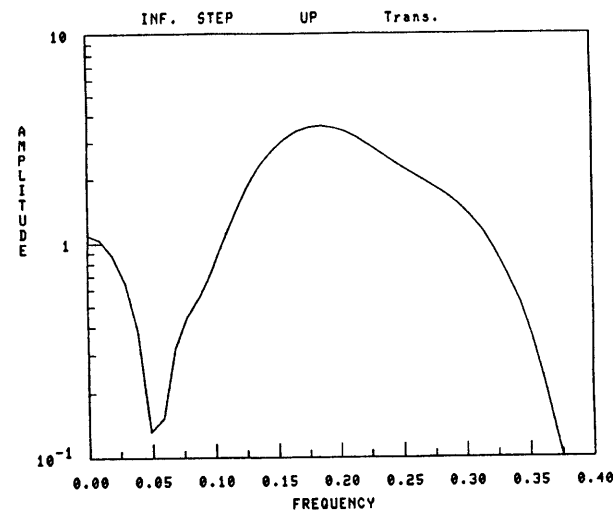
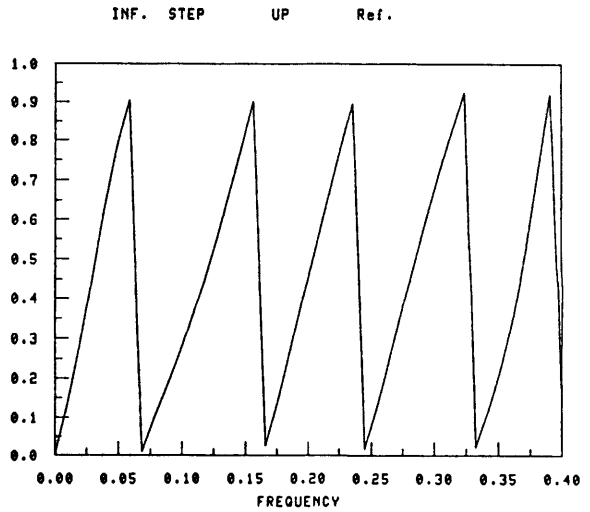
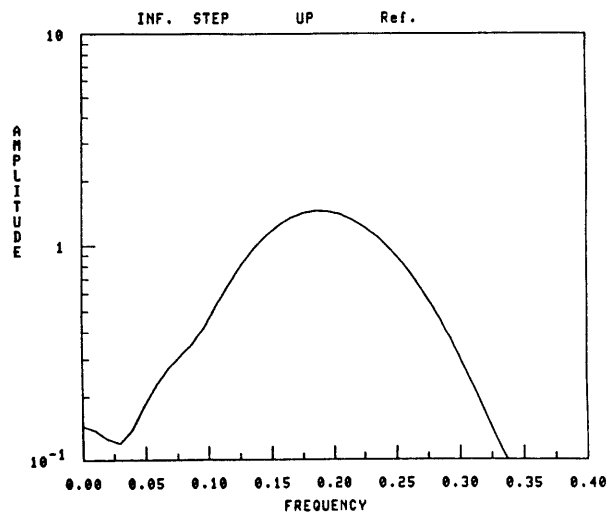
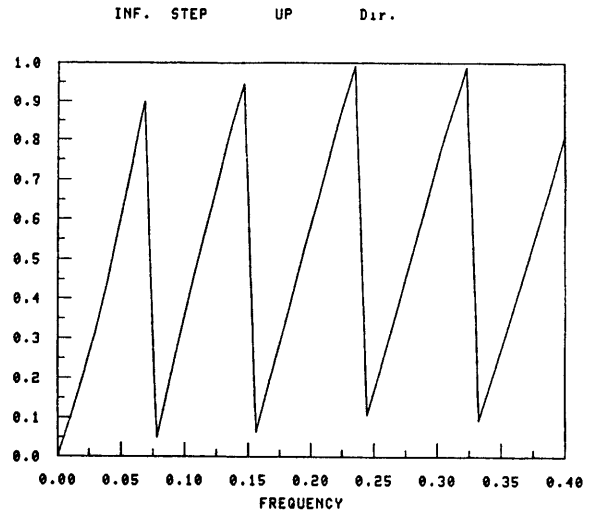
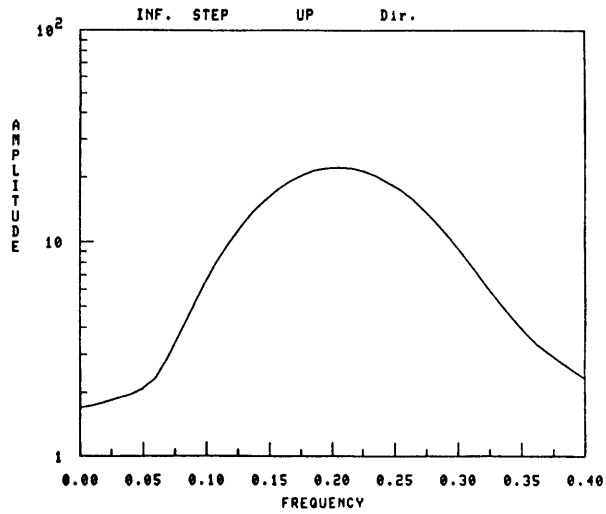


REF. COEFF. (h=19.997 UP)



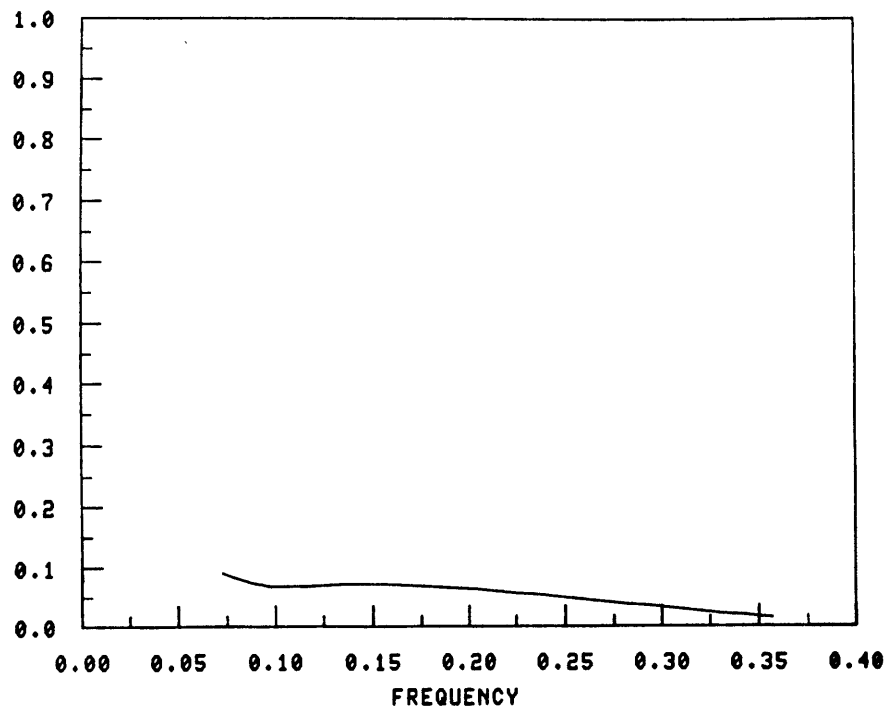
TRANS. COEFF. (h=19.997 UP)



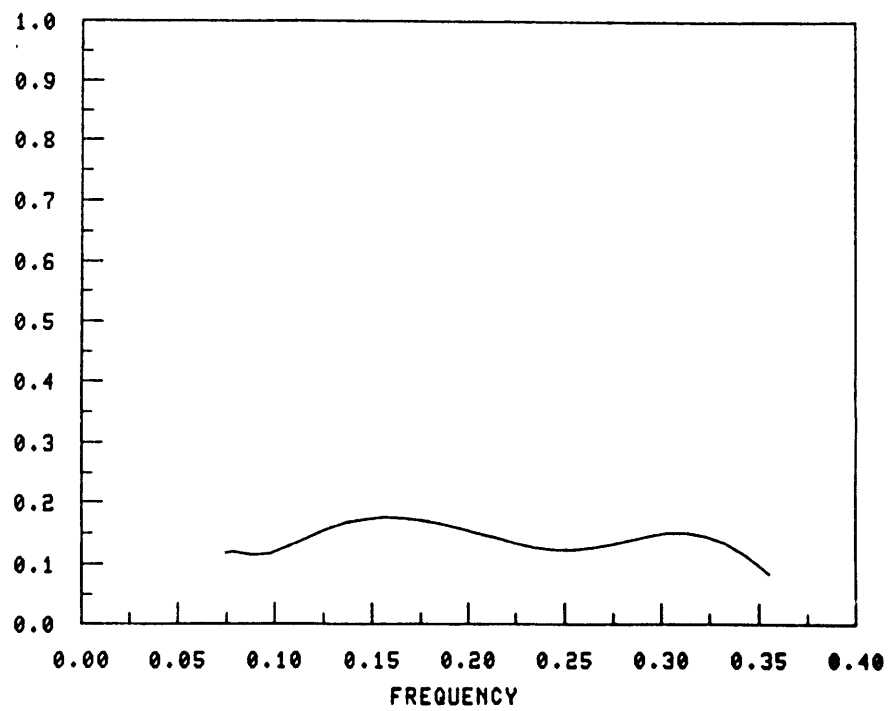


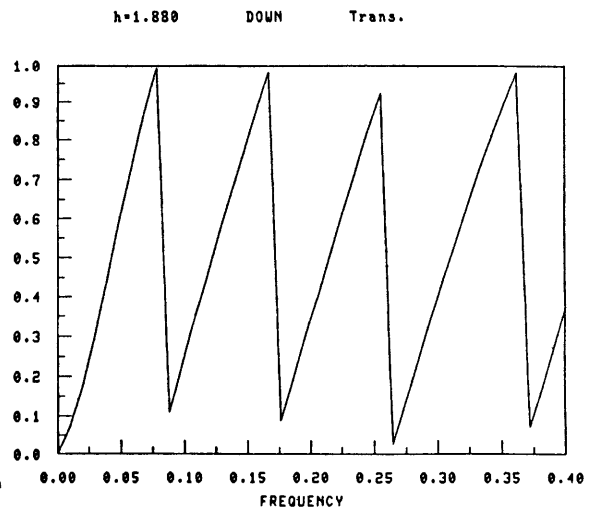
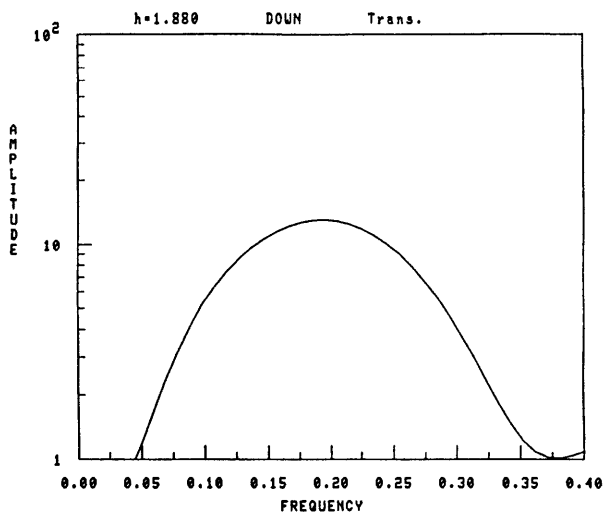
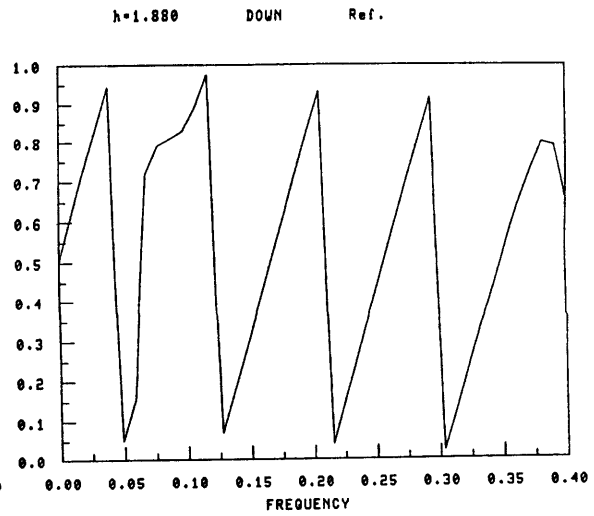
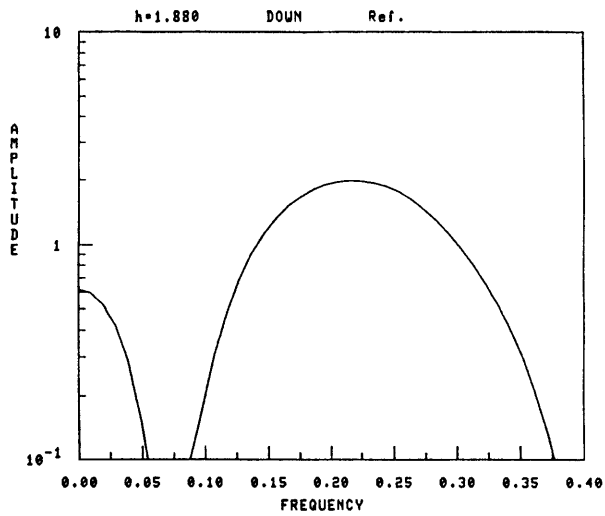
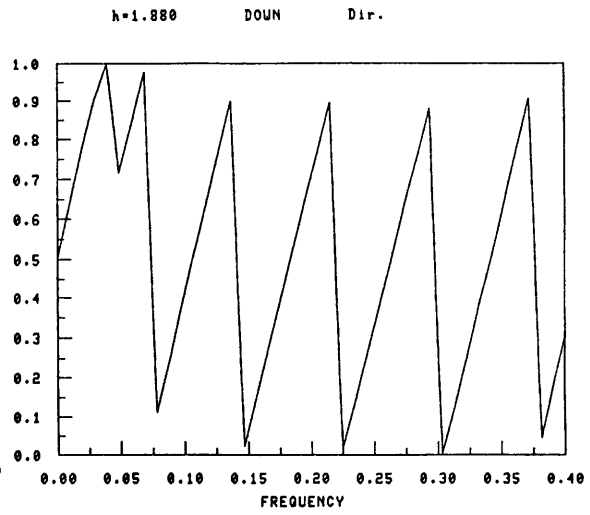
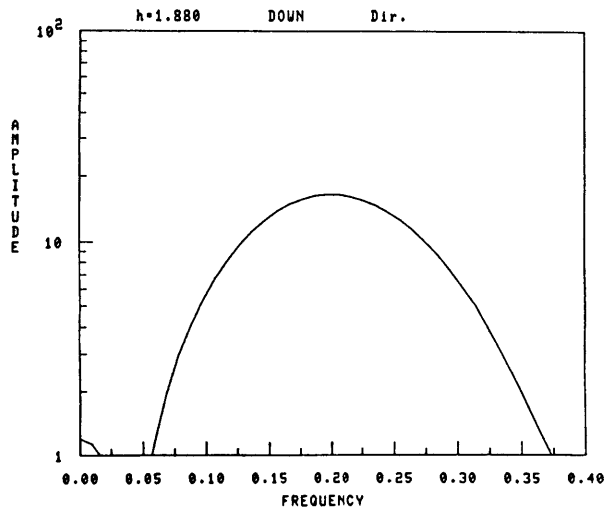


REF. COEFF. (Inf. Step UP)

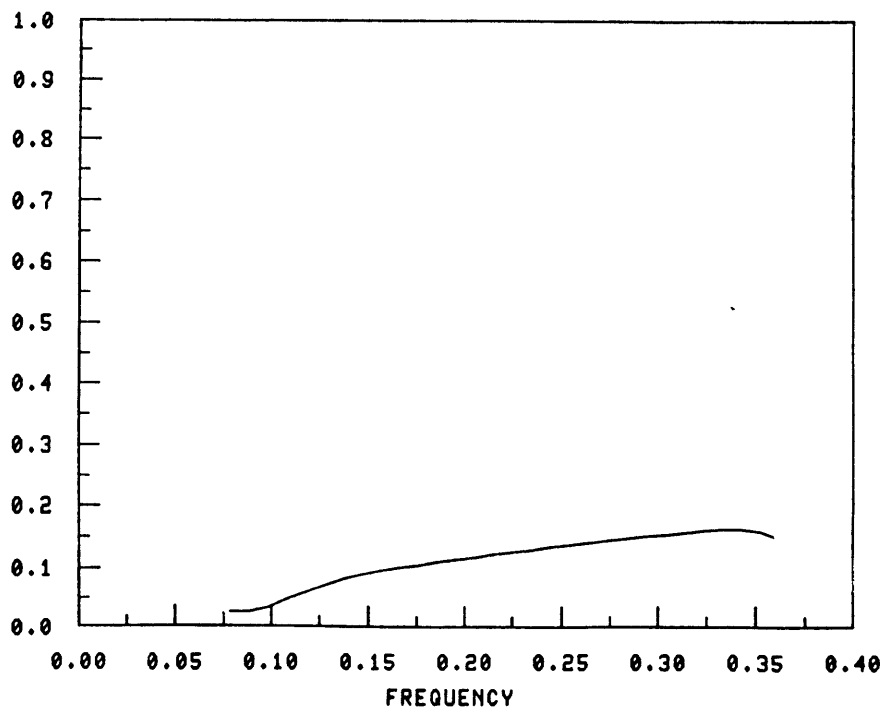


TRANS. COEFF. (Inf. Step UP)

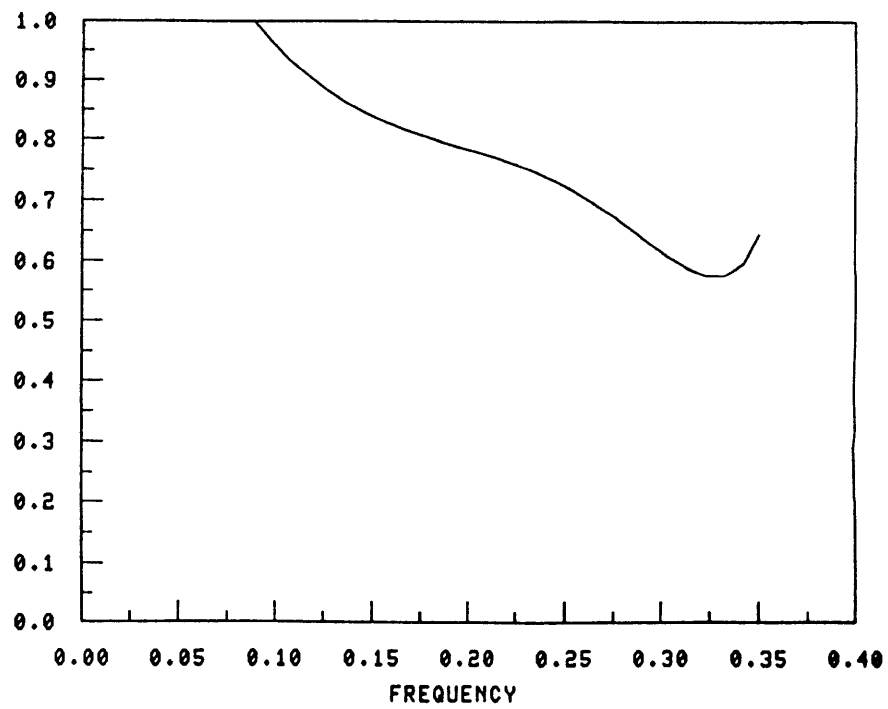


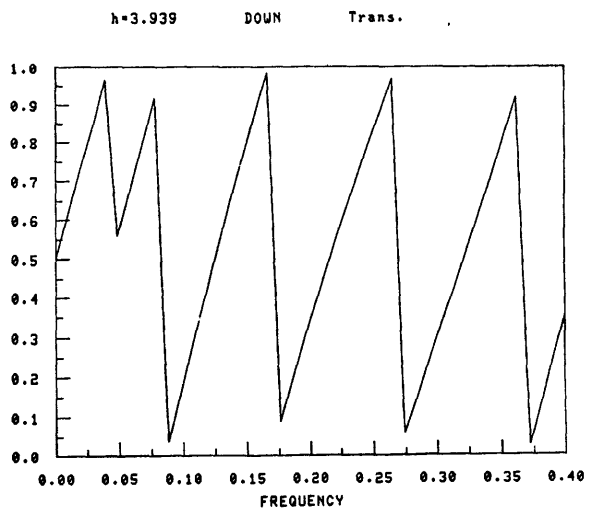
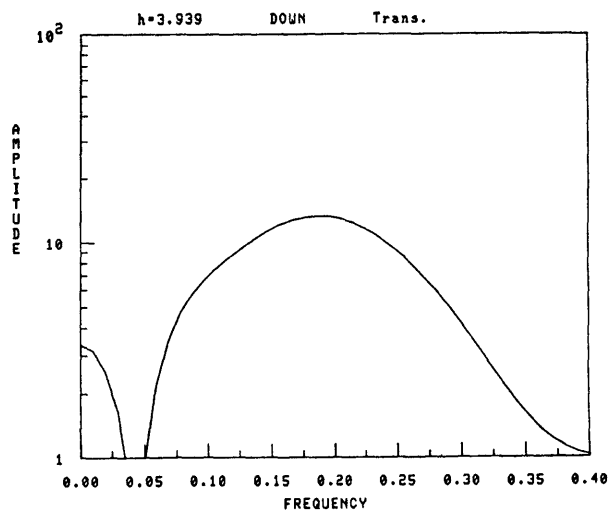
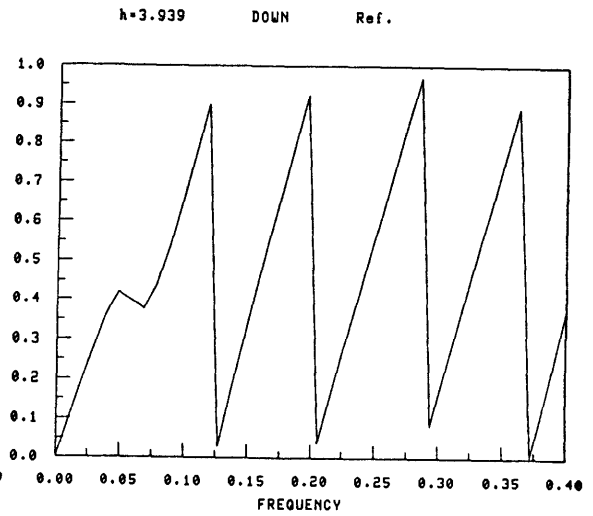
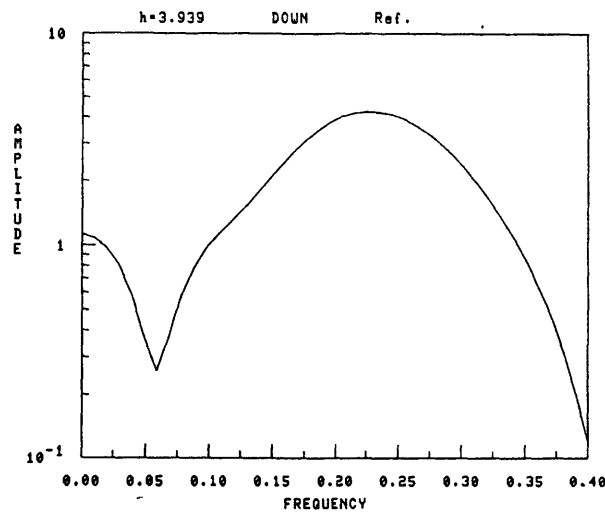
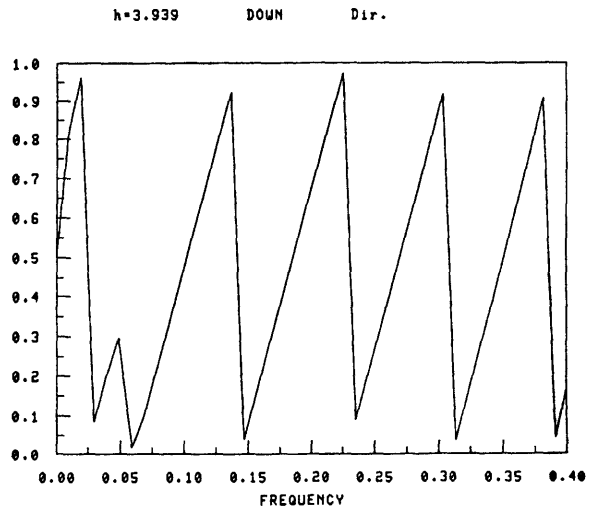
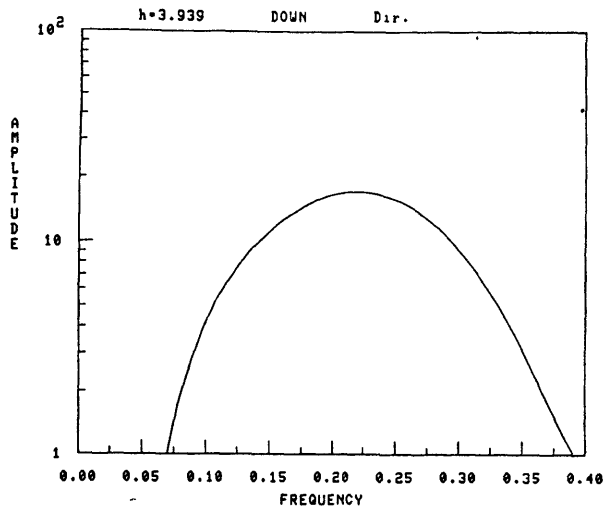


REF. COEFF. (h=1.880 DOWN)

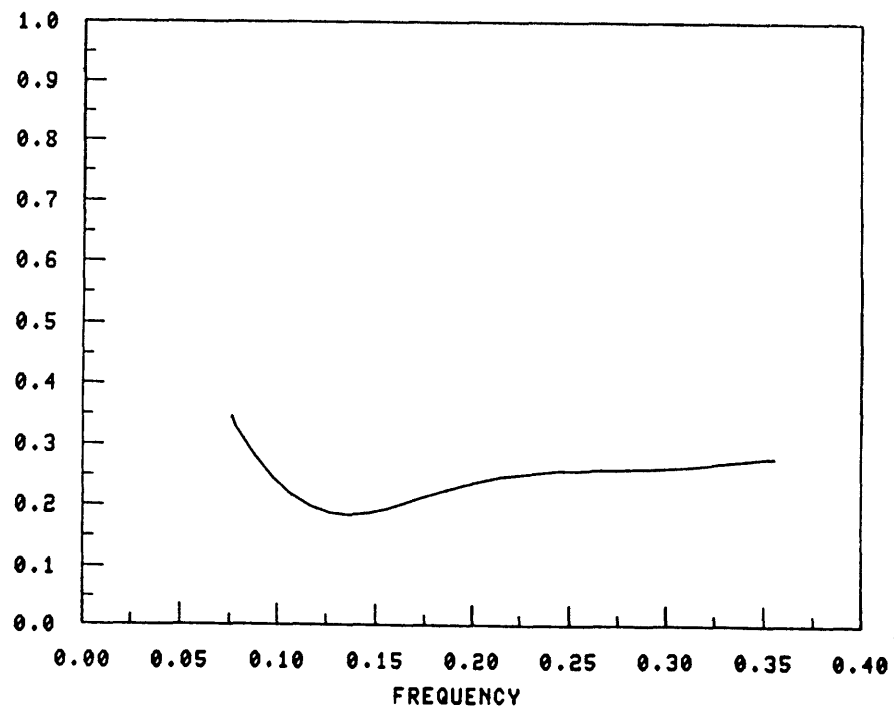


TRANS. COEFF. (h=1.880 DOWN)

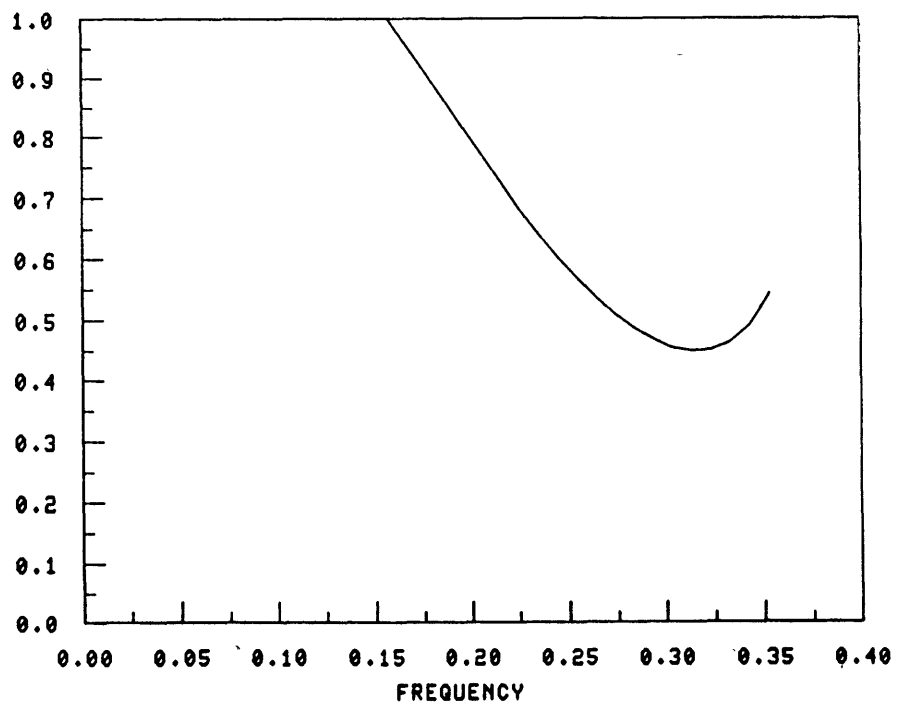


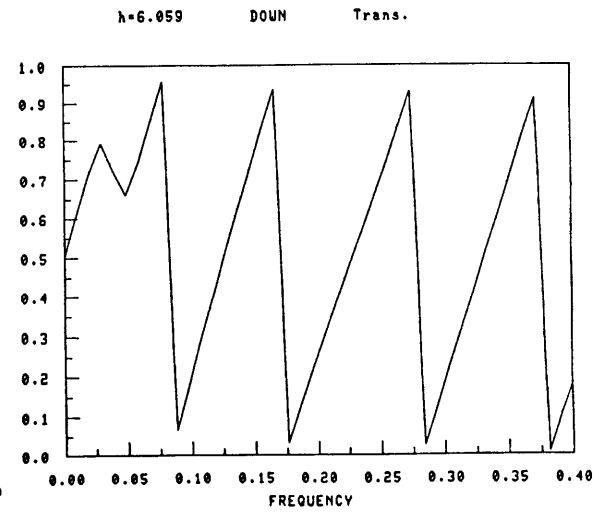
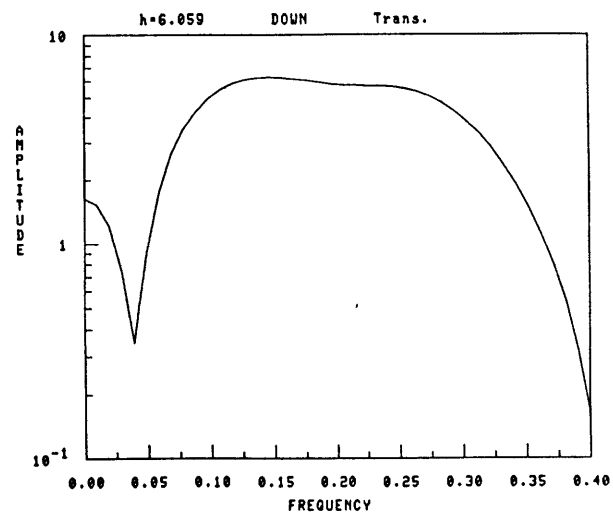
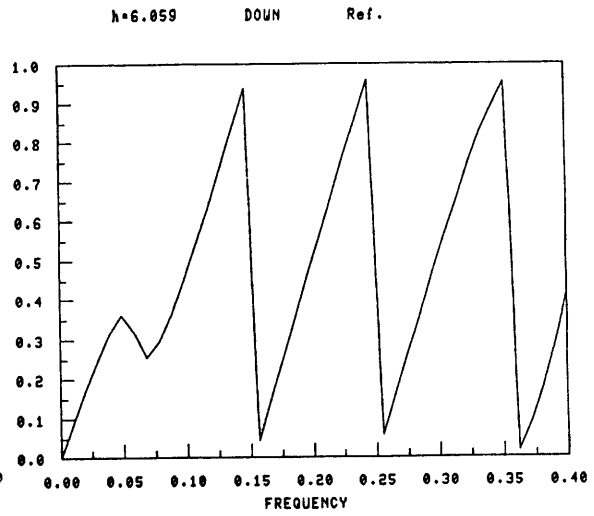
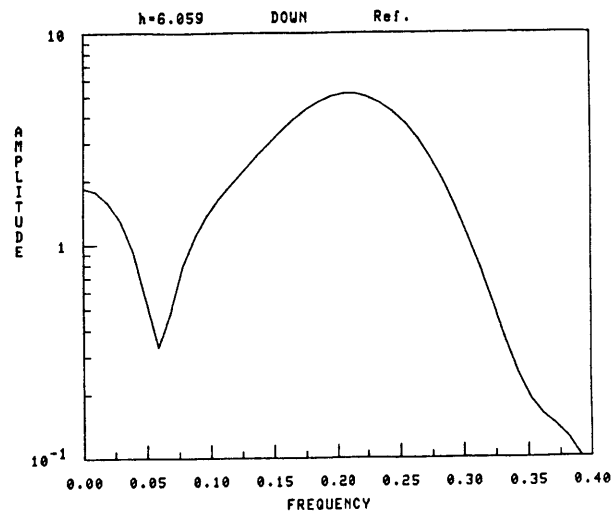
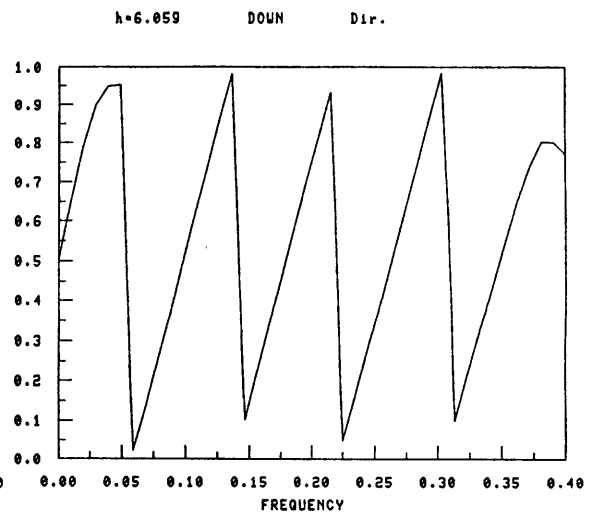
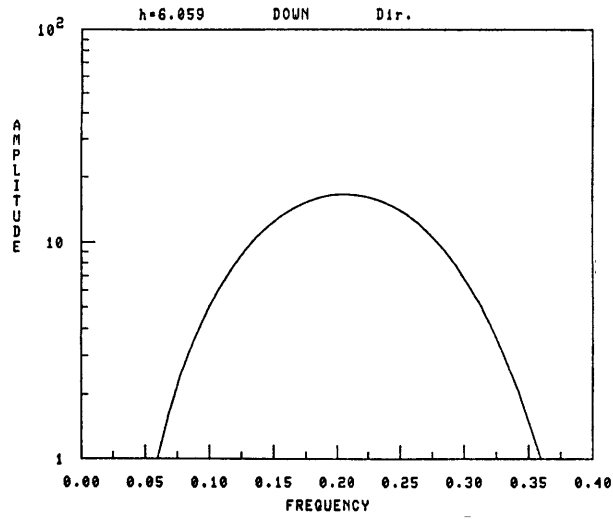


REF. COEFF. (h=3.939 DOWN)

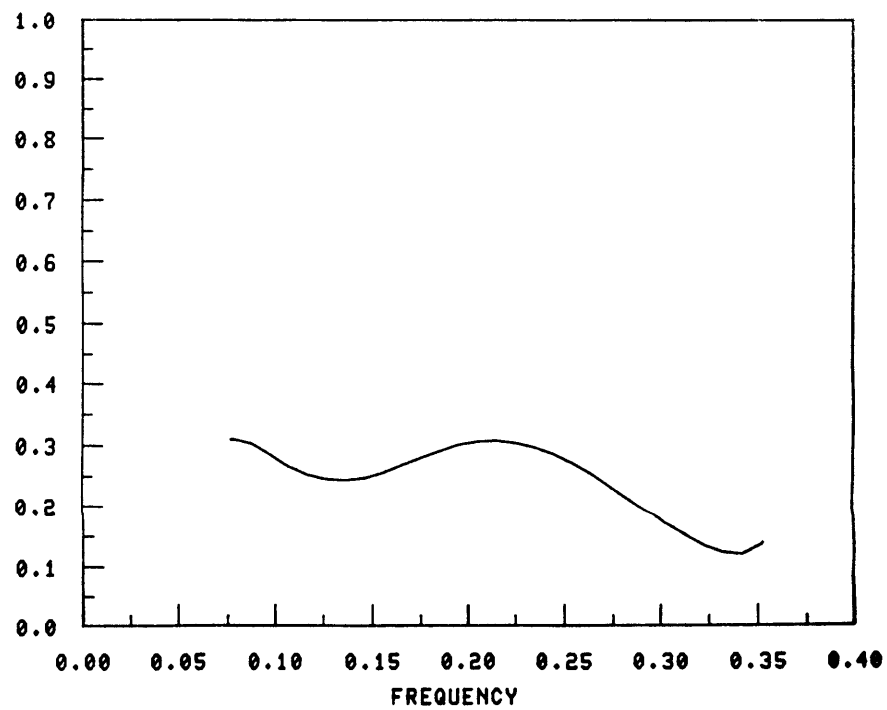


TRANS. COEFF. (h=3.939 DOWN)

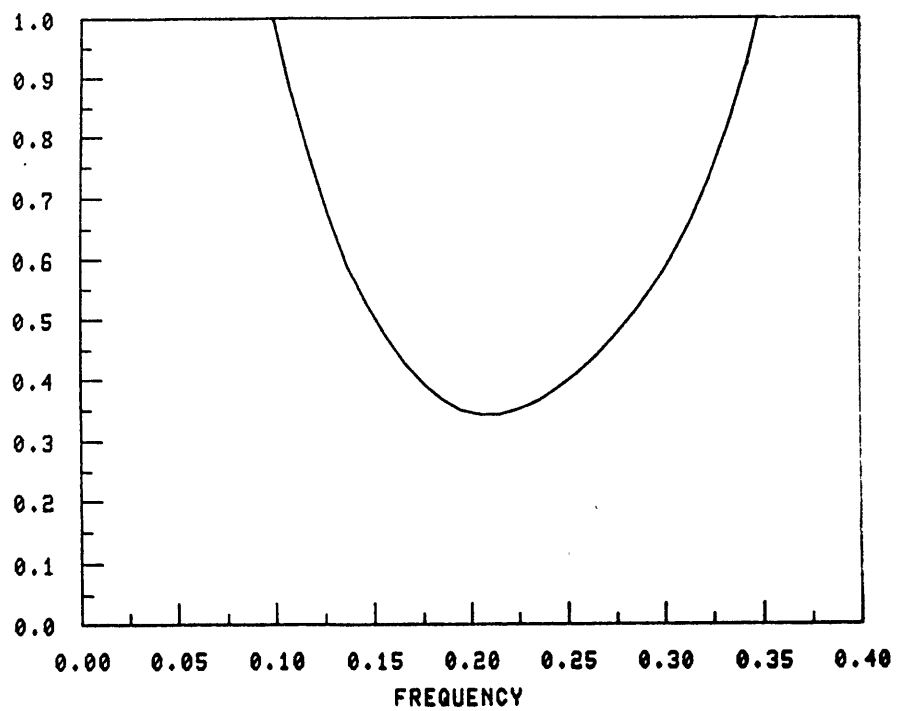


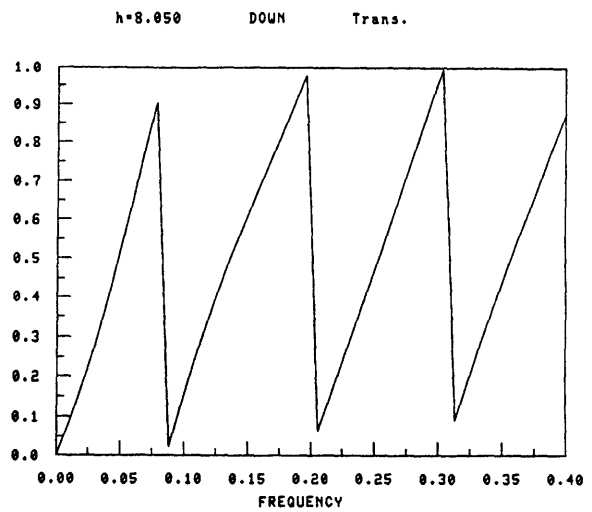
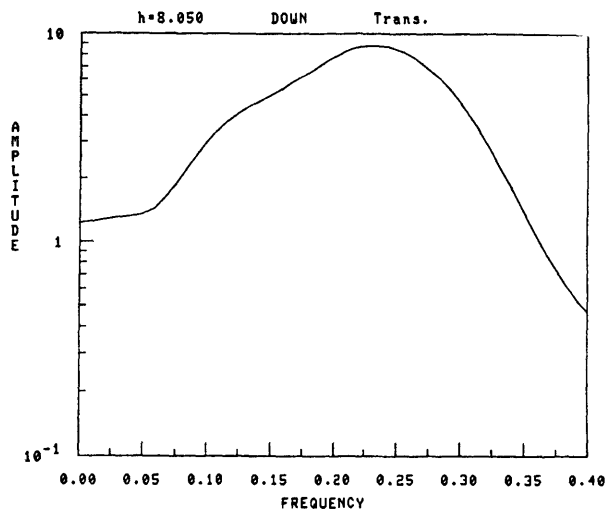
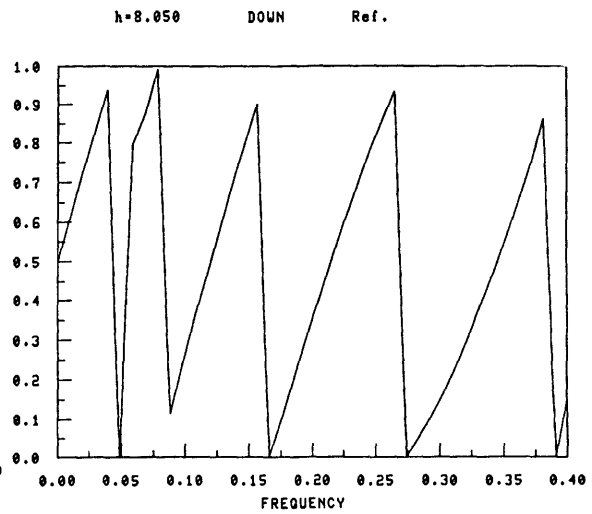
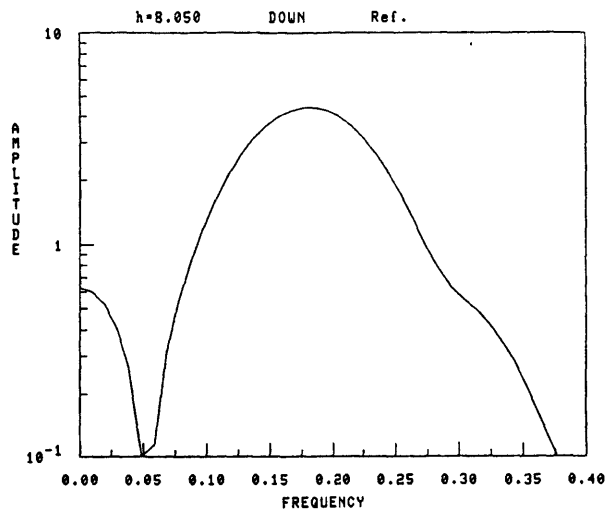
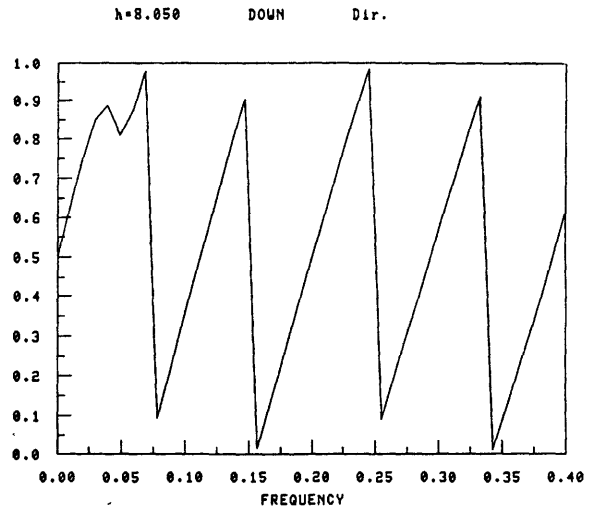
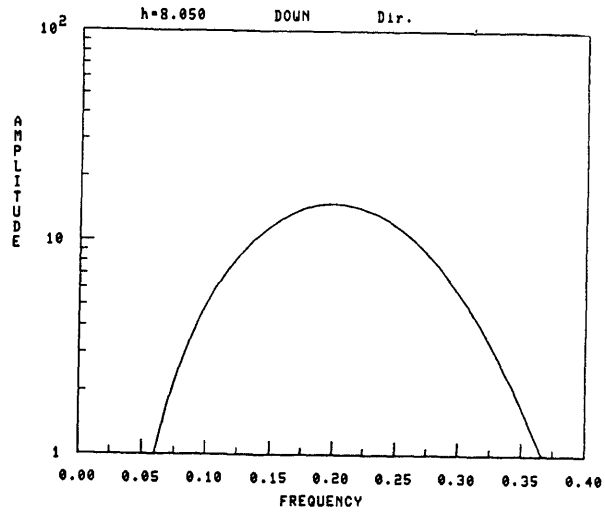


REF. COEFF. (h=6.059 DOWN)



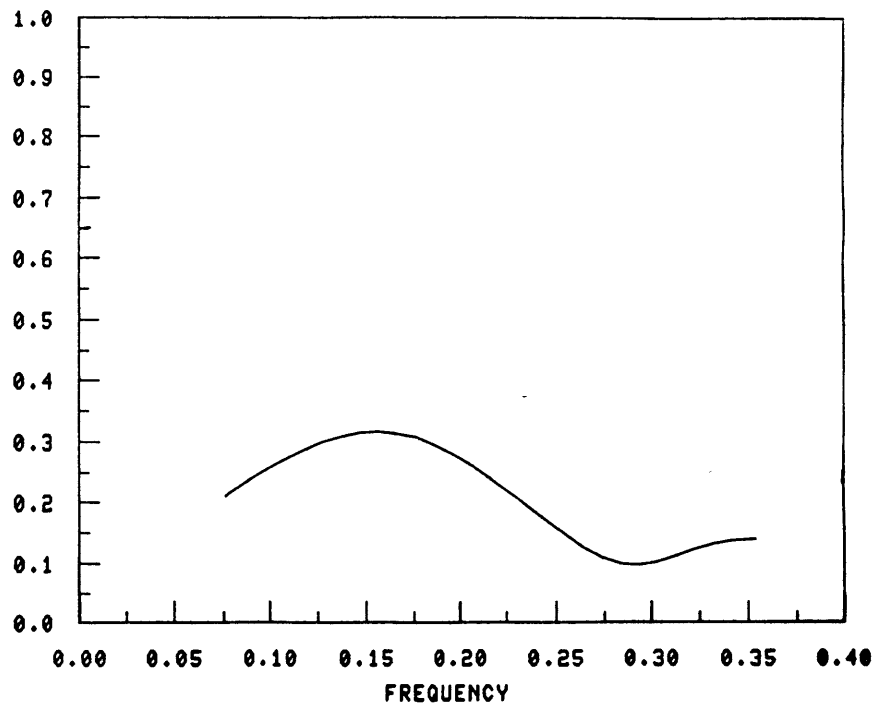
TRANS. COEFF. (h=6.059 DOWN)



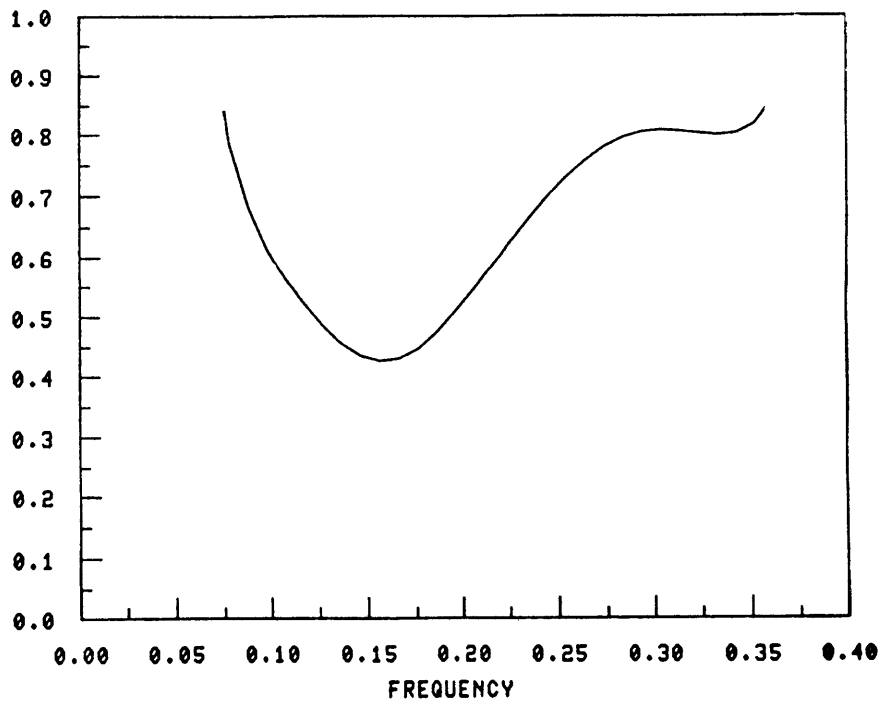


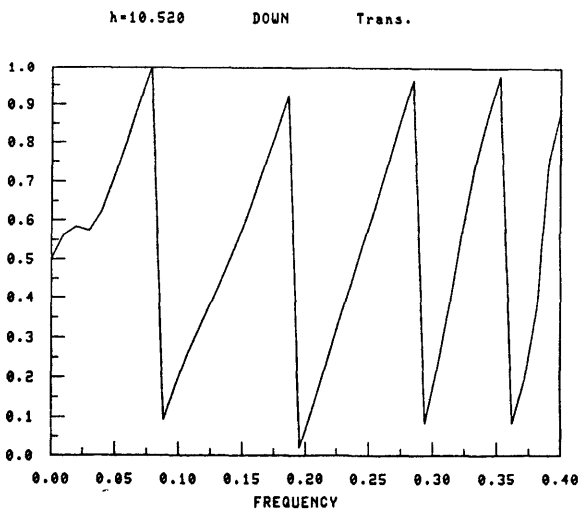
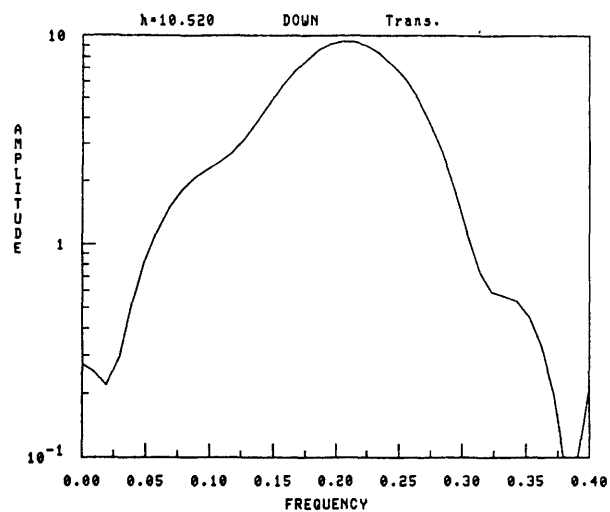
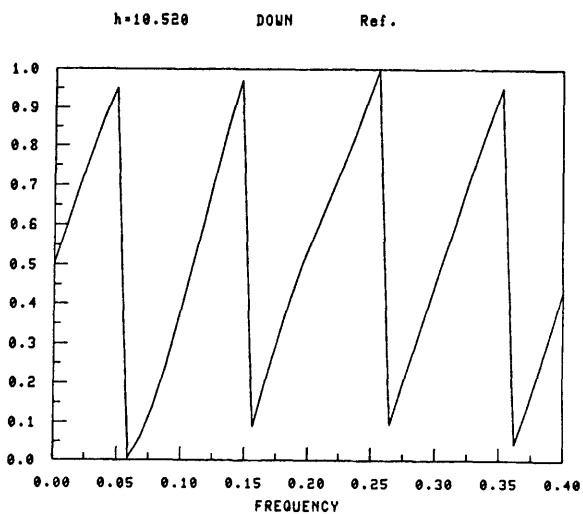
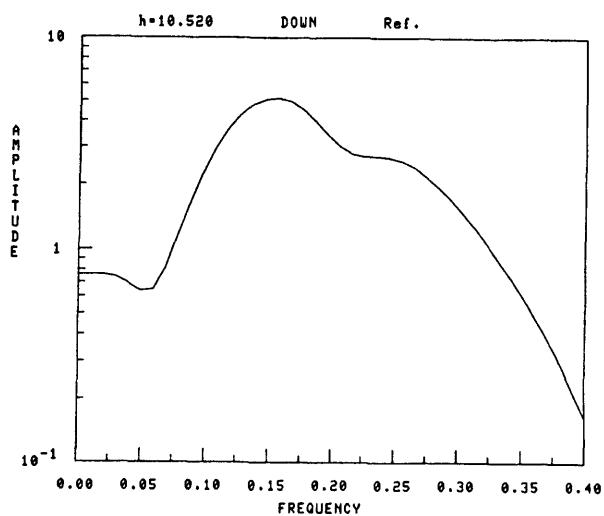
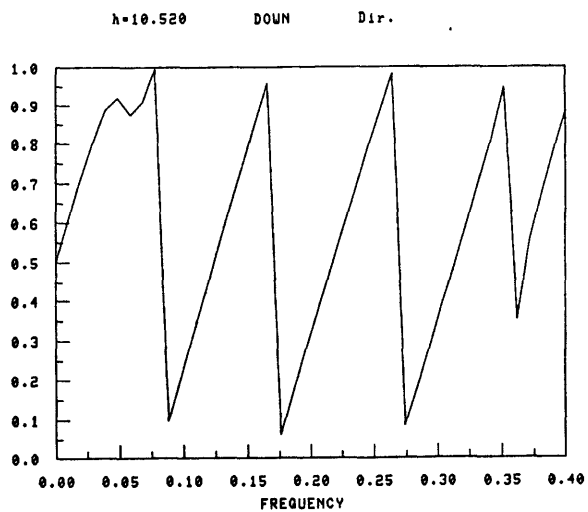
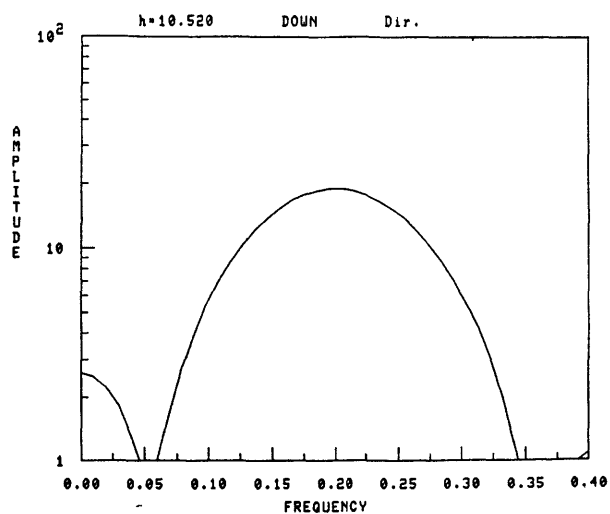


REF. COEFF. (h=8.050 DOWN)

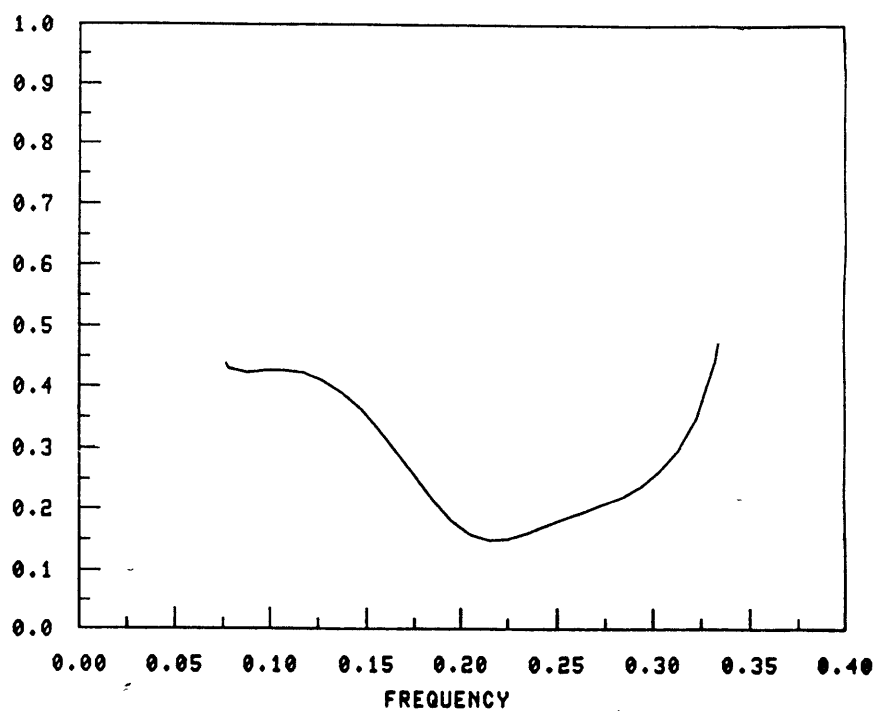


TRANS. COEFF. (h=8.050 DOWN)

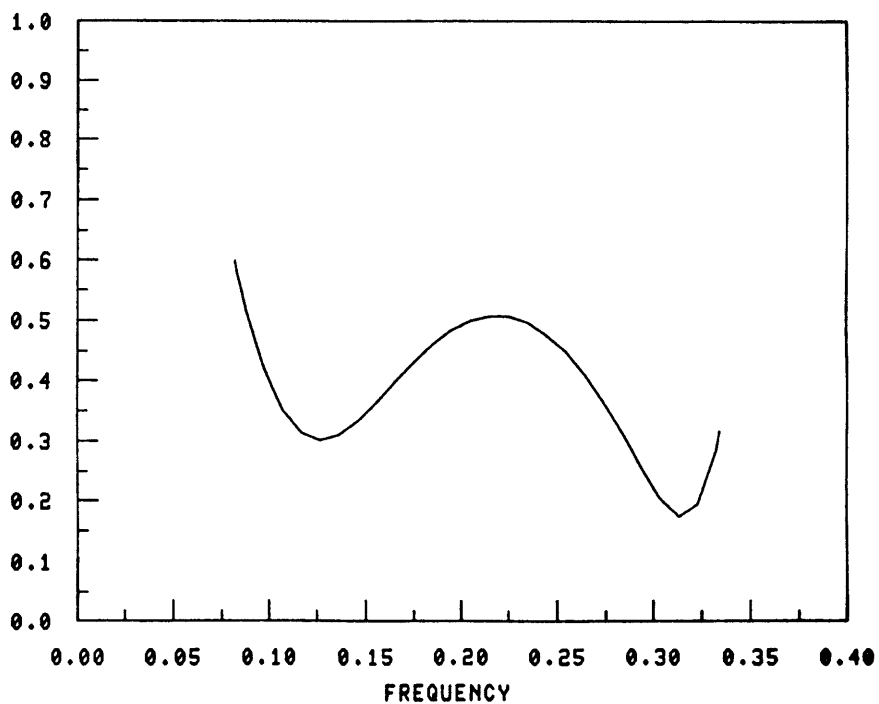


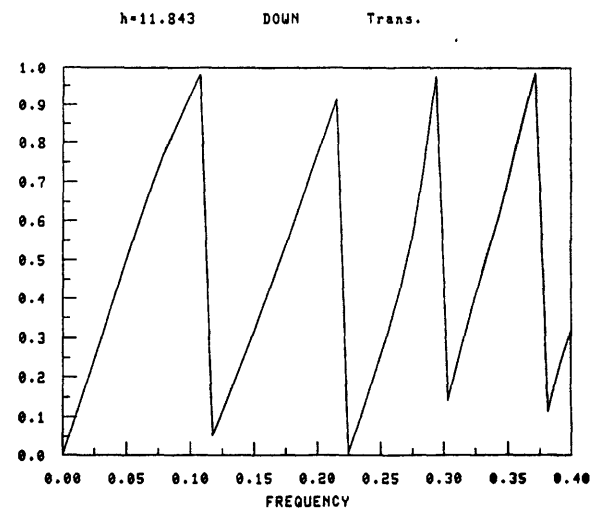
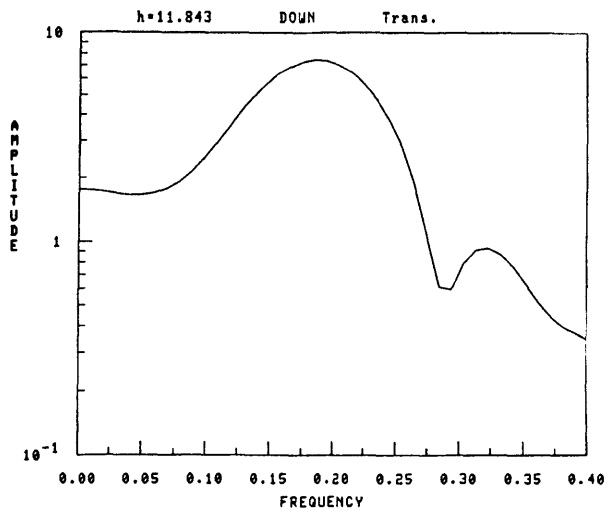
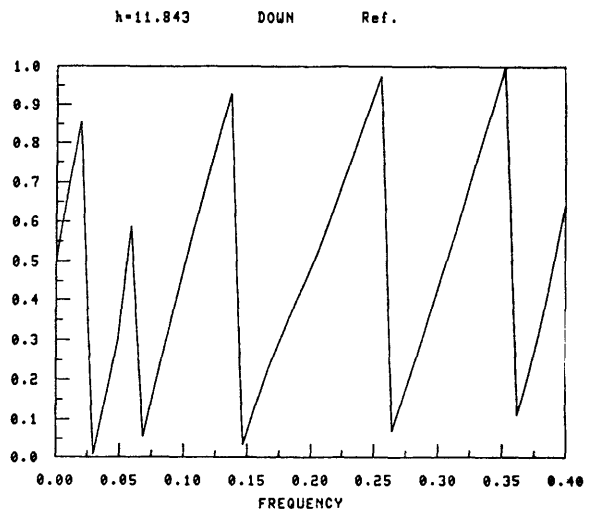
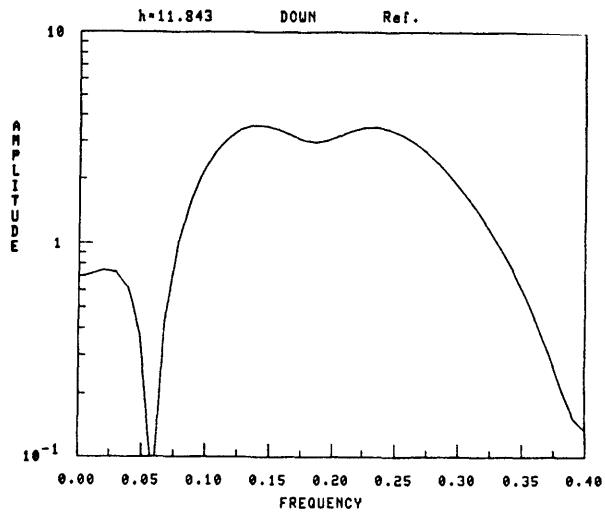
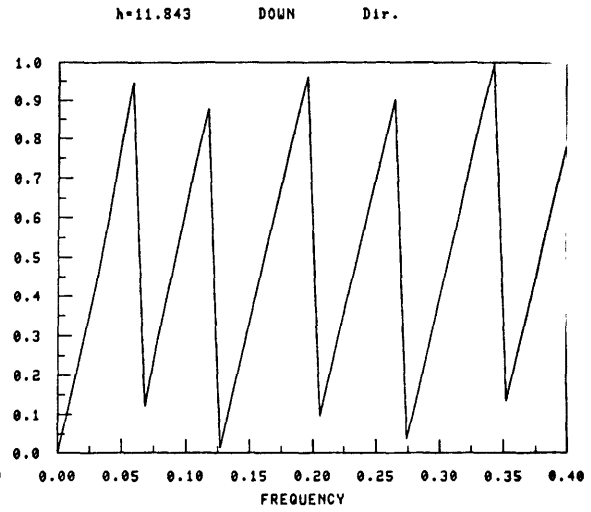
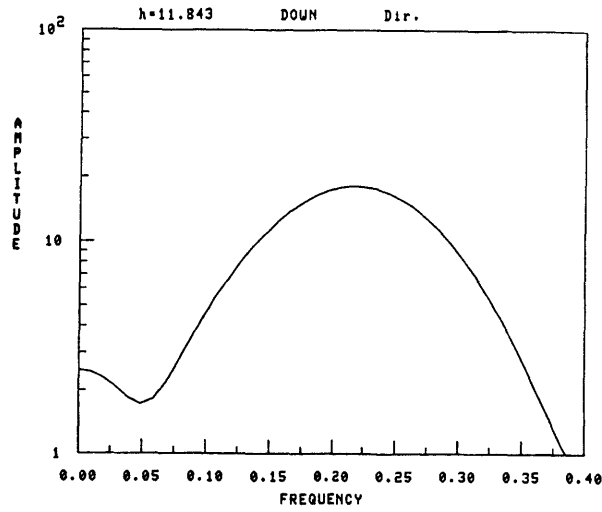


REF. COEFF. (h=10.520 DOWN)

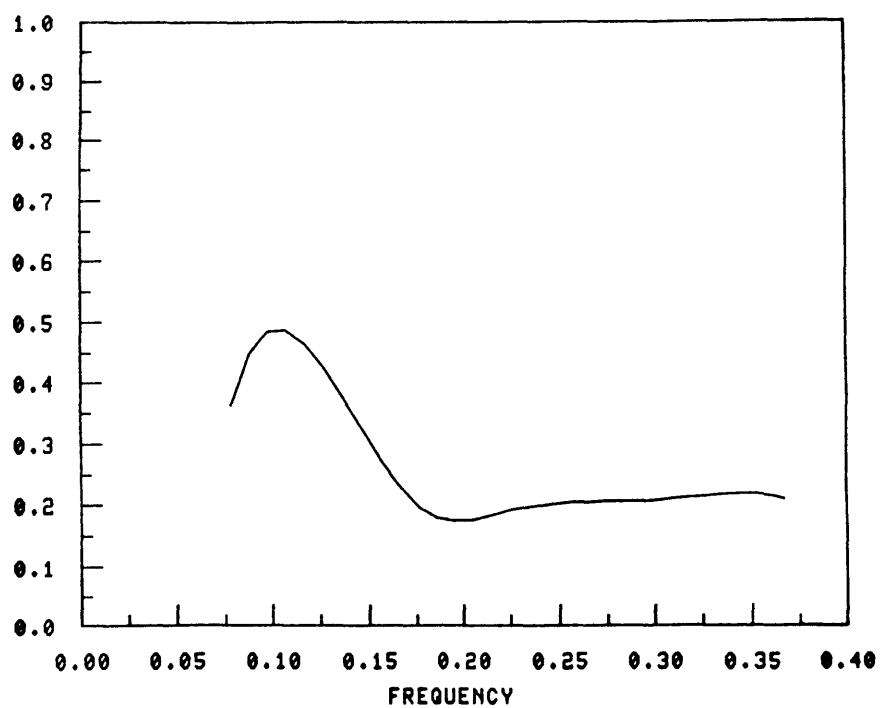


TRANS. COEFF. (h=10.520 DOWN)

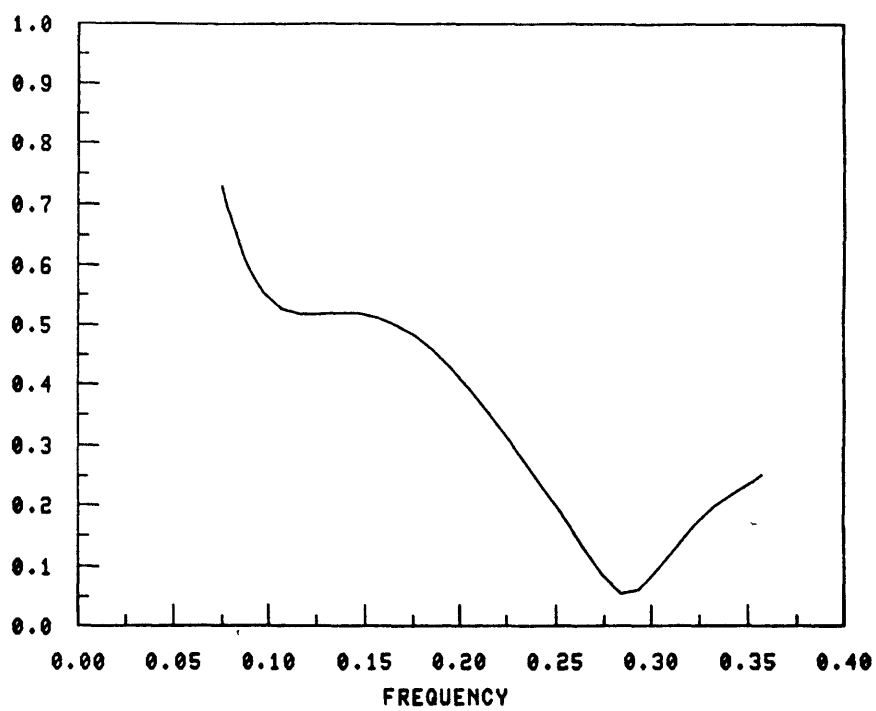


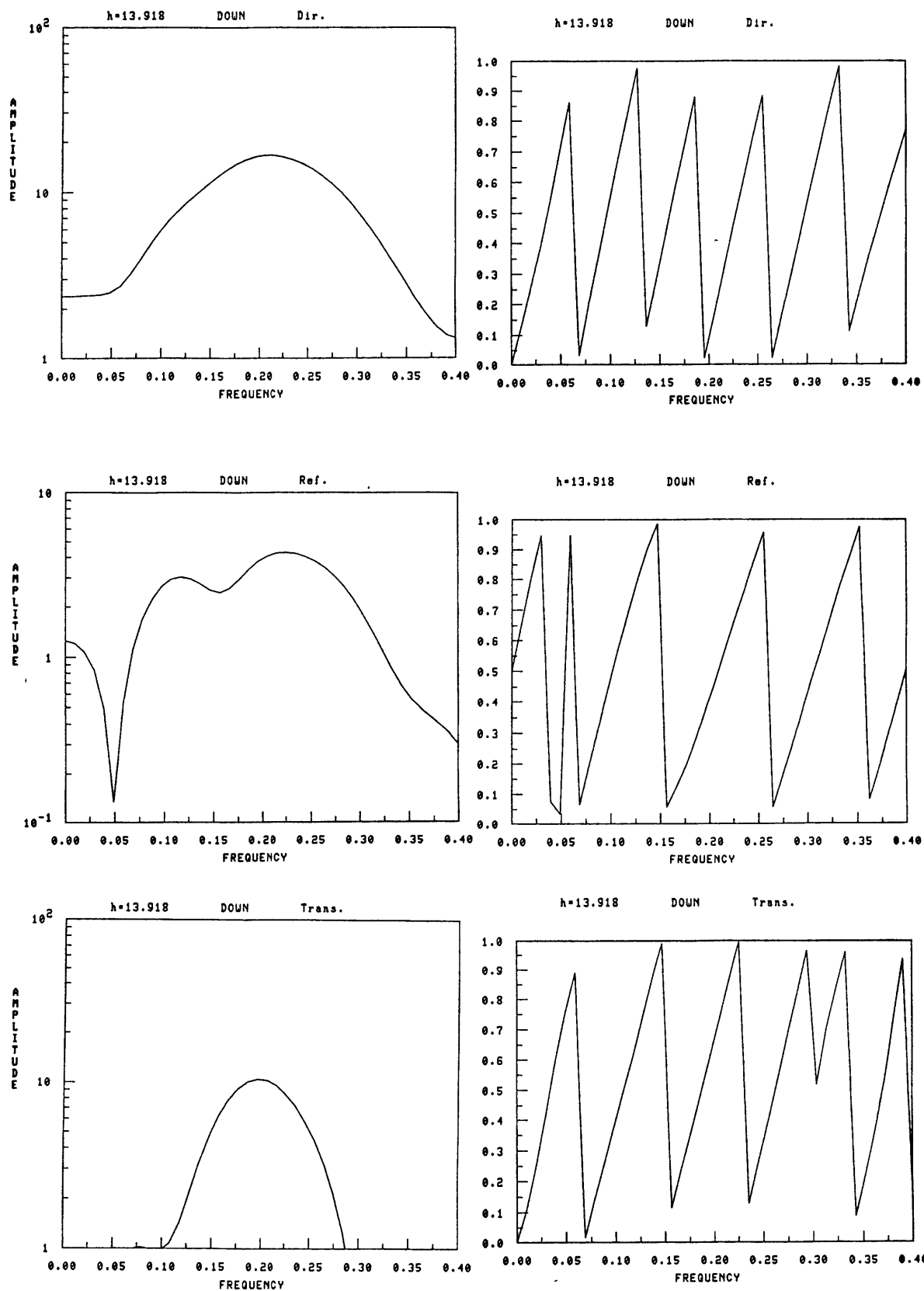


REF. COEFF. (h=11.843 DOWN)

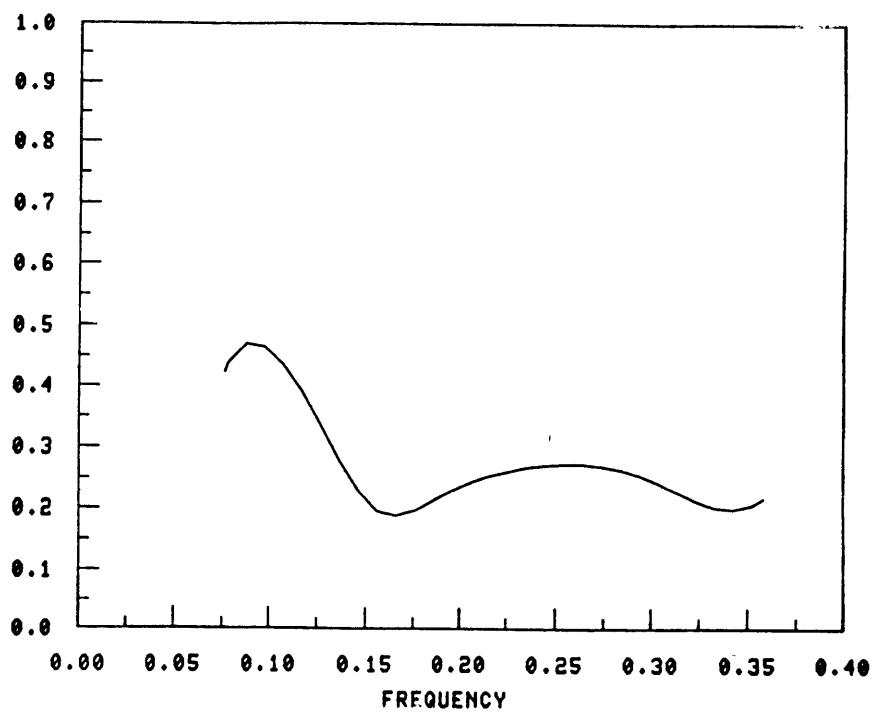


TRANS. COEFF. (h=11.843 DOWN)

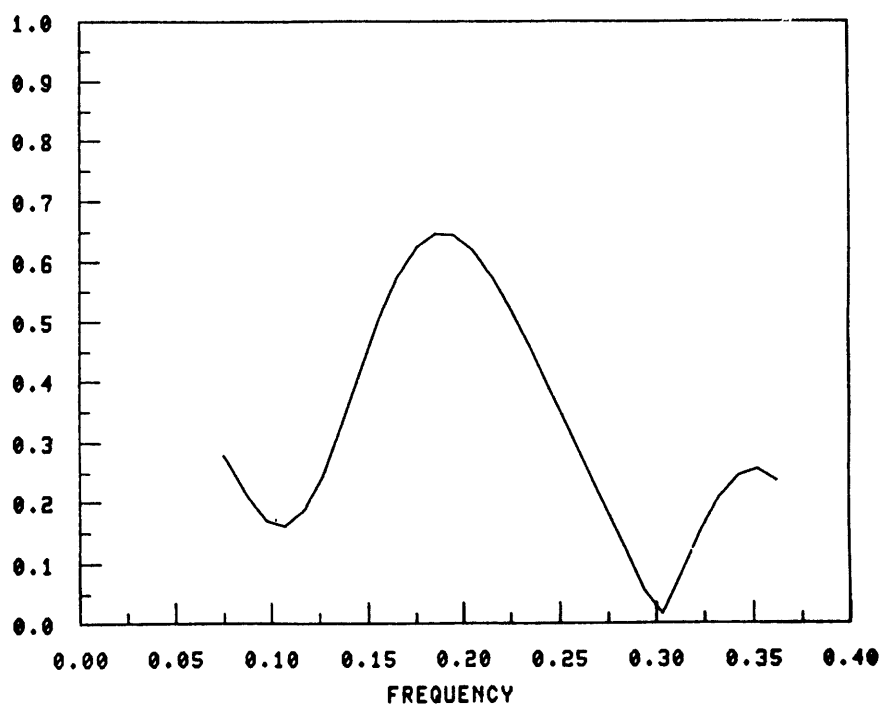


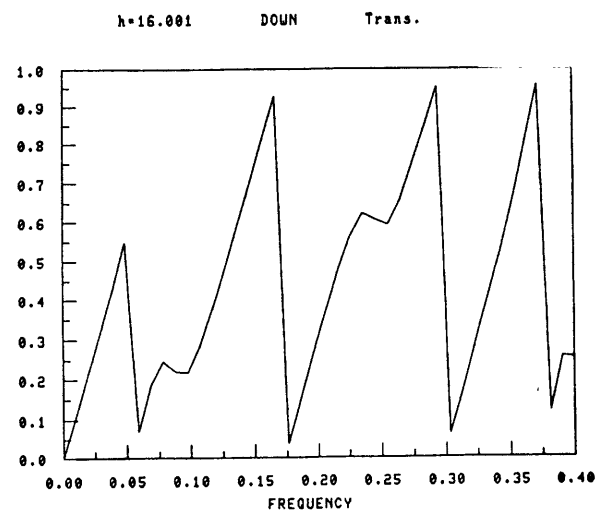
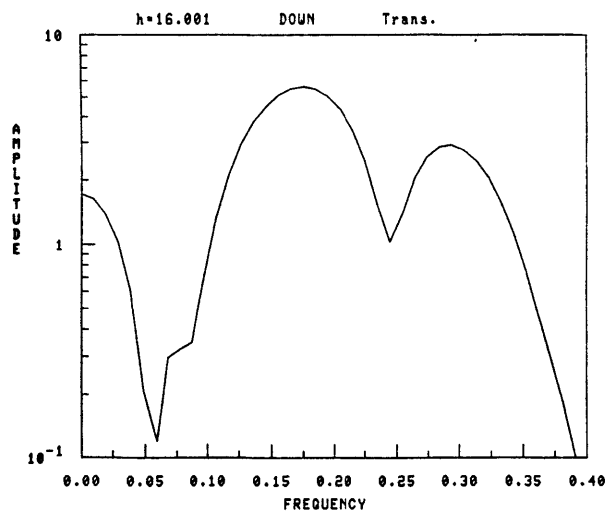
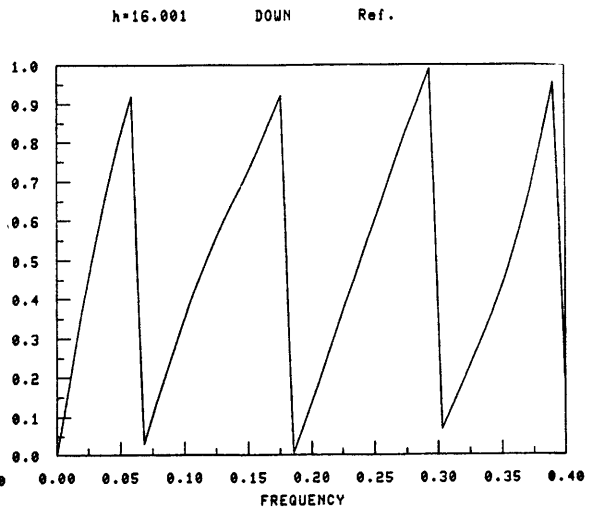
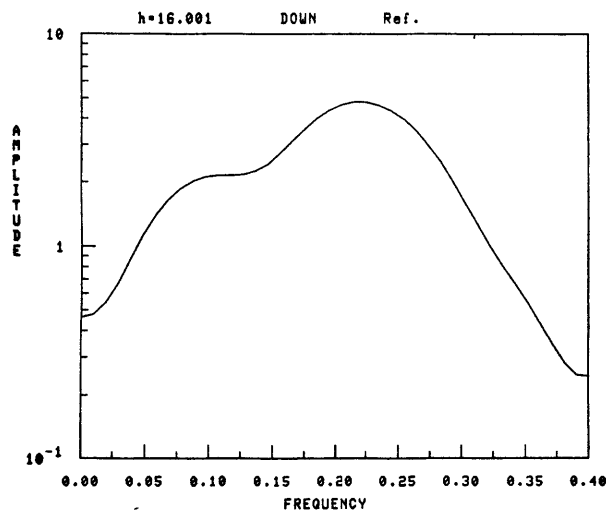
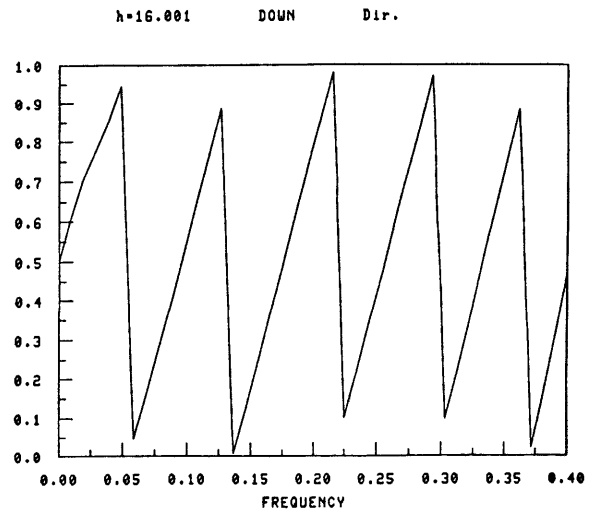
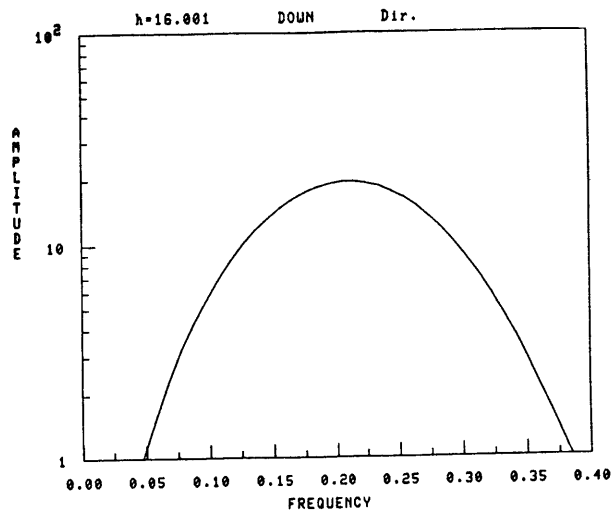


REF. COEFF. (h=13.918 DOWN)



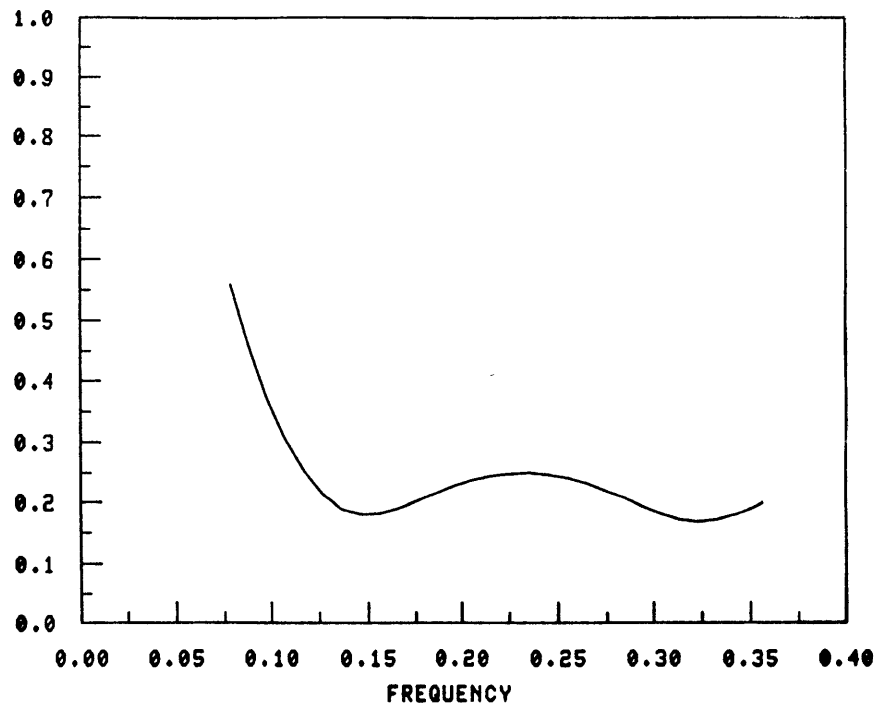
TRANS. COEFF. (h=13.918 DOWN)



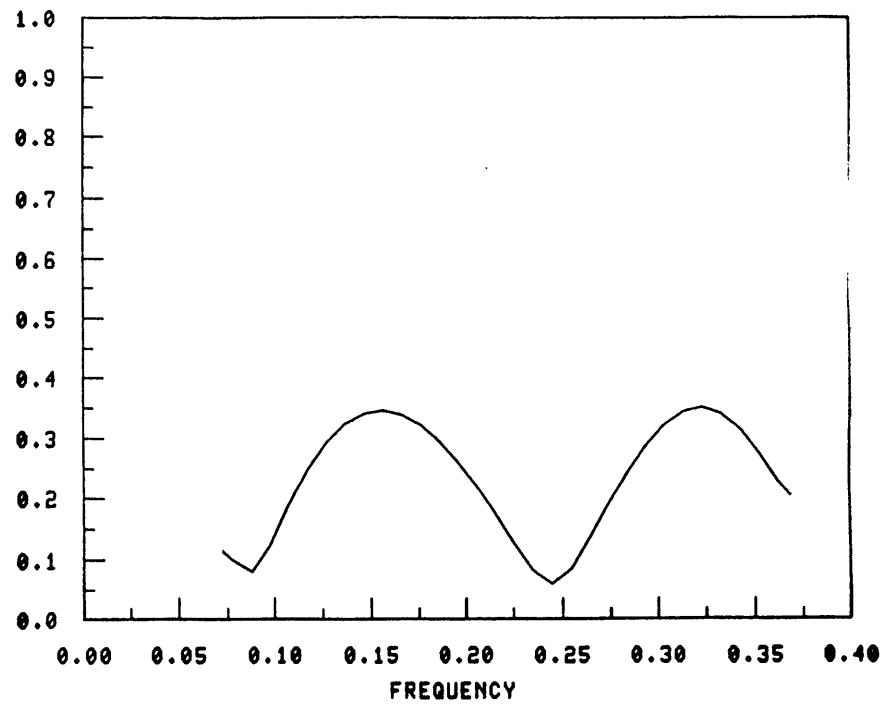


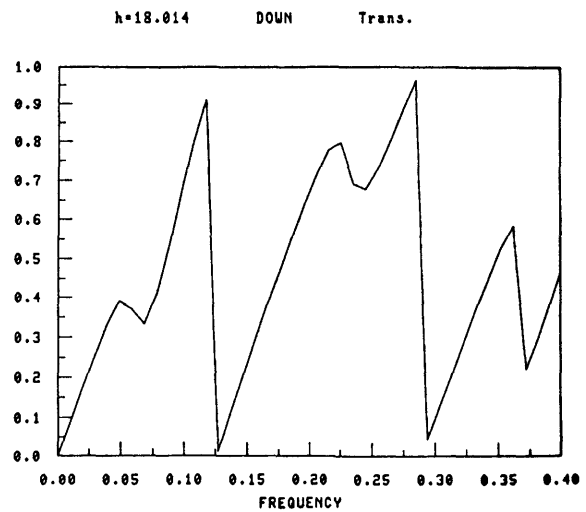
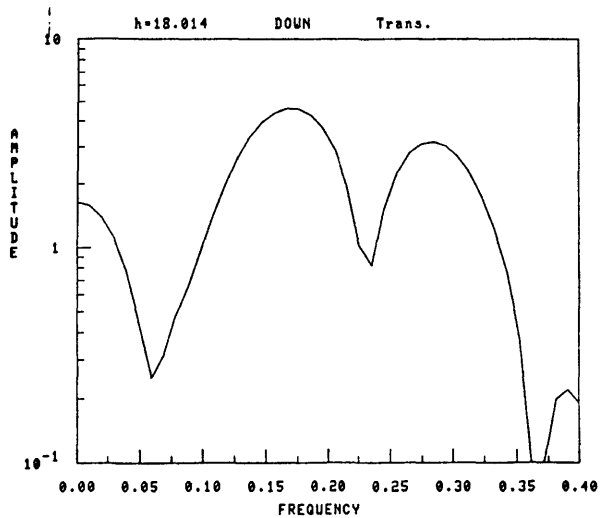
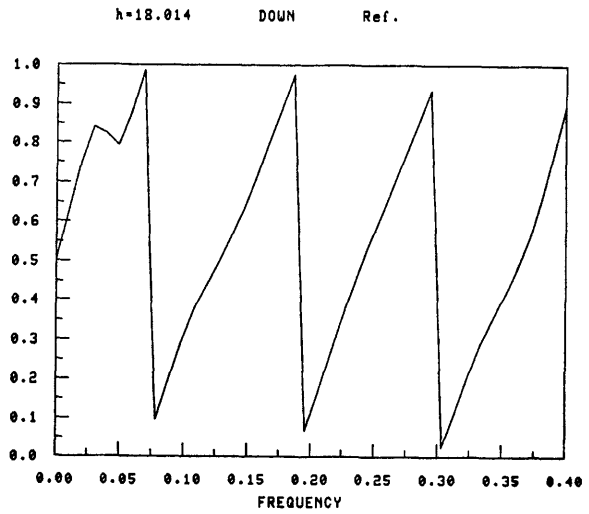
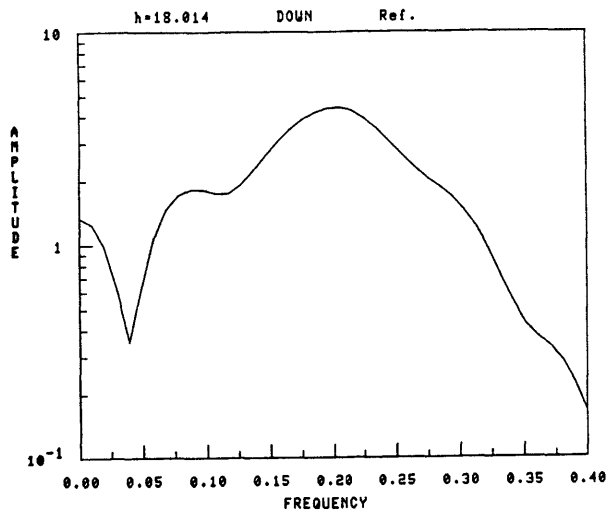
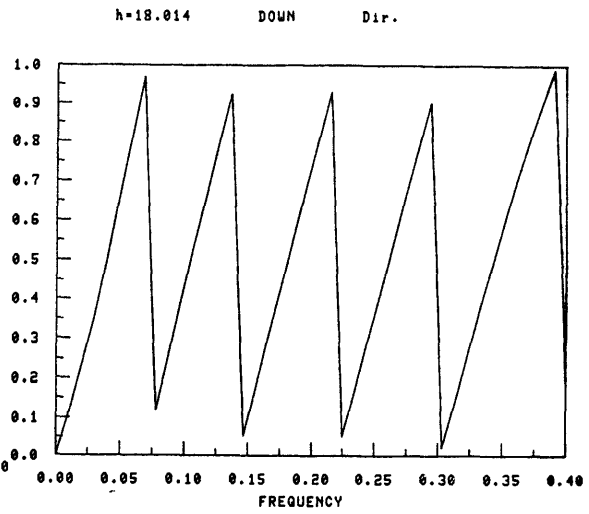
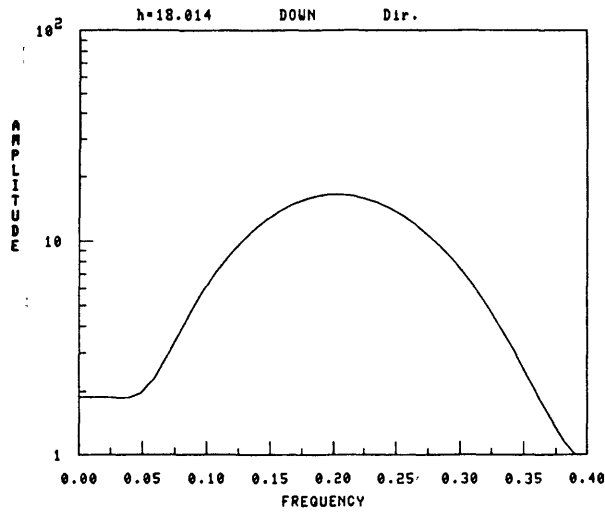


REF. COEFF. (h=16.001 DOWN)

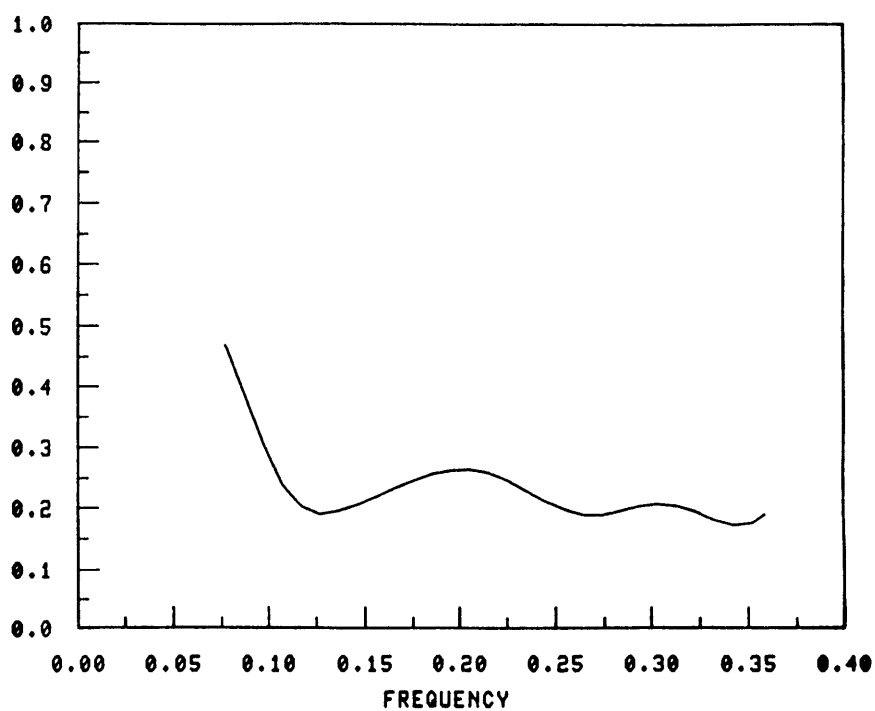


TRANS. COEFF. (h=16.001 DOWN)

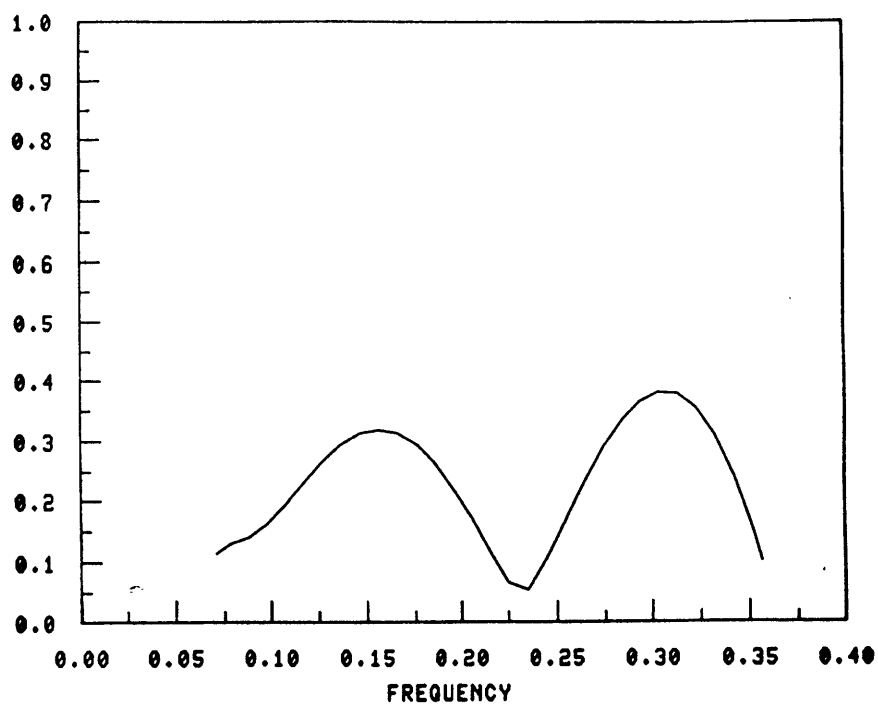


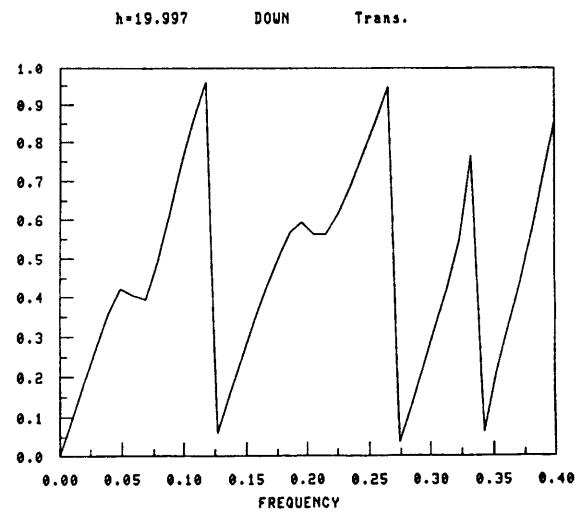
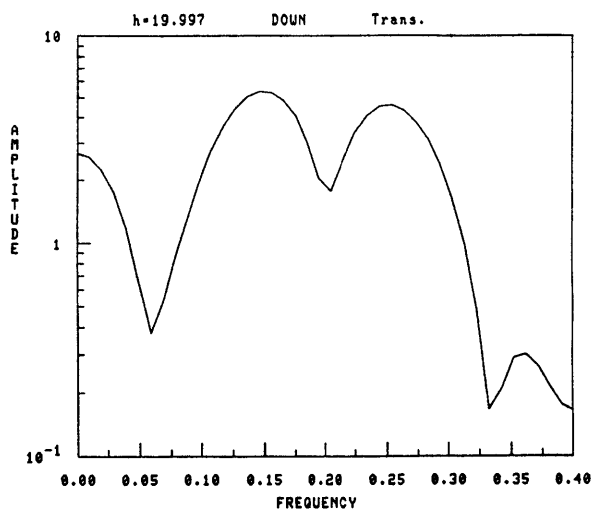
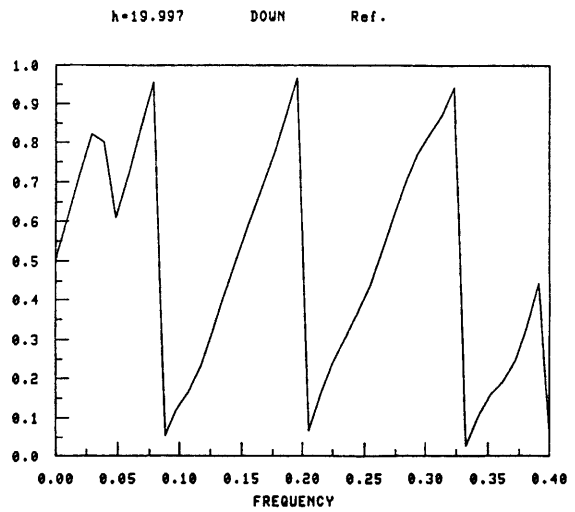
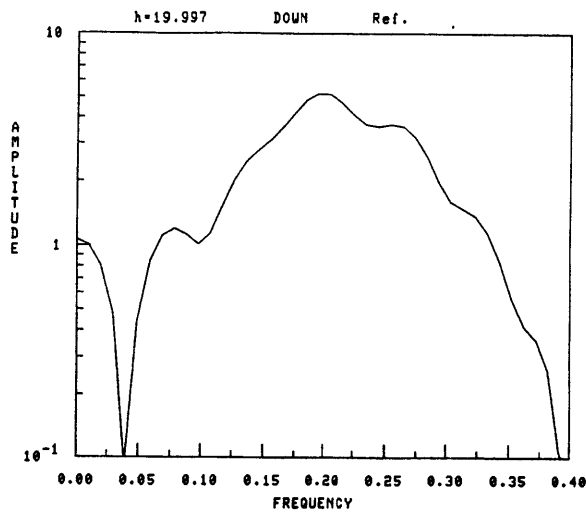
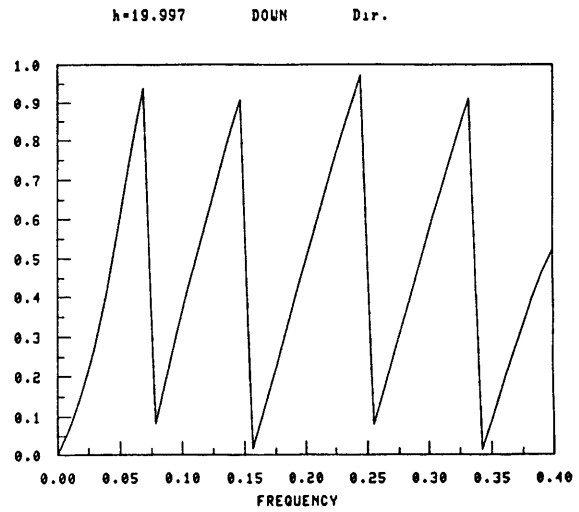
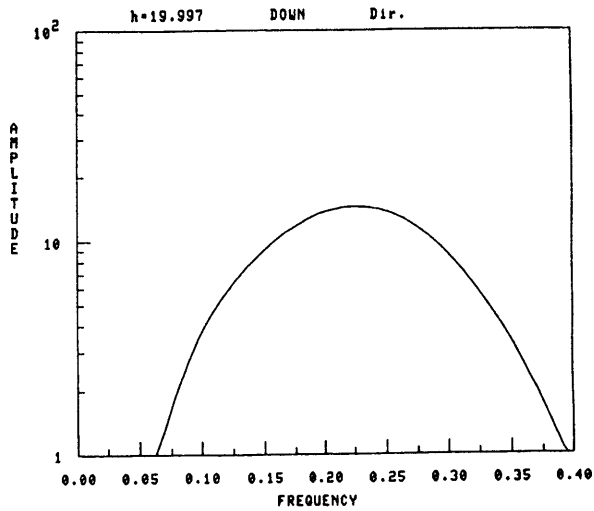


REF. COEFF. (h=18.014 DOWN)

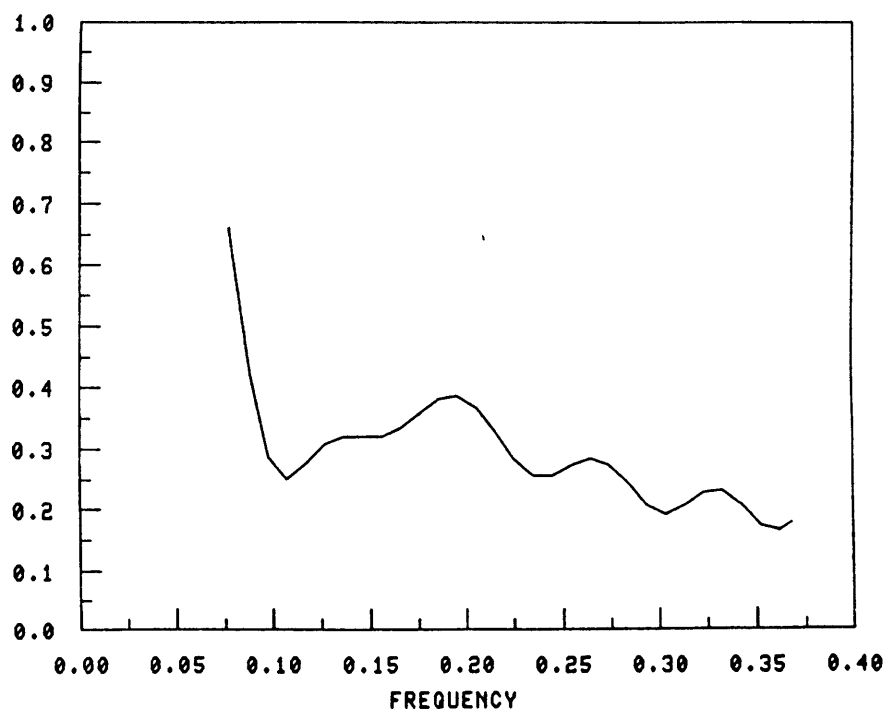


TRANS. COEFF. (h=18.014 DOWN)

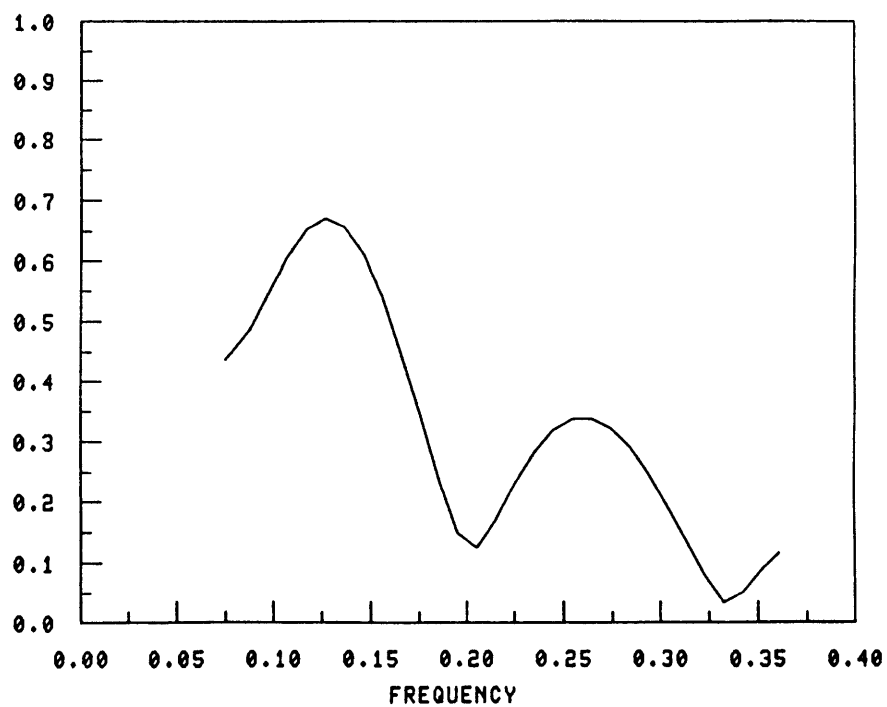


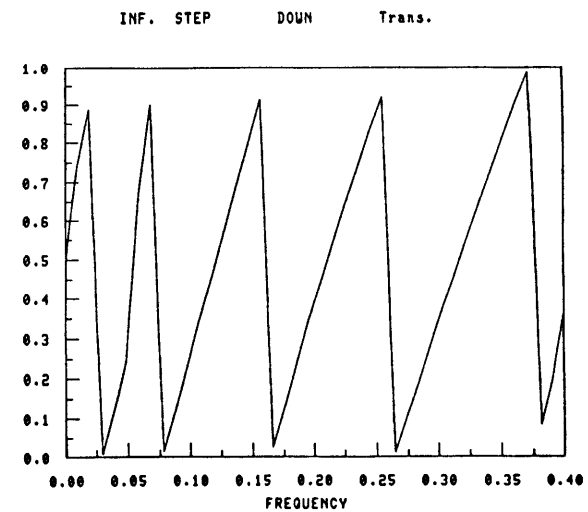
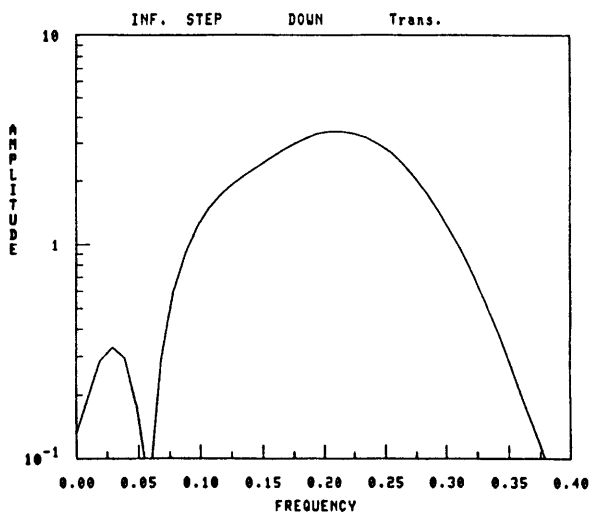
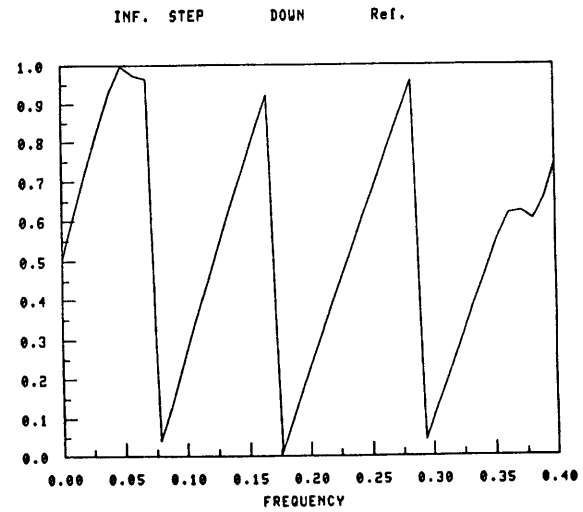
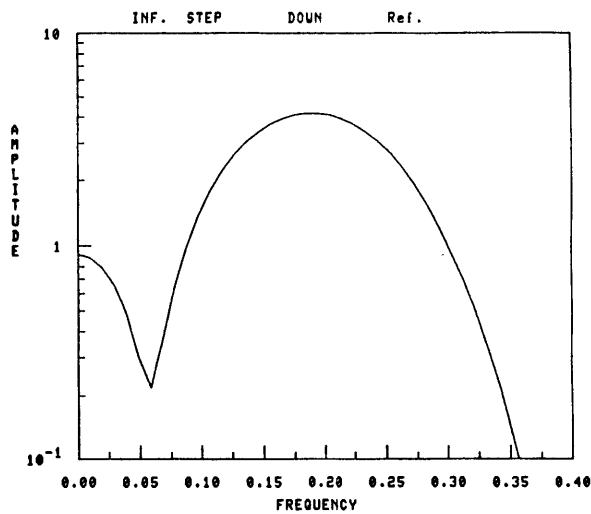
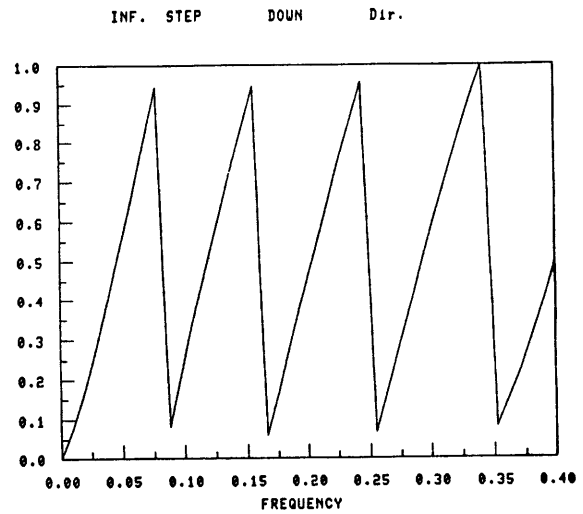
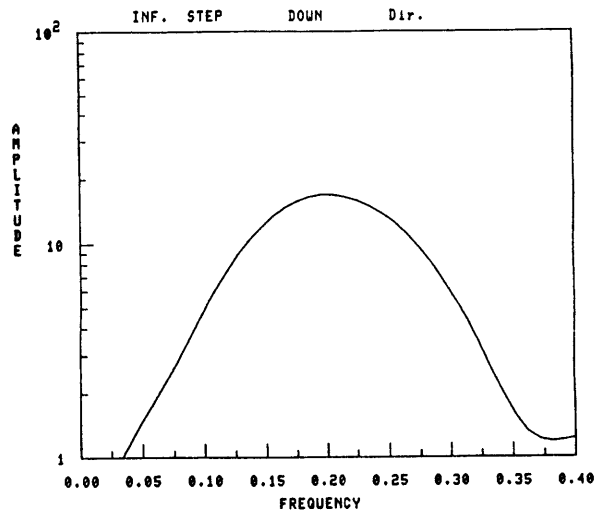


REF. COEFF. (h=19.997 DOWN)

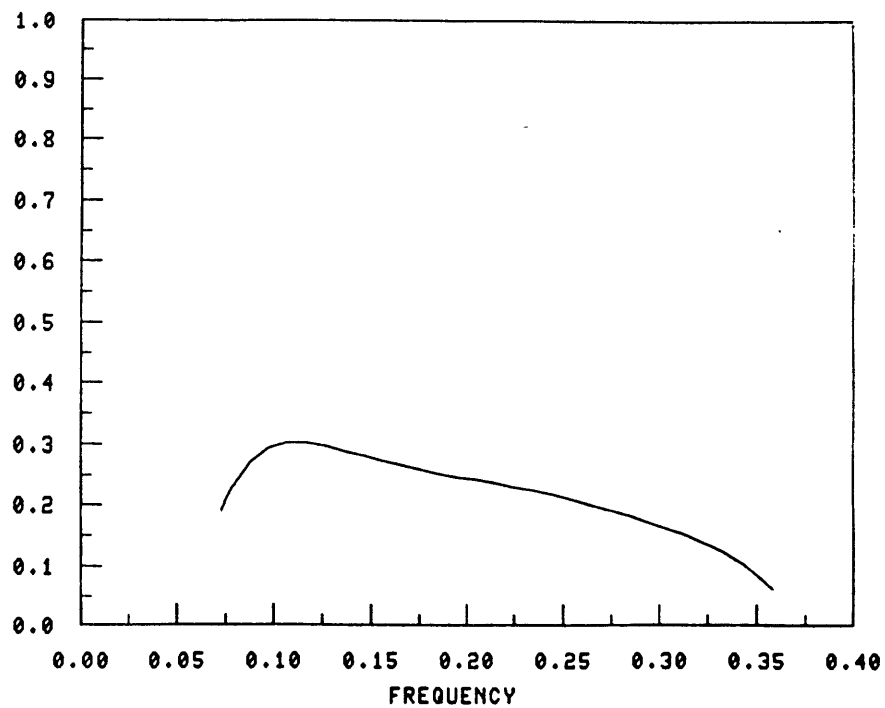


TRANS. COEFF. (h=19.997 DOWN)

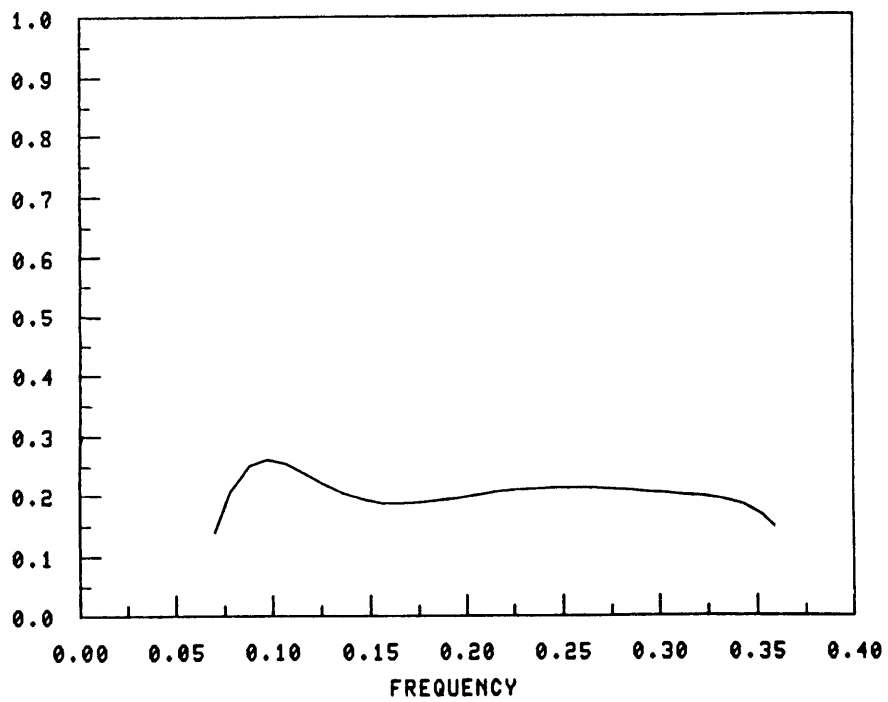




REF. COEFF. (Inf Step DOWN)



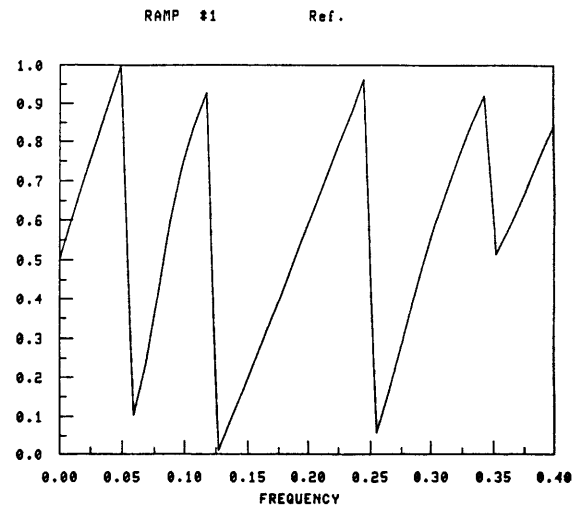
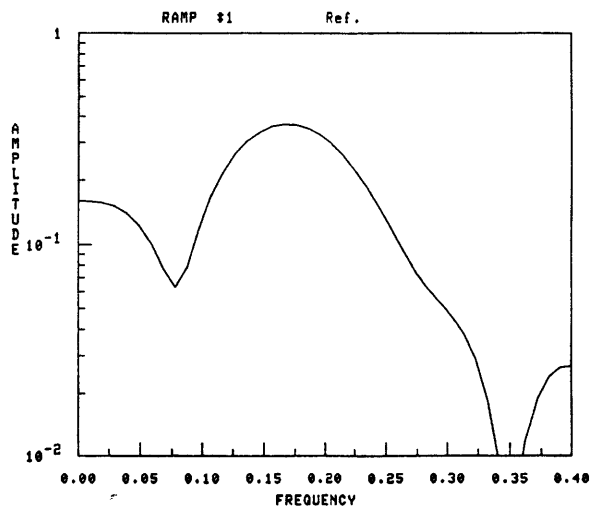
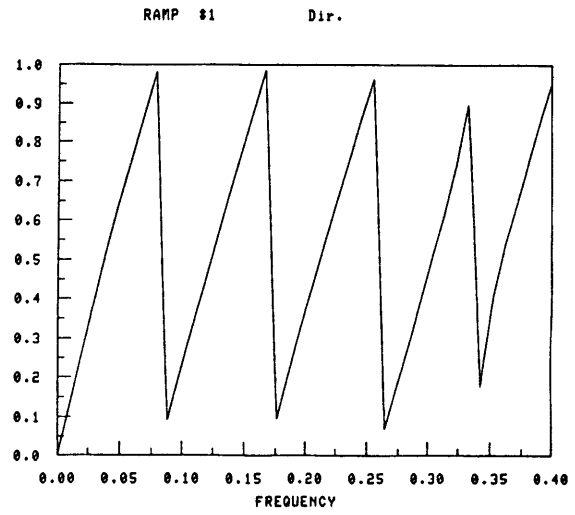
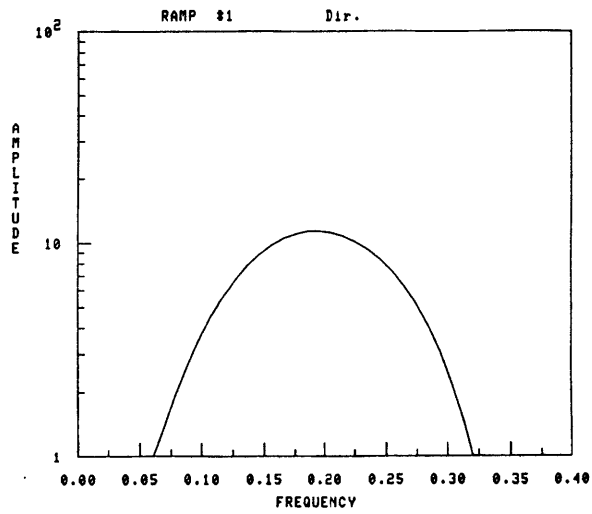
TRANS. COEFF. (Inf. Step DOWN)

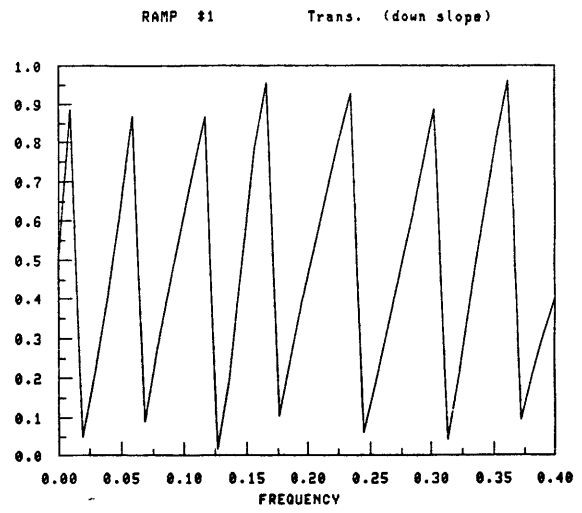
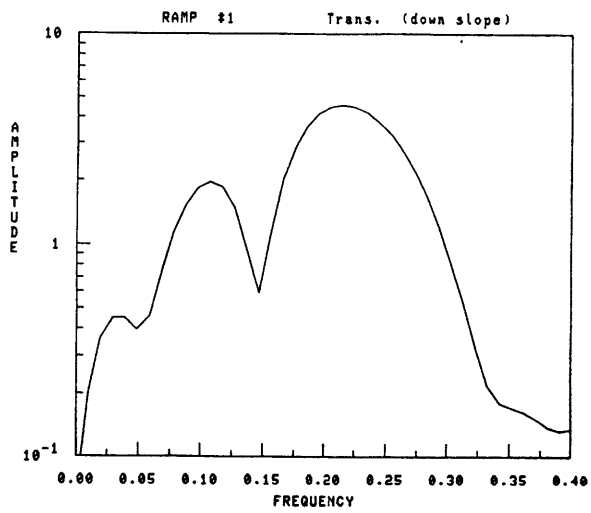
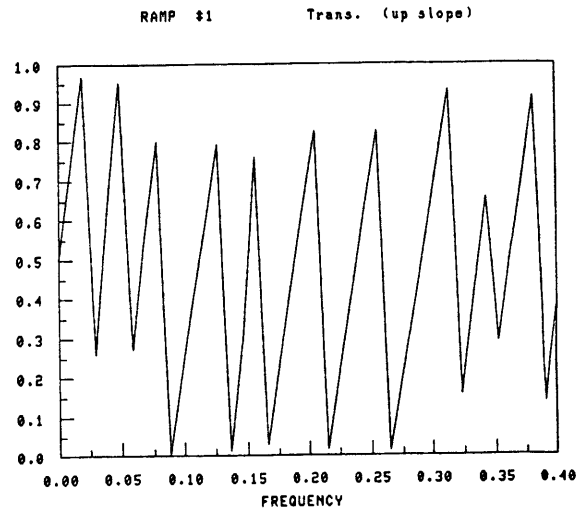
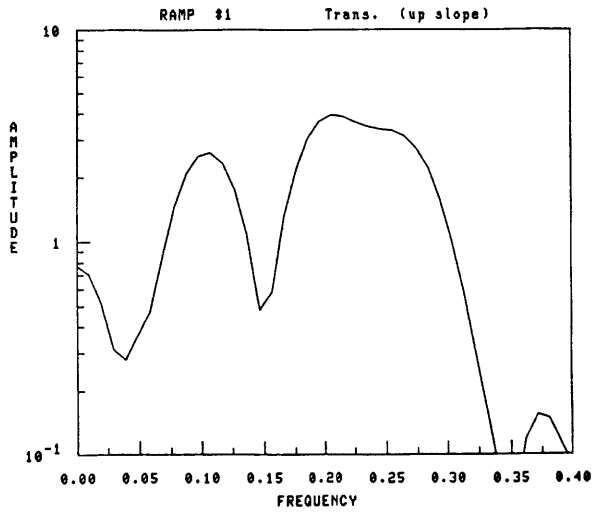


## APPENDIX B

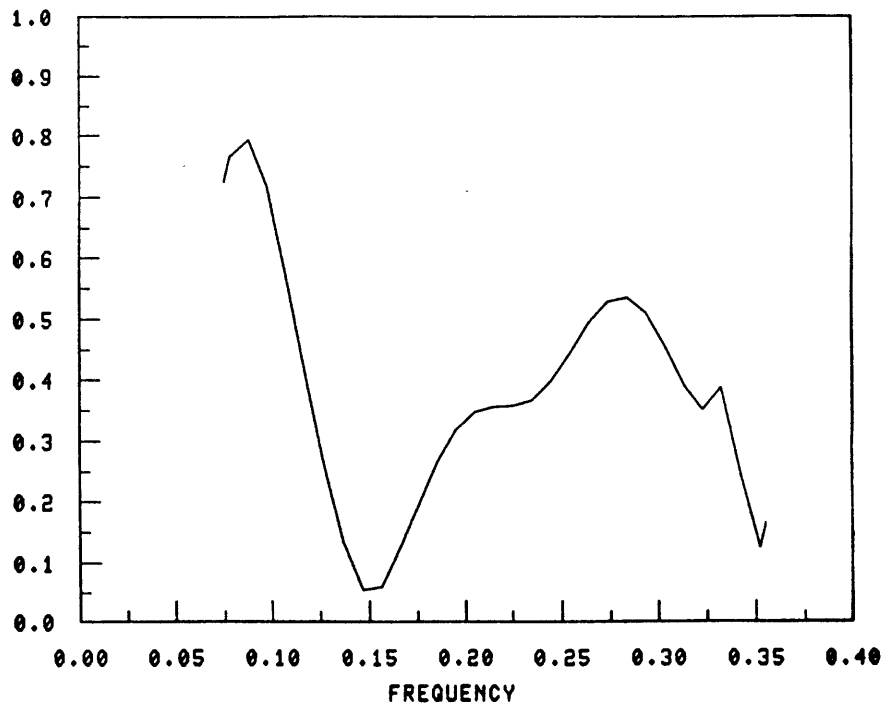
This appendix contains the amplitude and phase spectra plots as well as the reflection and transmission coefficient curves for all of the mountain-like features. The dimensions of the features are shown with the figures displaying their seismograms. (The amplitude spectra are displayed in the left column and the phase spectra are in the right column.) The seismograms were digitized and then the plots were generated by computer. The amplitude scale is in arbitrary units. The relative amplitude for each set (direct, reflected, and transmitted) represents the correct values. The phase spectra are shown in fractions of a cycle. The units on the frequency axis are in MHz.



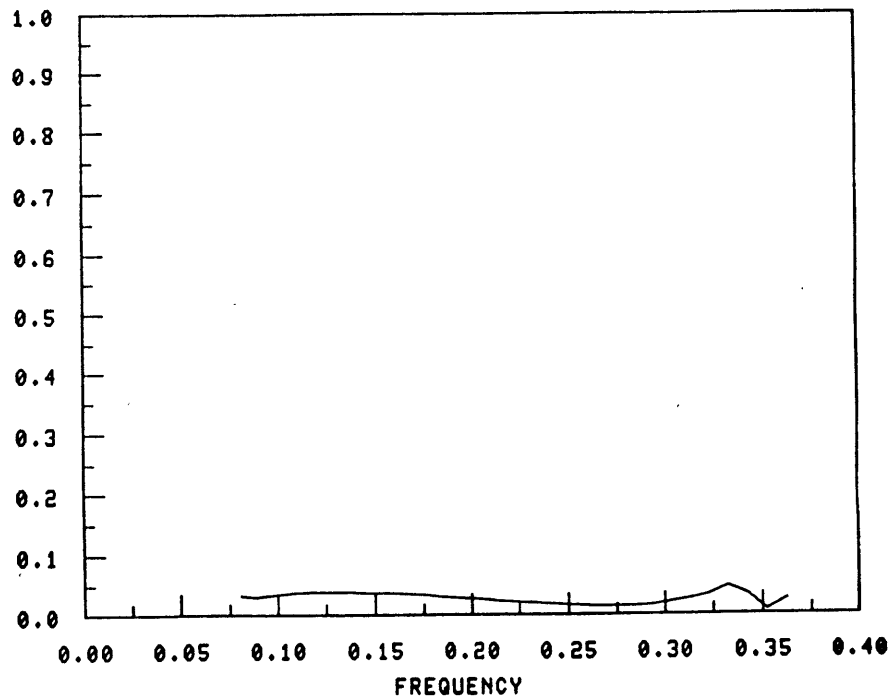




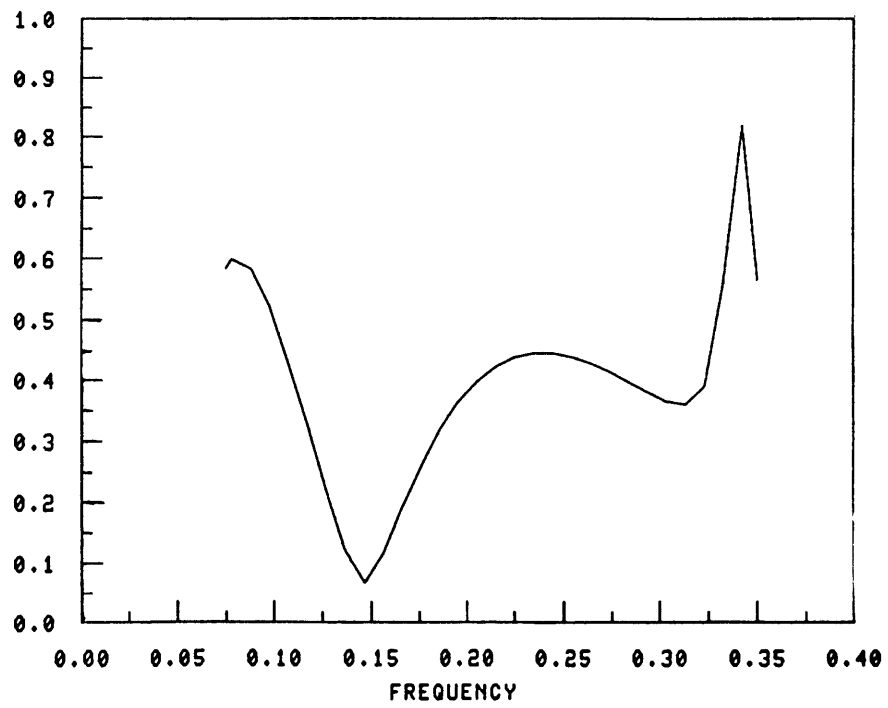
TRANS. COEFF. (up slope) (RAMP #1)

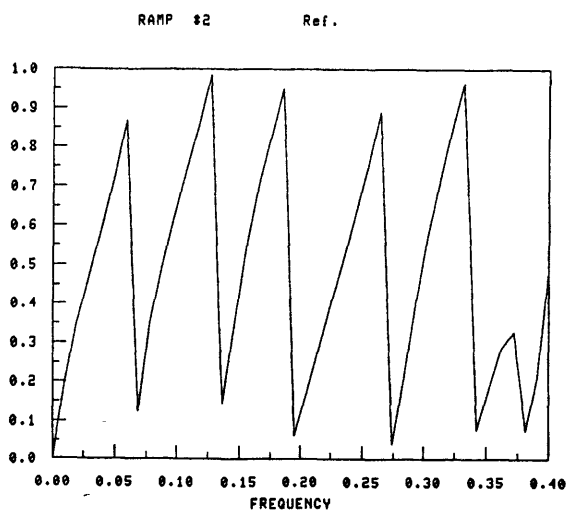
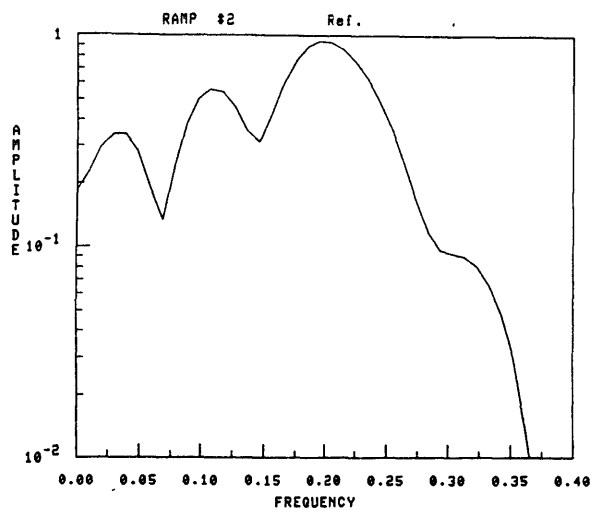
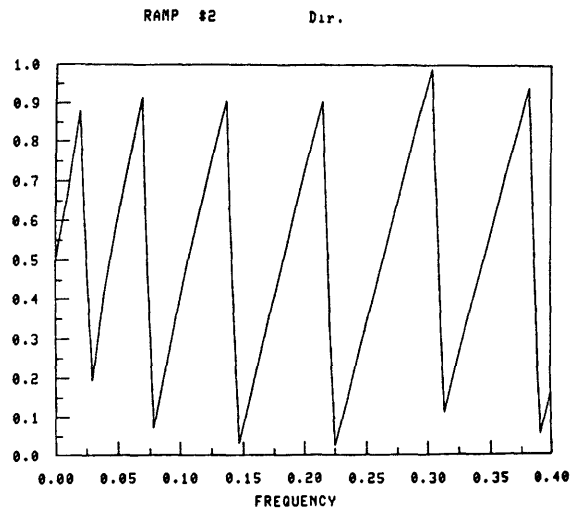
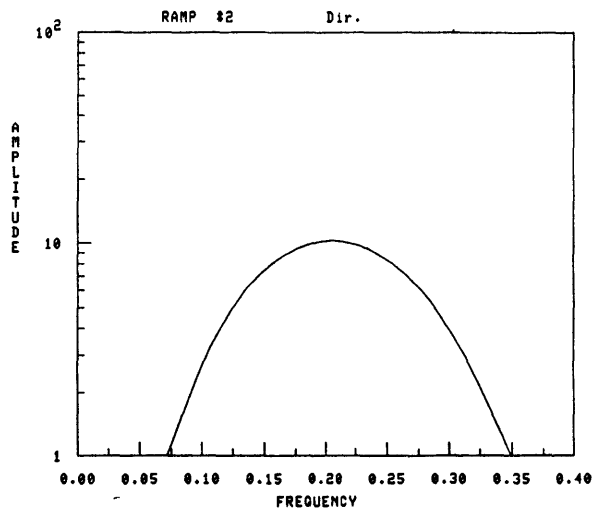


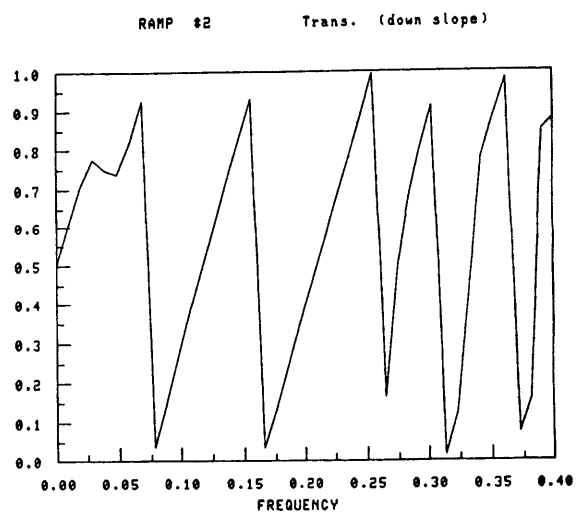
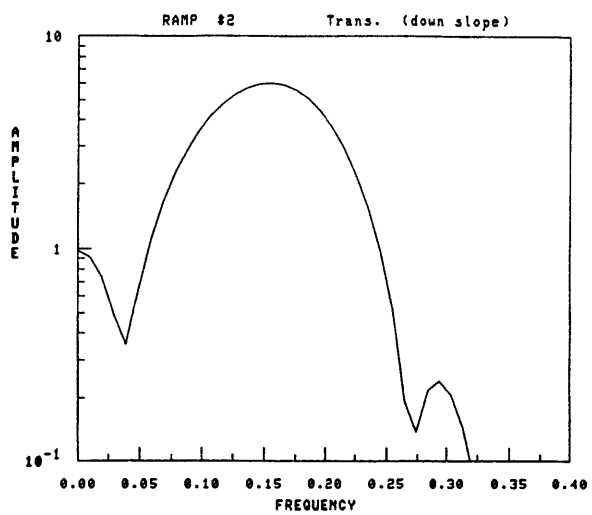
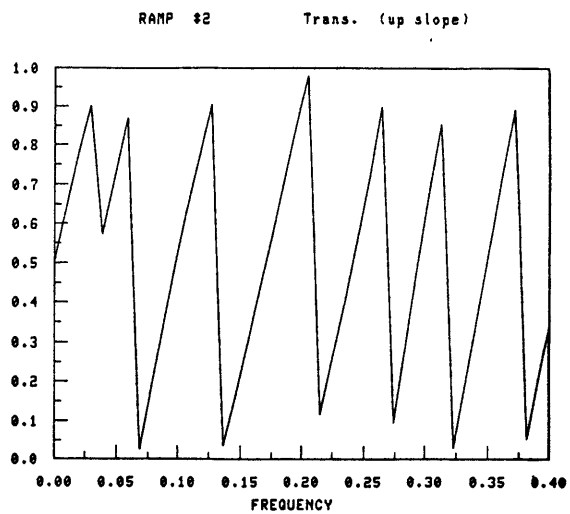
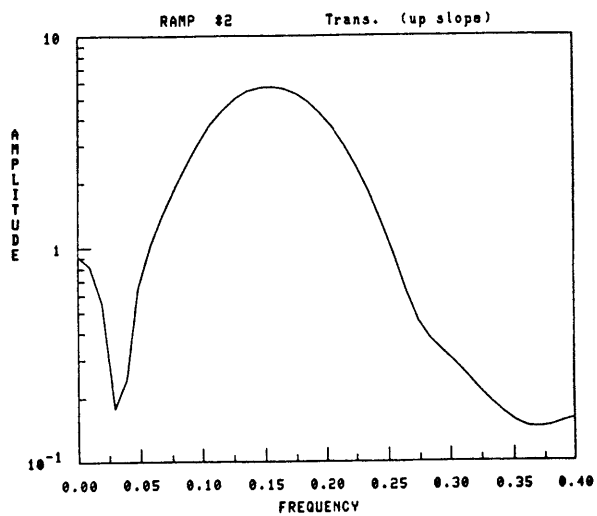
REF. COEFF. (RAMP #1)



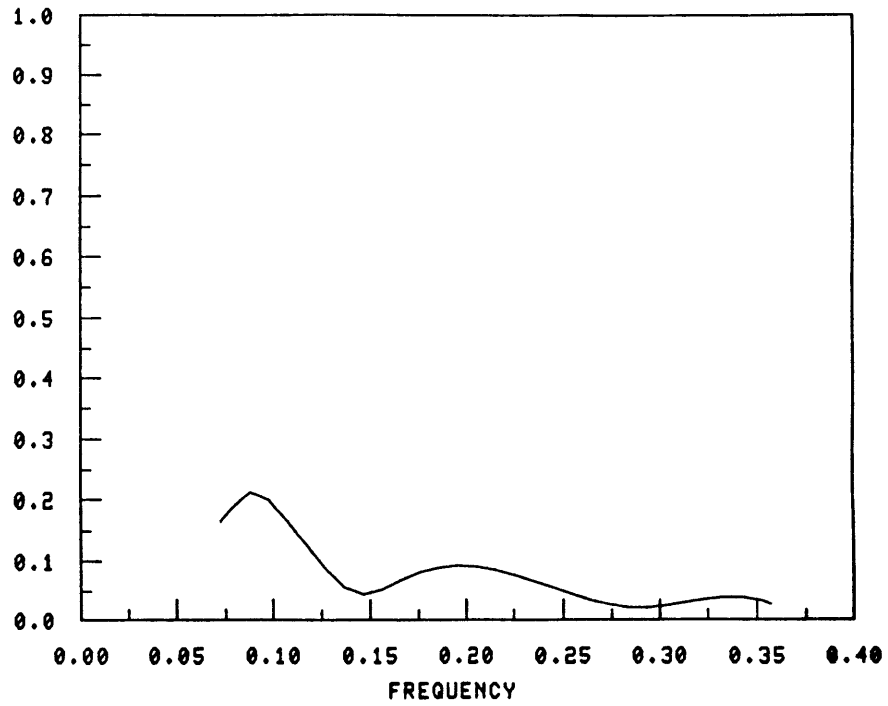
TRANS. COEFF. (down slope) (RAMP #1)



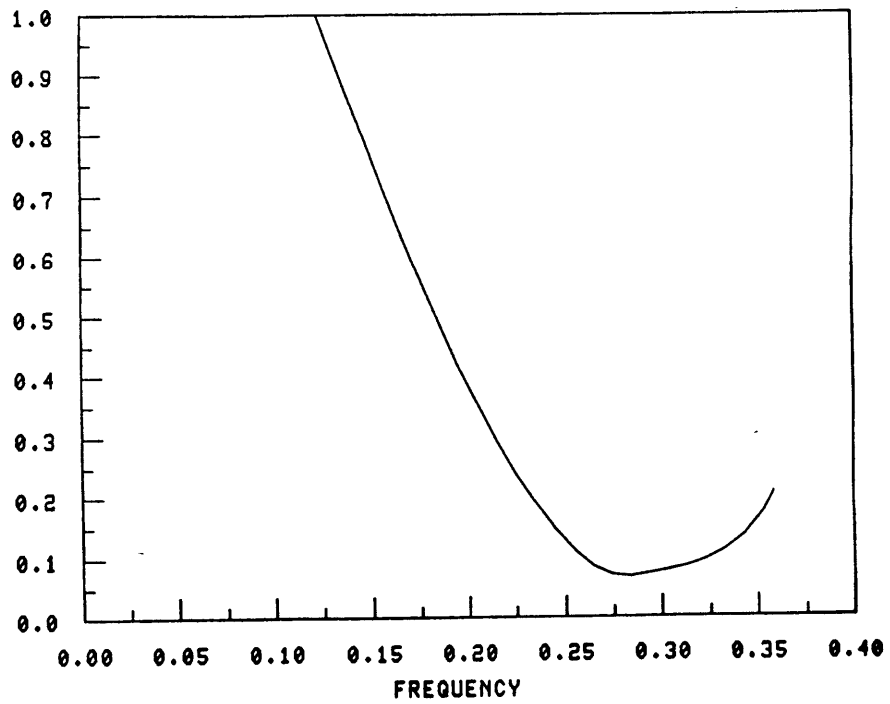




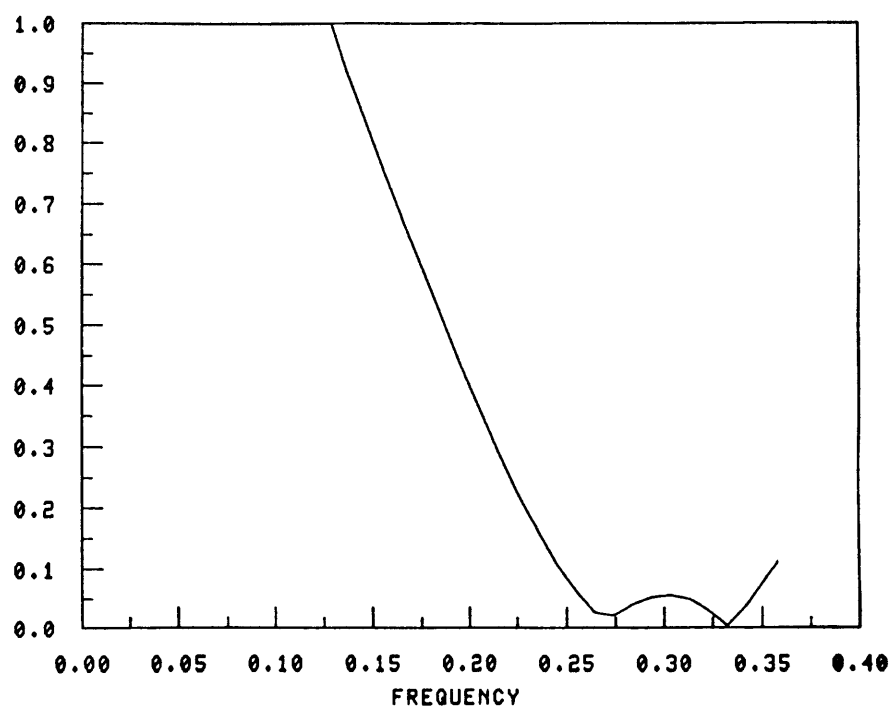
REF. COEFF. (RAMP #2)



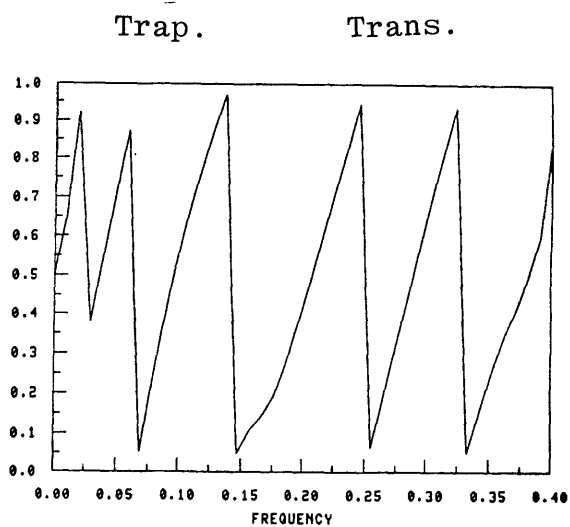
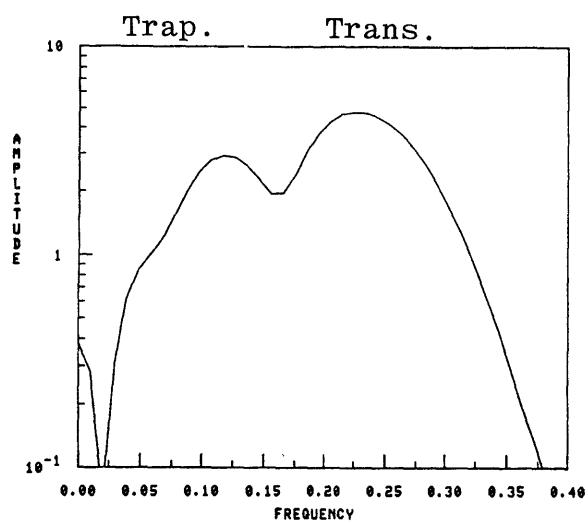
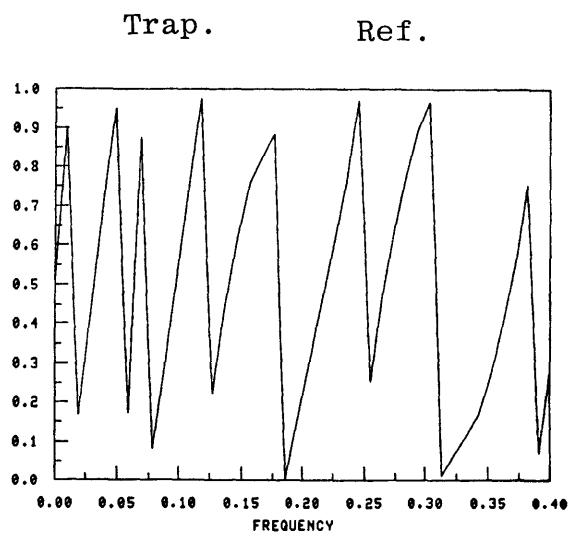
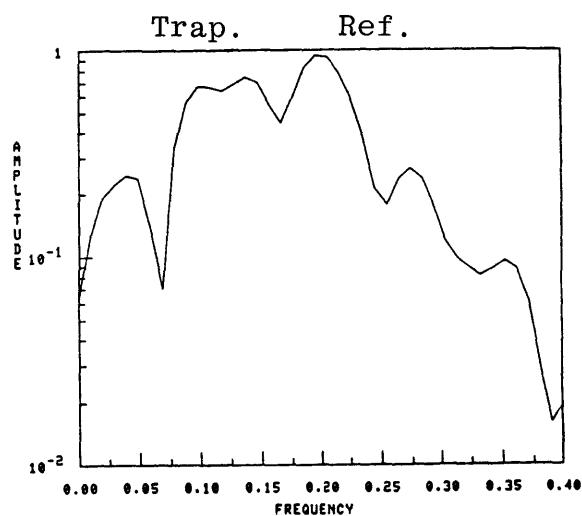
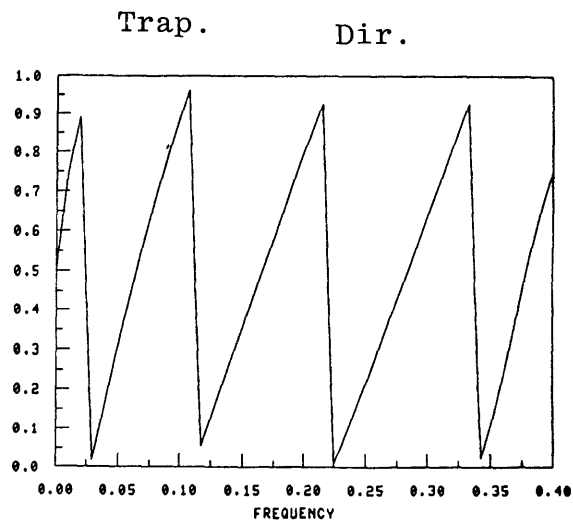
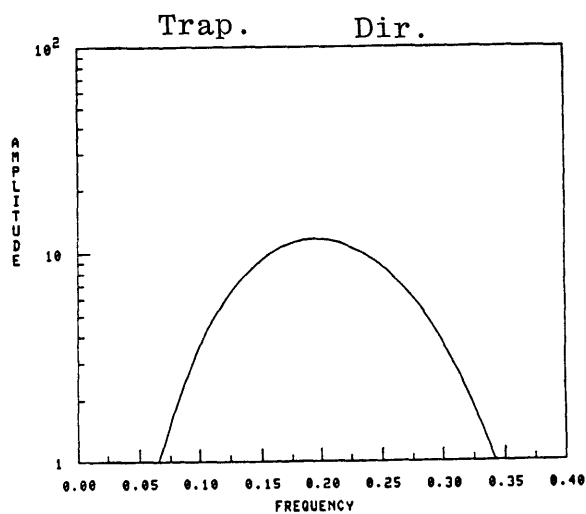
TRANS. COEFF. (up slope) (RAMP #2)



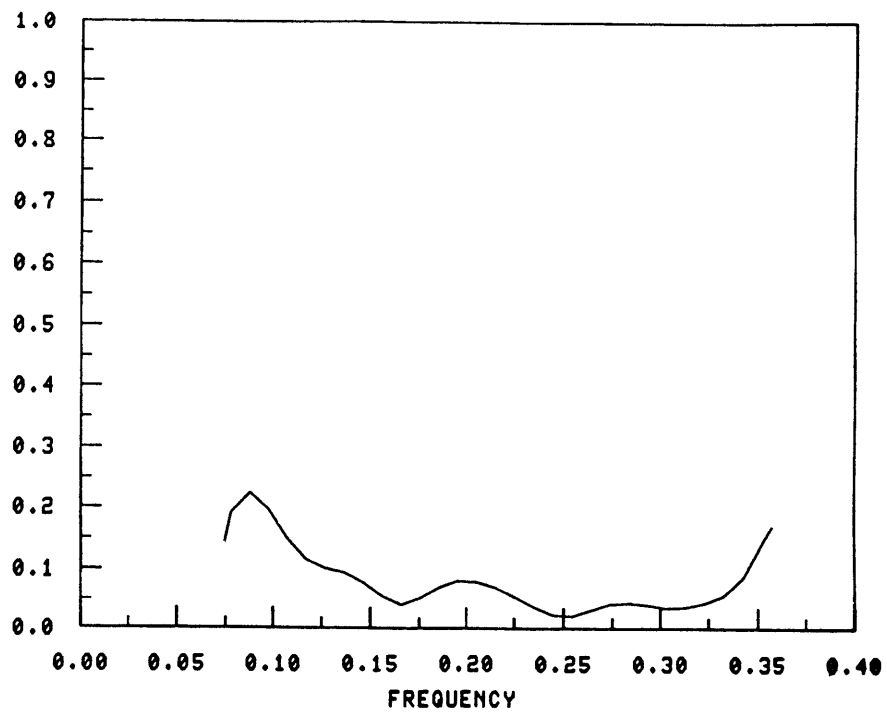
TRANS. COEFF. (down slope) (RAMP #2)



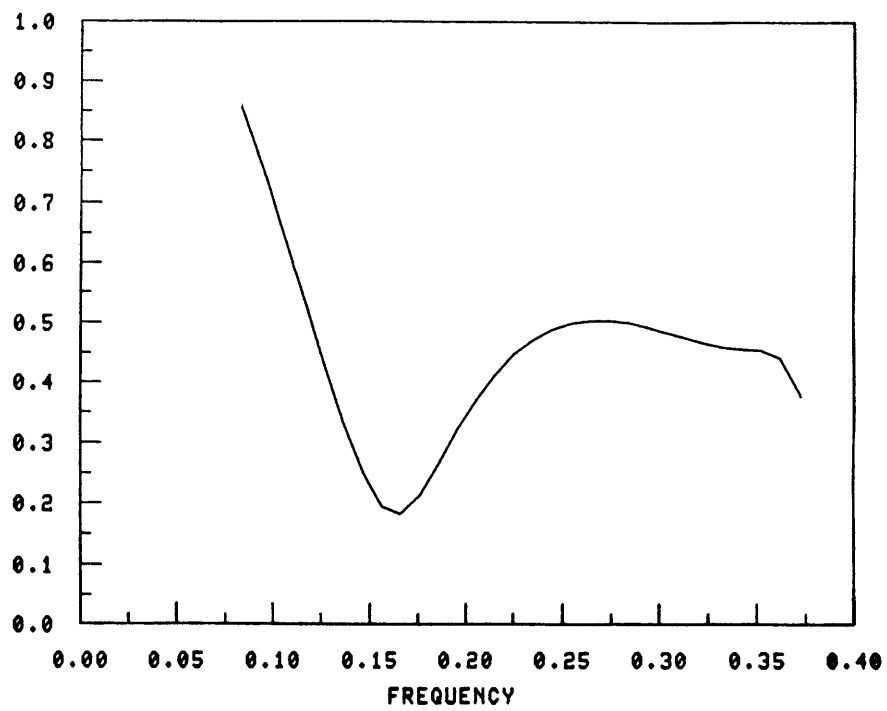


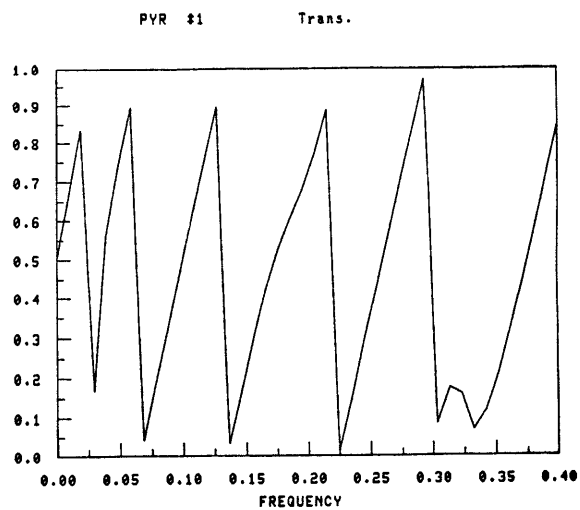
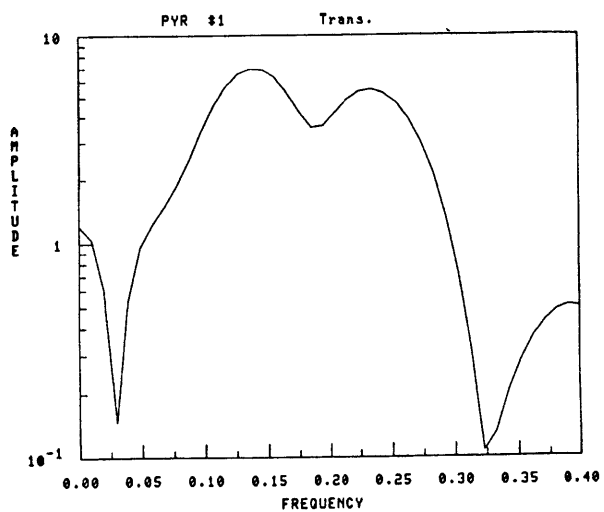
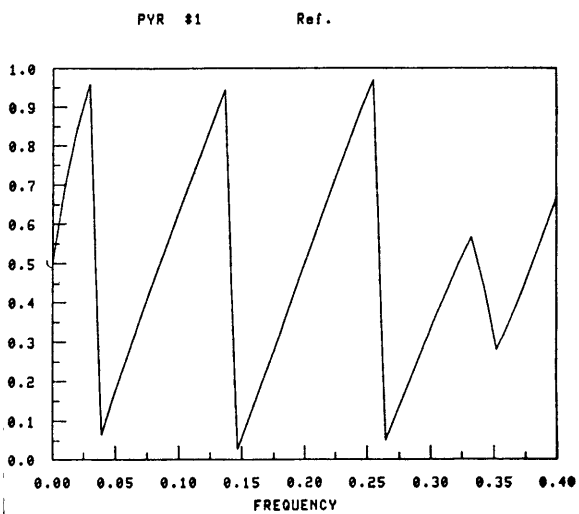
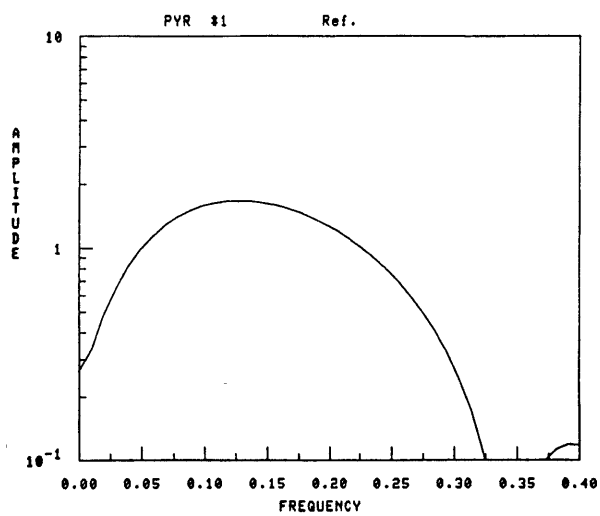
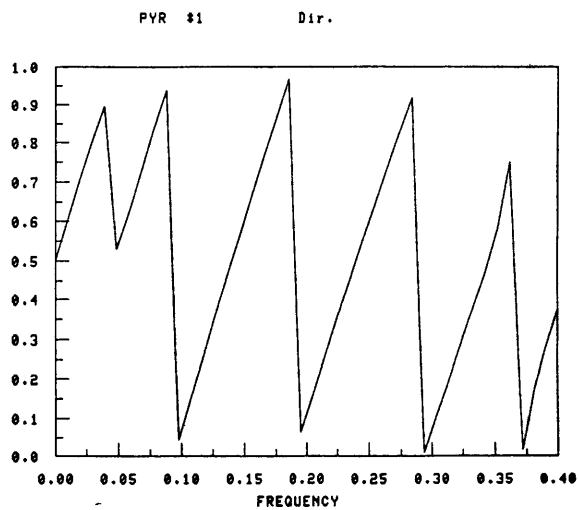
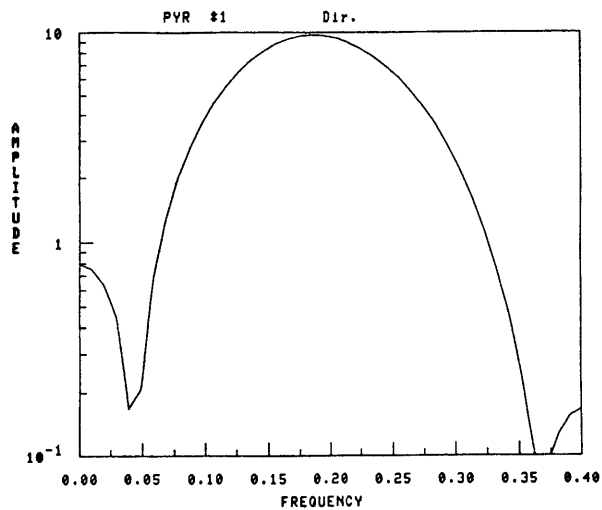


REF. COEFF. (Trap.)

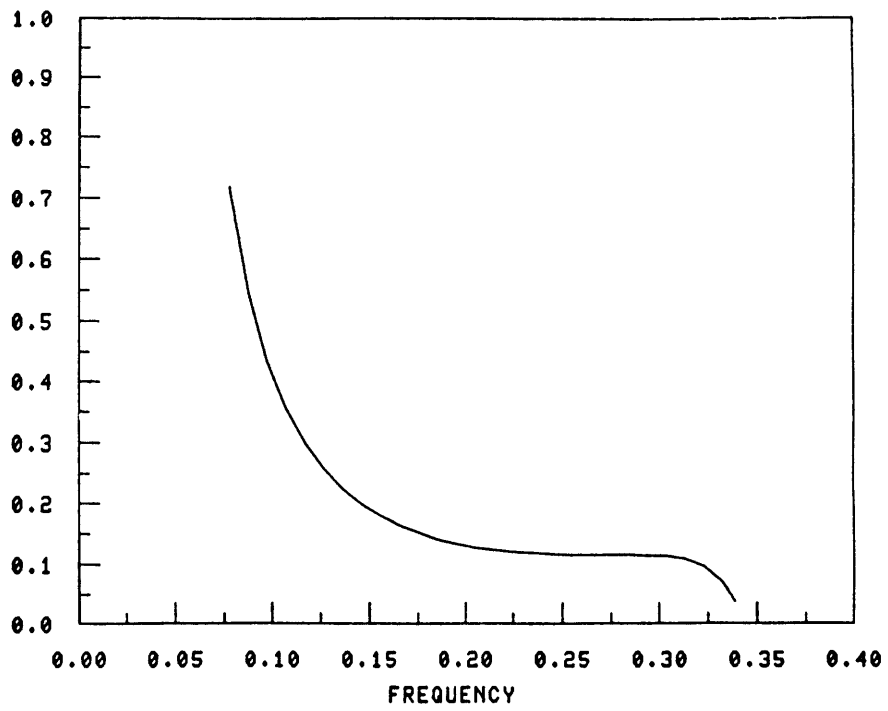


TRANS. COEFF. (Trap.)

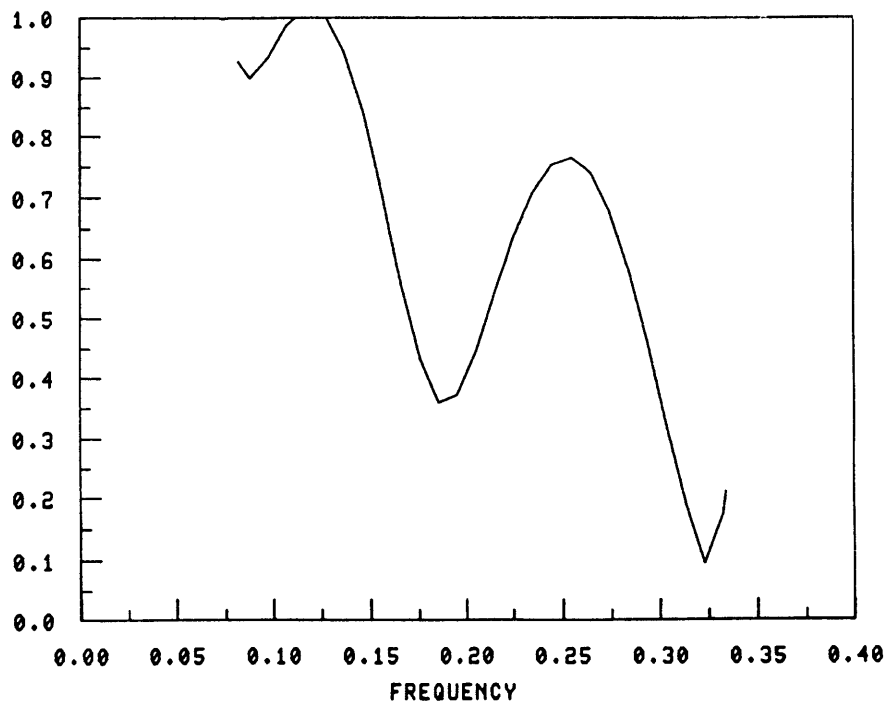


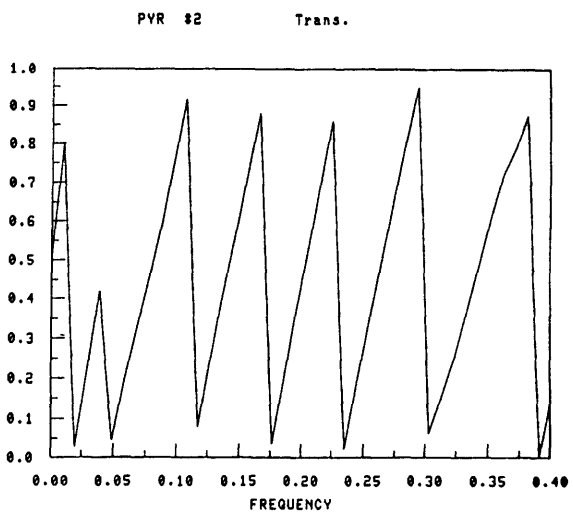
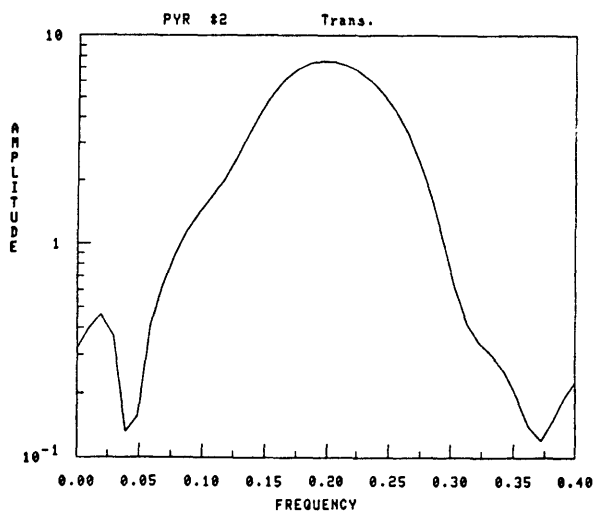
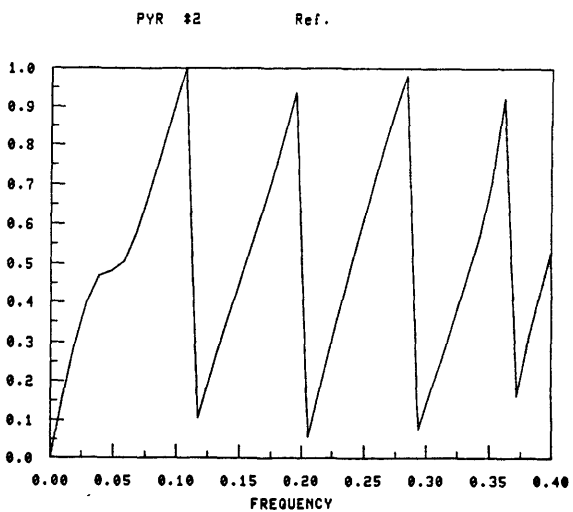
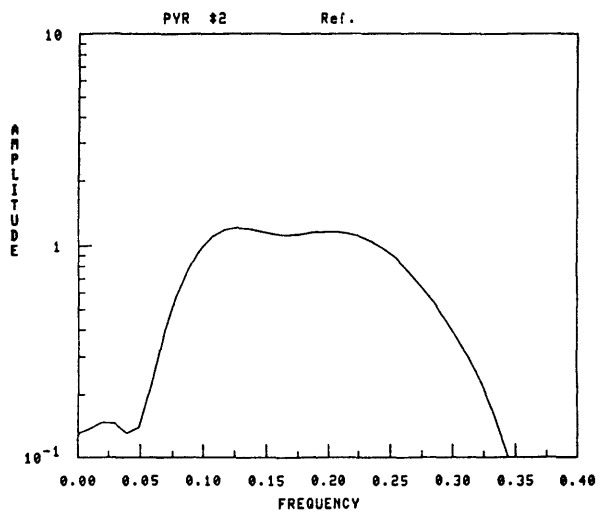
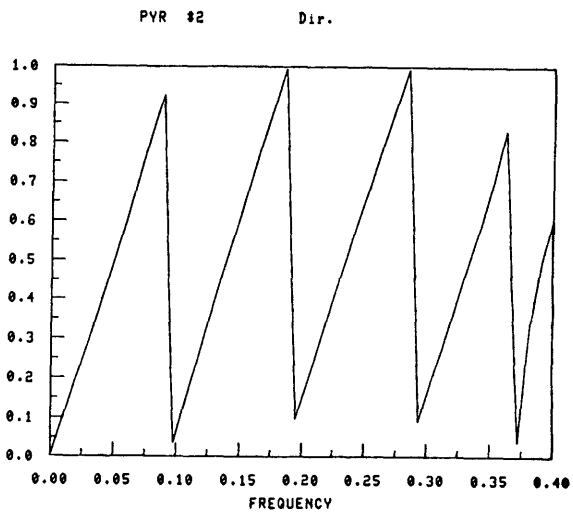
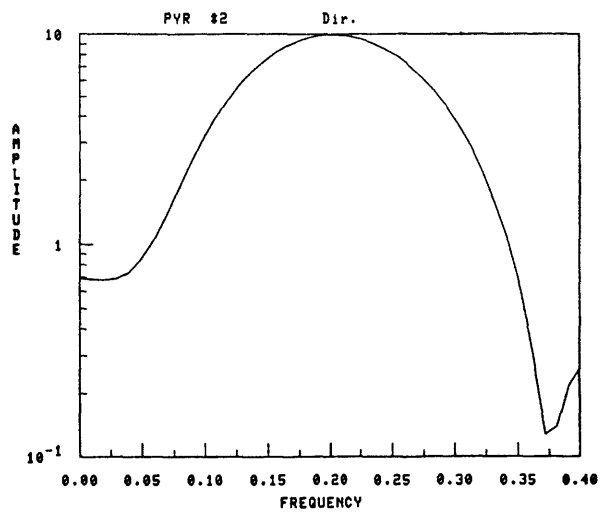


REF. COEFF. (PYR #1)

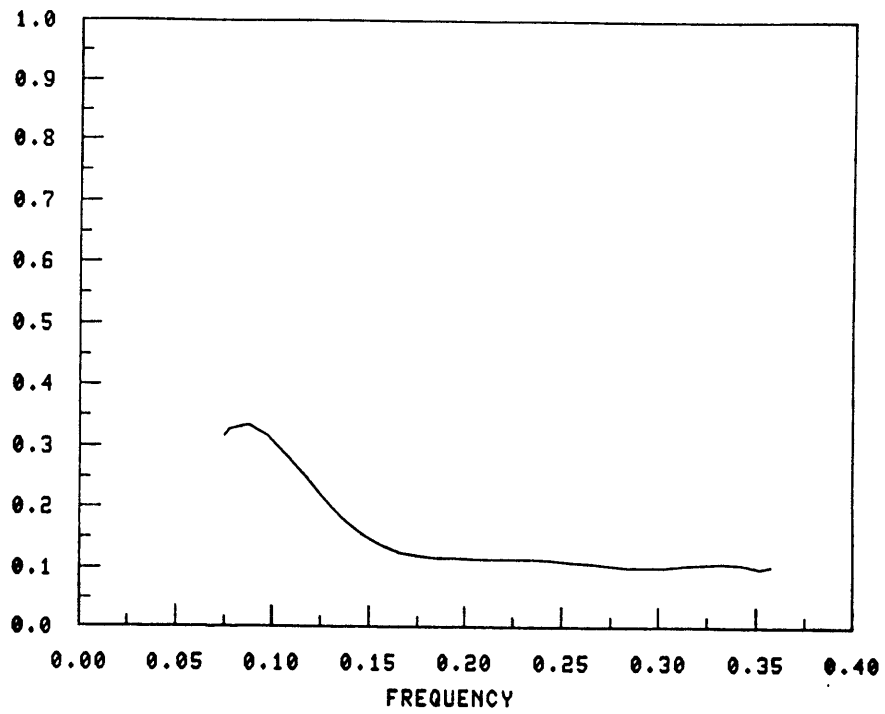


TRANS. COEFF. (PYR #1)

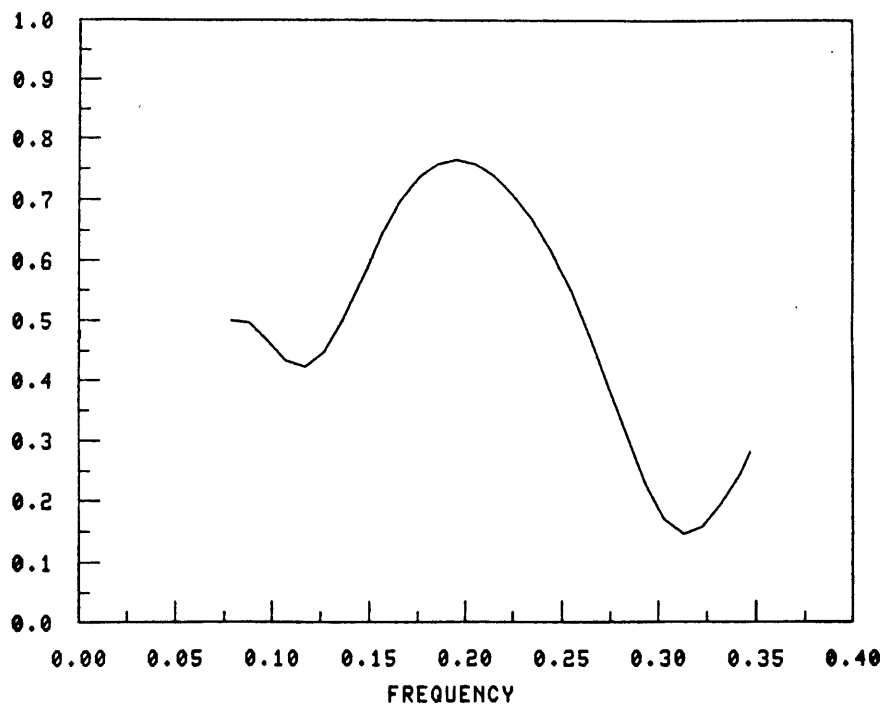


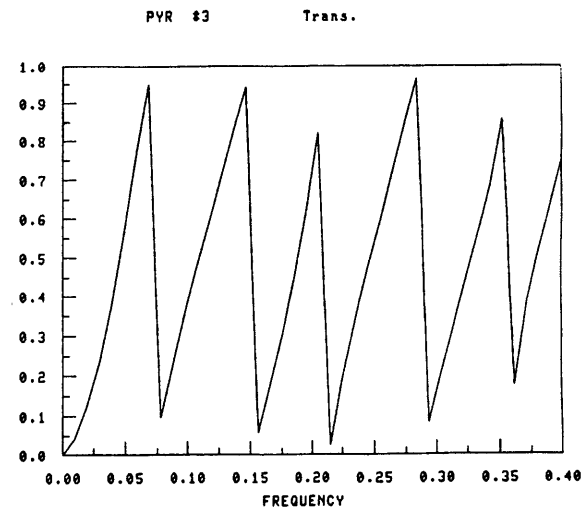
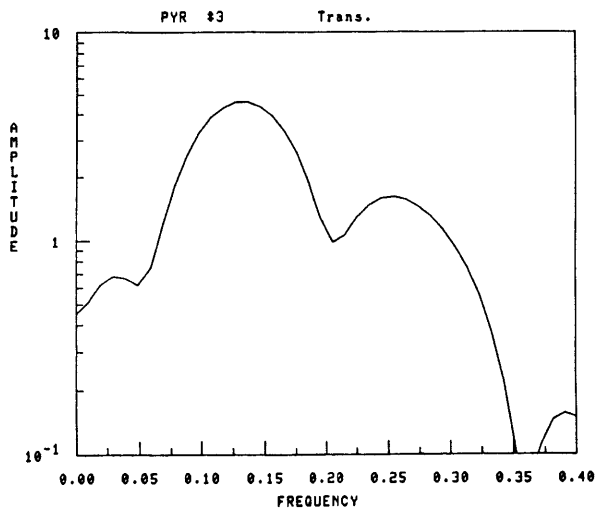
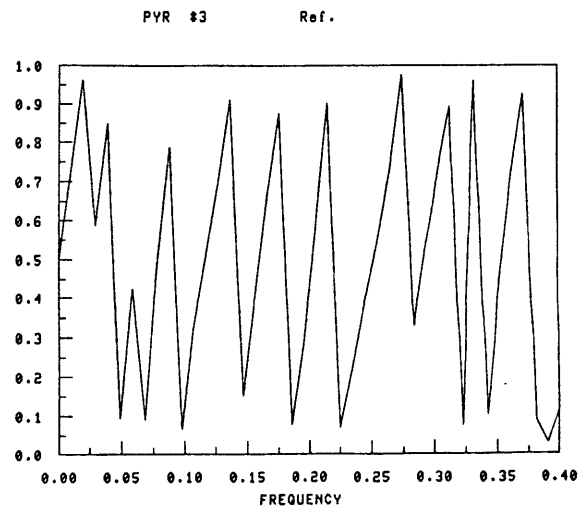
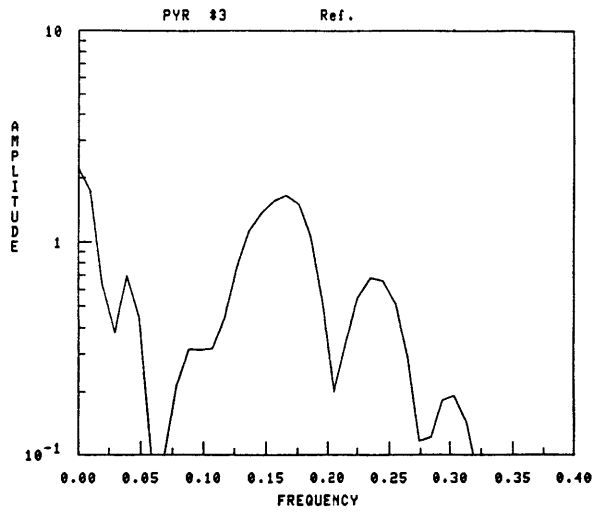
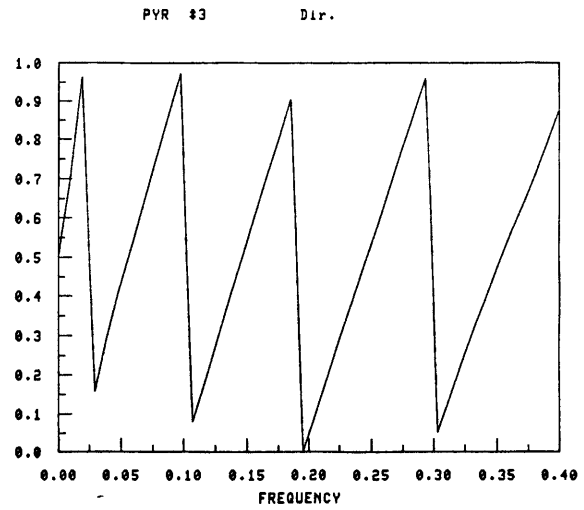
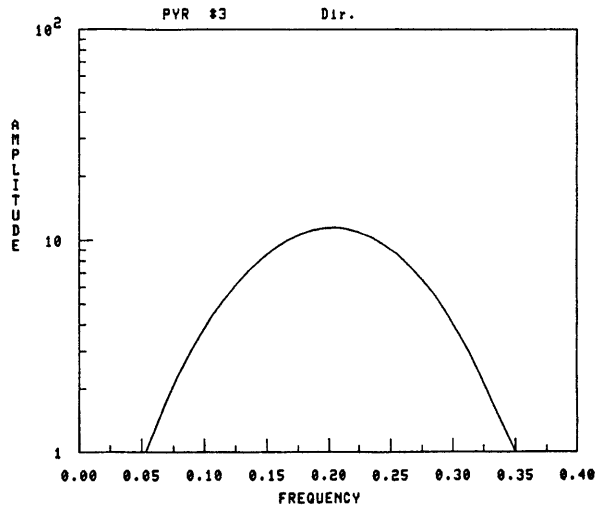


REF. COEFF. (PYR #2)

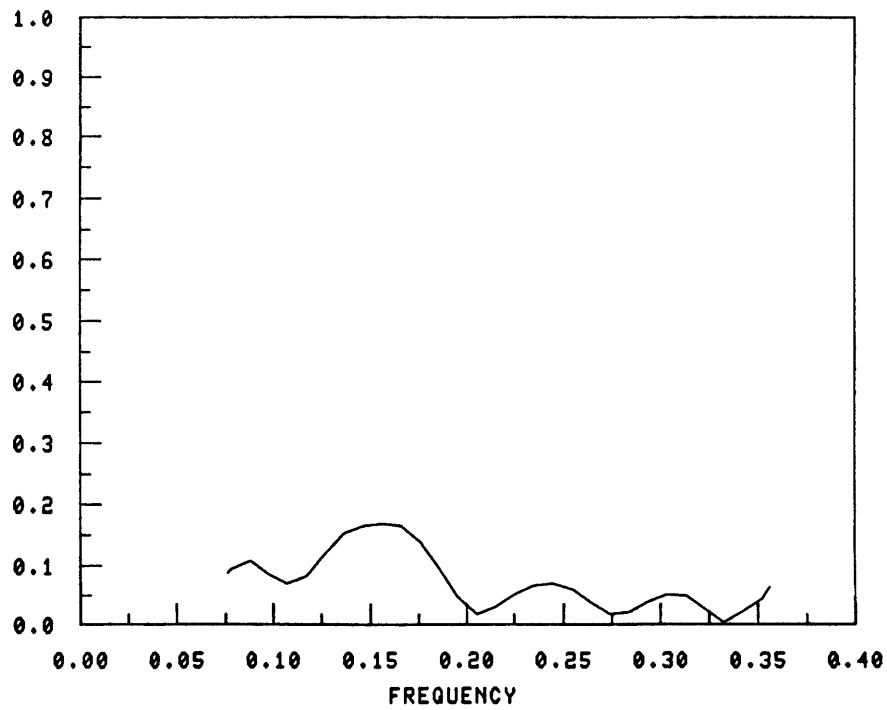


TRANS. COEFF. (PYR #2)

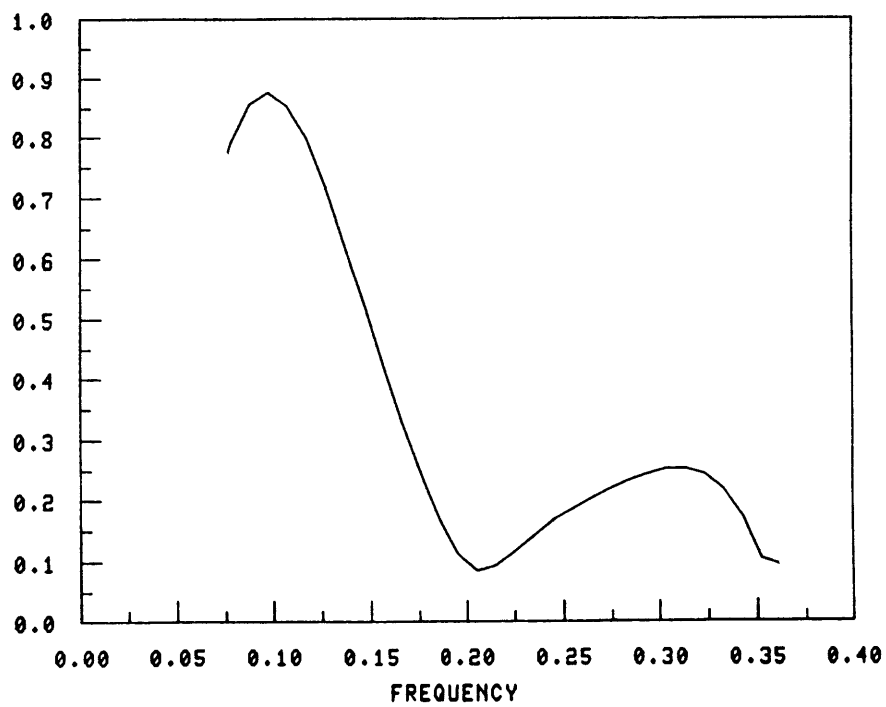




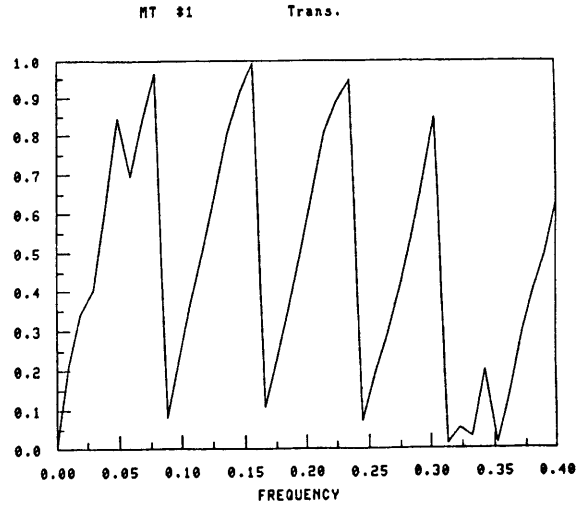
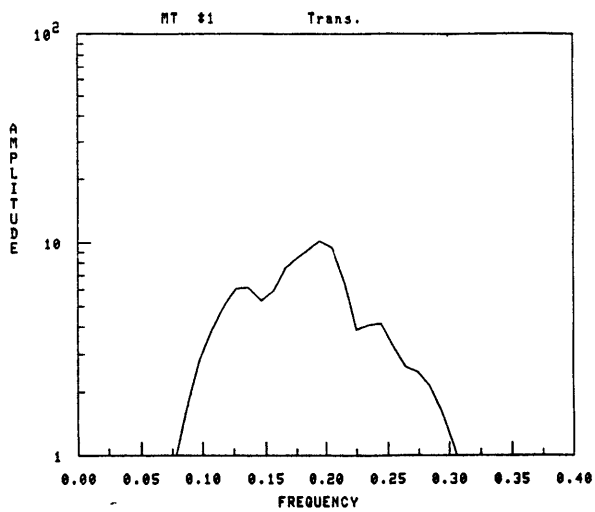
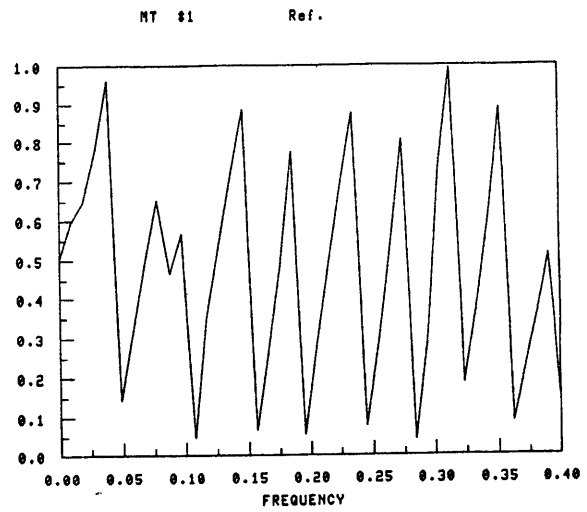
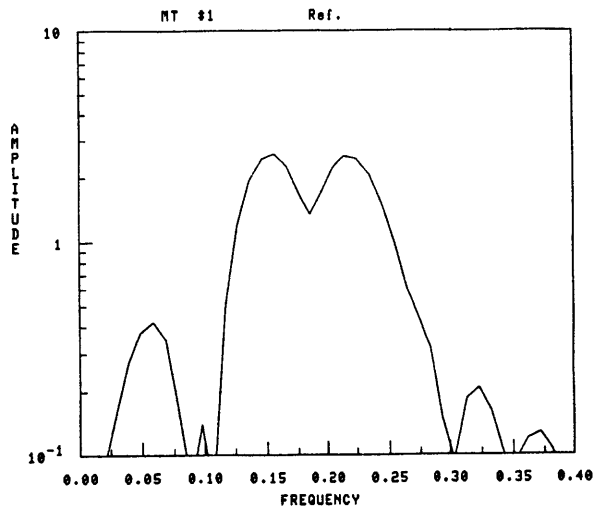
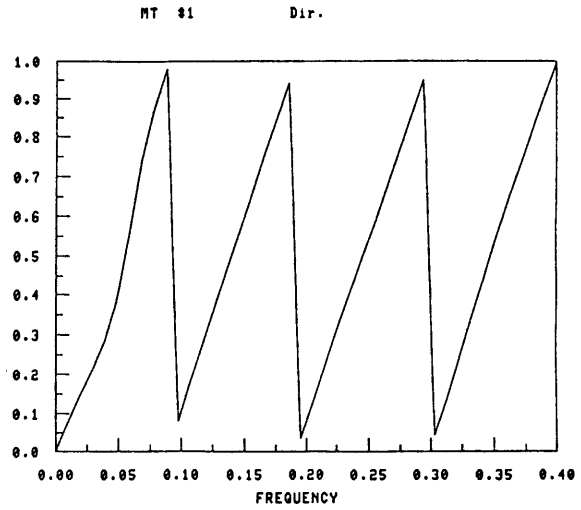
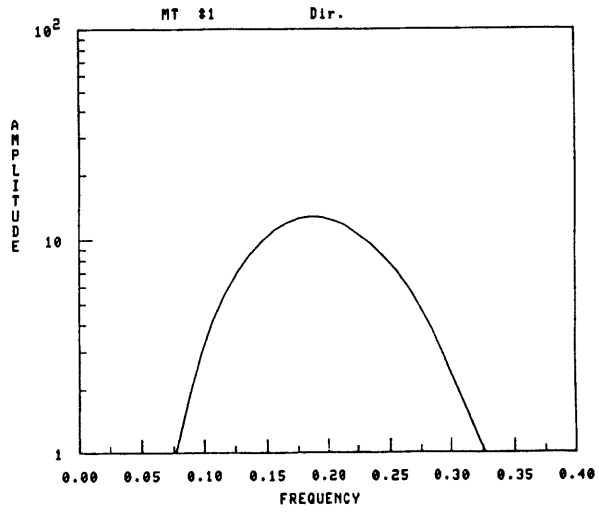
REF. COEFF. (PYR #3)



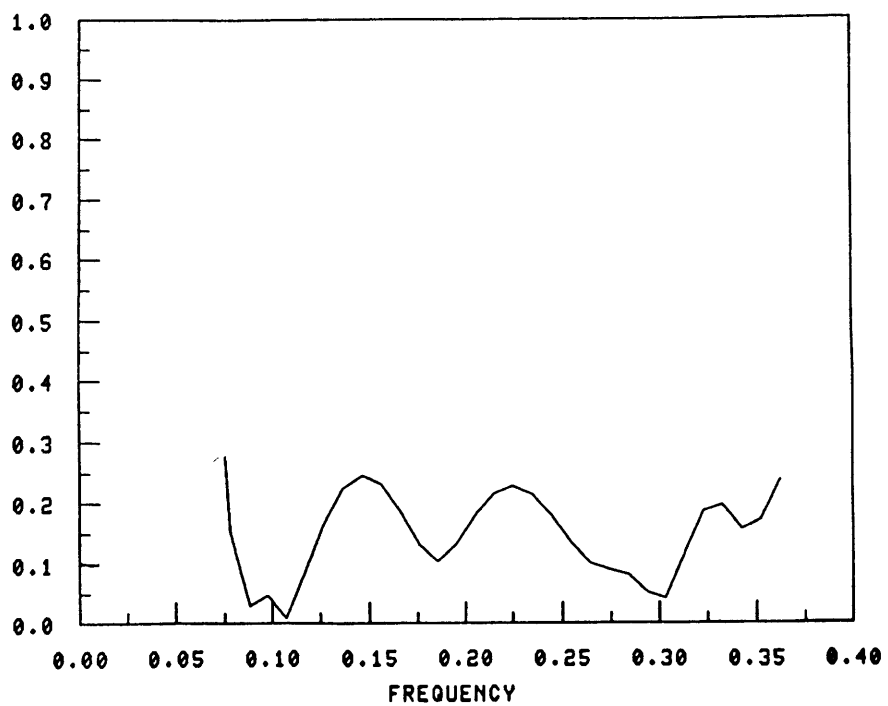
TRANS. COEFF. (PYR #3)



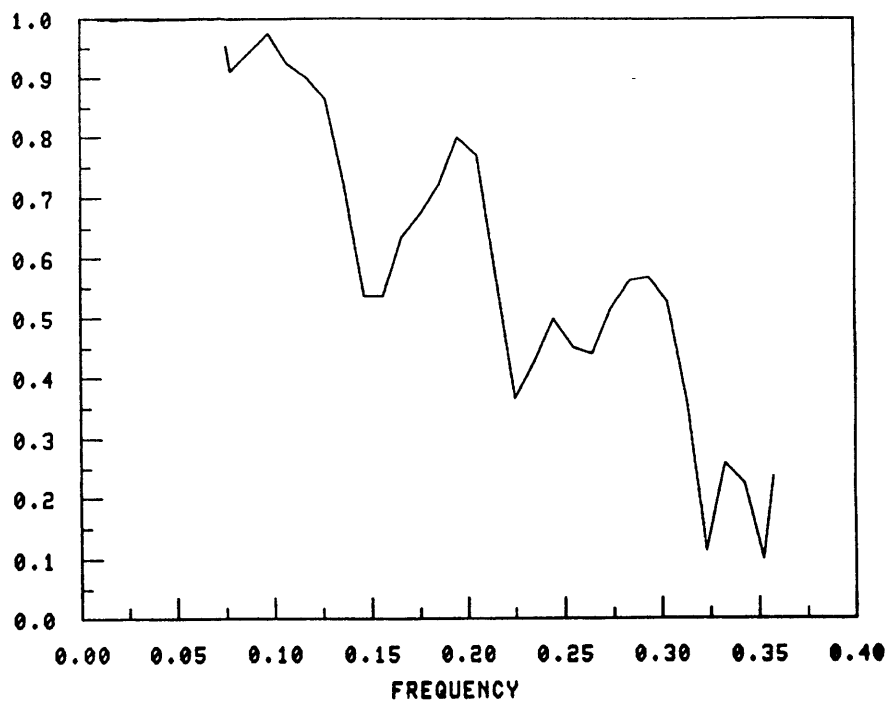


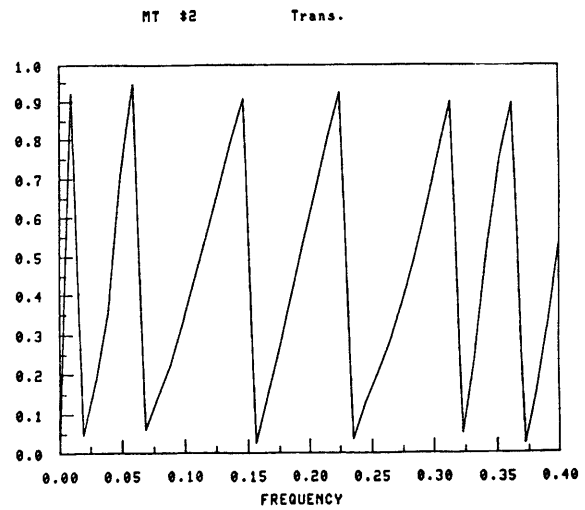
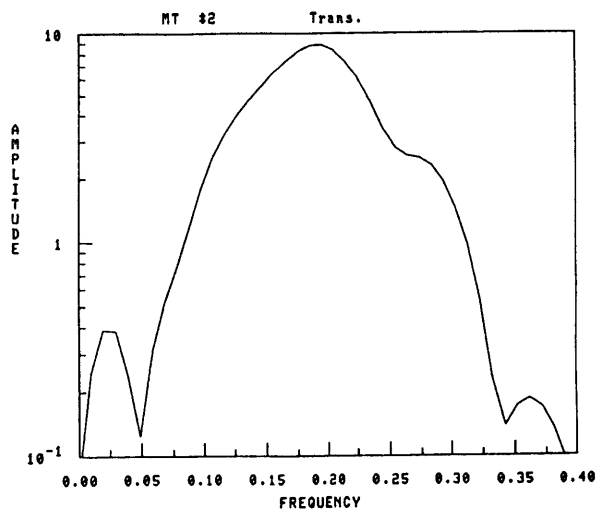
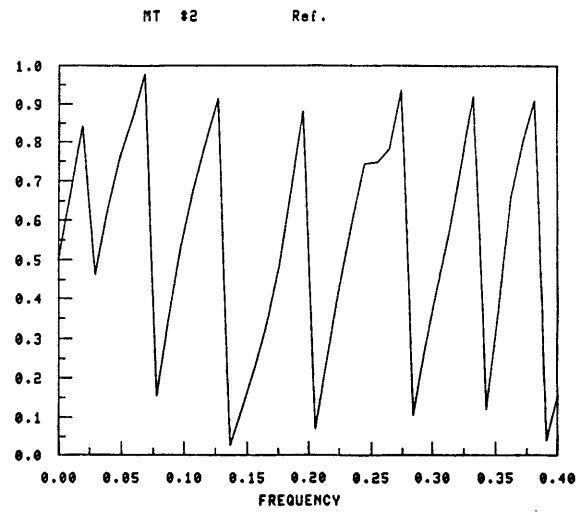
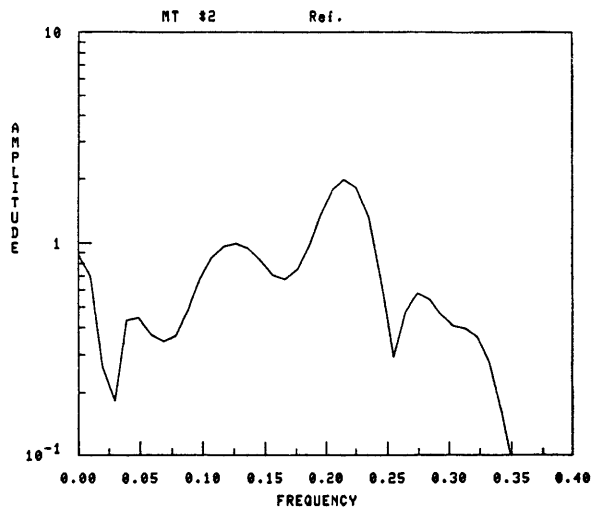
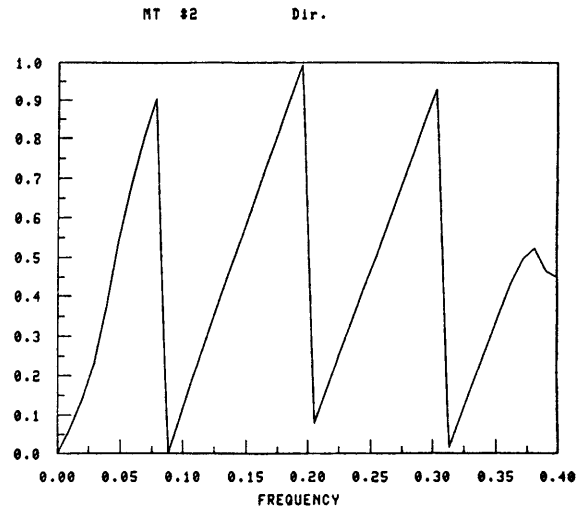
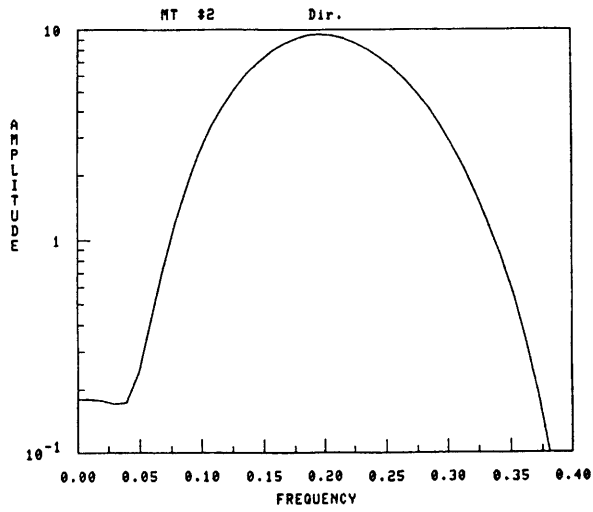


REF. COEFF. (MT #1)

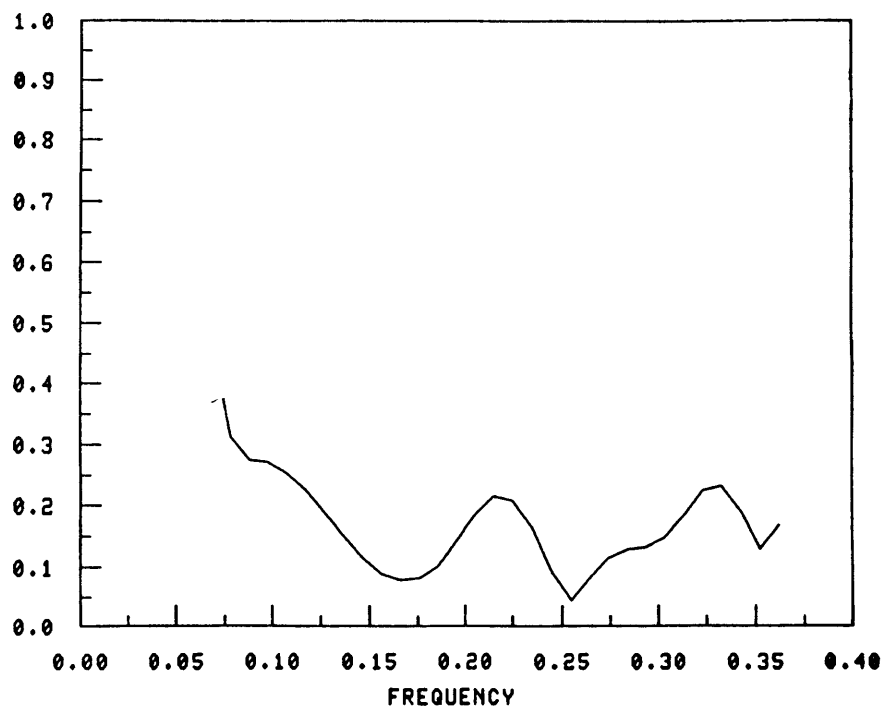


TRANS. COEFF. (MT #1)

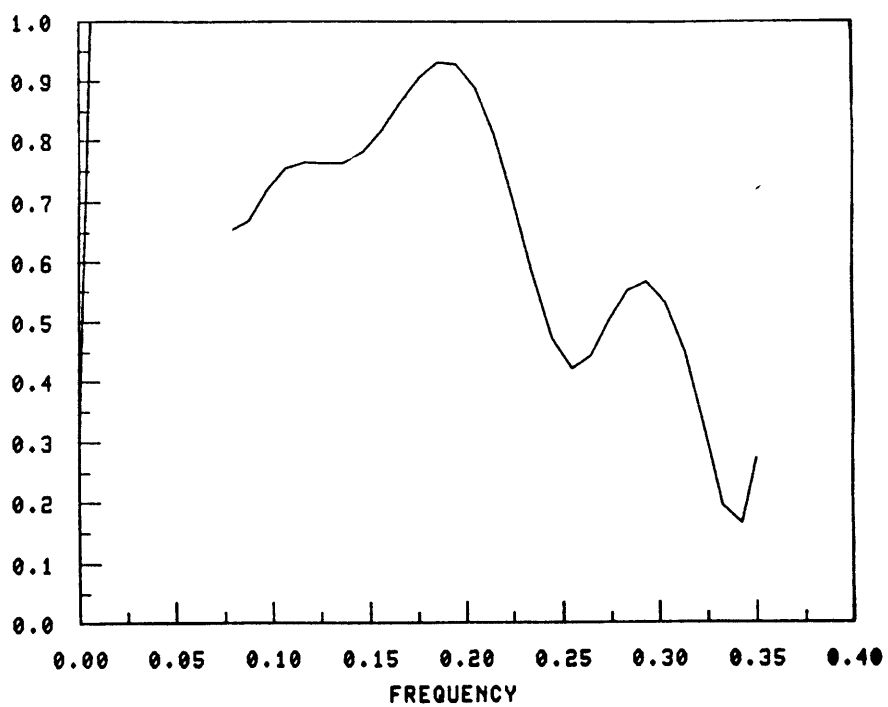


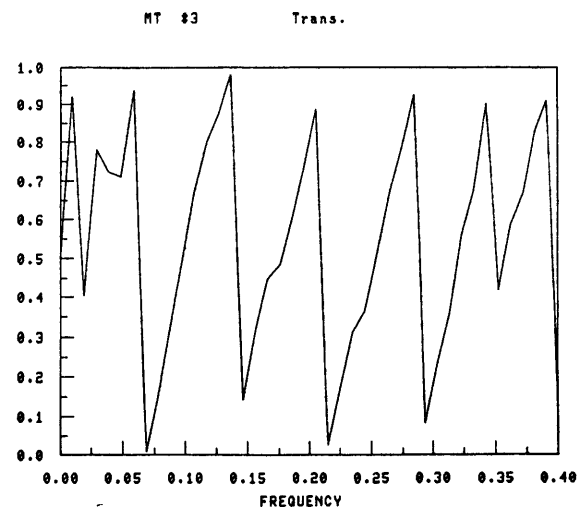
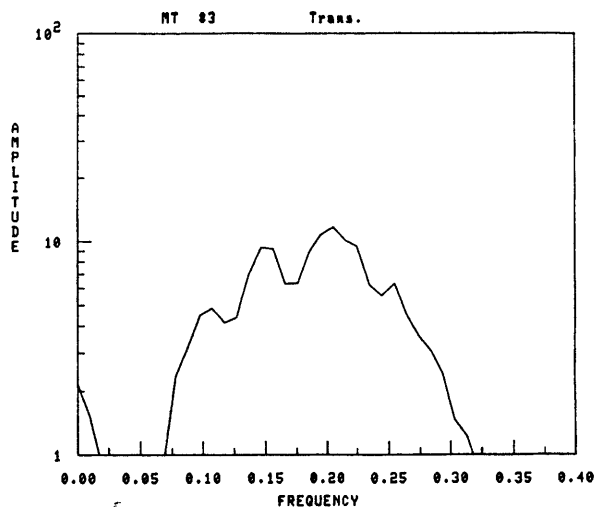
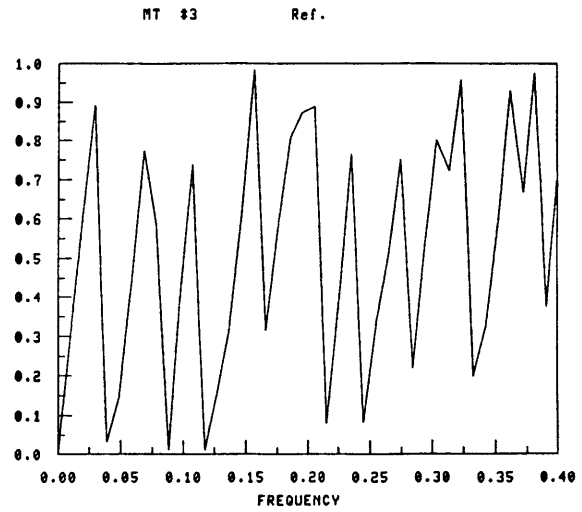
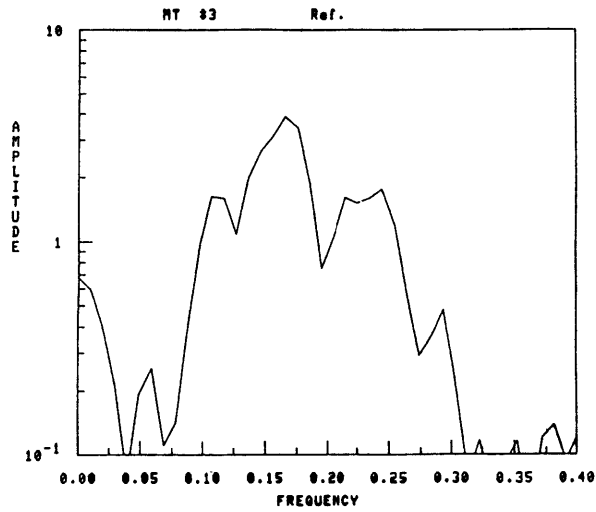
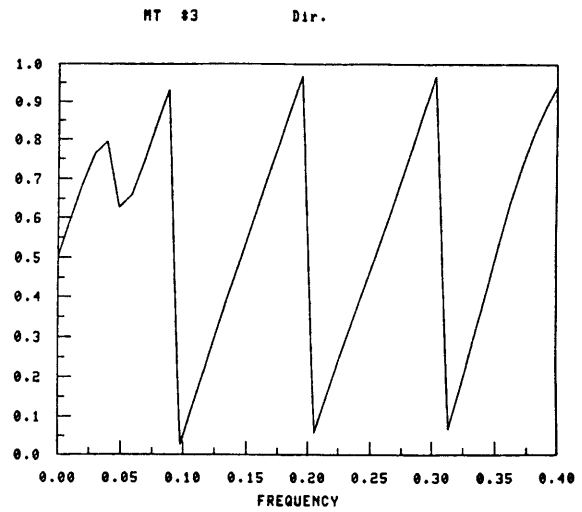
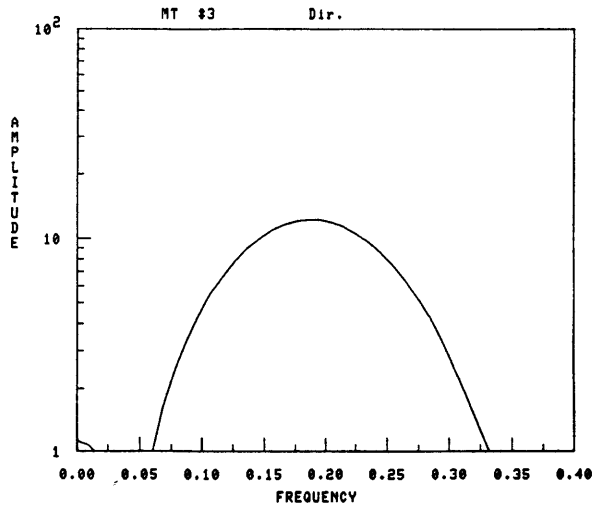


REF. COEFF. (MT #2)

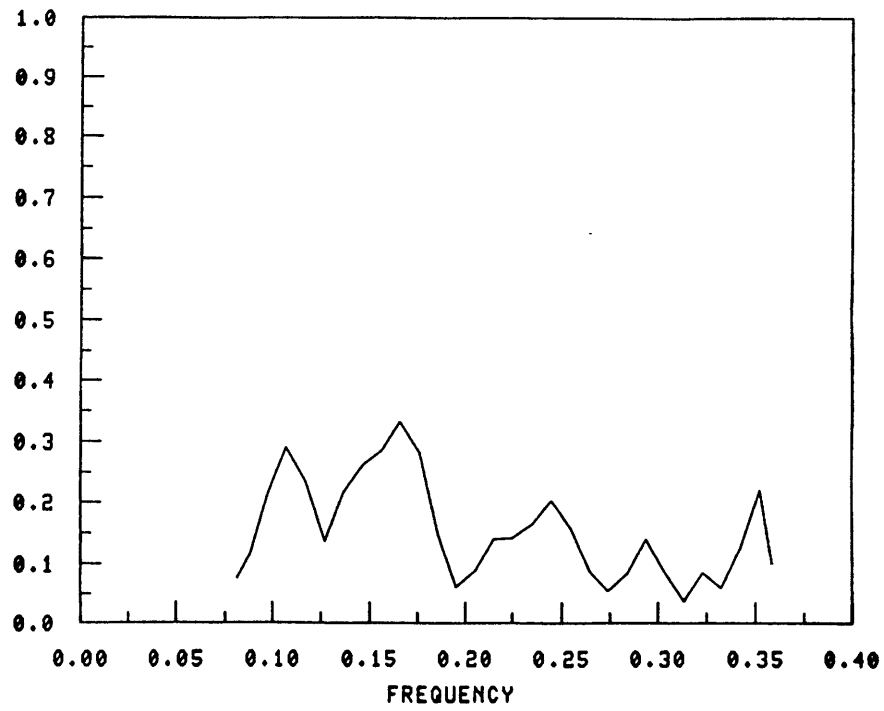


TRANS. COEFF. (MT #2)

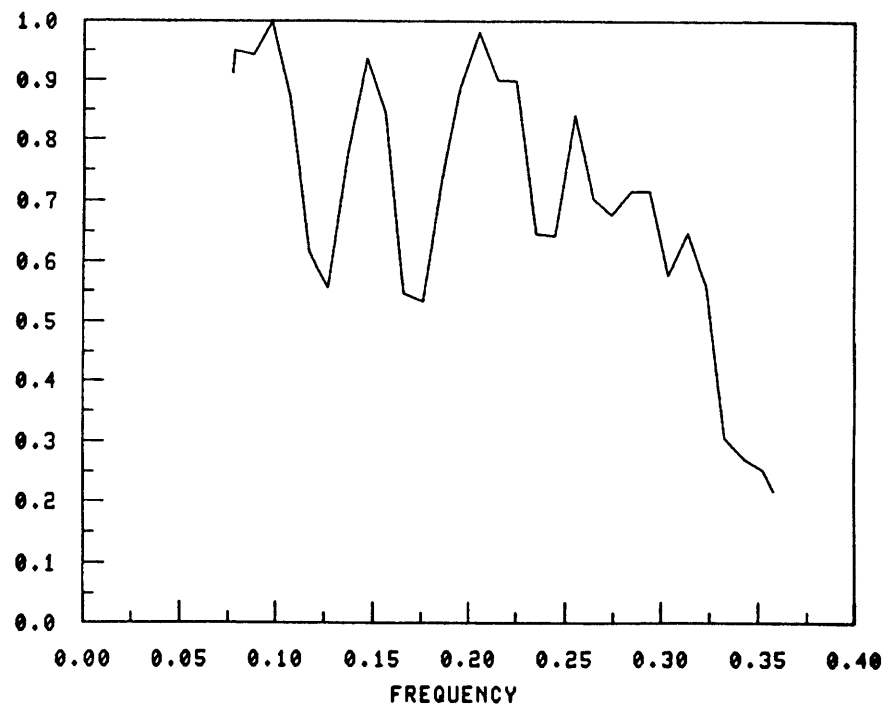


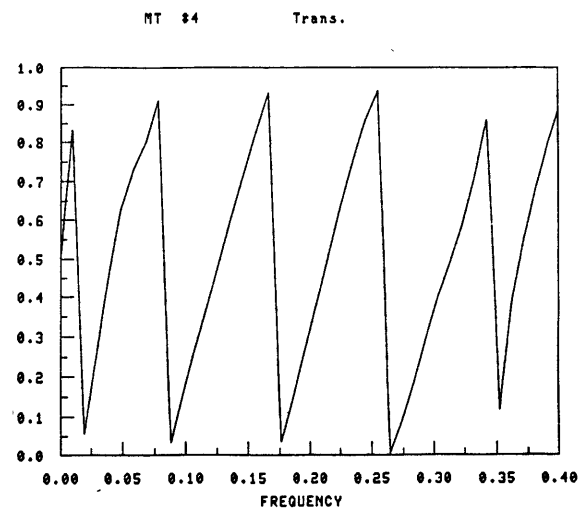
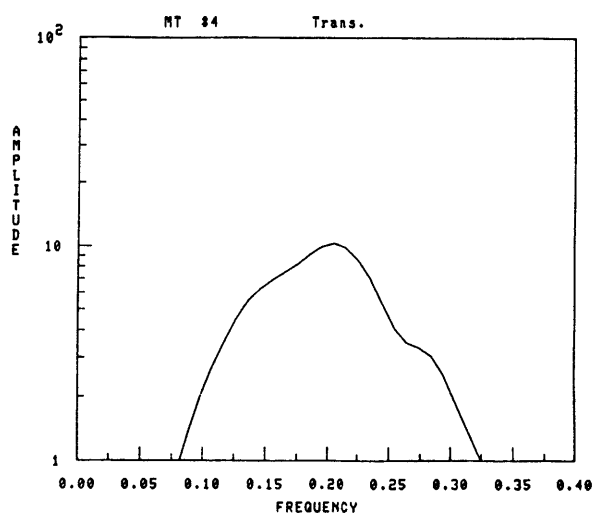
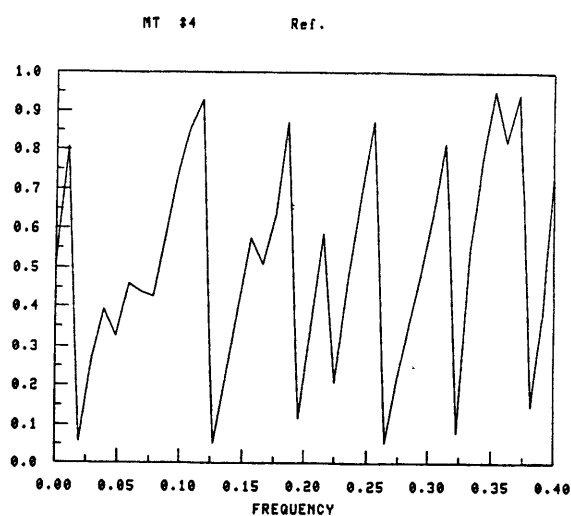
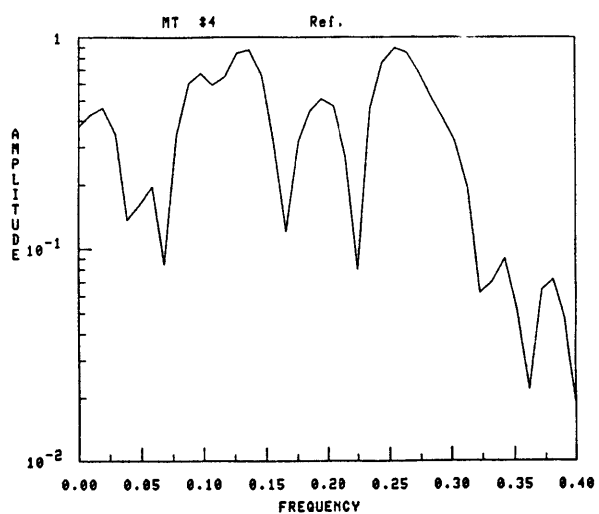
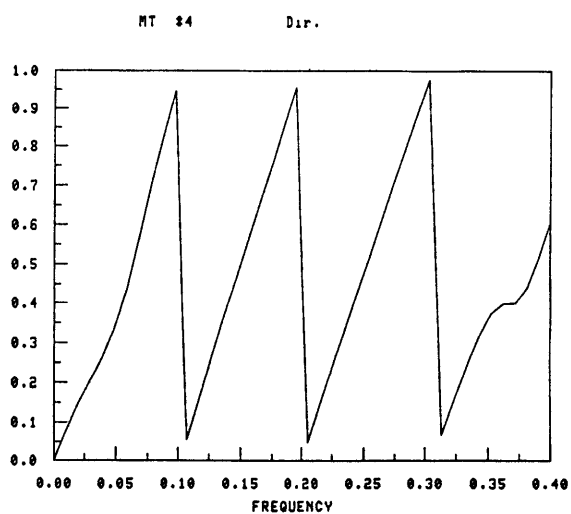
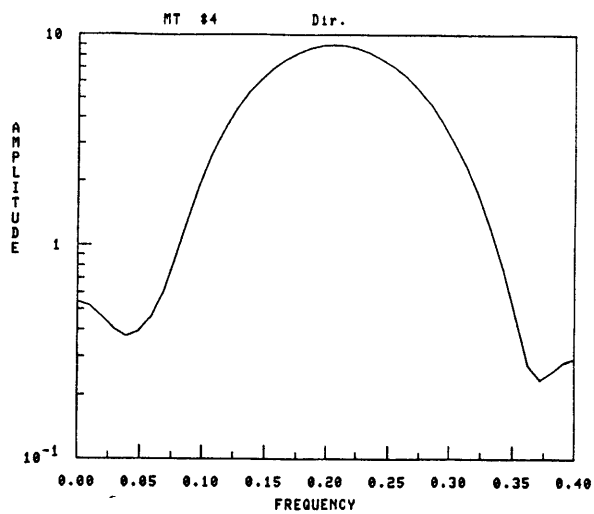


REF. COEFF. (MT #3)

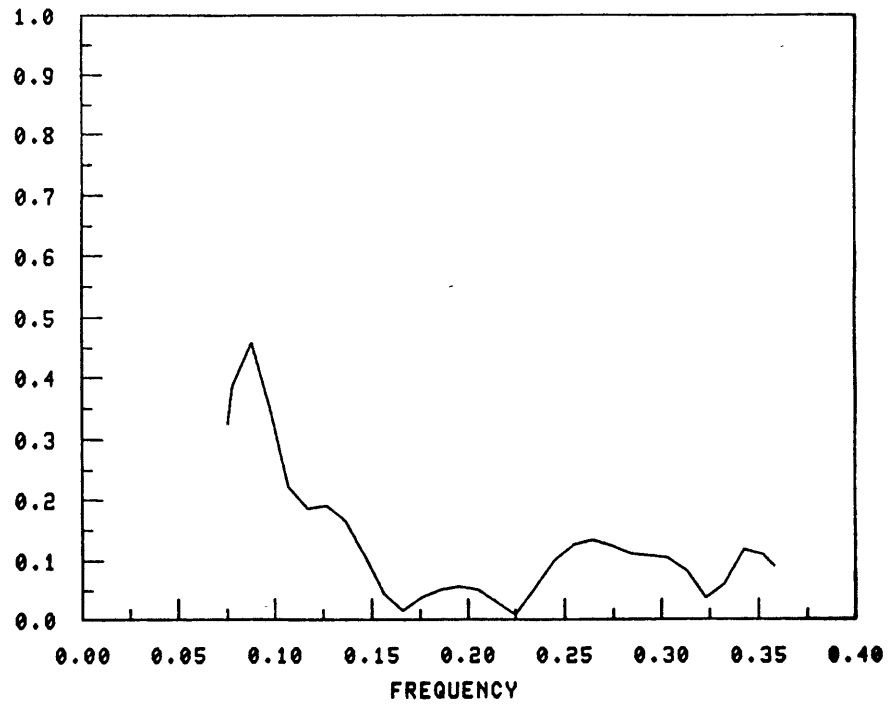


TRANS. COEFF. (MT #3)

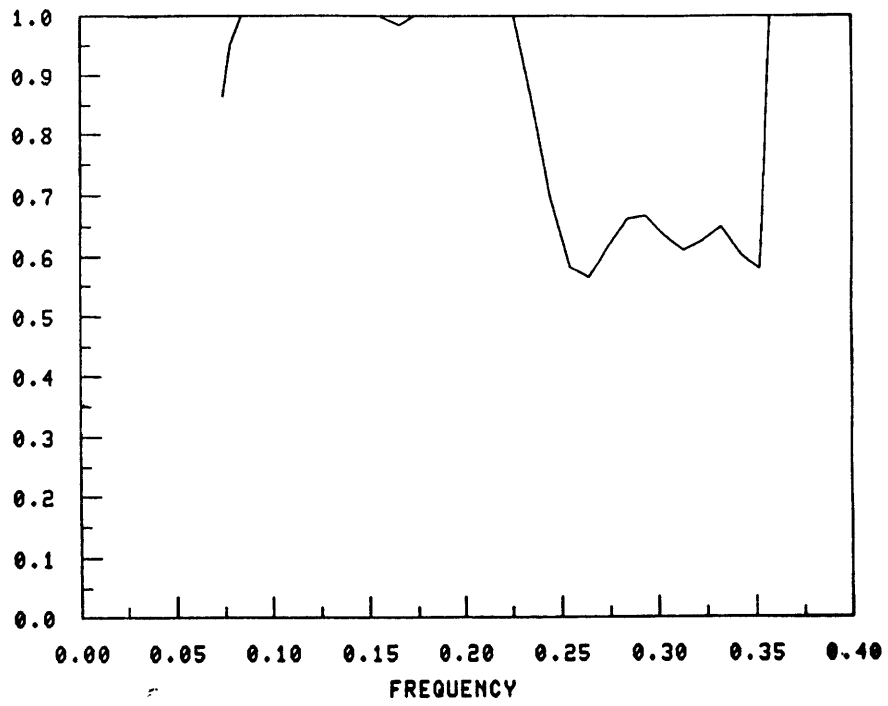




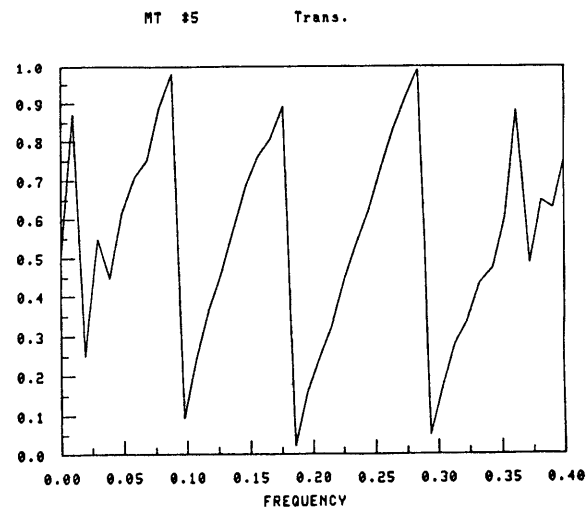
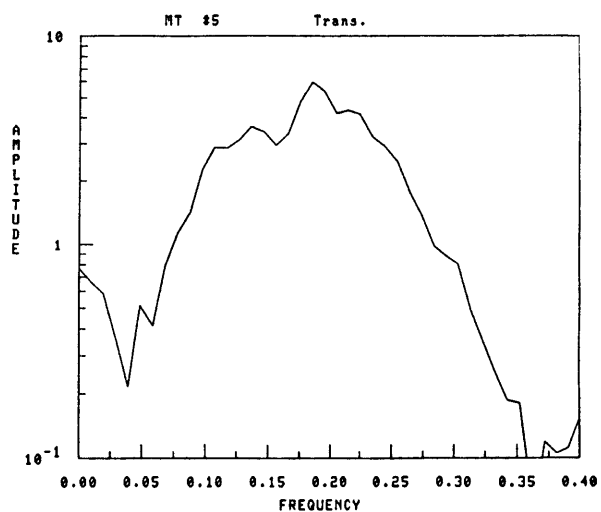
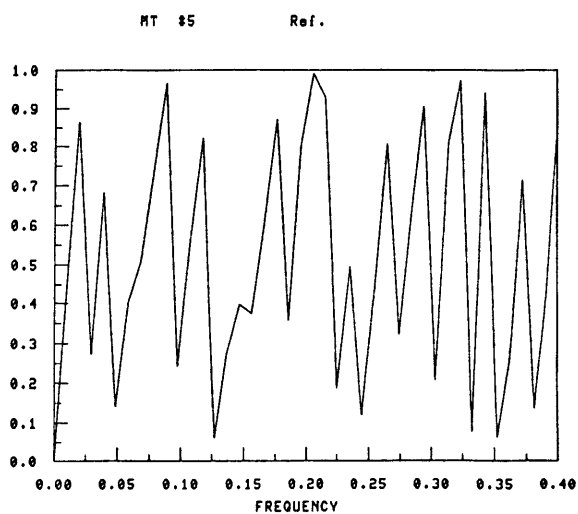
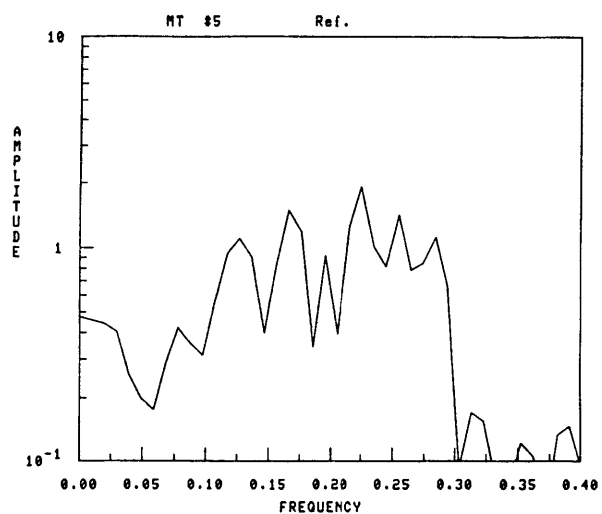
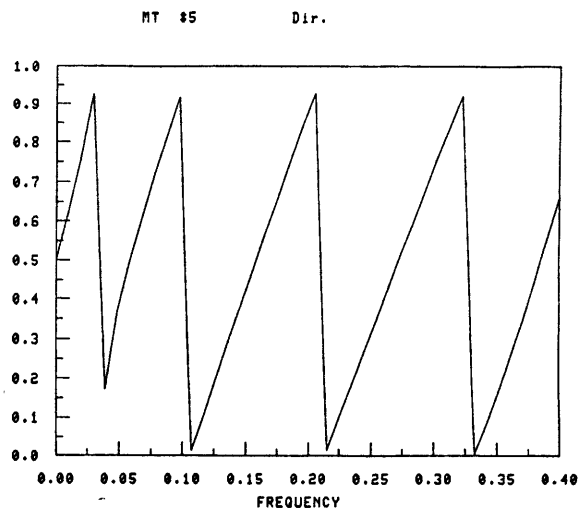
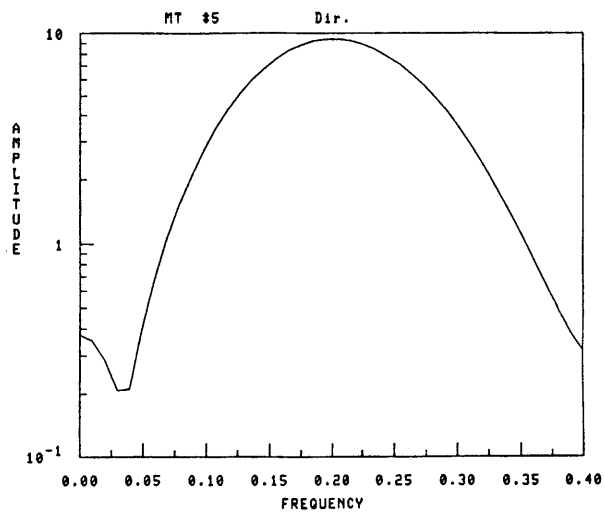
REF. COEFF. (MT #4)



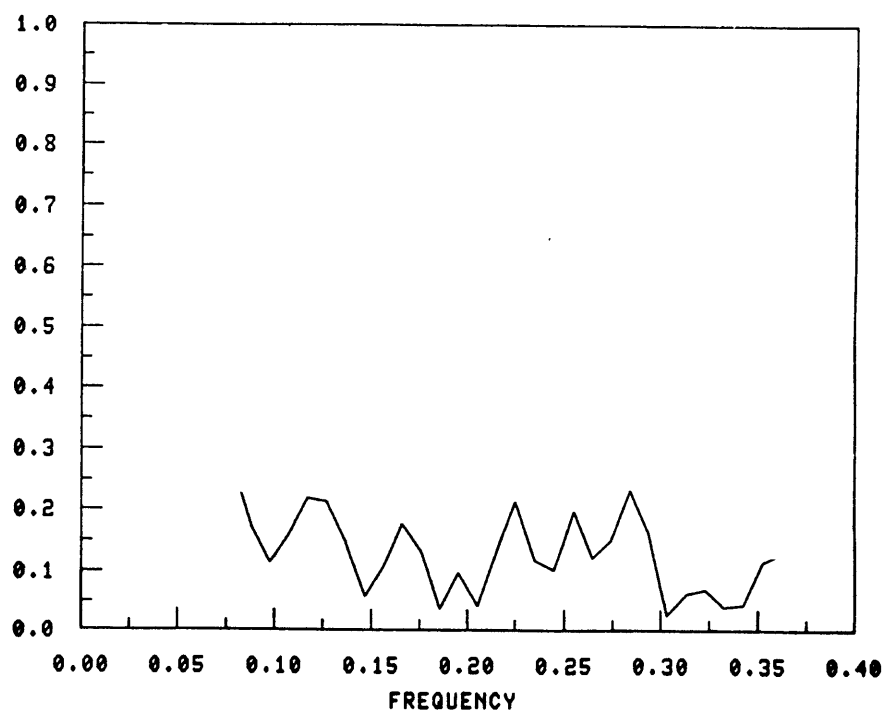
TRANS. COEFF. (MT #4)



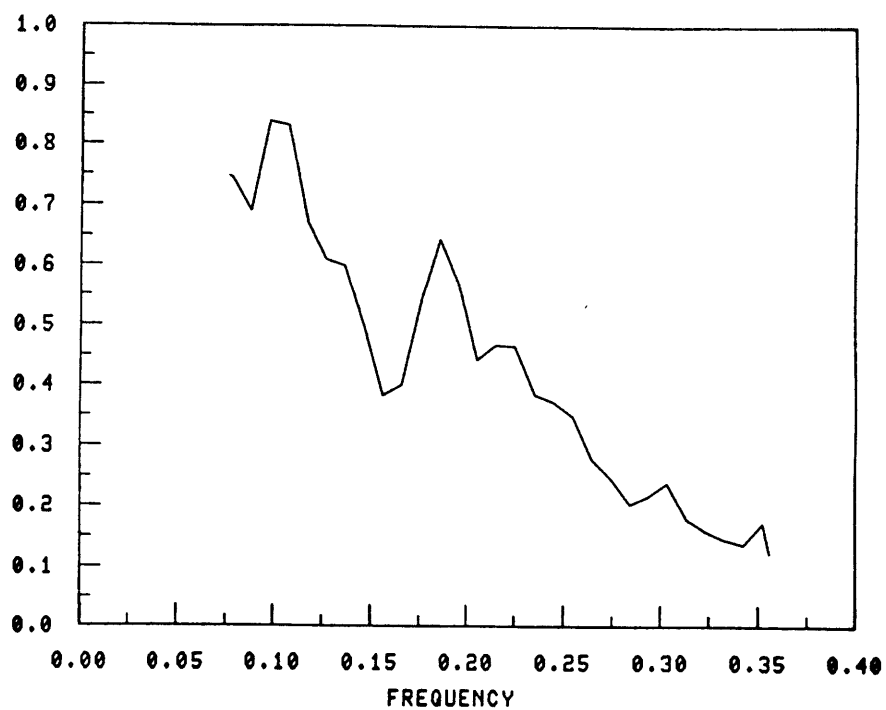


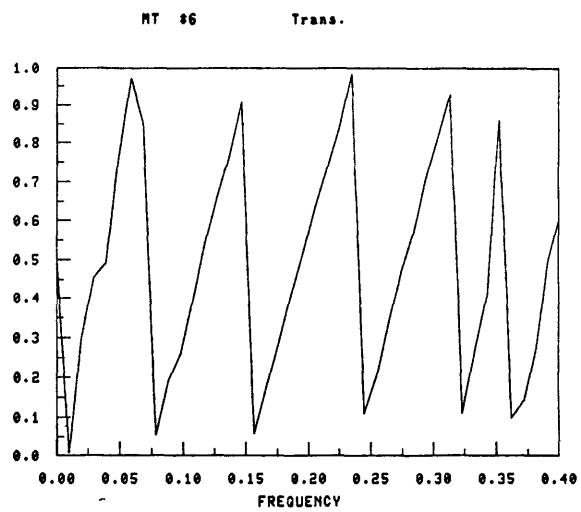
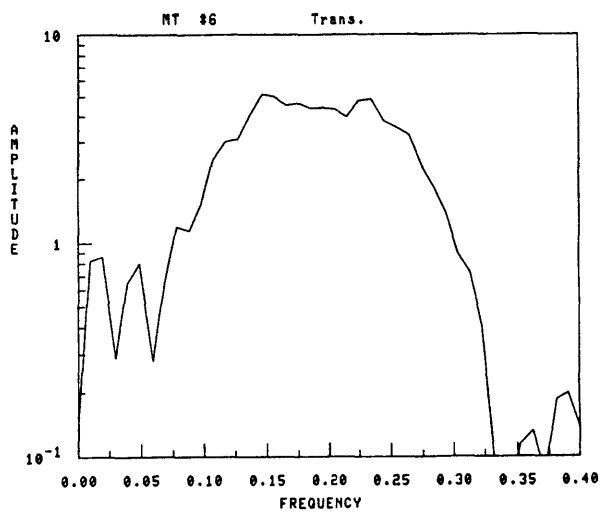
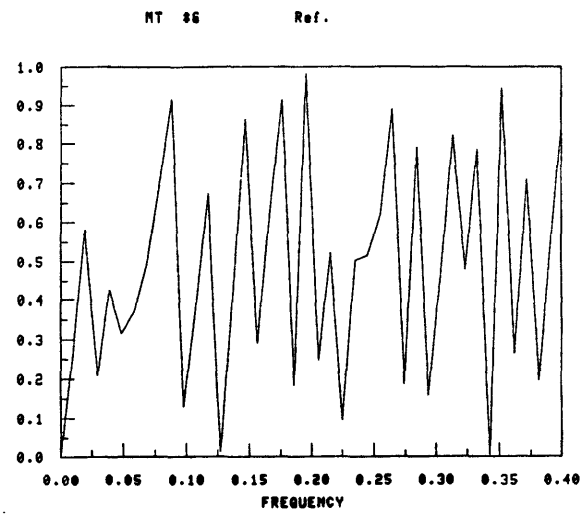
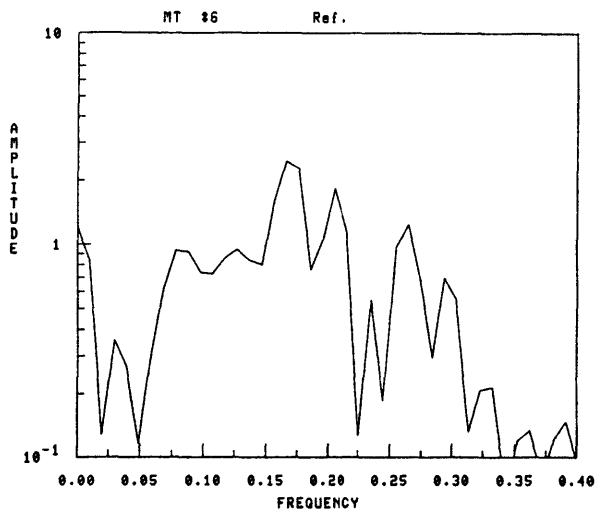
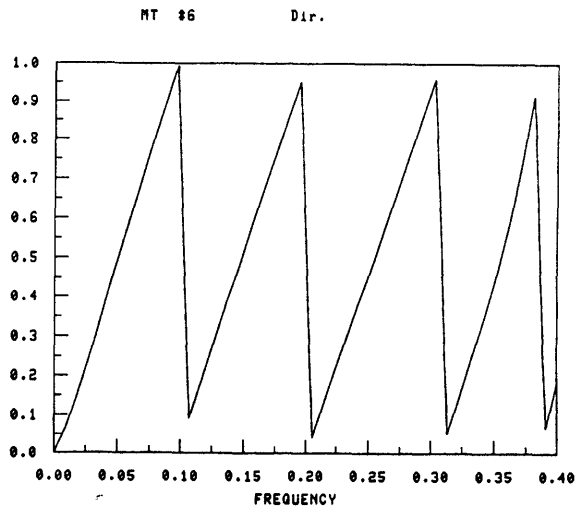
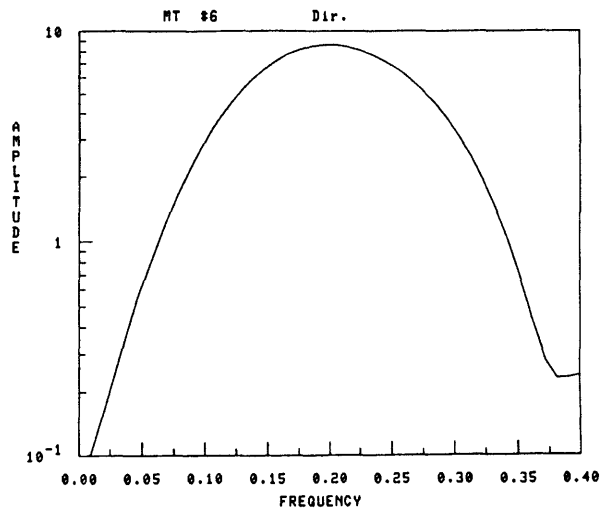


REF. COEFF. (MT #5)

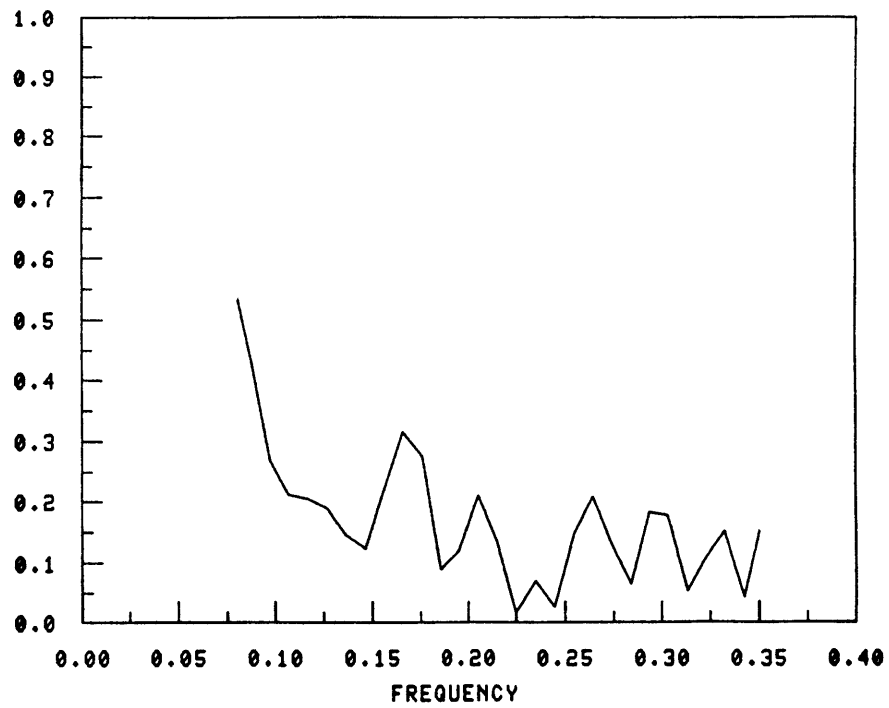


TRANS. COEFF. (MT #5)

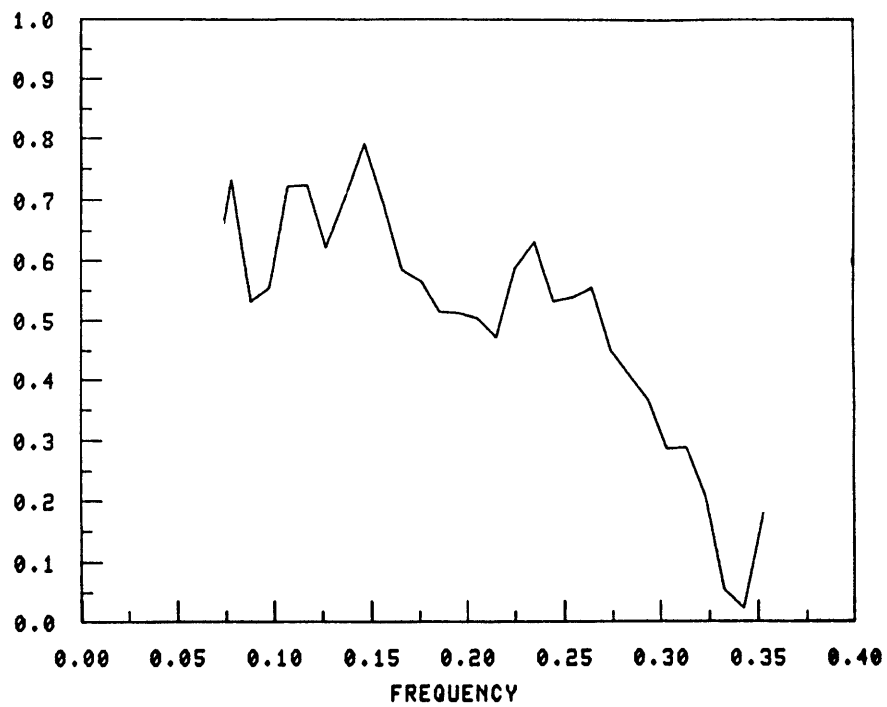


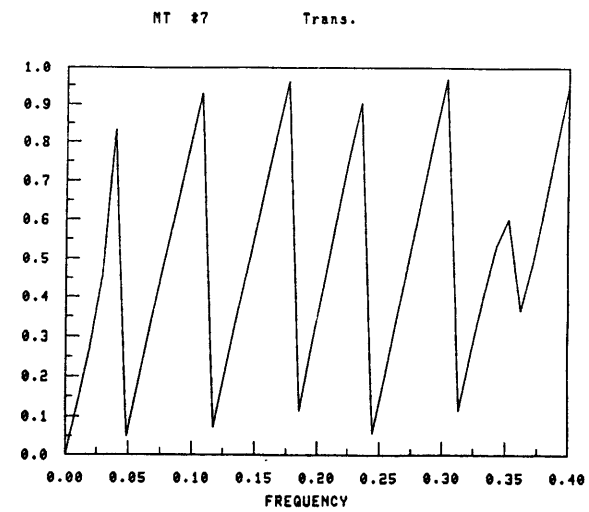
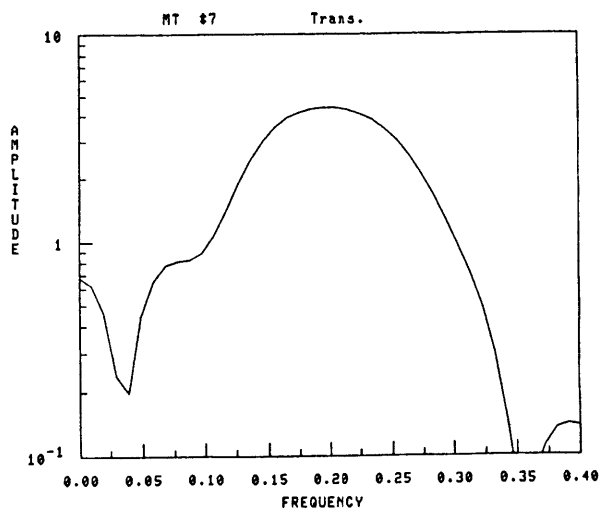
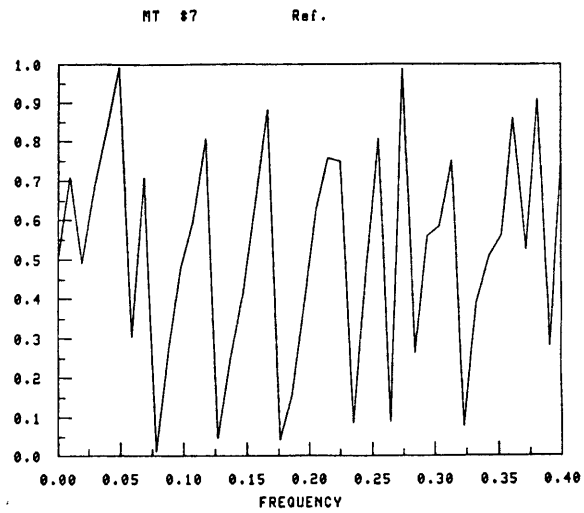
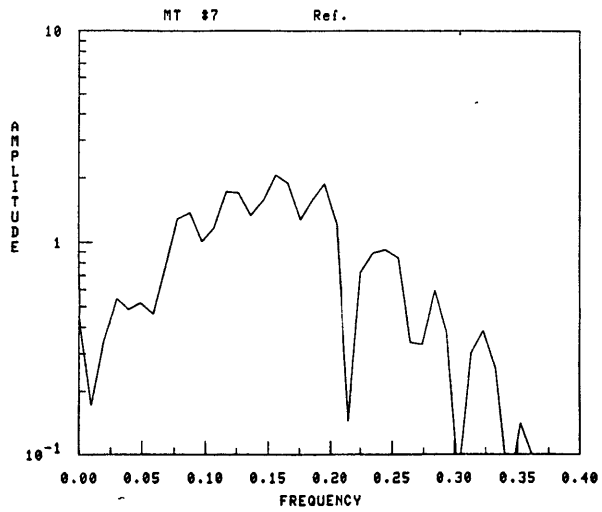
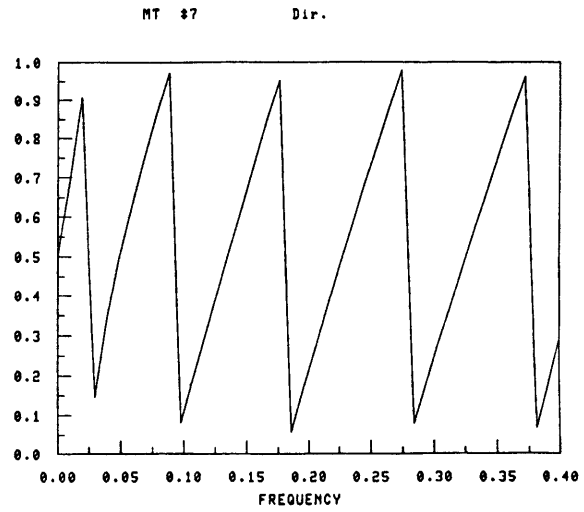
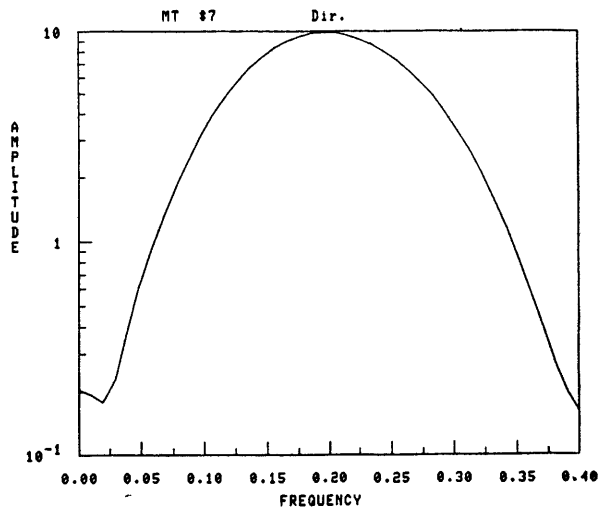


REF. COEFF. (MT #6)

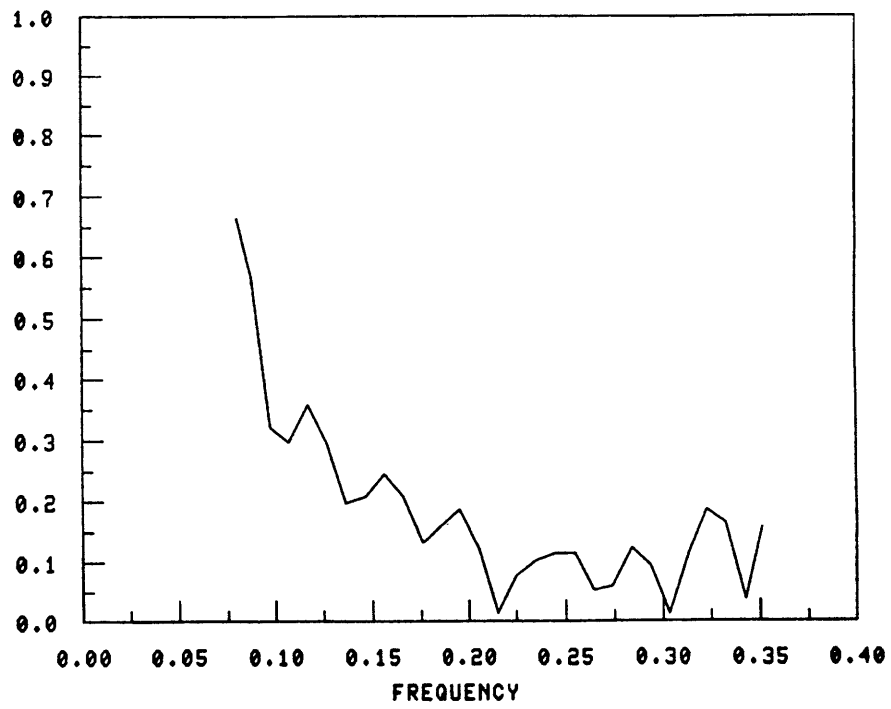


TRANS. COEFF. (MT #6)

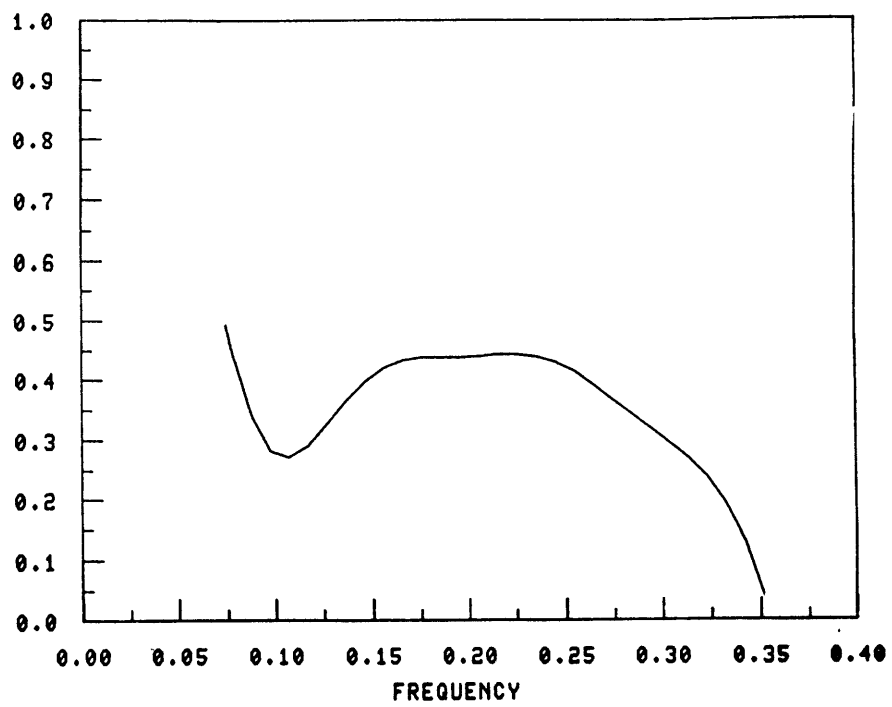




REF. COEFF. (MT #7)



TRANS. COEFF. (MT #7)



## REFERENCES

- Alsop, L.E., A.S. Goodman, S. Gregersen.  
Reflection and Transmission of Inhomogeneous Waves  
With Particular Application to Rayleigh Waves,  
Bull. Seism. Soc. Am., 64,  
1635 - 1652, 1974.
- Bjerkan, L., J.O. Fossum, K. Fossheim.  
The Surface Barrier Rayleigh Wave Transducer,  
J. Appl. Phys., 50,  
5307 - 5321, 1979.
- Bolt, B.A., and W.D. Smith.  
Finite-Element Computation of Seismic Anomalies For  
Bodies of Arbitrary Shape,  
Geophysics, 41,  
145 - 150, 1976.
- Bouchon, M.  
Effect of Topography On Surface Motion,  
Bull. Seism. Soc. Am., 63,  
615 - 632, 1973.
- Chamuel, J.R.  
Magnetostrictive Position Sensing Readouts For Commercial  
and Military Applications,  
C.S. Draper Lab, Report C - 4607,  
1976.

Chamuel, J.R.

Position Sensing Readout, U.S. Patent 4,035,762,  
12 July 1977.

Chamuel, J.R.

Seismic Ultrasonic Modeling,  
Presentation to Air Force, C.S. Draper Lab,  
Report No. 15L-79-081,  
18 May 1979.

Chamuel, J.R., and M.N. Toksöz.

Seismic Ultrasonic Modeling Program Final Report,  
C.S. Draper Lab,  
Report R-1385, 1980.

Chen, R.C., and L.E. Alsop.

Reflection and Transmission of Obliquely Incident  
Rayleigh Waves at a Vertical Discontinuity Between  
Two Welded Quarter-Spaces,  
Bull. Seism. Soc. Am., 69,  
1409 - 1423, 1979.

Curtis, R.G., and M. Redwood.

Approximate Analysis of the Reflection of Surface  
Acoustic Waves by Steps,  
J. Appl. Phys., 46.  
4627 - 4630, 1975.

Dally, J.W., and D. Lewis III.

A Photoelastic Analysis of Propagation of Rayleigh  
Waves Past a Step Change in Elevation,  
Bull. Seism. Soc. Am., 58,  
539 - 563, 1968.



de Bremaecker, J.Cl.

Transmission and Reflection of Rayleigh Waves at Corners,  
Geophysics, 23,  
253 - 266, 1958.

Deresiewicz, H.

The Effect of Boundaries on Wave Propagation in a  
Liquid-Filled Porous Solid,  
Bull. Seism. Soc. Am., 64,  
1901 - 1907, 1974.

Drake, L.A.

Rayleigh Waves at a Continental Boundary by the Finite  
Element Method,  
Bull. Seism. Soc. Am., 62,  
1259-1268, 1972.

Evernden, J.F.

Variation of Rayleigh-Wave Amplitude with Distance,  
Bull. Seism. Soc. Am., 61,  
231 - 240, 1971.

Farshad, J., and G. Ahmadi.

Effect of Boundaries on Wave Propagation in Media with  
Microstructure,  
Bull. Seism. Soc. Am., 64,  
387 - 392, 1974.

Gilbert, F., and L. Knopoff.

Seismic Scattering From Topographic Irregularities,  
J. Geophys. Res., 65,  
3437-3444, 1960.

Gregersen, S.

Possible Mode Conversion Between Love and Rayleigh Waves  
at a Continental Margin,  
Geophys. J. Roy. Astr. Soc., 54,  
121 - 127, 1978.

Gupta, I.N., and C. Kisslinger.

Model Study of Explosion-Generated Rayleigh Waves in  
a Half Space,  
Bull. Seism. Soc. Am., 54,  
475 - 484, 1964.

Hudson, J.A., and L. Knopoff.

Transmission and Reflection of Surface Waves at a Corner,  
(theoretical),  
J. Geophys. Res., 69,  
281 - 289, 1964.

Hudson, J.A., and L. Knopoff.

Statistical Properties of Rayleigh Waves Due to  
Scattering by Topography,  
Bull. Seism. Soc. Am., 57,  
83 - 90, 1967.

Kane, J., and J. Spence.

Rayleigh Wave Transmission on Elastic Wedges,  
Geophysics, 28,  
715 - 723, 1963

Kato, Y., and A. Takagi.

Wave Propagation in the Step-Shaped Structure and on  
the Cliff,  
Sci. Rep. Tohoku Univ., Ser.5, 8,  
212 - 224, 1957.

Knopoff, L., and A.F. Gangi.

Transmission and Reflection of Rayleigh Waves by Wedges,  
Geophysics, 25,  
1203 - 1214. 1960.

Kolsky, H.

Stress Waves in Solids,  
Dover Pub., N.Y., 1963.

Lapwood, E.R.

The Transmission of a Rayleigh Pulse Round a Corner,  
Geophys. J. Roy. Astr. Soc., 4,  
 174 - 196, 1961.

Lewis, D., and J.W. Dally.

Photoelastic Analysis of Rayleigh Wave Propagation  
 in Wedges,  
J. Geophys. Res., 75,  
 3387 - 3398, 1970.

Li, R.C.M.

Analysis of Surface Wave Reflection From a Periodic Array  
 of Grooves,  
IEEE 1972 Ultrasonics Symp. Proc.,  
 263 - 266.

Mal, A.K., and L. Knopoff.

Transmission of Rayleigh Waves Past a Step Change in  
 Elevation,  
Bull. Seism. Soc. Am., 55,  
 319 - 334, 1965.

Mal, A.K., and L. Knopoff.

Transmission of Rayleigh Waves at a Corner,  
Bull. Seism. Soc. Am., 56,  
 455 - 466, 1966.

Martel, L., M. Munasinghe, and G.W. Farnell.

Transmission and Reflection of Rayleigh Wave Through  
 a Step,  
Bull. Seism. Soc. Am., 67,  
 1277 - 1290, 1977.

Martel, L.

Love Wave Propagation Across a Step by Finite Elements  
 and Spatial Filtering,  
Geophys. J. Roy. Astr. Soc., 61,  
 659 - 677, 1980.

McGarr, A., and L.E. Alsop.

Transmission and Reflection of Rayleigh Waves at Vertical  
Boundaries,

J. Geophys. Res., 72,

2169 - 2180, 1967.

McGarr, A.

Amplitude Variations of Rayleigh Waves - Propagation Across  
a Continental Margin,

Bull. Seism. Soc. Am., 59,

1281 - 1305, 1969.

Miller, G.F., and H. Pursey.

On the Partition of Energy Between Elastic Waves in a  
Semi-Infinite Solid,

Proc. Roy. Soc. London, Ser. A, 233,

55 - 59, 1955.

Munasinghe, M., and G.W. Farnell.

Surface Wave Scattering at Vertical Discontinuities,

IEEE 1972 Ultrasonics Symp. Proc.,

267 - 270.

Munasinghe, M., and G.W. Farnell.

Finite Difference Analysis of Rayleigh Wave Scattering  
at Vertical Discontinuities,

J. Geophys. Res., 78,

2454 - 2466, 1973.

Oliver, J., F. Press, M. Ewing.

Two-Dimensional Model Seismology,

Geophysics, 19,

202 - 219, 1954.

Otto, O.W.

Scattering of Rayleigh Waves From Topographic Irregularities  
At Oblique Incidence,  
J. Appl. Phys., 48,  
5105 - 5110, 1977.

Parekh, J.P., and H.S. Tuan.

Reflection and Bulk-Wave Conversion of Rayleigh Wave at  
a Single Shallow Groove,  
J. Appl. Phys., 48,  
994 - 1003, 1977.

Pilant, W.L., L. Knopoff, and F. Schwab.

Transmission and Reflection of Surface Waves at a  
Corner (experimental),  
J. Geophys. Res., 69,  
291 - 297, 1964.

Sills, L.B.

Scattering of Horizontally-Polarized Shear Waves by  
Surface Irregularities,  
Geophys. J. Roy Astr. Soc., 54,  
319 - 348, 1978.

Thapar, M.R.

Rayleigh Wave Propagation and Perturbed Boundaries,  
Can. J. Earth Sci., 7,  
1449 - 1461, 1970.

Toksöz, M.N. and D.L. Anderson.

Generalized Two-dimensional Model Seismology with Application to  
Anisotropic Earth Models,  
J. Geophys. Res., 68,  
1121 - 1130, 1963.

Toksöz, M.N. and F. Schwab.

Bonding of Layers in Two-dimensional Seismic Modeling,  
Geophysics, 29,  
405 - 413, 1964.

Tuan, H-S, and R.C.M. Li.

Rayleigh Wave Reflection From Groove and Step  
Discontinuities,  
J. Acoust. Soc. Am., 55,  
1212 - 1217, 1974.

Viktorov, I.A.

The Effects of Surface Defects on the Propagation of  
Rayleigh Waves,  
Sov. Phys. Doklady, 3,  
304 - 306, 1958.

Viswanathan, K., J.T. Kuo and E.R. Lapwood.

Reflection and Transmission of Rayleigh Waves in a Wedge,  
Geophys. J. Roy. Astr. Soc., 24,  
401 - 414, 1971.

Viswanathan, K., and A. Roy.

Reflection and Transmission of Rayleigh Waves in a Wedge - II.  
Geophys. J. Roy. Astr. Soc., 32,

Wang, K.L. and H.A. Haus.

Scattering of Rayleigh Waves by Post Spacers,  
IEEE Trans. Sonics and Ultrasonics, 26,  
45 - 53, 1979.

Woods, R.D.

Screening of Surface Waves in Soils,  
J. Soil Mech. and Foundations Div., 94,  
951 - 979, 1968.